SINTEF Applied Chemistry

Address: N-7465 Trondheim, NORWAY
Location: S.P. Andersens vei 15A
Telephone: +47 73 59 20 80 / 12 12
Fax: +47 73 59 70 51

Enterprise No.: NO 948 007 029 MVA

SINTEF REPORT

TITLE

**DEEP SPILL JIP -
EXPERIMENTAL DISCHARGES OF GAS AND OIL AT HELLAND HANSEN – JUNE 2000,
TECHNICAL REPORT**

AUTHOR(S)

Øistein Johansen, Henrik Rye, Alf G. Melbye, Hans V. Jensen, Bjørn Serigstad, Tor Knutsen (IMR)

CLIENT(S)

DeepSpill JIP

REPORT NO.	CLASSIFICATION	CLIENTS REF.	
STF66 F01082	Confidential	Cort Cooper, Chevron Petroleum Technology Co.	
CLASS. THIS PAGE	ISBN	PROJECT NO.	NO. OF PAGES/APPENDICES
		661182	159
ELECTRONIC FILE CODE		PROJECT MANAGER (NAME, SIGN.)	CHECKED BY (NAME, SIGN.)
Final Report Part_total		Øistein Johansen	Mark Reed
FILE CODE	DATE	APPROVED BY (NAME, POSITION, SIGN.)	
	2001-06-05	Tore Aunaas, Research Director	

ABSTRACT

The DeepSpill experiment was conducted in the Norwegian Sea at the Helland Hansen site (65°00'N, 04°50'E) and included four controlled discharges of oil and gas from a water depth of 844 meters. The main objective of the experiments was to obtain data for verification and testing of numerical models for simulating accidental releases in deep waters. In addition, the experiments were aimed at testing equipment for monitoring and surveillance, and evaluation of the safety aspects of accidental releases of gas and oil in deep waters.

Three vessels took part in the experiment – one supply vessel (*Far Grip*) that carried the discharge equipment, and two research vessels (*Håkon Mosby* and *Johan Hjort*) carrying instruments for subsea monitoring and equipment for sampling of surface oil. A total of 42 scientists, operators and observers participated on the three vessels. In addition – surveillance airplanes from various countries were stationed at Kristiansund airport to be ready to make flights over the area. On the last two days of the experiment, seven Norwegian Clean Seas (NOFO) response vessels were present, in case any recovery of oil was necessary. Field operations started on June 21 when the supply vessel left Bergen and ended July 2 when the supply vessel returned to Mongstad. The field experiments took place from June 26 to June 29.

Mobilization of vessels, deployment of the discharge arrangement and conductance of the experimental discharges were all carried out according to plan, although with some delay due to adverse weather. Extensive observations and documentation were acquired during the experiments by use of wind and current meters, CTD instruments, aircraft surveillance, sampling of oil from the surface slicks, mapping of subsurface plumes with remotely operated vehicles (ROV) and echo sounder, as well as by chemical and biologic sampling in the water column. This report contains a description of the planning and execution of these experiments, a presentation of the observations and data acquired during the experiments, and some preliminary analyses of the data by use of simulation models.

KEYWORDS	ENGLISH	NORWEGIAN
GROUP 1	Environment	Miljø
GROUP 2	Oil	Olje
SELECTED BY AUTHOR	Blowouts	Utblåsning
	Deep water	Dypt vann
	Field trial	Feltforsøk

DEEP SPILL EXPERIMENTS – TECHNICAL REPORT

TABLE OF CONTENTS

1 INTRODUCTION

This report describes the findings from the DeepSpill sea trial carried out in the Norwegian Sea at the Helland Hansen location in June 2000. The sea trial was a part of the DeepSpill project, organized as a Joint Industry Project involving 23 oil companies and the US government agency Minerals Management Service (MMS). A complete list of the JIP members is given in Appendix B. Chevron US has acted as administrator of the JIP, while Norsk Chevron applied for the discharge permit on behalf of this organization. SINTEF Applied Chemistry was the main contractor, responsible for planning of the field trial and conductance of the scientific tasks in the project. The Norwegian authorities gave permission for the discharges on certain conditions. A cruise report has been issued previously – including a description of how these conditions were met and an overview of the field operations in general.

The present report provides a detailed technical presentation of all major findings from the DeepSpill field trial, including:

- Overall description of the experiment, including vessels, equipment for transport and discharge of oil and gas, monitoring instruments etc.
- Documentation of marine life at the experimental site.
- Description of environmental conditions during the experiments (sea state, hydrographic profiles, ocean currents as a function of depth).
- Description of discharges (discharge method, discharge rate of oil and gas, duration of discharges, observations of bubble and droplet formation at the exit).
- Observations of the deepwater plumes in each experiment (trajectory, depth of trapping, dilution, hydrate formation and dissolution of gas, comparison with model simulations).
- Observations of surfacing of oil droplets and formation of surface slick (extent and temporal changes, size distribution of surfacing droplets, weathering of surface slick).

In order to facilitate subsequent validation of deepwater plume models, a data set describing the experimental conditions, the development of the deepwater plumes and the formation of surface slicks has been produced in conjunction with the technical report. This data set is available to the JIP-participants on the CD-ROM containing this report.

2 OBJECTIVES OF FIELD EXPERIMENTS

The DeepSpill JIP was established with the aim of determining the fate of oil and gas released in deepwater by performing full-scale field experimental releases. The main purposes of these experiments were:

- to obtain data for verification and testing of numerical models for simulating accidental releases in deep waters;
- to test equipment for monitoring and surveillance of accidental releases in deep waters;
- to evaluate the safety aspect of accidental releases of gas and oil in deep waters.

Verified numerical models combined with improved surveillance of the releases should then provide a better basis for oil spill contingency planning and environmental impact assessments in conjunction with future deep water exploration, development and production.

3 PLANNING AND PREPARATIONS

This chapter provides an overview of the planning- and preparation activities that were conducted prior to the field operations. The planning activities started in June 1999 when SINTEF was commissioned by Chevron to prepare a feasibility study of experimental discharges of oil and gas in deep waters, and terminated almost exactly one year later with the participating vessels heading for the experimental site at Saturday June 24, 2000.

3.1 Feasibility Study

The feasibility study[1] was presented at a meeting arranged by Chevron in Stavanger the first of September 1999. The feasibility study concentrated on three major issues: a) options for transport and discharge of oil and gas in deepwater, b) instruments and methods for monitoring of the deepwater plume, and c) methods for monitoring the surface slick. Feasible solutions to these problems were identified. The study concluded with a plan for conducting field experiments in deep waters in the Norwegian Sea, including work scope, schedule and budget. This plan also formed the basis for the work scope adopted by the oil companies subsequently joining the *DeepSpill* JIP[2].

According to the original plan – a series of four experiments were to be conducted in June 2000 at one out of two optional sites in the Norwegian Sea, both with water depths in the range from 700 m and deeper (Helland Hansen or Ormen Lange). Sites with water depths in the order of, or deeper than 700 m were chosen to provide conditions for hydrate formation. June was chosen due to the high expectancy for favorable wind conditions in that month, while a second (optional) site were proposed to provide an alternative in case of adverse weather conditions at the first priority site. Later, the optional site Ormen Lange that was closest to the shoreline was dropped to minimize the risk for damage to sensitive biological resources and to facilitate the application for discharge permit that had to be submitted to the Norwegian Pollution Control Authority (SFT).

The experiments should be conducted during a three-day field trial – initiated with experimental discharges of nitrogen gas and natural gas in the first day, followed by two experiments with oil and gas during the next two days. The planned sea trial involved two vessels – a supply vessel equipped for transport and discharge of oil and gas, and a research vessel operating an ROV equipped with instruments for subsea monitoring of the plume. In addition, two workboats operated from the supply vessel should be used to monitor the formation of an eventual surface slick. In the actual field trial, a third vessel was added to provide a separate platform for operation of these workboats. Later the experimental schedule was shortened by one day by arranging for one gas experiment and one experiment with oil and gas combined each day. A light crude oil or condensate that was known not to form water-in-oil emulsion was proposed for the first combined oil and gas experiment, while a water-in-oil emulsion forming crude oil was proposed for the second.

The gas was to be transported to the experimental site in liquid state in cryogenic container tanks. The liquefied gas should be pumped through an air-heated evaporator mounted on the vessel and transported as pressurized gas to the seabed in coiled steel tubing. A separate coiled tubing line

[1] Johansen, Ø, 1999: Feasibility Study of a Field Experiment to Study the Behavior of a Deepwater Blowout. SINTEF report, STF66 F00101.44 pp.

[2] Johansen, Ø, 2000: Field Experiment to Study the Behavior of a Deepwater Blowout. Revised February 25, 2000. SINTEF Project Proposal, STF66-99043, 12 pp.

should be used for the oil discharge. According to the feasibility study, the proposed arrangement for transport and delivery of gas and the coiled tubing arrangement could be assembled from readymade and well proven units.

The planned arrangement was used during the actual experiment with some significant modifications. The air-heated evaporator was substituted by a seawater heated unit occupying less space, and the coiled tubing was deployed through the moon-pool (a 4×4 m well in the middle-deck of the vessel), rather than over the stern as indicated in the original plan.

As indicated above, the original plans were further detailed and to some extent modified in the subsequent planning phase. These modifications were to a large extent based on safety considerations put forward at the Technical Advisers Committee (TAC) meetings, or at special HAZOP sessions. Some major modifications were also made in response to recommendations from the various subcontractors participating in the design and conductance of the experiment. The decision to substitute the planned condensate discharge with marine diesel was in the latter category, motivated by the oil pump operator's caution against a potential cavitation problem.

3.2 Discharge permit

The preparation phase of the DeepSpill JIP included the task of preparing an application for discharge permit to be submitted to the Norwegian Pollution Control Authority (SFT). An informal meeting was held at December 15 1999 at SFT's premises in Horten to inform about the planned experiments. SFT told in response that the Norwegian Pollution Control Authority welcomes research and development activities related to deep water oil exploration contingency. However, according to regulations, a permit is required for any experimental release of oil in Norwegian waters. The application for permit had to be delivered 4 months before the start of the planned field trial and would be forwarded to 10-15 organisations for comments. A formal reply from SFT would be forwarded not later than 3 weeks prior to the experimental release. The application had to include the following items:

- Main objectives for the activities involving experimental release.
- Location(s) of the experimental release.
- Oil type, quantity and chemical/ physical/environmental properties.
- Weather and oil drift statistics for the location(s) involved.
- Environmental risk analysis.
- Contingency plan.
- Surveillance plan.
- Reporting.

Accordingly, Norsk Chevron delivered the application to SFT on February 18 2000 on behalf of the DeepSpill JIP. As required by SFT, the application was written in Norwegian with an English summary. The summary is enclosed in Appendix A. A positive reply to the application was received from SFT at May 23 2000, including a list of some specific requirements that had to be met:

1. Spills will take place during week 26, 2000 within the region N 64º 45' to 65º 15' and E 04º 00' to 05º 00'
2. Norsk Chevron will ensure that accidental spills on the way to and within the area do not occur and that each vessel is appraised of warning procedures.

3. Procedures for the mapping of seabirds, including which species are to be found in the area, and numbers. Acceptance criteria for maximum occurrence in potential influence areas will be included in the operation order. Criteria must be given before each single discharge, and for the decision for immediate action against oil on the surface after spills.
4. Acceptance criteria for wave height, visibility and wind speed must be established for each discharge. The criteria must ensure that effective standby measures can be started, that the position and spreading of oil are known at all times and that surface occurrences of oil can be detected by official inspection aircraft.
5. Acceptance criteria must be established for how far and for how long treatable oil can drift before recovery operations are initiated.
6. Before oil spills a procedure must be established to verify that the standby of the Norwegian Clean Sea Association (NOFO) is operative. The following minimum demands apply.
   A: At least one seagoing boom and skimmer system (NOFO) must be on standby in Kristiansund when the spill of condensate/light oil takes place.
   B: At least one seagoing boom and skimmer system (NOFO) must be stored on board a standby vessel in the area and ready for immediate use for 0-6 hours after the spill of emulsifying oil begins.
7. Standby must not be demobilised or leave the area before the SFT surveillance aircraft have confirmed that remaining oil is not recoverable. Flyovers must take place in daylight and good visibility. The costs for these flights will be borne equally between Norsk Chevron and NOFO.
8. Maximum spill volume for each spill must not be exceeded, preferably in that the oil volume over 60 m^3 is not held in the system carrying out the spills.
9. If other types of oil than Oseberg Blend and Sleipner condensate are used weathering data for the chosen oil types must be sent to SFT with the Operation Order.
10. Any fishing vessels in the vicinity of the area must be warned of spill positions.
11. Information regarding the position and start and finish times of trials with oil must be reported to the Coast Directorate, National Coordinator.
12. A report of the trial and results must be sent to SFT and other involved instances (according to the enclosed address list) by 01.09.2000.

Moreover, SFT required a description of how these conditions would be fulfilled as a part of an Operation Order to be sent to SFT by June 19 2000. It should also be noted that SFT requested a report from the field trial by the first of September 2000. This report is later referred to as the Cruise Report.

The Operation Order was delivered by the June 19 as requested by SFT. The Operation Order was written in English with a Norwegian summary, and was made to serve as a common reference document for all units participating in the experiment. Among other things, it included a detailed time schedule for each of the three participating vessels, as well as a description of the acceptance criteria for conductance of the experiments and a description of the oil spill response plans involving oil recovery units from NOFO.

3.3 TAC conferences

The DeepSpill TAC members had frequent meetings during the planning phase of the project – two of these were arranged as workshops – both held at grand Hotel in Oslo, while the others were arranged as telephone-conferences.

The first JIP meeting was held on 30 November 1999 as a telephone conference. At that time, commitments to participation had been received from the US Governmental agency Minerals Management Services (MMS) and four oil companies – Chevron, Conoco, Texaco and Elf. Beside some organizational issues, the major issues of concern at the meeting were the choice of oils in the experiment and the clean-up liability issue. It was agreed that Norwegian crude oils should be used in the experiment, however with the intent of covering a range in oil quality similar to the range observed in the US Gulf of Mexico. Regarding the clean-up issue, SINTEF was told to contact NOFO with the aim of obtaining a stand-by vessel free of charge to the DeepSpill JIP. The TAC also expressed concern about SFT's conditions for discharge permit. Among other things, SFT seemed to require that the data from the experiment should be publicly released. Such a requirement would contradict the intentions of reserving the results from the experiment for the participating parties in the DeepSpill JIP. Chevron's representative was asked to clear up these matters with SFT. As a result, SFT accepted the project's right to keep the actual data from the experiments restricted, but SFT asked to be informed of the more general outcome of the experiments in terms of a cruise report.

The next TAC meeting was held on January 10 2000 as a workshop at Grand Hotel in Oslo. At this time, commitments to participation had been received from two additional oil companies – BP-Amoco and Norsk Hydro. MMS and the six committed oil companies were all represented at the meeting. In addition, five persons participated from the SINTEF project team, supported by four invited experts from companies subcontracted by SINTEF – Argus, Institute of Marine Research (IMR), JM Consult and MARINTEK. Finally, two invited observers were present, one from NOFO and one from the Norwegian Institute for Water Research (NIVA) – representing the CO_2 disposal project. The primary objective of the meeting was to review the experimental plan developed so far by SINTEF, including the issue of stand-by oil recovery vessels. At the meeting, the representative from NOFO expressed strong interests in conducting the planned NOFO oil-on-sea trials at the end of the DeepSpill experiment, thus providing on-scene recovery units free of charge to the experiment. In subsequent meetings set up to clarify the conditions for such an arrangement – NOFO asked to get the right to use data from the experiments for the purpose of verification of an updated NOFO/SFT oil drift forecast model. The TAC finally accepted this condition given that the use of the updated forecast model would be limited to accidental spills or exercises initiated by NOFO or SFT.

The TAC also discussed the issue of an optional experimental site, and decided unanimously to focus on the Helland Hansen site and drop the Ormen Lange site because it was considered too environmentally and politically sensitive.

Another issue of major concern at the meeting was the discharge arrangement for oil and gas. The feasibility of coiled steel tubing for injection of oil and gas was under debate, mainly due to the unexpected expensive skid arrangement required for deployment of the tubing from the stern of the supply vessel. Meanwhile, SINTEF had identified an option based on a geotechnical drilling vessel *Bucentaur*. The alternative plan was to pump oil down the drill pipe and gas down coiled tubing attached to the drill pipe. Even if the hire cost of such a vessel would be significantly higher than of a supply vessel, the use of build-in equipment rather than specially designed units would compensate for the extra cost. As this option would imply significant increases in the costs per day on sea, SINTEF was asked to explore the potential for shortening the experimental schedule without reducing the number of experiments.

Figure 3.1 Picture of the geotechnical drilling vessel Bucentaur.

The next TAC meeting was arranged as a telephone conference on February 16 2000. At that time, the number of participants had increased to 8 including MMS, with one more oil company (Shell) committed to the project. SINTEF presented a revised operational plan with a one-day reduction in time on sea. The new schedule implied a rearrangement of the experiments with one experiment with gas and one combined oil and gas experiment per day in two days. SINTEF also informed the TAC that *Bucentaur* would not be available in the period reserved for the DeepSpill experiment due to unexpected delays in an ongoing drilling project. SINTEF and members of the TAC group had looked for another vessel of the same type, but as no option was available, the focus was returned to the original proposal with coiled tubing deployed from a supply vessel. As a result – a new and less expensive design was launched that utilized the moon-pool located in the middle-deck of the supply vessel for deployment of the coiled tubing.

A second TAC workshop was arranged in Oslo at Grand Hotel on March 30 2000. At that time, written commitments had been received from 17 participants (MMS together with 16 oil companies). Before this TAC meeting, a special two-day safety session (HAZOP) had been arranged in the same hotel on March 16 and 17. This and a second HAZOP was facilitated by experts hired from the Norwegian maritime classification company Veritas (DnV). More details on these sessions are given in the next section. Beside a review on the status of the preparation tasks, the report from the HAZOP session was the major issue at the TAC-workshop. After the review of the HAZOP-report SINTEF was asked to provide estimates of the extra costs involved fulfilling the various recommendations stated in the report. Among other things, the TAC also expressed serious concern about basing the subsea surveillance program on a single ROV, and asked SINTEF to look more closely at getting and using a second ROV.

A revised budget including the costs of implementing the HAZOP recommendations was presented by SINTEF at the next TAC telephone conference on April 14 2000. The budget increases were approved unanimously by the TAC representatives, with the note that additional increases might come with a second ROV. However, as SINTEF had failed to come up with a solution to this problem, the TAC representatives were urged to consult with their European branches to see if they were aware of suitable ROVs. SINTEF would provide the relevant specifications.

At the next TAC telephone conference held on May 30 2000, SINTEF could report that a suitable second ROV had been located thanks to the involvement of the TAC members. At that time, most

of the details were worked out, including cost estimates from the ROV operator. At the same meeting, Chevron reported that the project team had been extended with Bob Watson, serving as project manager for the JIP, while Odd Arne Follum from Norsk Hydro had accepted the role as Response Officer during the sea trial. Moreover – Roger Tailby, an external consultant had been assigned as safety officer in the project. Prior to the meeting, on May 23, a positive reply to the application had been received from SFT. As mentioned above, the permit was given on certain conditions, but none of these were unforeseen or could be showstoppers of any kind.

Another issue of concern at the telephone conference was the report from the second HAZOP session that had been held on May 23 and 24 in Asker outside Oslo.

3.4 HAZOP workshops

The first hazard review workshop (HAZOP) was arranged in Oslo during March 16th and 17th 2000. In total19 people participated at the workshop; 6 from participating oil companies; 4 from SINTEF's project team; 7 specialists from companies sub-contracted by SINTEF including two ship captains; and finally 2 experts from *Det Norske Veritas* (DnV) hired as workshop facilitator and recorder.

It was decided to conduct the workshop at two levels – starting with a high-level review of the operational schedule, followed by more detailed reviews focusing personnel risk (safety review) and risks for loosing experimental results (project risk review). The reviews were based on a tentative operational plan for the experiment, formulated as a timetable with action points. A total of 69 recommendations were recorded from these sessions, of which 33 were reported from the safety review. As could be expected, the majority of the recommendations were related to planning requirements, with much emphasis on fire and explosion hazards caused by introduction of LNG and high pressure CNG on the aft deck of an otherwise ordinary supply vessel. It was concluded that careful planning of the layout of the equipment would be necessary to ensure that the risk of ignition of eventual leaks from these systems could be reduced to a minimum.

A considerable part of the recommendations related to potential causes of project failure ("show stoppers"). The method of deployment of the discharge unit and the arrangement of the coiled tubing on deck of the vessel was a central issue at this stage. Two options were available – one with the coiled tubing deployed over the stern of the vessel, and one with the coiled tubing deployed through a 4×4 meter open well in the centre of the vessel (the moon pool). The participants at the workshop agreed that both options were feasible, but the final decision was in favour of the moon pool option. This was partly because the moon pool option was the simplest solution from a design point of view (no need for special skids to move the arrangement to operating position), and partly because the coiled tubing would be more exposed to heave when deployed from the stern of the vessel. However, some uncertainties existed as to whether the relevant authorities and DnV (the maritime classification company) would approve the moon pool option. Subsequently, as informal requests indicated that this would be the case, the moon pool option was chosen as the basis for further planning.

The risk of loosing critical measurements was another important issue at the workshop – particularly the risk related to potential ROV failure. At that time, the current plan included two ROVs, but the availability of ROVs with the required specifications (particularly with respect to length of umbilical) was limited. Based on operational experience, some participants urged for a second ROV to be brought along for the experiment, either as spare – or with both to be used operationally. Out of the total package of instruments planned to be used for subsea monitoring

during the experiment, the ROV was identified as the most critical "single point of failure" that could possibly result in failure to reach the project objectives. However, due to the difficulties in getting hold of a second ROV, it was agreed that the possibility of having to run the experiment with one ROV only had to be taken into account in the operational plans. At the same time, the SINTEF team, as well as the JIP members were urged to continue the search for a second suitable ROV.

Subsequently, persons in charge were appointed to each of the recommendations to assure that the appropriate actions were taken, either in terms of more detailed planning, documentation or development of operational procedures.

A second HAZOP was arranged in Asker outside Oslo May 23 and 24 2000. This time, 17 people participated at the workshop. Four participants – including the newly appointed project manager from Norsk Chevron (Bob Watson) and the safety officer appointed directly by the TAC (Roger Tailby) represented the JIP. As last time, four from the SINTEF project team were present, supported by seven experts from subcontracted companies – including two from an ROV company that would operate the second ROV that finally had been secured for the experiment. Finally, as at the previous HAZOP workshop – two experts from DnV were serving as facilitator and recorder.

The main objective of the second HAZOP was to review the status of risk reducing activities recommended at the first HAZOP. In addition, the 2nd HAZOP should focus on procedures for deployment and retrieval of the discharge unit and for discharges of gas and oil during the four planned experiments, with special focus on issues related to personnel safety.

Most of the recommendations were at that time in progress, already closed or made unnecessary by alterations of plans. The newly appointed project manager together with the safety manager were in the process of gathering relevant operational procedures and documentation in a Quality Plan, and to collect safety related procedures in a Bridging document. A second ROV that could operate safely from the discharge vessel had been identified and secured for the project, and IMR had offered a second research vessel (*Johan Hjort*) that would make room for SINTEF's oil chemists with their laboratory container and serve as platform for sampling boat operations.

However, some new and important safety issues were brought up as a result of the workshop:

- The planned mobilization schedule for the discharge vessel in Stavanger would be too tight.
- More rest time would needed between the deployment operation in the evening after arrival on site and start of the first experiment next morning.
- To avoid that potential hydrate blockage of the gas line should be a showstopper, the most risky experiment in such terms (i.e. the LNG discharge) should be moved to the end of the field trial.
- The operator of the high-pressure oil pump (Schlumberger) could not recommend pumping of condensate due to risk of vapour formation on the suction side of the pump (cavitation).

Subsequently, the first two issues were solved by arranging for an earlier arrival of the discharge vessel in Stavanger and by rearranging the sailing plans for two of the vessels. The planned intermediate stop in Kristiansund on the way to the experimental site was skipped *for Håkon Mosby* and *Far Grip*. For this reason the LNG had to be transported by truck container all the way from the LNG plant at *Tjelbergodden* near Kristiansund to Sotra outside Bergen – a distance of about 500 km. Finally, the TAC decided to move the LNG experiment to the end of the sea trial

as recommended by the HAZOP, and to use marine diesel as a replacement for the planned condensate discharge.

The replacement of condensate by marine diesel also contributed to the demanded extension of mobilization time and to enhanced safety. Marine diesel could be loaded where the vessel filled bunker oil, and the planned stop at the *Kårstø* gas terminal for filling condensate could be skipped. Secondly, as marine diesel could be stored in the vessels oil-recovery tanks, the in-built methanol tanks that were originally reserved for storage of condensate could now be used for the crude oil, and the mobile container tanks to be mounted on decks for storage of crude oil could be skipped. In this way, a safest possible compartment for storage of crude oil was found, and at the same time, valuable deck space was made free on an otherwise crowded deck.

4 DISCHARGE EQUIPMENT AND LOGISTICS

4.1 Participating units

The sea trial as such involved three vessels – the supply vessel *Far Grip* from Farstad Shipping and the two research vessels *Johan Hjort* from Institute of Marine Research (IMR) and *Håkon Mosby* from University of Bergen (UiB) (see Figure 4.1). The overall length of the supply vessel (*Far Grip*) was 74.5 meters, while the corresponding dimensions of the two research vessels (*Johan Hjort* and *Håkon Mosby*) were 65 meters and 47 meters respectively. Two workboats were used to collect samples of surface oil and monitor the water column under the slick. *Johan Hjort* carried one of the workboats, while the second workboat was carried by *Far Grip*. A total of 43 scientist, specialists and JIP representatives participated on the three vessels, with 17 on Far Grip, 12 on Håkon Mosby and 14 at Johan Hjort (see Appendix B for a complete list of participants).

By coordinating their annual oil-on-sea trial with the DeepSpill project, the Norwegian Clean Sea Association (NOFO) provided the demanded oil spill response capability for the DeepSpill experiment. NOFO's oil-on-sea trial involved three oil recovery vessels and two towing vessels. As planned, the recovery units started to arrive at the experimental site in the evening of June 28, with the aim of conducting the NOFO trials in the morning of June 29. However, due to adverse weather conditions, the NOFO trials were postponed to the day after, and finally canceled as the conditions at the site were judged to be unsuitable for the planned tests. However, when it was decided to conduct the crude oil experiment the following day, the NOFO vessels stayed on site until it was found acceptable to leave the remaining oil slick without any attempt of recovery.

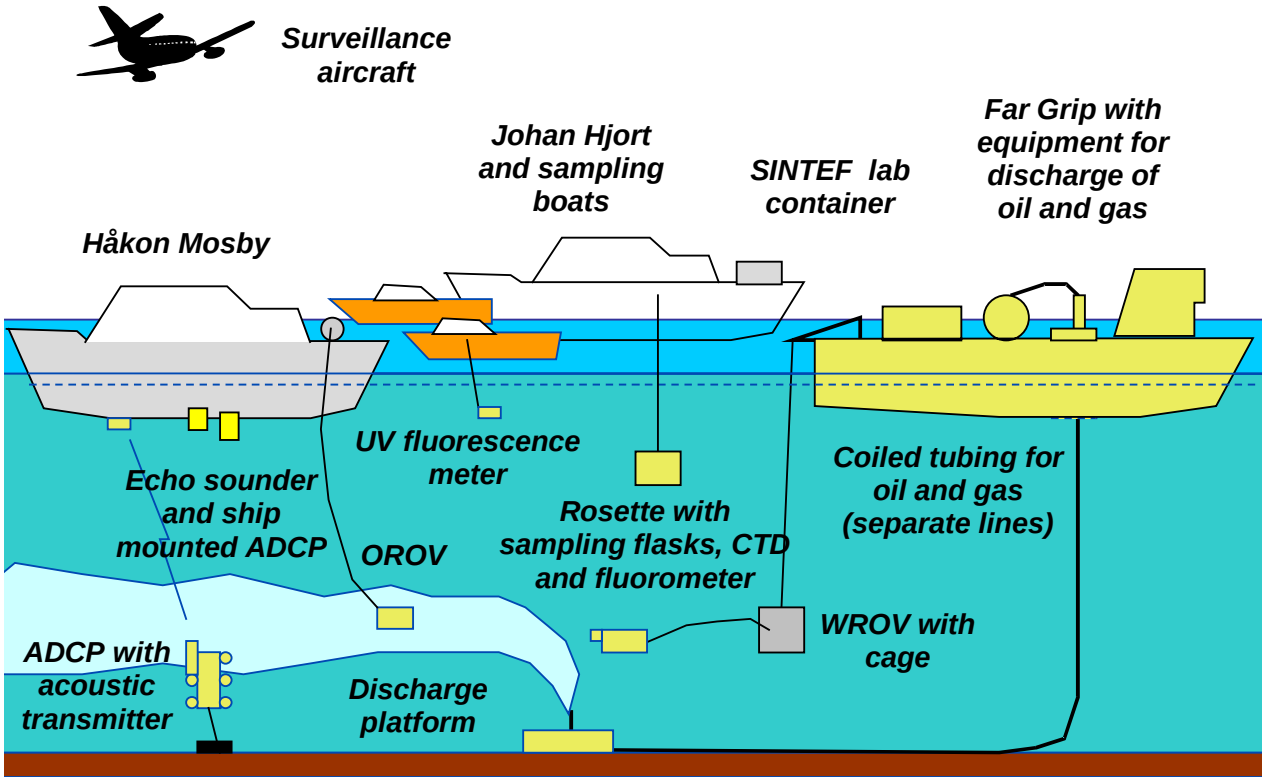

Figure 4.1 Schematic oveview of participating units at the DeepSpill experiment.

In addition, 7 airplanes from different North Sea countries were involved in aerial surveillance of the oil slicks. A dedicated flight commander was stationed at the Kristiansund airport to organize this activity and secure videotapes and pictures taken during the flights. More details on the tasks of the participating vessels are given in the next sections.

4.1.1 Far Grip

The hire of *Far Grip* started when it sailed from Mongstad Wednesday June 21 at 0500 Norwegian Local Time[3] (NLT) for transit to the ASCO Base in Tananger (see map at Figure 4.2). After a short stop at the CCB base at Ågotnes, Sotra for bunkering fuel oil, the vessel arrived in Tananger at 2300 NLT to make the vessel ready for the sea trial. The 60 m^3 of marine diesel to be discharged in the experiment was also loaded during the stop at the CCB base.

Figure 4.2 Sailing route for Far Grip to the experimental site (Helland Hansen). The vessel was chartered at Mongstad and sailed to Stavanger to mobilize equipment and personnel. Next stop was at Sotra outside Bergen to load crude oil and LNG.

[3] Norwegian Local Time – referred to as NLT in the following – corresponds to UTC + 2 hours in summer.

The work at the ASCO-base involved loading, installation and sea fastening of the work ROV (WROV) with related equipment, as well as various heavy equipment designed for discharge of oil and gas (Figure 4.3). Besides - the liquid nitrogen tank was filled from a truck tank in this harbor. In addition to the installation and sea fastening crews, key personnel from the DeepSpill project were present on the vessel to supervise the installation work. An inspector from the classification company Norske Veritas (DnV) came onboard on the afternoon of Friday June 23 to conduct a final inspection/approval of the installations before the vessel could leave Tanager.

The ASCO base was left Friday June 23 at 2240 NLT for transit to the CCB base at Ågotnes, Sotra. The vessel arrived there in the morning of Saturday June 24 for loading the 60 m^3 of crude oil and 18 m^3 of LNG to be discharged in the experiments. Two tank trucks that had been filled at the Sture oil terminal delivered the Oseberg Blend crude oil, while the LNG was delivered with a cryogenic tank truck filled at the *Tjelbergodden* gas plant near Kristiansund.

The vessel departed the CCB base practically on schedule at 1645 NLT the same day for transit to the Helland Hansen site. *Far Grip* arrived at the planned site Sunday June 25 at 1855 NLT – delayed about three hours relative to schedule due to unexpected heavy northerly winds.

Figure 4.3 Far Grip on transit from Tananger to Sotra.

4.1.2 Håkon Mosby

The Aglantha observation ROV (OROV) with related equipment was loaded onboard *Håkon Mosby* at *Marineholmen* harbor in Bergen Saturday June 24. When the SINTEF personnel and the JIP observers had been embarked, the vessel moved to *Nykirkekaien* harbor to load the current meter instrument (ADCP) with mooring, and ropes and wire for the deployment operation. After a safety rehearsal, *Håkon Mosby* left Bergen the same day about 1700 NLT for transit to the experimental site (Figure 4.4). The vessel arrived on the experimental site Sunday June 25 at 1945 NLT – about 4 hours after schedule – a delay mainly caused by the above mentioned unexpected heavy northerly winds.

Figure 4.4 Picture of research vessel Håkon Mosby *arriving at the experimental site.*

Figure 4.5 Picture of research vessel Johan Hjort *arriving at the experimental site.*

4.1.3 Johan Hjort

Johan Hjort left Bergen harbor Thursday June 22 at 2100 NLT for transit to Helland Hansen to conduct a biological survey in the experimental area. The vessel arrived in the experimental area Friday June 23 at 2400 NLT . An ornithologist from the Norwegian Institute of Natural Research (NINA) participated on this survey to make the sea bird observations required by the spill permit. *Johan Hjort* reported to the cruise commander on *Far Grip* at 1700 NLT Saturday June 24 and was granted 3 extra hours on site before leave to Kristiansund.

The research vessel left the experimental area Saturday June 24 about 2000 NLT to pick up SINTEF's laboratory container, SINTEF personnel and JIP observers in Kristiansund. *Johan Hjort* arrived there the next morning at 0945 NLT and departed at 1700 NLT the same day to join the two other vessels at the experimental site (see Figure 4.5 and 4.6). Reported time of arrival at the experimental site was Monday June 26 at 0800 NLT.

Figure 4.6 Work boat in front of Far Grip (front left) and Johan Hjort (front right), with one of the oil recovery vessel behind.

4.2 Transport and delivery of gas and oil

As mentioned above, *Far Grip* served as discharge vessel and carried all equipment for transport and delivery of oil and gas. An overview of the major special arrangements made for this purpose on *Far Grip* is shown at Figure 4.7. Figure 4.8 shows a picture of the cryogenic pump and evaporator for delivery of natural gas and nitrogen. Figure 4.9 shows a picture of the coiled tubing arrangement, and a close up of the discharge platform mounted in the moon pool is shown at Figure 4.10.

4.2.1 Gas supply system

The gas supply system was designed and operated by specialists from the Norwegian Marine Technology Research Institute (MARINTEK)[4]. Some of the major components of the system was made specially for the project, including the 3 cylinder reciprocating cryogenic pump designed for

[4] A more detailed description of the cryogenic system is found in MARINTEK Report MT23 F00-229: *DeepSpill JIP – Design of Gas Supply System*, Trondheim August 2000.

delivery of 100 L/minute of liquefied gas, and the high pressure evaporator, both manufactured by the German cryo-technical factory *Krytem GmbH* in *Willich*. To assist during the assembly and testing phase, two specialists from *Krytem* boarded *Far Grip* during mobilization in Tananger and stayed onboard until the vessel arrived at the CCB base at Sotra outside Bergen for loading of LNG and crude oil. After these specialists left the vessel, two experts from MARINTEK was in charge of the operation of the system.

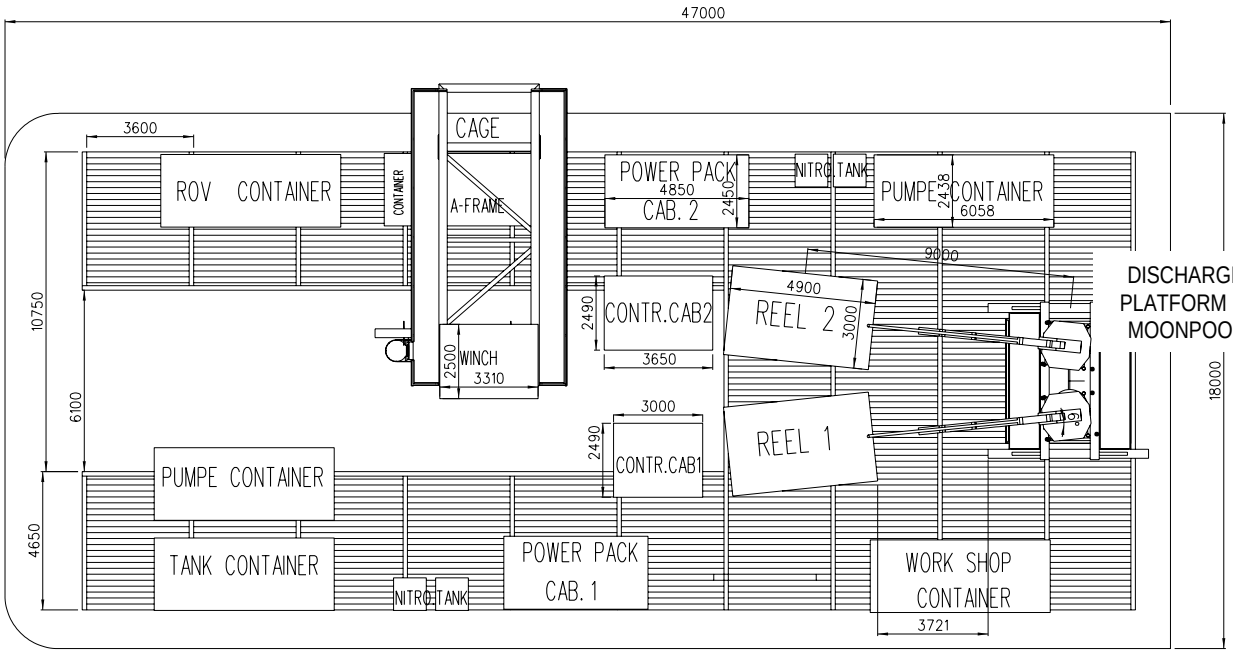

Figure 4.7 Sketch of aft deck of Far Grip showing placement of discharge equipment

Top left to right:
The ROV CONTAINER is the control cabin for the ROV. Next comes the platform installed for the ROV, supporting the WINCH and the AFRAME used for launching of the CAGE with the ROV. The maintenance CONTAINER for the ROV is placed below the platform. Next comes the hydraulic POWER PACK for the portside coiled tubing unit, a packet of pressurized NITROGEN flasks, and the PUMP CONTAINER with the high-pressure pump powered by a diesel engine.

Middle left to right:
CONTROL CABINS 1 and 2 for portside and starboard coiled tubing reel (REEL 1 and 2) followed by the support frame for the injectors mounted on top of the moonpool (a 4x4 meter well in the deck). The DISCHARGE PLATFORM is located in the moonpool during transit.

Bottom left to right:
TANK CONTAINER for transport of liquefied gases (LNG and LIN) and PUMP CONTAINER with the cryogenic pump and the seawater heated evaporator. Next comes a second package of pressurized nitrogen flasks, followed by the POWER PACK for the starboard coiled tubing unit, and the WORKSHOP CONTAINER for maintenance of coiled tubing system.

Below deck:
The 60 m^3 of crude oil to be discharged in the experiment was stored in the methanol tank located under the aft deck, while the same volume of marine diesel was stored in one of the combined bunkers and oil recovery wing tanks. Onboard pumps fitted to these tanks were used to feed oil to the high-pressure pump.

The two cryogenic storage tanks for Liquefied Natural gas (LNG) and Liquefied Nitrogen (LIN) were also mounted on Far Grip during the mobilization in Tanager. Each tank had a filling capacity of 16 m^3 and a design pressure of 10 bars, and were delivered from Rotterdam by a tank container leasing *specialist Taylor Minster Leasing Ltd*. The LIN tank was filled in Tanager to provide liquid for testing of the cryogenic system, while as mentioned before, the LNG tank was filled at the CCB base at Sotra outside Bergen with LNG transported by a cryogenic tanker truck from the *Tjelbergodden* gas processing plant outside Kristiansund.

Figure 4.8 Far Grip *in Tananger. Sea fastening of LIN and LNG tanks with pump unit and evaporator.*

4.2.2 Storage and pumping of oil

The oil supply system included the following main components:

- A high-pressure positive displacement pump powered by its own diesel-hydraulic unit.
- A built in 121 m^3 methanol tank with inert gas system (N_2) used for storage of crude oil.
- A combined oil recovery and fuel oil wing tank used for storage of marine diesel.

The crude oil was fed to the high-pressure pump by a low-pressure pump in the methanol tank, while one of the vessels fuel oil pumps were used as feed pump for the marine diesel oil.

4.2.3 Coiled steel tubing and discharge platform

The coiled steel tubing (CT) package that was provided by Schlumberger consisted of the following main components:

- Two CT injectors with goosenecks. Pulling capacity approximately 50 tons each.
- Two reels with 1200m CT with outer diameter 2 7/8” (ID 2 ½ ”), one line for oil and one line for gas.
- Two control cabins w/ hydraulic power packs.
- One workshop container.
- High-pressure piping w/ flexible couplings to connect the reels and pumps.

As there would be no need for spooling in or out during the experiments, the high-pressure piping was connected direct to the reel drum, bypassing the swivel coupling.

The injectors were placed over the moon-pool of the discharge vessel, supported on a specially designed frame (see Figure 4.9). The coiled tubing were connected to the discharge platform by short sections of armored rubber hoses with swivel couplings in-between to remove torsion stresses from the coiled tubing (see Figure 4.10). Two steel chains were mounted between the swivel couplings and the discharge platform to relieve the tensile load on the rubber hoses. The rubber tubes fed oil and gas into a manifold with a vertical exit section (120 mm internal diameter) where the two fluids mixed (oil on the outside, gas on the inside). The discharge platform with a total weight of about 4000 kg was only suspended in the coiled tubing during deployment and recovery. However, in order to avoid twisting of the tubing, a horizontal towing line was connected to the research vessel *Håkon Mosby* during these operations (Figure 4.11). The towing line was dropped to the seabed after deployment and brought up to the surface by a float ball connected to an acoustic release mechanism before recovery of the platform.

Figure 4.9 View of main deck on supply vessel Far Grip during mobilization at the ASCO base in Tananger. Reels with coiled steel tubing, goose necks and injector heads seen from the rear of the vessel.

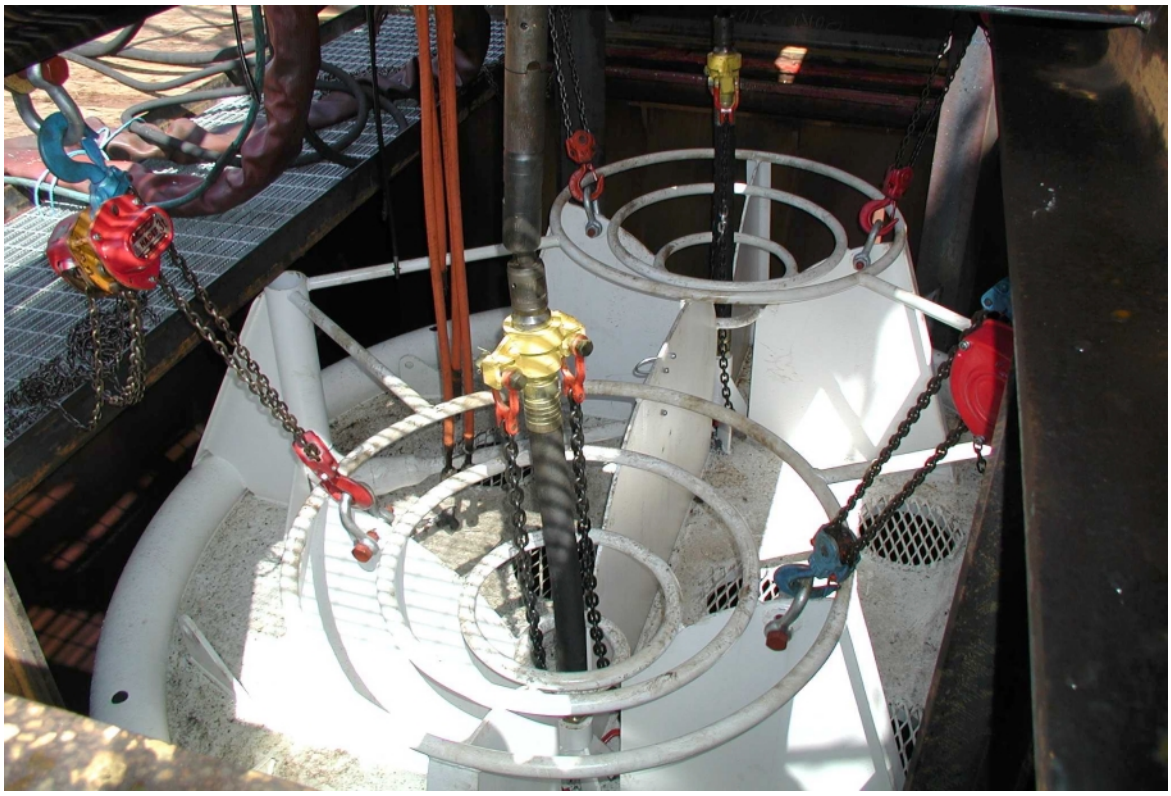

Figure 4.10 Far Grip *in Tananger. Picture of discharge platform secured by chains in the* 4×4 *meter moonpool.*

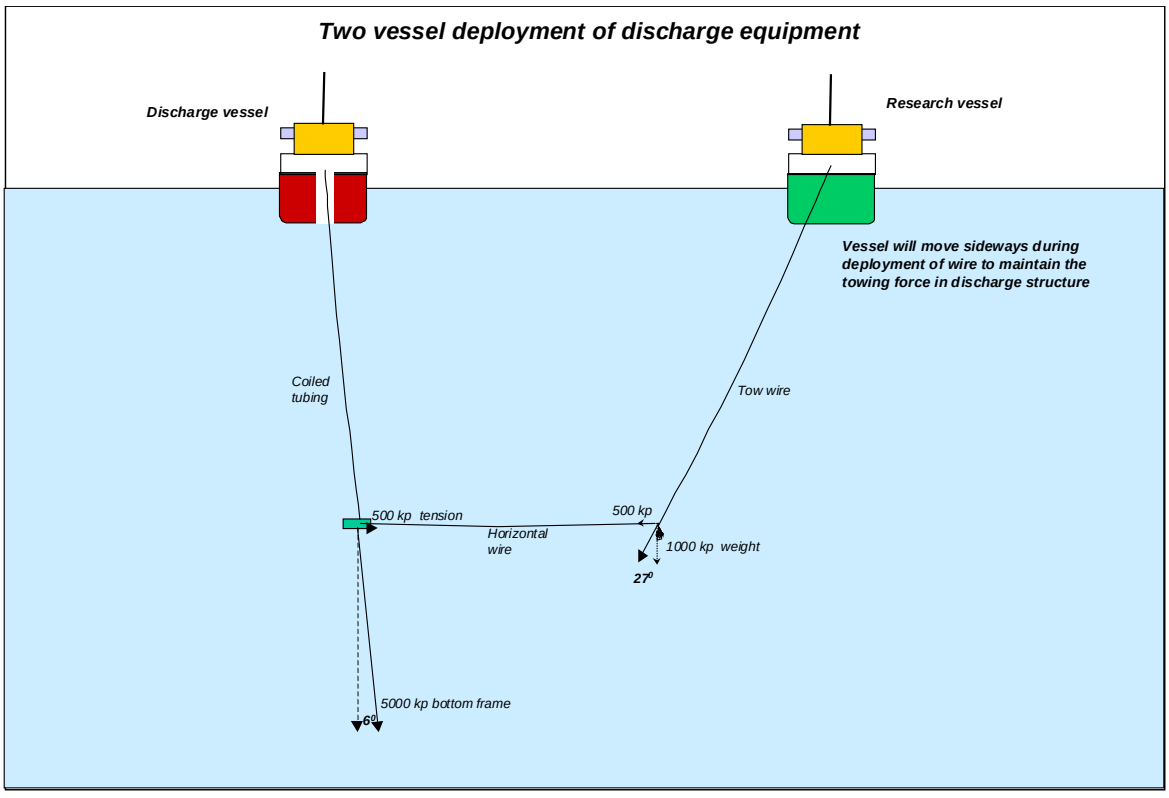

Figure 4.11 Sketch of the arrangement used for deployment of the discharge platform.

4.3 Field Operations

While the field operations are described in detail in the DeepSpill Cruise Report, only a brief chronological summary of the major events is presented here (see table 4.1), together with an overview of the timing of the different experiments (see Figure 4.13). For later reference, the discharge conditions at the four experiments are listed in Table 4.2, while the relevant properties of the discharged fluids are given in Table 4.3.

Table 4.1 Overview of field operations. Note that time is given in Norwegian Local Time, corresponding to UTC + 2 hours in summer.

Date	***Local time***	***Event***	***Comments***
June 21	0500	Supply vessel Far Grip on charter	Far Grip departs Mongstad on transit to the ASCO base in Tananger for mobilization.
June 22	2100	Research vessel Johan Hjort departs from Bergen harbor.	Johan Hjort heading for experimental site to conduct biological survey prior to experiment.
June 23	2400	Johan Hjort arrives in the experimental area	Reports to Far Grip one hour later
	2240	Mobilization in Tanager finished on schedule	Far Grip heading for the CCB base at Ågotnes, Sotra.
June 24	1645	Loading of crude oil and LNG finished on schedule	Far Grip heading for experimental site
	1700	Mobilization of Håkon Mosby finished on schedule	Håkon Mosby heading for experimental site
	2000	Johan Hjort departs experimental area temporarily	Johan Hjort heading for Kristiansund to pick up SINTEF crew and equipment
June 25	0945	Johan Hjort arrives Kristiansund harbor	JIP observers, SINTEF personnel and lab container loaded on Johan Hjort
	1700	Johan Hjort departs Kristansund	
	1855	Arrival of Far Grip in the experimental area	Vessels arrived about three hours after schedule due to strong Northernly winds
	1930	Arrival of Håkon Mosby	
	1930	Work ROV launched from Far Grip to inspect sea bed	Depth 844 m – sea bed consisted of clay with a few cm thick soft top layer.
	2345	Start of deployment operation	Transfer of tow wire from Far Grip to Håkon Mosby
June 26	0230	Discharge platform at sea bed	Discharge platform deployed through moon pool on Far Grip with assistance from Håkon Mosby. Visual observations made with WROV during deployment.
	0300	Deployment operation finished 3 hours after schedule	Håkon Mosby deployed tow wire, rope and acoustic release with floats for later retrieval.
	0430	Håkon Mosby deploys ADCP on sea bed	Contact problems reported with ADCP.
	0800	Johan Hjort back in experimental area	Vessel arrives with JIP observers, SINTEF personnel and equipment picked up in Kristiansund

Date	*Local time*	*Event*	*Comments*
	1650	Far Grip starts preparations for discharge of nitrogen and dyed seawater	Communication problems with ADCP and entanglement of OROV caused delayed start of the first experiment.
	1810	Liquid nitrogen pumped at full rate	Temporary problems with power supply to high pressure sea water pump
	1947	First experiment finished	Nitrogen pumped for two hours with variable rate due to temporary overheating problems with power generator for the high-pressure sea water pump. Due to the serious delay of the first experiment – the marine diesel discharge was postponed until next morning.
June 27	0620	Preparations for marine diesel experiment started	OROV launched from Håkon Mosby. Problems with the video transmission lines were reported shortly after and the ROV had to be recovered due to damaged video cable.
	0838	Full rate pumping of diesel and LNG	Experiment commenced after some minor problems with high-pressure pump.
	0930	All pumps stopped - discharge finished	Experimental discharge of marine diesel and LNG conducted successfully.
	0935	Oil spotted on sea surface	Workboats from Johan Hjort starts monitoring surface slick
	1012	First aircraft on site	SFT's surveillance airplane first on site – followed by airplanes from Germany, France, Denmark, Netherlanss and UK.
	1230	Workboats return to Johan Hjort due to adverse sea conditions	Next experiment postponed due to adverse weather conditions
	1800	NOFO oil recovery vessels starts to arrive on site	Oil recovery vessel (ORV) Northern Commander arrives at 1800, ORV Troms Skarven arrives at 2200, and ORV Far Sun comes later in the night..
June 28		Experiments postponed until next day	Adverse sea conditions prohibits launching of workboats and ROV's. All surveillance airplanes, except the SFT aircraft leave site. NOFO oil recovery vessels determined to wait for crude oil discharge.
June 29	0345	Preparations started for conducting crude oil discharge from 0600	Sea conditions declared acceptable for conducting crude oil discharge
	0510	Sea conditions prohibits deployment of WROV	ROV observations could not be made during crude oil discharge.
	0714	Crude oil experiment started	Crude oil pump started. LNG and crude oil pumped at full rate at 0723
	0810	LNG and diesel discharge stopped	Cryogenic pump switched to LIN. Marine diesel supply exhausted.
	0821	Crude oil reported on sea surface	Surface slick monitored by workboat from Johan Hjort. The MOB boat from Far Grip could not be launched due to sea conditions (swell).
	0950	SFT aircraft on site	Guiding workboat
	1047	Starting preparations for experiment #4, discharge of LNG and sea water.	Pumping LIN. WROV going down to discharge platform to observe plume and gas bubbles.
	1108	Full rate LNG	Last experiment started
	1247	LNG discharge stopped	End of last experimental discharge

Date	*Local time*	*Event*	*Comments*
	1420	Recovery of discharge platform started	Far Grip assisted by HåkonMosby
	1625	Far Grip and Håkon Mosby depart experimental site	SFT aircraft has declared slick not recoverable
	2000	Johan Hjort departs site	Heading for Kristiansund
June 30	0500	Far Grip arrives Kristiansund	Unloading power pack for high pressure pump
	0950	Johan Hjort arrives Kristiansund	Unloading laboratory container and SINTEF personnel
	1300	Johan Hjort departs Kristiansund	Heading for Bergen
	0830	Håkon Mosby arrives in Bergen	Unloading OROV
July 01	0825	Far Grip arrives in Tanager	Unloading equipment and cleaning oil tanks
	0830	Johan Hjort arrives in Bergen	Cruise finished for IMR
July 02	0150	Far Grip departs from Tanager	Heading for Mongstad
	1400	Far Grip arrives in Mongstad	End of charter

4.3.1 Experimental discharges

A description of the four discharges is given in Table 4.2. As indicated, the discharge rates of both oils and seawater were 60 m^3/hour. The chosen discharge rate of 60 m^3/hour corresponds to a release rate of 1440 m^3/day. Such a release rate will not be too far from a realistic spill situation. Moreover, the same release rates were used during the experimental subsea discharges released from 100 meters depth in the North Sea in 1995 and 1996.

The discharge rate of gas was planned to be 1 Sm^3/s, but the nominal rates varied between 0.6 and 0.7 Sm^3/s due to an error in the set up of the cryogenic pump regulator. For this reason, the volume of gas remaining before the last experiment was greater than planned, and consequently, the last discharge were extended in time (from one hour to two hours).

In all experiments with oil and gas, the fluids were discharged in a certain sequence to avoid or reduce the risk for blocking of the lines with hydrate. The pumping sequences were initiated with nitrogen gas together with seawater, then switching from seawater to oil and then from nitrogen to methane. At the end of the discharge period, the nitrogen was replacing methane, and then oil by seawater before closing off the pumps. The length of each of these periods varied from one experiment to the other for different reasons (start up trouble with the pumps etc.), but the actual pumping sequences are depicted in Figure 4.13.

The physical properties of the discharged fluids are given in Table 4.3, while the boiling point curves for the two oils are given in Figure 4.12. The distillation data for Oseberg Blend is taken from the Crude Assay issued by Statoil February 1997, while the corresponding data for marine Diesel is taken from a study made by the SINTEF Petroleum Research in 1991.

Table 4.2 Discharge conditions during oil and gas experiments. All discharges were released from an exit pipe with 120 mm internal diameter with an exit temperature close to the sea temperature near the sea bed (about 0 °C).

Experiment	*Start (local time)*	*Duration*	*Gas rate*	*Water/Oil Rate*
Nitrogen gas and dyed sea water	June 26th, 18:05	40 minutes	0.6 Sm^3/s	60 m^3/hour
Marine diesel and LNG	June 27th, 08:20	60 minutes (oil)	0.6 Sm^3/s	60 m^3/hour
Crude oil and LNG	June 29th, 07:15	60 minutes (oil)	0.7 Sm^3/s	60 m^3/hour
LNG and sea water	June 29th, 11:05	120 minutes	0.7 Sm^3/s	60 m^3/hour

Table 4.3 Properties of discharged fluids

Fluid	*Content*	*Density at 1 atm, 15 °C*	*Viscosity*
Nitrogen gas	N_2	1.17 kg/m^3	
LNG	99% (min) CH_4, rest C_2H_6 and N_2	0.67 kg/m^3	
Marine Diesel	Marine Gasoil	854.8 kg/m^3	3.9 cP at 13 °C
Oseberg Blend	Mixture of crude oils	842.5 kg/m^3	84 cP at 10 °C

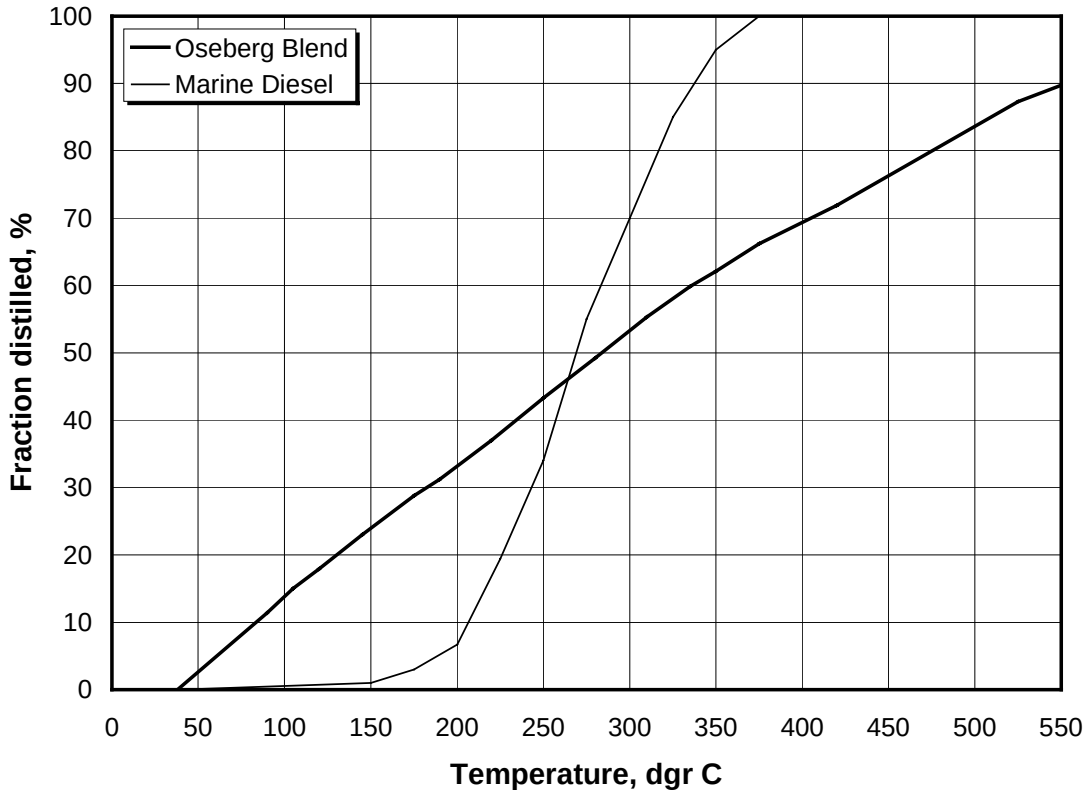

Figure 4.12 Boiling point curves for the two oils discharged in the experiment – Marine Diesel Oil and Oseberg Blend Crude. Volume fraction distilled vs. boiling point.

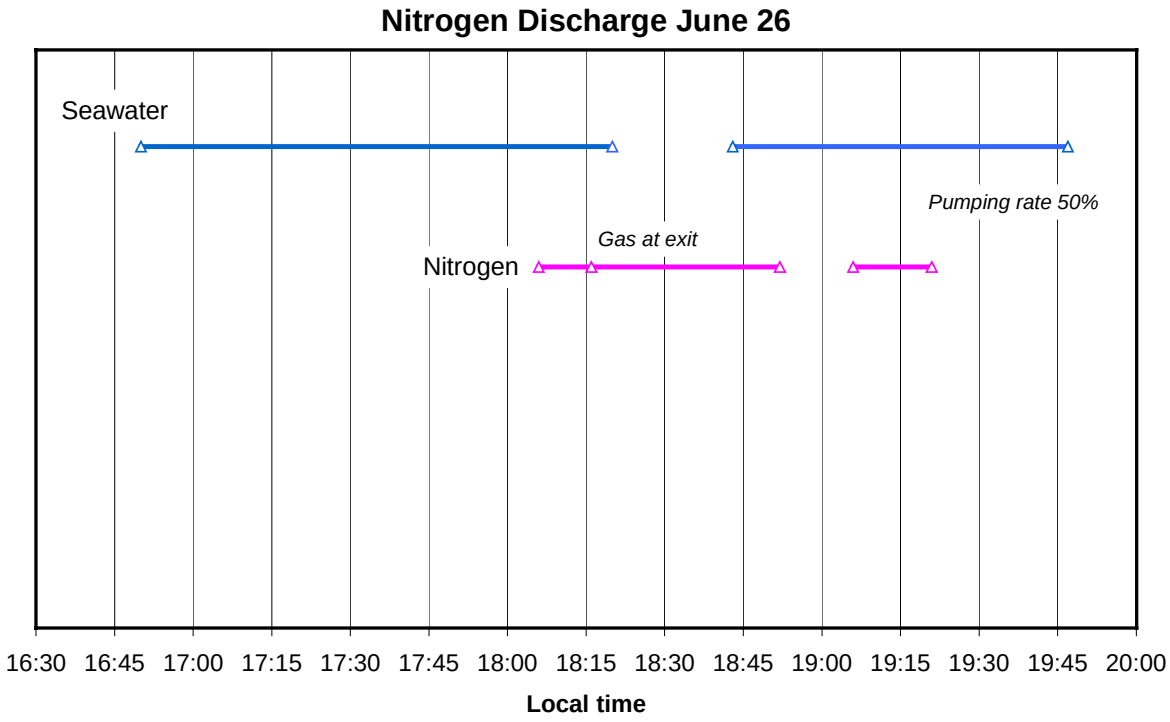

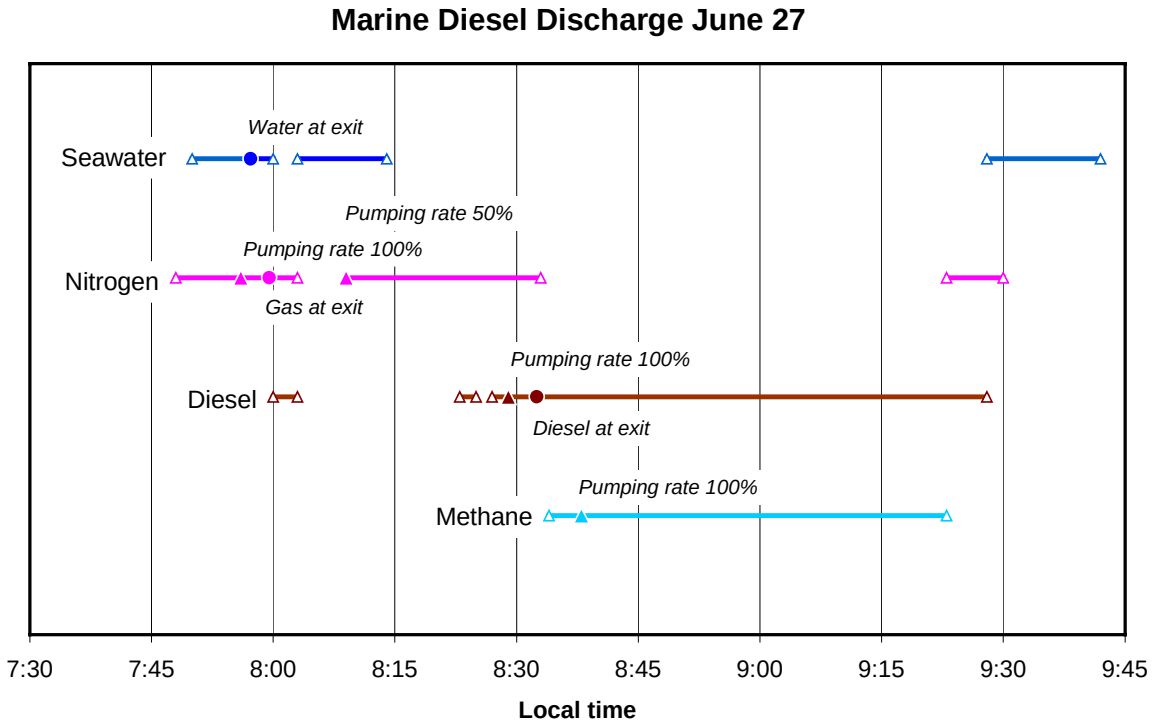

Figure 4.13 Timing of the gas and oil discharges. The bars indicates when pumping of the different fluids took place. Continued on next page.

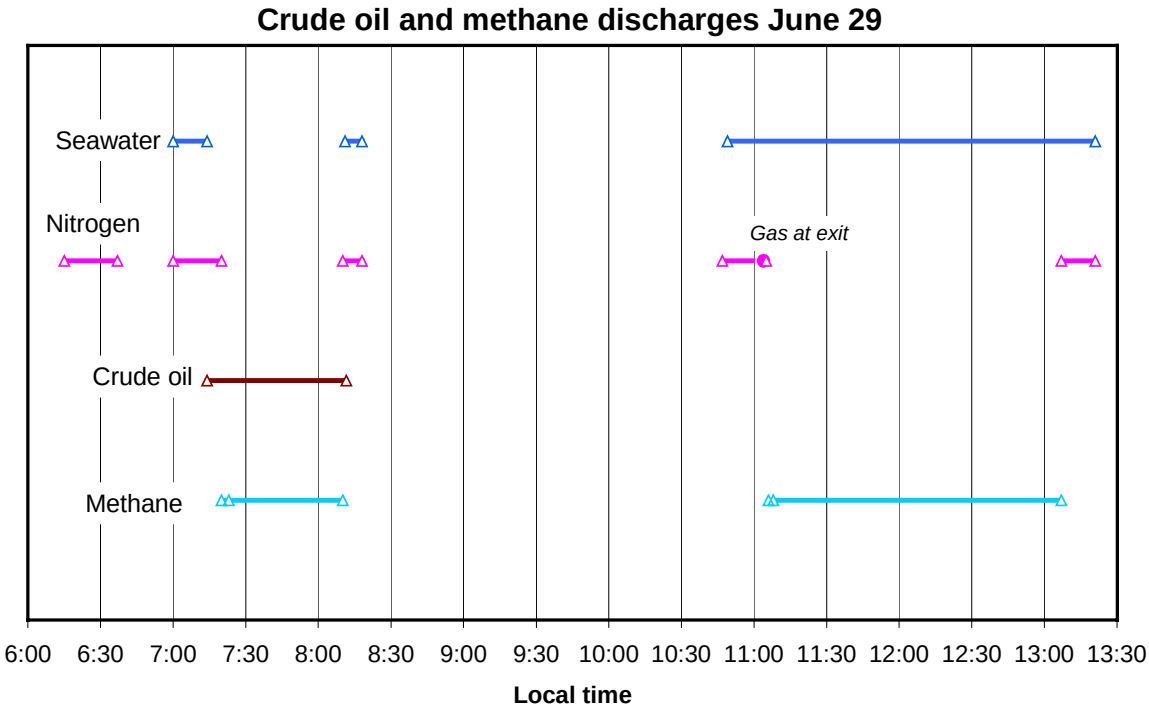

Figure 4.13 continued. *Timing of experimental discharges. The bars indicates when pumping of the different fluids took place.*

5 MONITORING INSTRUMENTS AND SAMPLING EQUIPMENT

5.1 Instruments operated from ROVs

5.1.1 Observation ROV

The observation ROV (OROV), owned by the University of Bergen and operated by Argus AS, was used as a platform for instrumentation capable of studying the plume formation, droplet sizes and water sampling. Table 5.1 gives an overview of the specifications of the OROV, and the OROV is shown on Figure 5.1

Table 5.1. Specifications of OROV

Weight	700kg
Maximum depth	2000m
Thrusters	3 hp each
Speed	Max. 2.5 knots forward and sideways Max. 1.5 knots vertical
Potential payload	Variable, 10kg (+\-5) at 2,000m, more at shallower depths Fixed payloads 150 kg
Cable	3 power leads 6 optical fibres Negatively buoyant except last 100m
Power	12kW 3 phase 1000V, 50-60Hz
Lighting	White flash, continuous red dark field illumination 2 macro ranges: 1:2 & 1:10 Oblique white light for distance work
Cameras	6 cameras Broadcast quality 3xCCD video + zoom lens
Add-ons	Robot arm

Figure 5.1 Observation ROV (OROV) on deck of R/V Håkon Mosby prior to deployment

Fluorimeter for Hydrocarbon detection
A fluorimeter for detection and quantification of oil components in water was attached to the OROV, and interfaced to the OROV's digital interfacing system. The fluorimeter, UVAQUAtracka, is a proven instrument delivered by Chelsea Instruments Ltd. The instrument is tested for depths up to 2,000 m, and has a minimum detection level of 10 ng/L (for Carbazole). Figure 5.2 shows the instrument.

Figure 5.2. The UVAQUAtracka fluorimeter

Fluorometer for Rhodamin detection
A fluorometer from Seapoint Sensors Inc., was mounted on the OROV for detection of dissolved Rhodamin in water. The sensor was interfaced via the CTD on the OROV. The minimum detection level of Rhodamin was 20 ng/L.

Figure 5.3. The Rhodamine fluorometer

CTD

The OROV was equipped with a CTD from SAIV environmental sensor and systems A/S for measurement of conductivity, temperatures and depth. The rhodamine fluorometer was interfaced to this CTD. The specifications for the CTD are given in Table 5.2, and the instrument is shown in Figure 5.3.

Table 5.2. Specification of CTD

Conductivity (inductive cell)	0-70 ms/cm
Salinity	Calculated from conductivity, temperature and depth
Temperature (thermistor)	2°C ± 40°C
Pressure (Piezo resistive)	Up to 6 000 meters

Figure 5.3. The CTD

Methane sensor

The METS methane sensor, delivered by ADS Sensortechnik GmbH was mounted on the OROV for detection and semi-quantification of dissolved methane in the water phase. The sensor was interfaced to the OROV´s digital data transfer system. The sensor has a sensitivity of approx. 20 nmol/l (methane in water). The METS sensor is shown in Figure 5.4.

Figure 5.4. The METS methane sensor

Video cameras (standard)
The standard video cameras mounted on the OROV were planned to visually detect the plume of oil and gas, both in the near-zone and downstream of the discharge.

Macro video camera
A macro video camera for close-up details of oil droplets, gas bubbles and transition to hydrate was mounted on the OROV. The camera was equipped with an enlightened slit with an attached ruler, to enable an image analysis of the droplet size distributions of oil and gas bubbles.

Sonar
The OROV was equipped with 675 KHz sonar for detection of the plume of oil and gas. The vertically mounted sonar was planned for imaging of cross sections spaced at 10-m intervals along the plume centreline from the depth of trapping.

Water sampler
The OROV was equipped with a water sampler (multiple flasks), to sample water from different locations downstream of the discharge point. The results were planned used to post-calibrate the data from the fluorimeter. The water sampler skid was especially designed to fit the Aglantha OROV.

Field experience
The OROW failed to give any meaningful data during the field trial. The reasons for this were:

- Too low thruster capacity to withstand drag forces on the umbilical from the ambient currents.
- Tangling problems with the coiled steel tubing on the sea floor.
- Problems with launching the OROV due to swell induced ship motions.

5.1.2 Work ROV (OCEANEERING)

The ROV company OCEANEERING was subcontracted to carry out the ROV operations from *Far Grip*.

The ROV consisted of two parts. The first part consisted of a non-movable cage that was launched into the water and lowered down to (or close to) the sea floor. From the cage, the ROV movable part (by thrusters) was free to move within 200 m from the cage. Figure 5.5 shows a picture of the cage and the ROV during launching from "*Far Grip*".

The detailed specifications are given in the Memo from the ROV recordings [5]. Some of the specifications are as follows:

<u>ROV Type Scorpion 10:</u>
Depth rating 1500 msw fitted with TMS (Tether Management System)
Hydraulic power unit: Electro-hydraulic power unit provides 75 HP
Thrusters: 6 ea Innerspace thrusters

[5] Rye, 2001: "*ROV sonar and visual pictures from the field trial "Deep Spill", June 2000. Final data report.*" Memo prepared for the "*Deep Spill*" project dated February 22, 2001. 55 pages.

Speed: 1.5 knots horizontal, 1 knot lateral , 1 knot vertical
Tether length: 150m

Figure 5.5 Work ROV launched from Far Grip in preparation for deployment operation. Research vessel Håkon Mosby seen in the background.

Sonar Specifications:
Type: Mesotech MS 900 Color Imaging, deep head sonar
Frequency: 675 kHz
Beam width: 1.7°horizontal, 60°vertical
Mechanical resolution: 0.225° (step angle)

SIT Camera SIMRAD 1324:
Horizontal Resolution: 700 TV Lines (typical
Light Sensitivity (limiting): 2 x 10-4 Lux (faceplate)
Light Sensitivity (full video): 1 x 10-3 Lux (faceplate)

OE1366/67 Colour Zoom Camera:
Horizontal Resolution: 450 TV Lines for OE1366, 460 TV Lines for OE1367
Light Sensitivity: 0.1 Lux (faceplate)
Standard Lens: Zoom Lens 12:1, 5.4mm to 65mm f/1.8 - 2.7

SIMRAD RPT324 Transponder

Overall length : 350 mm
Operational depth : 2000 m max

Transducer beam : 45 degrees

Video recorders
JVC BR - S 600 E SVHS players.

Ruler montage
A ruler was mounted on the ROV for droplet and bubble size determination. Distance from color camera lens to ruler was 41 cm. Ruler was mounted on front center of ROV skids beneath camera pan/tilt unit

Field experience
The WROW worked well during the field trial. Problems encountered were:

- Problems with receiving clear signals from the side scan sonar due to electronic noise generated by the cryogenic pumps (both units were operated from a common power supply)
- Problems with receiving positioning signal on *Far Grip*, probably due to fouling on the transceiver unit.
- Occasionally problems with launching the WROV due to swell induced ship motions. For this reason, the WROV had to be kept onboard *Far Grip* during the crude oil discharge.

The results from the WROV recordings are given in Chapter 7.1.

5.2 Instruments operated from research vessels

5.2.1 Echo sounder

On RV Johan Hjort continuous acoustic measurements were performed using the Simrad EK500 scientific echosounder operating with 18, 38, 120 and 200 kHz transducers. All transducers are mounted on a retractable keel in order to obtain high quality data, during potentially sever weather conditions. The Bergen Echo Integrator (BEI) was used to store all acoustic data in a database, as well as for inspection of the acquired data during the cruise. With respect to the 18 and 38 kHz transducers, data were acquired with a range setting of 0-750 m or 0-1000 m, while the 120 and 200 kHz transducers were operated with a range setting of 0-250 m.

On board Håkon Mosby the EK500 and BEI system was used in a similar way as on RV Johan Hjort. Data were however, mainly acquired at 38 kHz during the oil spills, using an identical range setting as on RV Johan Hjort. A limited amount of recordings were also made at 120 kHz, but with a range setting of 0-1000 m.

Results from the echo sounder measurements are given in Chapter 7.2.

5.2.2 Acoustic Doppler Current Profilers (ADCP)

On RV H. Mosby a RD Instruments 150 kHz narrowband hull mounted Acoustic Doppler Current Profiler (ADCP) was used to monitor the current pattern in the upper part of the water column from approximately 20 - 400 m depth. Two different configurations were used (1 and 2 below), the first setting only for a short period on 25 June 2000.

1. ADCP averaging interval: 600 s, number of depth bins: 32, depth bin length: 32 m, transducer depth: 4.2 m, pulse length: 32 m, blank length interval: 16 m, ping interval: 0.65 seconds.

2. ADCP averaging interval: 600 s, number of depth bins: 64, depth bin length: 16 m, transducer depth: 4.2 m, pulse length: 16 m, blank length interval: 8 m, ping interval: 0.65 seconds.

In order to perform near continuous measurements of currents in the deeper part of the water column, a RDI Long Ranger 75 kHz ADCP were mounted on a moored rig at a bottom depth of around 840 m (Fig. 5.6). The rig consisted of an anchor, two MORS (AR 661) acoustic release units, and a LinkQuest Inc. acoustic modem (UWM 2000) with external battery pack. The acoustic modem, battery pack and the LR ADCP were mutually connected with Y-cable in order to supply the acoustic modem with external power and for data transfer between the ADCP and the acoustic modem.

Figure 5.6 Picture of bottom mounted ADCP with buoyancy and acoustic release mechanism.

A pressure resistant ARGOS-transmitter was attached to the rig in case it would be difficult to retrieve, due to weather conditions or visibility, when it surfaced after the experiment. A total of 10 air-filled glass floats (Nautilius Deep Sea 17” glass floatation spheres), were used to bring the rig to the surface after terminating the experiment. The current measurements were performed for 25 m depth bins, ranging approximately 33.3 m to 508.3 m from the instrument, corresponding to an actual depth range of 800 – 320 m depth.

During the field experiments the LinkQuest UWM 2000 acoustic modem was used to download a subset of the acquired data in near real time, in order to provide the command vessel in charge of the operation with data on deep-water current velocity and direction. Such data were downloaded on several occasion during the experiment, especially prior to the gas and oil spills conducted.

Results from the ADCP measurements are given in Chapter 6.1.

5.2.3 CTD and Carousel Water Sampler

A Seabird 911 CTD with a rosette sampler was used to obtain information on the hydrography as well as obtaining water samples for chemical analysis of oil components in the experimental region (Figure 5.7). For the purpose of obtaining independent data on oil concentrations in connection with the oil spills, a Sea & Sun Technology, PAH-probe SNO.02/UV-fluorimeter was attached and connected to the Seabird 911. The PAH-probe is designed to measure aromatic hydrocarbons, using a Xenon flash lamp light source, type Perkin Elmer FX1104, and as detector two silicon photodiodes with center wavelengths of 254 and 360 nanometers respectively. Two of the Seabird 911 auxiliary channels (0 and 1) were used to transfer data in real time to the Seabird deck unit and store these on a computer along with the standard Seabird 911 measurements.

Figure 5.7. The carousel water sampler.

However, for some unforeseen reason – but probably due to contamination of the optical lens – the fluorometer produced a noisy response that could not be related to oil concentrations. For this reason, the rosette sampler had to be launched based on readings from the echo sounder, rather than – as planned – on the fluorometer readings.

Results from the CTD measurements are given in Chapter 6.1. Results from the analysis of the carousel water sampler data are given in Chapter 7.3.

5.3 Sampling equipment operated from work boats

5.3.1 Work boats

Two workboats (MOB-boats) were used for subsurface and surface oil monitoring:

- **Workboat from Johan Hjort:** Allocated for "shallow" subsurface measurements (i.e. oil droplet size distribution, oil concentration and water sampling at 1 – 5 m depth) during and after discharge of marine diesel. Due to problems of using the workboat from Far Grip during the crude oil spill, this workboat was also used for oil sampling and oil film measurements during the crude oil spill.
- **Workboat from Far Grip:** Allocated for surface oil sampling and oil film thickness measurements. This workboat was only used during the marine diesel discharge.

5.3.2 Water sampling and UV-Fluorometers

Fluorometers operating at two different depths were used for measurement of hydrocarbon concentration under the oil slick and in areas where oil droplets was surfacing. The technique is based upon pumping water from two separate depths into the fluorometers. The fluorometers were calibrated for a response for the oils used in the experiment. In addition, water samples was taken for a post-calibration of the UVF-data obtained *in-situ.* The water samples was processed and analysed at SINTEF's laboratories in Trondheim for analysis of total concentration of oil (THC) and more detailed chemical composition of the oil in the water. The measurements have been coupled with data for position (from GPS) for accurate geographical visualisation of the hydrocarbon concentrations.

Results from the water sampling and UV-fluorometers are given in Chapter 8.1.

5.3.3 Oil film thickness measurements

Different sampling / measurement techniques was used depending on the oil film thickness within the slicks:

Method	*Tentative thickness*
3M PP pad	> Rainbow (from 1-5 μm to 2-3- mm)
Teflon sheet	< Rainbow (from 0.1 μm to 5 μm)

Pad / net sampling techniques
For sampling of thinner film thickness two various pad techniques are used:

- 3M polypropylene pad (25 × 25 cm) was operated in the thickness area from 2-3 mm down to about 1-5 μm. The pads was carefully placed on the slick surface for 5-10 seconds and transferred to an airtight bottle, and transported to SINTEF for quantification. In the SINTEF laboratories, the oil adsorbed on the pad was extracted and quantitatively analysed using gas-chromatography techniques and UV spectrophotometer
- For very thin oil films (< rainbow; i.e. from 0.1 μm to 5 μm) a ETFE Teflon net (SEFAR, 25 × 25 cm sheet) was used to skim/adsorb the thin oilfilm over a certain surface distance. As an alternatively, the Teflon net was used to skim/adsorb the oil within a defined surface area. After skimming, the Teflon sheet was carefully transferred to a tight bottle and extracted by an organic solvent (DCM) in the laboratory container on board Johan Hjort. The extract was brought to SINTEF laboratories for quantification using gas-chromatography techniques.

Results from the oil film thickness measurements are given in Chapter 8.2.

5.3.4 Determination of weathering characterisation of surface oil

Different methods for determination of weathering characteristics were used as listed in Tables 5.3 and 5.4 below. The analytical methods described in Table 5.3 was performed in the laboratory container on board research vessel immediately after receiving the samples from the workboats, Analytical methods described in Table 5.4 was performed at SINTEF's laboratories.

Table 5.3 Physical chemical analyses performed on surface oil in the laboratory container onboard Research vessel Johan Hjort.

Parameter	*Method*
Evaporative loss	Prediction based on waterfree oil density
Water content	Alcopol O 60 % and heating
Viscosity/rheology of w/o emulsion	Bohlin Visco 88
Stability of w/o emulsion	By settling and use of emulsion breaker
Effectiveness of emulsion breaker	Alcopol O 60 %
Dispersibility (with Dasic NS)	CONCAWE / SINTEF FET

Table 5.4 Analyses carried out at SINTEF's laboratories on selected samples.

Parameter	*Method*
Evaporative loss *	Gas chromatography
Dissolution potential of WAF components *	Gas chromatography / Mass spectrometry
Density *	Densiometer – ASTM D 4052-81
Water content	Karl Fischer Titration
Density of emulsion	Calculated based on density of sea water and oil residue and emulsion water content
Film thickness	Analysis of pad samples

* Measured on water free residue.

Results from the determination of the weathering characterization of surface oil are given in Chapter 8.2.

5.4 Aerial surveillance

5.4.1 Aerial surveillance of surface slicks

Aerial surveillance was provided by six airplanes from the same number of European countries – Norway, Denmark, Germany, The Netherlands, France and UK. The flights were arranged as a part of a Bonn Agreement project with its own agenda – namely to test a special color code designed for determination of oil slick thickness. All planes were operating from Kristiansund Airport, about 250 km south east of the experimental site. These surveillance airplanes are in general equipped with special imaging facilities, such as infrared (IR) and ultraviolet (UV) scanners and a side scanning radar (SLAR) for mapping oil slicks.

Results from the aerial surveillance of surface slicks are given in Chapter 8.3.

6. ENVIRONMENTAL CONDITIONS

6.1 Met-ocean data

In this section, measurements of oceanographic and meteorological data will be reported. The data comprises wind data from an Aaanderaa met-station mounted on *Håkon Mosby*, hydrographical measurements from CTD instruments operated from *Håkon Mosby* and *Johan Hjort*, as well as ocean current data from the bottom mounted ADCP and the ADCP mounted on *Håkon Mosby*. Where relevant, references will be given in this and the following sections to folders and files where data are stored on the CD-ROM accompanying the present report. An overview of the content of this CD-ROM is given in Appendix C.

6.1.1 Wind data

The wind data which was sampled at 10 minutes intervals are shown in Figure 6.1 as East and North component of the wind velocity, defined according to the meteorological convention (East component = wind blowing from East, North component = wind blowing from North). Data includes some noise that may be due to inappropriate compensations for ship motion. The data from June 27 00:04 UTC to June 29 23:04 UTC are stored at 10 minutes intervals as wind speed and direction in the ASCII file HAKON_MOSBY_WIND.DAT in the WINDdata directory. A smoothed curve that has been drawn for both components forms the basis for the graph of smoothed wind speed and direction shown in Figure 6.2.

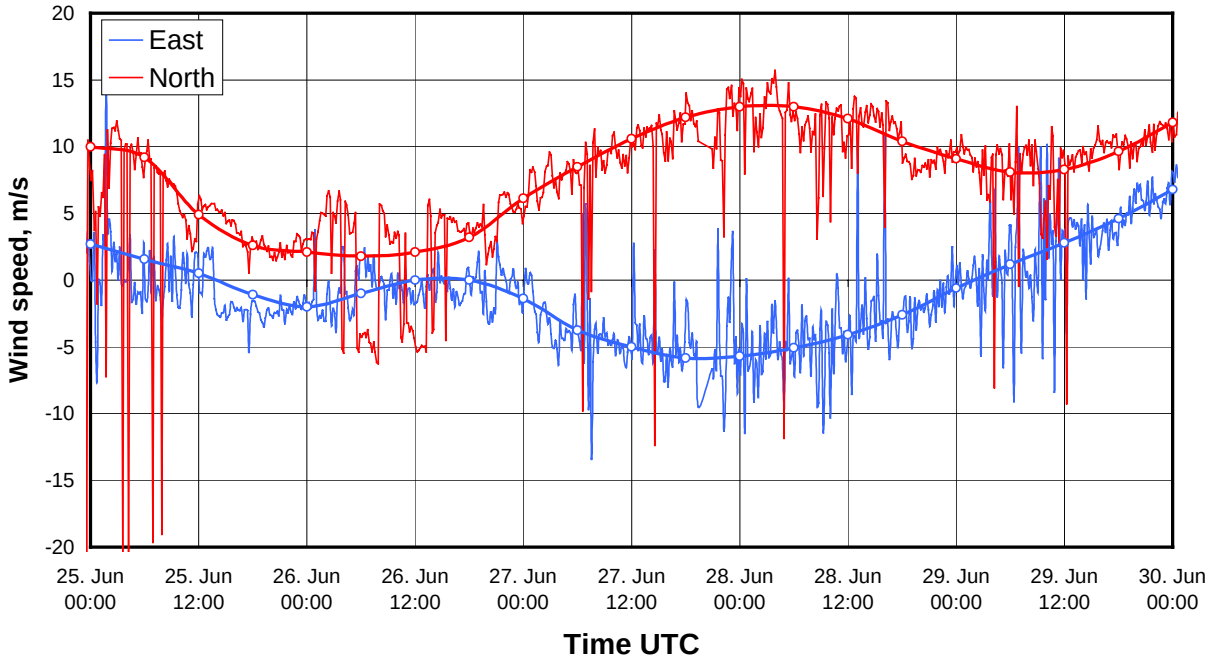

Figure 6.1 Wind measurements from the Aanderaa weather station on Håkon Mosby. Wind shown as north and east components. The ship motion has been subtracted from the measurements, but the noisy character of the data may in part be due to ineffective correction for vessel motions. Solid lines shows smoothed data used as a basis for the speed/direction plot shown at Figure 6.2.

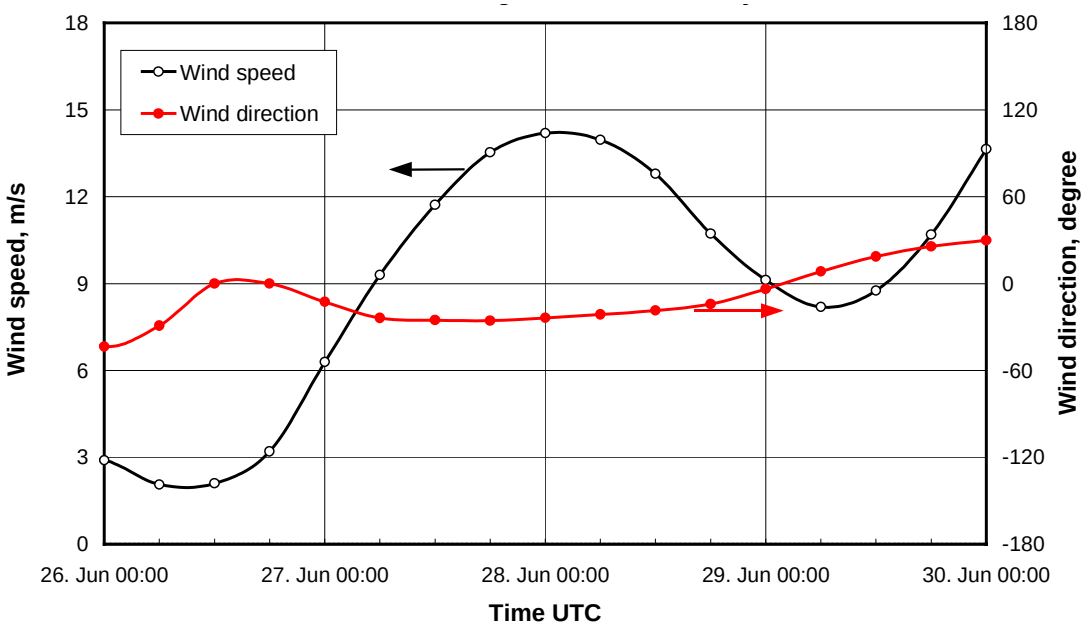

Figure 6.2 Plot of wind speed and direction at the Helland Hansen site during the DeepSpill sea trial. Based on smoothed data as shown in Figure 6.1.

6.1.2 CTD data

CTD profiles were measured on 10 occasions in the experimental period. Table 6.1 gives the date, time and location of the different profiles. Note that all measurements were made within a distance of less than 5 km from the discharge point. The same information (Table 6.1) and the results from each profile are stored in ASCI-files with names CTD_***.prn in the CTDdata directory. Figure 6.3 shows mean profiles of sea temperature and salinity based on the data for all stations. A file with the mean profile – sampled at 25 m intervals – is included as CTD_MeanProfiles.prn in the CTDdata directory.

Table 6.1 Date and location of CTD-profiles measured during the DeepSpill experiment. Max depth is the maximum depth covered by the respective profile. Profiles marked HM are measured from Håkon Mosby, while profiles marked JH are measured from Johan Hjort.

Station	*Date and time UTC*	*Lat*	*Long*	*Max depth*
HM 2001	Jun 25 17:45	64.9833	4.8167	798
HM 2002	Jun 27 08:54	65.0033	4.8349	803
JH 488	Jun 26 15:23	64.9857	4.8502	793
JH 489	Jun 27 00:23	64.9982	4.7663	840
JH 490	Jun 27 01:20	64.9960	4.9155	762
JH 494	Jun 27 16:20	64.9847	4.8897	774
JH 495	Jun 28 00:07	64.9602	4.8052	814
JH 496	Jun 28 16:57	65.0215	4.8748	814
JH 499	Jun 28 23:17	64.9750	4.8827	771
JH 500	Jun 29 06:05	64.9987	4.8365	497

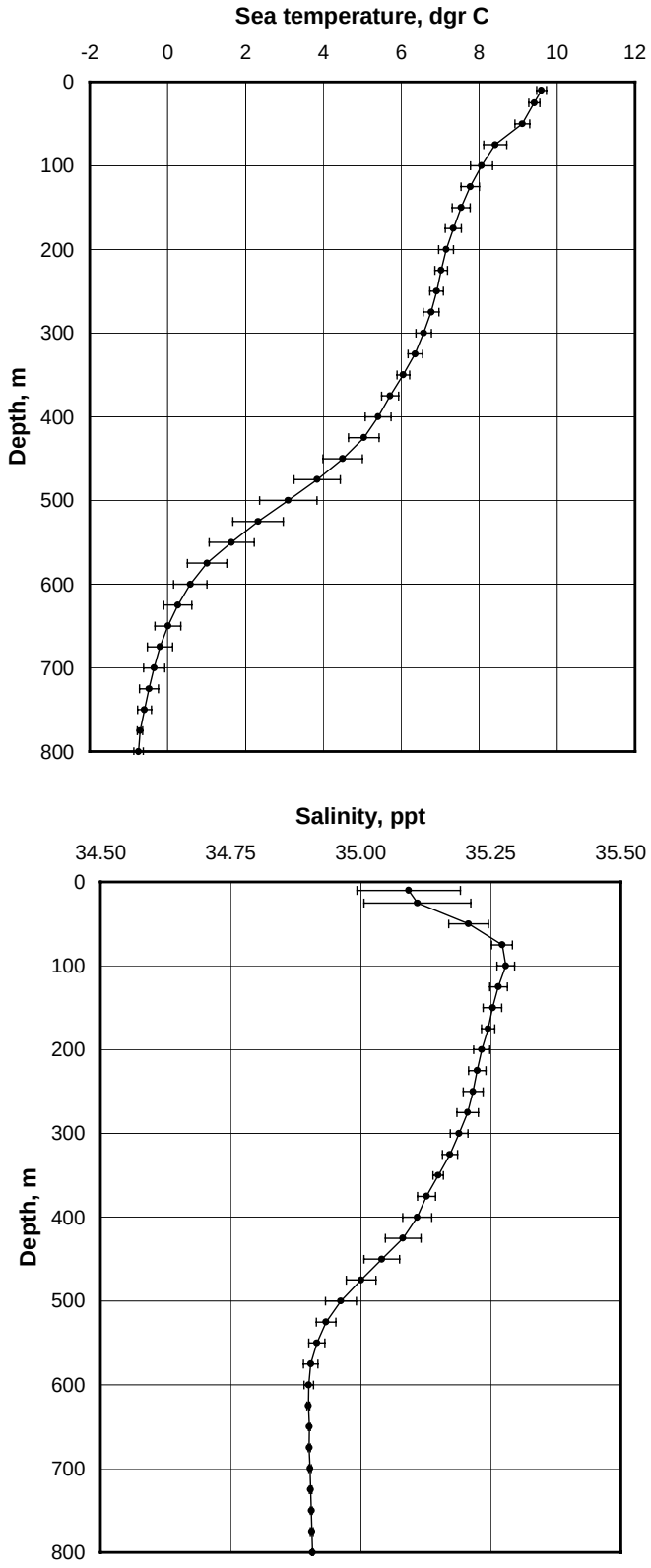

Figure 6.3 Vertical mean temperature and salinity profiles based on 10 profiles measured at the Helland Hansen site in the experimental period. Horizontal bars indicate the variability in data represented by ± 1 standard deviation. Data from the CTD instrument operated from Håkon Mosby and Johan Hjort.

6.1.3 ADCP data

Ocean current data were obtained from two instruments, one upwards looking ADCP mounted in a rig anchored on the seabed, and one downwards looking ADCP mounted under the hull of *Håkon Mosby*. The former instrument covered a depth range from 800 m to about 325 m in 25 m intervals, while the latter covered the depth range from 25 to 425 m in the same intervals (see section 5.2.2 for more details). In theory, the current measurements from the ship-mounted ADCP should have been fully compensated for ship motion, but this compensation proved to be ineffective – probably due to the rather long integration time that was chosen for the measurements (10 minutes). However, reasonable data could be recovered by application of the following method:

- Differential current profiles were obtained for each time step by using the currents measured at 350 m meter with the ship mounted ADCP as reference (*HM = Håkon Mosby*):

$$\hat{U}_i^{(HM)} = U_i^{(HM)} - U_{350}^{(HM)}$$

- To obtain absolute current velocities, these differential velocities were added to the currents measured at the corresponding depth with the bottom mounted ADCP (*BM* = Bottom Mounted):

$$U_i = U_{350}^{(BM)} + \hat{U}_i^{(HM)}$$

The measurements from the two instruments were made at 10 minutes intervals, but the two instruments were not fully synchronized. For this reason, the sampling periods of the bottom-mounted instrument were used as a basis, and the data from the bottom-mounted instrument were paired with the data from the ship-mounted instrument measured closest in time with these periods. The data set containing these recovered measurements and the data from the bottom mounted ADCP have been stored in the Excel-file ADCP_DATA.xls in the directory ADCPdata at depth intervals of 50 meters.

This Excel file includes worksheets with time series of current data for each depth, as well as a facility for extracting current profiles at chosen times. Figure 6.4 shows an example of such profiles from the start of the three experiments. Figure 6.5 shows a progressive vector diagram for a selection of depths based on data from the period from June 27 00:17 UTC to June 29 13:26 UTC.

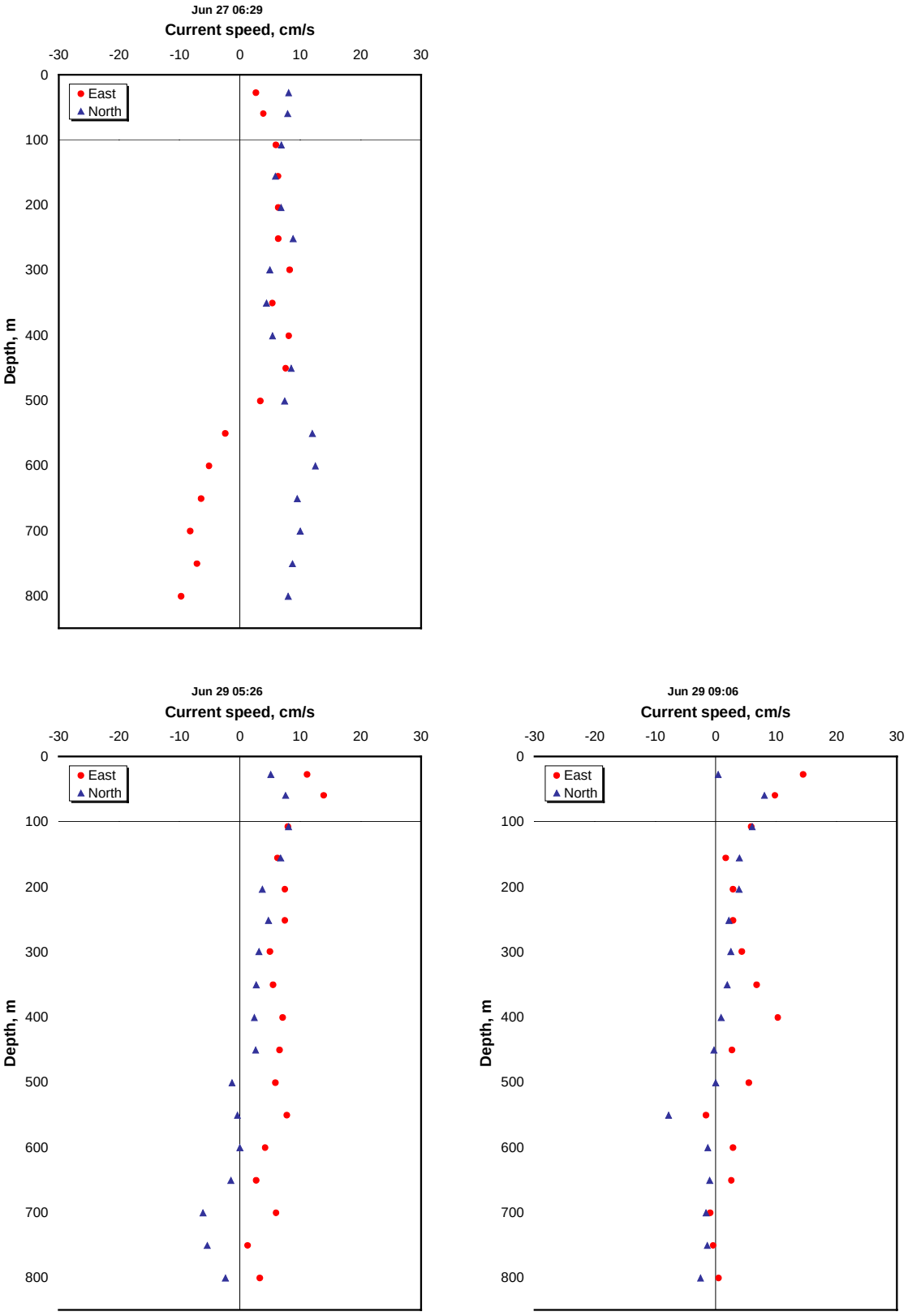

Figure 6.4 Current profiles from the start of the three experimental discharges. Marine Diesel (top), Crude Oil (bottom left) and LNG (bottom right). Examples of output from the Excel-file ADCP_DATA.xls.

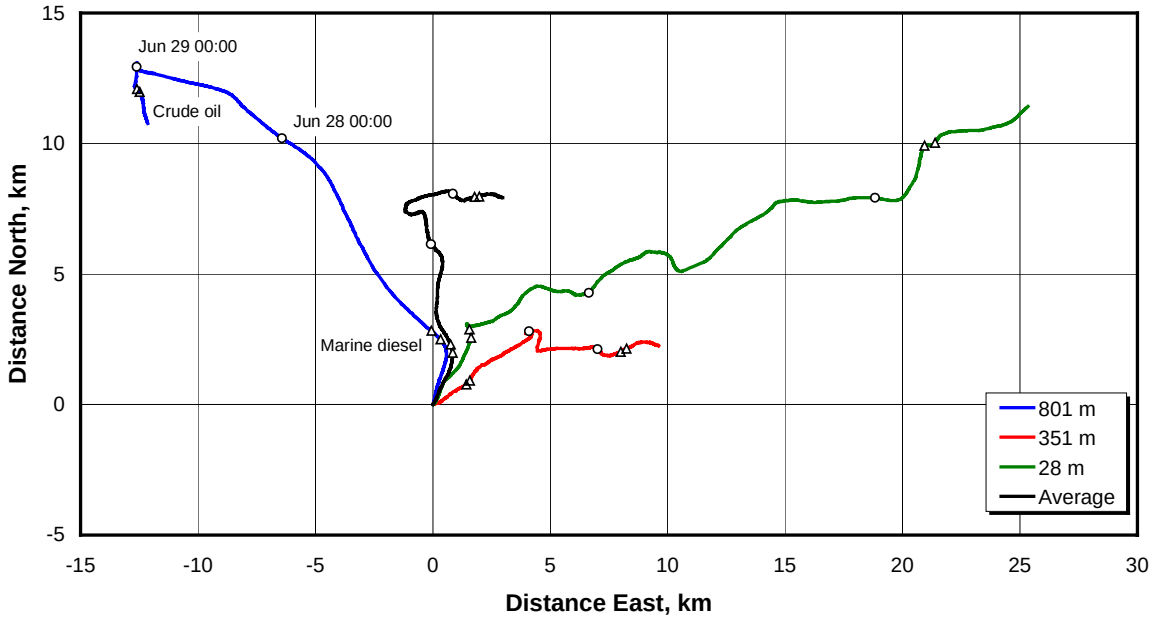

Figure 6.5 Progressive vector diagram based on the current measurements from the bottom mounted and ship mounted ADCPs. Open circles mark the start of a new day, while the duration of the two experiments with oil is marked with triangles. Data from 801, 351 and 28 m depths, covering the period from June 27 00:17 UTC to June 29 13:26 UTC. Black line marked "average" is based on the depth-averaged currents in the same period.

6.2 Marine Life

6.2.1 Marine organisms

Within the framework of the present report only a brief sketch of the biological material collected in trawl and net samples together with a general description of the scattering structures observed by the echo sounders throughout the experimental period are presented. These observations are qualitative in nature, and as such of restricted value with regard to an evaluation of potential effects of the oil and gas spills on the biological community. A more detailed description and analysis will be presented in an additional report as jointly agreed upon by Chevron as the head coordinator of the JIP, Statoil and the Institute of Marine Research, Bergen.

Acoustic scattering structures
The acoustic registrations recorded throughout the water column (20 - 840 m depth) at 18 and 38 kHz are in agreement with what could be expected from a biological point of view. At 38 kHz a regular and more or less constant deep scattering layer (DSL) was observed around 300-500 m depth during daytime. Near the surface down to approximately 50 m depth, another distinct scattering layer could be distinguished also at 38 kHz. As light conditions slightly changed during evening the lowermost DSL slowly disintegrated into less defined scattering structures, suggesting that what was first observed as a more or less homogeneous layer, are composed of different scattering organisms that have definite and different vertical migration patterns. Some of these deep scattering structures rose towards surface waters at night. Based on previous knowledge the

organisms that undertake the most extensive diel vertical excursion in this region, is euphausiids or krill. Hence the well-defined deep scattering layer (DSL) that was regularly observed during daytime most probably consists of a range of species of larger zooplankton (pelagic shrimps and krill) as well as mesopelagic fish.

The higher frequencies (120 and 200 kHz) observing particularly the upper 250 m of the water column, suggest the regular presence of weaker and smaller scatterers within this depth range, particularly closer to the surface in the 0- 75 m depth range.

Few if any registrations of large schools of fish were recorded throughout the water column, and no acoustic registrations of what can be interpreted as Norwegian Spring Spawning herring, which is the most important fish stock in the Norwegian Sea during summer, was recorded in the experimental region.

Fish and larger zooplankton
Trawl samples, whether obtained from deep, mid or surface waters showed no high number of individuals of particular fish or larger zooplankton species. A scattered distribution of organisms throughout the depth ranges sampled, might be deduced. However, the acoustic scattering layers suggest that some organisms are more abundant than others, but are probably confined to a narrow or restricted depth range. Some species were mainly recorded in the deepwater samples, while others were only found in samples from mid and surface waters.

The surface hawls [0-35 m] suggested the regular occurrence of 0-group haddock, 0-group herring and 0-group saithe. Adult herring, mackerel and lumpsucker as well as juveniles of the squid *Gonatus fabricii*, which is a regular inhabitant of the Norwegian Sea surface waters, where also recorded in small numbers. No records of North Atlantic salmon (*Salmo salar*) which is also an important inhabitant of the surface waters was found in the experimental region.

Deeper in the water column mesopelagic fishes like the lantern fish *Benthosema glaciale*, blue whiting (*Micromesistius poutassou*), white barracudina (Notolepis rissoi kroyeri) and hatchet fish (*Argyropelecus* spp.) were found. Of the larger zooplankton occurring in the deeper part of the water column, the shrimps *Hymenodora* sp., *Sergestes arcticus* and *Pasiphea* spp. were observed regularly as was also euphausiids or krill, mainly *Meganyctiphanes norvegica* and *Thysanoessa longicaudata*.

Mesozooplankton
The small copepod crustacean *Calanus finmarchicus* also called “raudåte” in Norwegian because of its deep-red appearance when found in the surface waters, were numerous in the uppermost part of the water column. This species is by far the most important zooplankter in the Norwegian Sea, as well as being the primary feed for Norwegian Spring Spawning herring on its feeding excursions into the Norwegian Sea during summer. Its abundance seemed to decrease towards the bottom waters. In the deepwater, carnivorous zooplankton like chaetognaths (Sagitta spp.), the copepod Euchaeta spp. and the jellyfish Aglantha spp. were more numerous.

6.2.2 Sea bird observations

As part of the project planning NINA researcher Svein-Håkon Lorentsen made an assessment of the occurrence of vulnerable seabirds within the potentially risk area on Helland-Hansen oil field

in July 2000. On the basis of existing knowledge, he concluded that vulnerable seabirds would probably not be effected at the population level by possible oil pollution in the experiment area. However, it was recommended that seabird observations should be carried out before and during the experiment, because vulnerable auk species from nearby breeding colonies might occur in the area. Furthermore, it was pointed out that controlled oil spill situations represent good opportunities to study seabird behaviour in relation oil on the sea surface. To accumulate knowledge in this field increases our ability to assess possible effects of oil spill at sea. NINA worked out a proposal to a procedure for seabird monitoring and accept criteria for the oil spill experiment. It was decided that a seabird researcher from NINA should take part in the experiment as an adviser. He stayed on board RV Johan Hjort.

Seabird observations were carried out in the area before the start of the experiment, and an assessment of the seabird density was made on the basis of the accept criteria. Observations were also made during the experiment period in order to detect possible damage to seabirds caused by the oil slick, as well as acquire general knowledge about bird seabird behaviour.

Methods

Seabirds were surveyed by internationally accepted methods[1]. In order to obtain knowledge about the seabird situation before the oil spill, censuses were made on the route to the experiment area and between this area and Kristiansund during 23 – 26 June. A scan in the 180^o sector forward of the ship was made. All birds were recorded as numbers seen per ten-minute period (later converted using the ships speed, to numbers of birds seen per kilometre travelled). A transect to record the number of birds within a fixed sea area, providing an estimate of the density of birds per square kilometre. Altogether 29 ten-minute periods in five transects were surveyed, between 63^{o}28’ N, 4^{o}47’E and the experimental area and between this area and 64^{o}50’, 5^{o}10’E. These surveys covered a total 26.9 km^2. In periods during the experiment observations were made in order to detect possible oil damage to seabirds and to record their behaviour.

Results and comments

The Fulmar *Fulmarus glacialis* was the most common seabird in the area. Other birds occurred only in low numbers (Table 1).

Table 6.1. Results of seabird surveys before the experiment started. Density values are given as number of birds per km^2.

Species	Density	Number observed	Variation within ten-minute period	
			Minimum	Maximum
Fulmar *Fulmarus glacialis*	3.6	96	0	10
Gannet *Sula bassana*	0.04	1	0	1
Kittiwake *Rissa tridactyla*	0.2	6	0	2
Guillemot *Uria aalgae*	0.3	7	0	4

If we suppose that an area of e.g. 100 km^2 would be effected by the oil spill, our calculations indicate that about 350 Fulmars would be found within the area. This is significantly less than the number given by the accept criteria. Although Fulmars may sometimes rest on the sea surface they are usually flying birds, and accordingly considerable less vulnerable to oil spill than e.g. auks. On the basis of the results that were obtained, the following message was given to the experiment leader: ”The number of vulnerable seabirds in the potential influence area is far less

[1] Tasker, M.L., Jones, P.H., Dixon, T. & Blake, B.F. 1984. Counting seabirds at sea from ships: A review of methods employed and a suggestion for a standardised approach. – Auk 101: 567-577.

than the accept criterion for the oil spill experiment." A message was forwarded that no organic waste from ships should be thrown overboard during the experiment, so that flying seabirds should not be attracted to the oil spill area.

The day before the oil spill, several ships were concentrated within the experimental area. Environmental sampling and trawling took place. Moreover, organic garbage was probably thrown into the sea from the vessels at that time. Probably as a result of this situation a considerable number of Fulmars concentrated in the area (Table 2). In periods many of these birds were resting on the sea.

Table 6.2. Results of Fulmar counts within the potential experimental area on 24 June.

Time	0910	1115	1300	1630	1830
Number observed	300	500	500	190	180

The maximum number corresponds to the number of Fulmars that would be found within a 140-km^2 large sea area (given the density that was calculated). If we regard such an area to have a circular form, the radius would be 6.7 km. This indicates that the birds that normally would have been found within a distance of 6-7 km from the experimental site had assembled by the ongoing activity in the area. It is well known that Fulmars are often attracted to fishing activity[2]. The birds probably regarded the assembly of vessels in the area as an indication of fishing activity, as well as possible availability of organic garbage. Concentrations of Fulmars in connection with oil spill experiments has also earlier been recorded[3].

By request, the vessels probably did not throw organic garbage overboard during the experiment period. As shown in the Table 2, the number of Fulmars decreased during the day before the experiment started, and when the release of oil started on 27 June, most birds had left the area. During the experiment 2-5 Fulmars were usually observed in the area. An exception was at 1630 on 29 June, when 35 birds were observed on the sea outside the oil slick. Beside Fulmars a number of other species were observed. Gannets were most common, but also several Gull and Skua species (Table 3). Two Killer whales were seen outside the oil-slick area

Table 6.3. Observed seabirds and sea mammals in the experiment area, 26 – 29 June. Fulmars are not included.

Species	Number
Gannet *Sula bassana*	8
Lesser black-backed Gull *Larus fuscus*	1
Greater black-backed Gull *Larus marinus*	1
Kittiwake *Rissa tridactyla*	4
Pomarine Skua *Stercorarius pomarinus*	1

[2] Tasker, M.L., Webb, A., Hall, A.J., Pienkowski, M.W. & Langslow, D. R. 1987. Seabirds in the North Sea. Final report of phase 2 of the Nature Conservancy Council Seabird at Sea Project. - Nature Conservancy Council, Aberdeen.

[3] Lorentsen, S.-H. 1995. Observasjoner av sjøfugl i forbindelse med eksperimentelt oljeutslipp Friggfeltet august 1995. – NINA Oppdragsmelding 372: 1-11.

Arctic Skua *Stercorarius parasiticua*	1
Great Skua *Catharacta skua*	2
Puffin *Fratecula arctica*	1
Killer whale *Orcinus orca*	2

Seabird behaviour in relation to the oil spill

Fulmars were often observed flying over the oil slick, but none were seen lying on the sea where there was oil on the sea surface. This has been observed also on earlier oil spill experiments and indicates that the birds generally avoid contact with oil. Areas with blue-shine oil slick may be an exception. On the other hand, the observations indicate that the oil attracted Fulmars to a certain degree. Fulmars and their relatives are able to detect food by their smell over long distances. The birds probably connect the smell of oil components to food availability. However, the general low number of birds seen during the oil spill period, shows that the experiment did not cause any particular concentration of seabirds.

In two occasions Gannets were seen flying across or along the oil slick. On 29 June, an adult bird was seen flying along the front of the oil slick. The bird plunge-dived into the sea and caught a fish. After two minutes it took to its wings. Shortly afterwards the Gannet was attacked by a Great Skua which forced it down to the sea and probably stole its fish. It is well known that flying seabirds often search for food along visible ocean-fronts, because these are often high production areas with an abundance of food. The observed Gannet may have interpreted the oil slick front in that way.

Damage to seabirds caused by to oil spill experiment

In one occasion a flying adult Kittiwake was observed with a small oil patch on its neck. Otherwise no indication of damage to seabirds were seen.

Conclusion

One the basis of the results, our conclusion will be than the DeepSpill experiment did not cause any significant damage to seabirds. The seabird surveys that were undertaken in the area, as well as observations of seabird behaviour gave valuable results that are relevant to environmental impact assessment and planning of future oil-spill experiments. It may also be concluded that both the locality and time of the year seemed to be favourable for such experiments. It is recommended that seabird researchers should participate also in future oil-spill experiments.

7 SUBSEA PLUME OBSERVATIONS

7.1 Results from the ROV recordings

The work ROV recorded visual and sonar images of the underwater plume on analog tapes during the experiments. The visual images switched between the color camera and the black/white camera, while the sonar recorded the plume by side scans. Both signals were recorded simultaneously on two different tapes. Details of the work ROV equipment are given in Chapter 5.1.

In the following, the notation "ROV" is used for the work ROV, for short.

ROV recordings were performed during the nitrogen release (release #1), the diesel release (release #2) and the pure methane release (release #4). In the following, the results from the recordings are summarized. Further details are given in a separate report on the ROV recordings made during the experiment (Rye, 2001)[4].

7.1.1 Sonar recordings.

Sonar recordings were made simultaneously with the video picture recordings. Unfortunately, the cryogenic pump (used for pumping the gas) distorted the sonar signal so that it was not possible to interpret the plume signal. However, the potential for use of the sonar for recordings of plumes was clearly demonstrated during the experiment, because some clear signals were recorded both before and after the pumping of the gas. Figure 7.1.1 shows one example of the picture from the sonar recordings made just after the cryogenic pump has been switched off. While the noise from the cryogenic pump is fading away from the sonar signal (as seen to the right), the signature from the nitrogen plume appears clearly on the sonar signal. This gas plume was generated just before the cryogenic pump was switched off. The plume will cease to occur shortly after this instance, because the gas release stops immediately when the cryogenic pump is switched off. The plume example here is therefore just an instant of opportunity, showing the gas plume clearly on the sonar screen.

7.1.2 The visual recording of the underwater plume.

While the sonar failed to record the underwater plume, the black/white camera made some good recordings of the plumes generated during the experiment. The following pictures show some typical examples of underwater gas plumes from the nitrogen and the diesel releases. Figure 7.1.2 shows the nitrogen release upon arrival of the gas at the release arrangement. Figure 7.1.3 shows a more developed nitrogen plume.

[4] Rye, 2001: *ROV sonar and visual pictures from the field trial "Deep Spill", June 2000. Final data report.* SINTEF Applied Chemistry. Memo prepared for the "*Deep Spill*" project dated February 22, 2001. 55 pages.

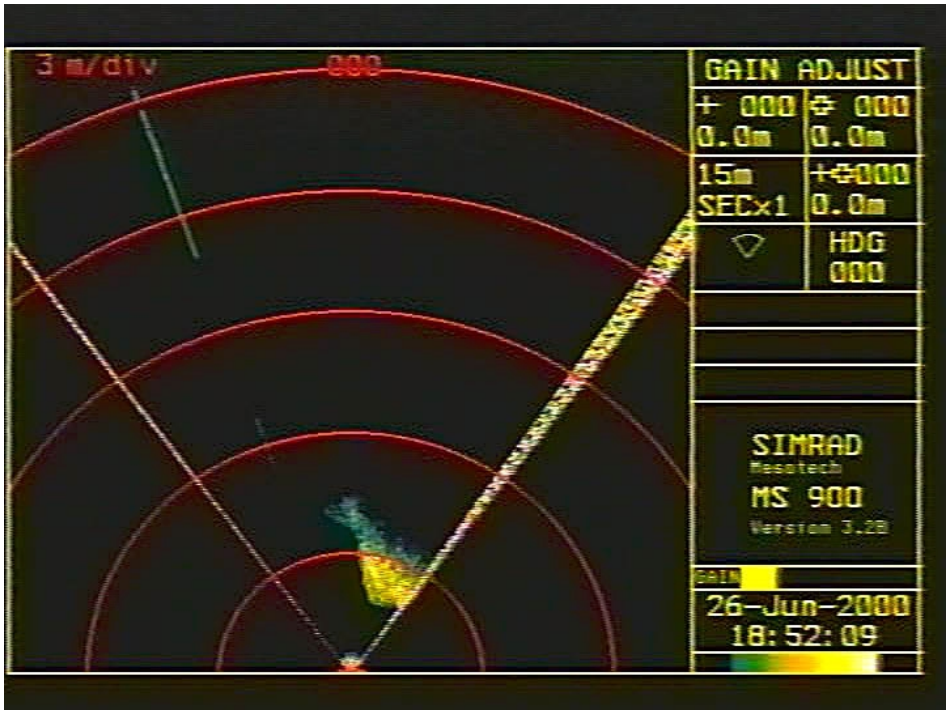

Figure 7.1.1. Sonar recordings of nitrogen plume.

Figure 7.1.2. Initiation of the nitrogen plume.

Figure 7.1.3. Well developed nitrogen plume.

Pictures are shown similarly for the diesel release. It behaves apparently like the gas plume. This is expected, because the buoyancy of the plume will be governed by the gas and to a lesser extent by the oil. The plume is shown for somewhat larger distances from the release arrangement in this case as well. The plume will tend to break up in a more “puff-like” behavior at larger distances, similar to what would be expected from patterns generated by growing meanders in the plume.

Figures 7.1.4 –7.1.7 show a series of pictures of the diesel plume, starting with a close-up on the release (taken with the color camera), and then three pictures following, taken from increasing distances from the source.

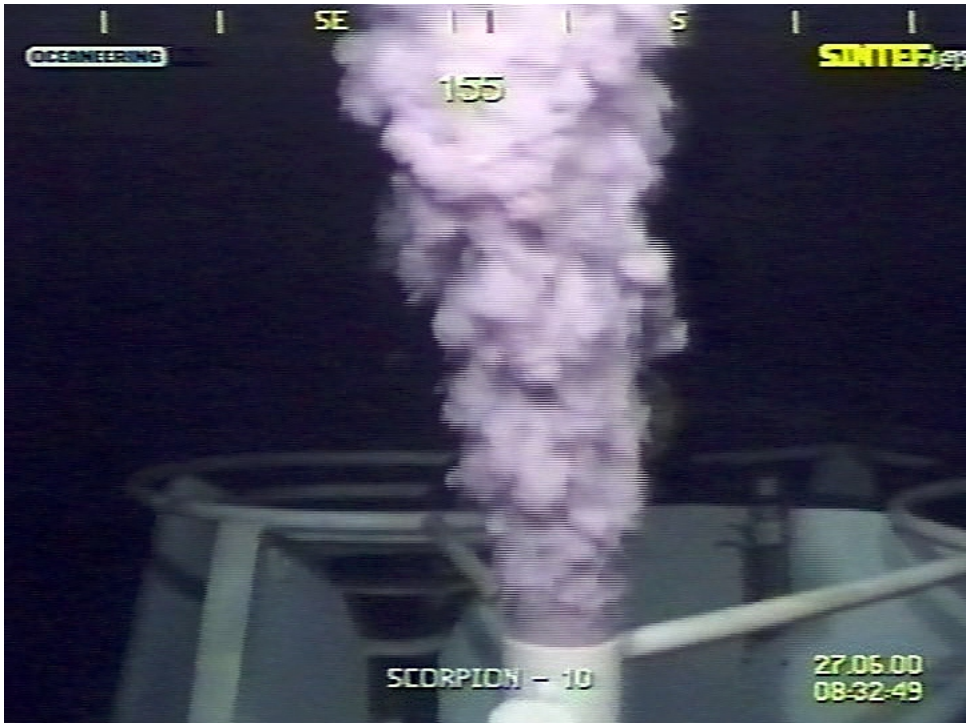

Figure 7.1.4. Release of diesel and nitrogen just after the arrival of diesel at the release opening.

Figure 7.1.5. Development of the plume for the diesel and methane release.

Figure 7.1.6. Further development of the diesel and methane plume. Undulating or meandering plume.

Figure 7.1.7. Further breakup of the plume at larger distances from the release.

7.1.3 Determination of gas bubbles and diesel droplet sizes.

The ROV was equipped with a ruler that was mounted in front of one of the cameras (the color camera). This camera was basically used for close-up pictures. The distance from color camera lens to the ruler was 41 cm. The ruler was mounted on front center of ROV skids beneath the camera pan/tilt unit. Figure 7.1.8 shows the ruler pictured by the color camera.

When the close-up picture camera was switched on, the oil droplets or the gas bubbles were observed to pass the volume of water between the ruler and the color camera. This would happen while the ROV was located within the plume volume. Most of the droplets were too unclear and also passing too fast for a proper size determination. However, under some circumstances, it turned out that the droplets were reasonably sharp to be considered further. This would happen when all the three following circumstances took place at the same time:

- The gas bubbles or diesel droplets were moving sufficiently close to the ruler so that the droplet/bubble was in focus.
- The droplet/bubble was moving sufficiently slow (relative to the ROV) so that the individual pictures of the droplets/bubbles became sharp enough for size determination.
- The ROV operator was able to focus the color camera on the ruler combined with sufficient light.

All these three conditions occurred frequently during all the three releases, although the bulk of the “plume visits” were less successful in this respect. However, it turned out to be sufficient that only some pictures were of reasonable quality for droplets/bubbles determination.

Figure 7.1.8. A color picture of the ruler mounted on the ROV.

The VHS picture generation for this purpose is rather large. As an example, just one minute of ROV recording of droplets/bubbles produce approximately 25 x 60 = 1500 pictures for further examination of the presence of droplets/bubbles. Therefore, a selection of pictures was made at various distances from the source (bottom).

I the following, two pictures are shown as examples that have a potential for being read off for droplet or bubble size determination. Figure 7.1.9 shows 2 – 3 bubbles that may be clear enough for size determination, by comparing the diameter against the size of a millimeter shown on the ruler. Figure 7.1.10 show some diesel droplets that appear to be relatively sharp at the upper part of the picture.

Counts were carried out for the methane release case (release #4) and for the diesel release case (release #2). In the following, results from 8 cases selected for droplet and/or bubble size distributions are described, 4 cases for the gas bubble size distribution and 4 cases for the diesel droplet size distribution. All cases were selected with an increasing distance from the source or the bottom.

It should be stressed that it was necessary to read off the individual bubbles and droplets manually. The video sampled pictures rather frequently, and it became therefore evident that the same bubble/droplet appears on many pictures in a sequence. The observer had then to keep track of the different bubbles/droplets that appeared on the screen, in order to avoid counting the same droplet/bubble more than one time.

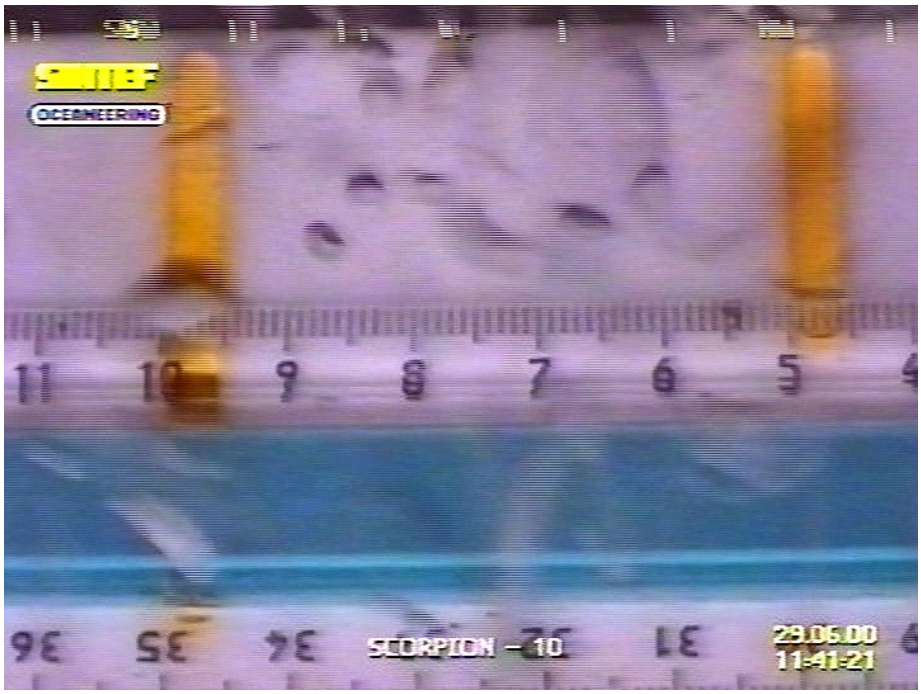

Figure 7.1.9. Example of reading gas bubble sizes from the video recording. Methane release.

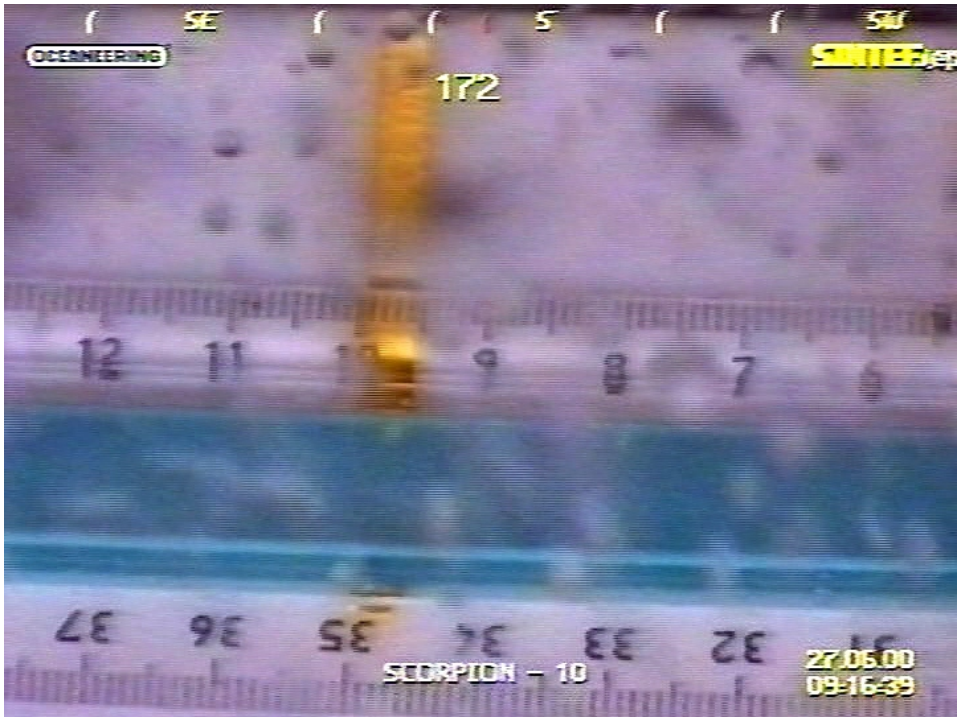

Figure 7.1.10. Example of reading droplet sizes from the video recording. Diesel droplets, mainly.

7.1.4 Gas bubble size distribution.

4 cases were selected for reading off the gas bubble size distributions. The criterion for selecting the cases was to look at the distribution at various distances from the source. Gas bubbles with a reasonable quality to be read off from the pictures were found between about 9 and 85 m above the source.

Table 7.1.1. Counts of methane gas bubble sizes at release #4 carried out 29. June 2000. Each second recorded represents 25 pictures read off for bubble sizes. A total of 667 bubbles were read off from a total of 3400 pictures.

Case No.	*Time interval, local time*	*Depth interval*	*No. of bubbles counted*
1	11:17:45 - 11:18:15	836 – 826 m	124
2	11:18:16 - 11:18:27	826 – 822 m	184
3	11:19:15 - 11:20:05	806 – 787 m	201
4	11:43:50 - 11:44:35	780 – 760 m	158

The results from the counts are shown in Figures 7.1.11 and 7.1.12. Figure 7.1.11 shows the distribution of the methane bubbles diameters for cases 1 and 2. The count is separated into two parts, the distribution determined within the depth range 836 – 826 m depth (closest to the source) and the depth range 826 – 822 m depth (at a longer distance from the source). Both distributions appear to concentrate within the range 1 – 5 mm diameter sizes of the bubbles, with some gas bubbles appearing with sizes closer to 8 mm diameter.

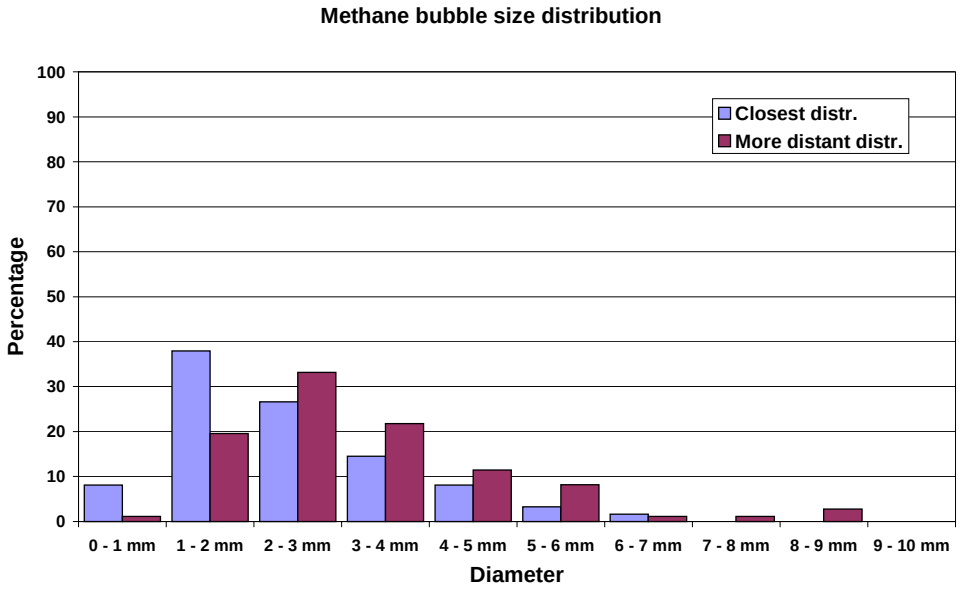

Figure 7.1.11. Distribution of the gas (methane) bubble diameters, below 822 m depth. Cases 1 (closest distribution) an 2 (more distant distribution). "Close" and "more distant" refer to distance to bottom.

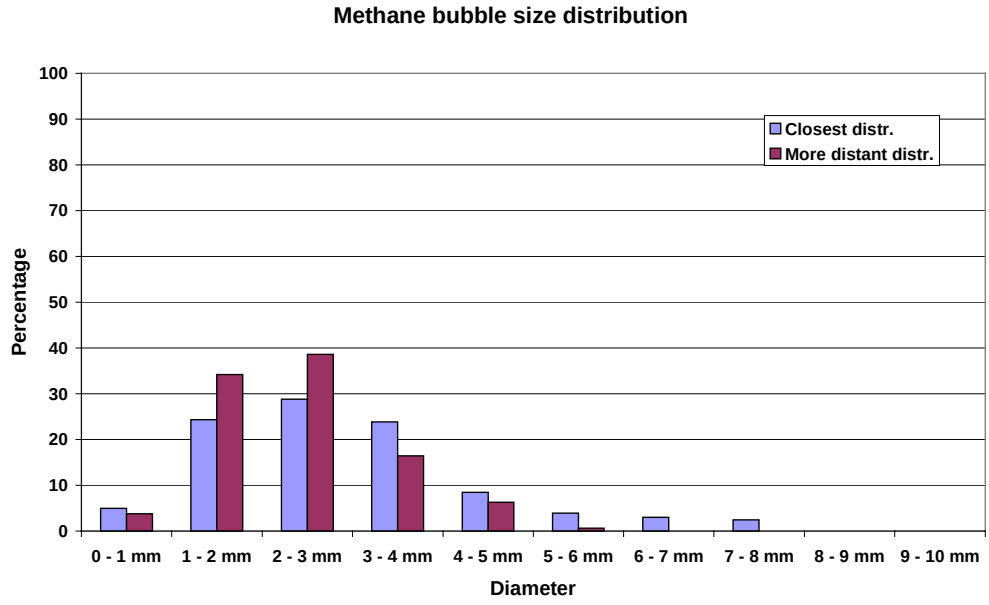

Figure 7.1.12. Distribution of the gas (methane) bubble diameters, between 806 and 760 m depth. Cases 3 (closest distribution) and 4 (more distant distribution). "Close" and "more distant" refer to distance to bottom.

A similar distribution is shown for the volume of the gas bubbles, see Figures 7.1.13 and 7.1.14. This distribution is based on the same material as for the diameter distribution, except that the diameter is taken to the third power (in order to arrive at volume estimates). In this diagram, the volume distribution is distorted towards larger gas bubbles, compared to the distribution shown in Figures 7.1.11 and 7.1.12. The reason for this distortion is that bubbles increase the mass (volume) faster than the corresponding increase in diameter.

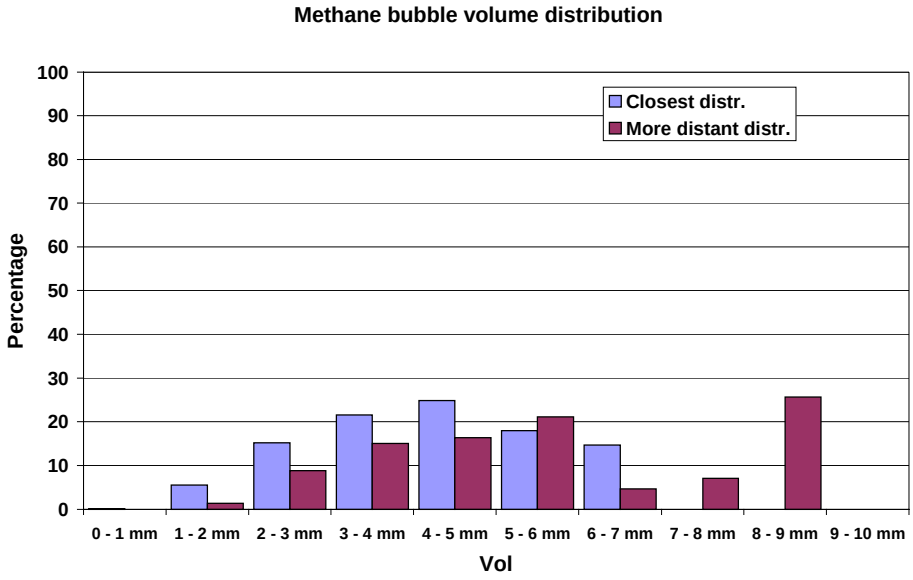

Figure 7.1.13. Distribution of the gas (methane) bubble volumes, below 822 m depth. Cases 1 (closest distribution) and 2 (more distant distribution). "Close" and "more distant" refer to distance to bottom.

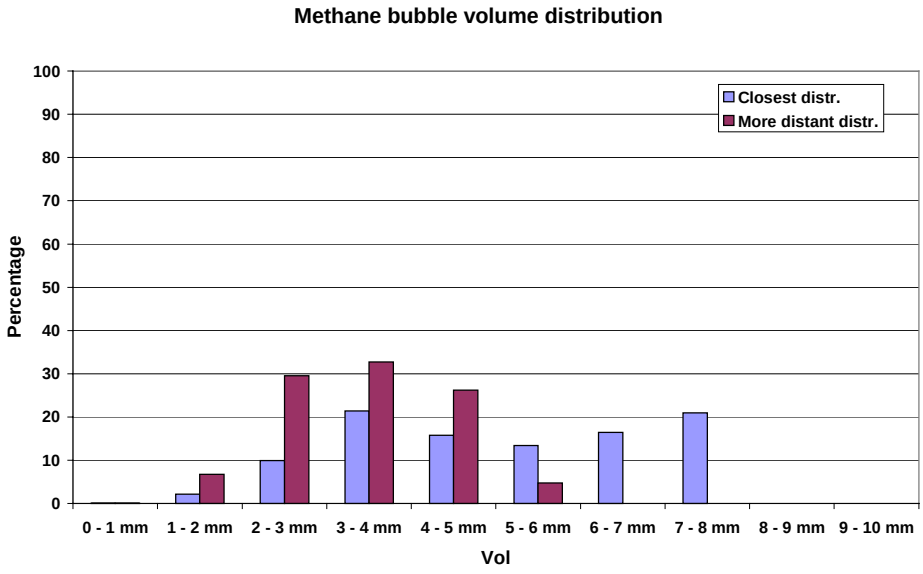

Figure 7.1.14. Distribution of the gas (methane) bubble volumes, between 806 and 760 m depth. Cases 3 (closest distribution) and 4 (more distant distribution). "Close" and "more distant" refer to distance to bottom.

Note that any increase in volume corresponding to the gas expansion effect is negligible for the cases considered. The change in gas volume for one single bubble moving between 760 and 836 m depth will be about 10 %, and the corresponding change in radius will be about 3 %. This change is negligible compared to the uncertainty in the drop size read-off carried out manually (ranging the bubbles into 10 different mm intervals).

One of the purposes to read off distributions for gas bubbles at various distances from the source was to look for some "separation" effect in terms that larger gas bubbles may follow another path through the water column than smaller gas bubbles. Due to this separation, the gas bubble distribution may change with the distance from the source (narrowing the distribution at increasing distance from the source). This effect is however not evident from the data that was read off. The reason for this is attributed to the fact that the rise velocity for gas bubbles is more or less the same for gas bubble diameters larger than about 2 mm. The bubbles will tend to break up at about 8 mm diameter. The rise velocity is close to 0.3 m/s for "clean" bubbles in this gas bubble diameter interval. Therefore, no "separation" effects are expected to be apparent in the data for the bubble size distribution.

This conclusion seems also to be supported by Figure 7.1.15, where the data from the first and second bubble count are considered together. The theoretical distribution that is drawn on the same chart is based on the two-parameter Rosin-Rammler distribution [5], where the volume contained in droplets with diameter larger than D is expressed by

$$V(D) = 1 - \exp\left[-2.996\left(D / D_{95}\right)^{n}\right]$$

where D_{95} is the maximum droplet size and n is a spreading parameter, here chosen as n = 2.5.

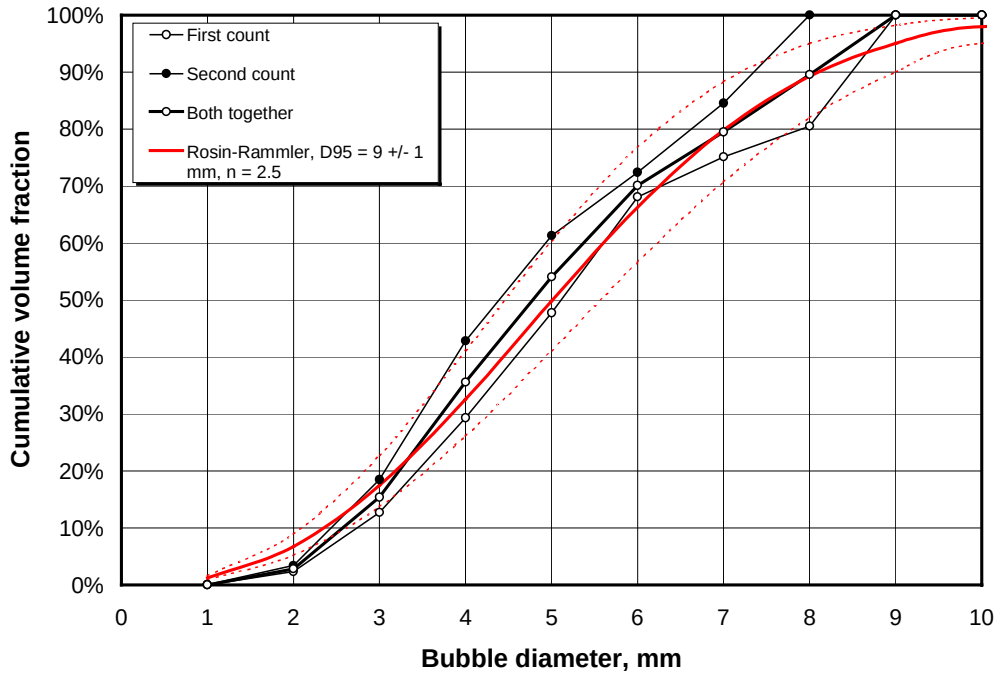

Figure 7.1.15 Cumulative distribution of bubble sizes, compared with theoretical curves based on the two-parameter Rosin-Rammler distribution.

[5] See Chapter 3 in Lefevbre, A.H, 1989: Atomization and Sprays. Taylor & Francis, USA.

7.1.5 Diesel droplet size distribution.

4 cases were selected for reading off the diesel droplet size distributions. The criterion for selecting the cases was the same as for the gas bubble size distribution, that is, to look at the distribution at various distances from the source. Diesel droplets with a reasonable quality to be read off from the pictures were found between about 5 and 56 m above the source (bottom).

Table 7.1.2. Counts of diesel droplets at release #2 carried out 27. June 2000. Each second recorded represents 25 pictures read off for droplet sizes. A total of 677 droplets were read off from a total of 5325 pictures.

Case No.	*Time interval, local time*	*Depth interval*	*No. of droplets counted*
5	09:16:29 - 09:16:32	840 – 839 m	215
6	09:16:48 - 09:16:52	835 – 834 m	129
7	09:21:50 - 09:22:40	830 – 822 m	139
8	09:28:14 - 09:30:49	810 – 789 m	194

The results from the counts of the diesel droplets are shown in Figures 7.1.16 – 7.1.19. Figures 7.1.16 and 7.1.17 show the distribution of the droplet diameters.

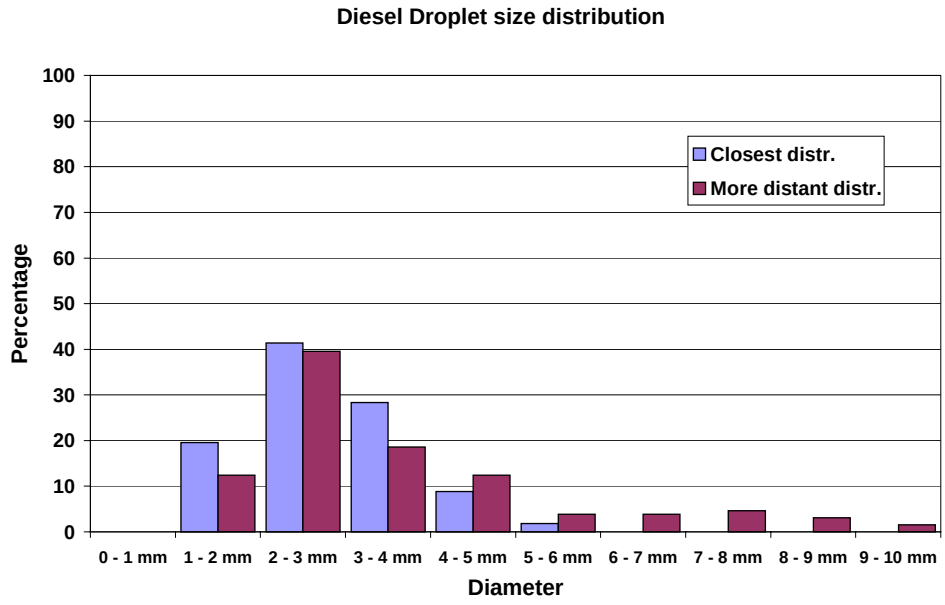

Figure 7.1.16. Distribution of the diesel droplet diameters below 834 m depth. Cases 5 (closest distribution) and 6 (more distant distribution). "Close" and "more distant" refer to distance to bottom.

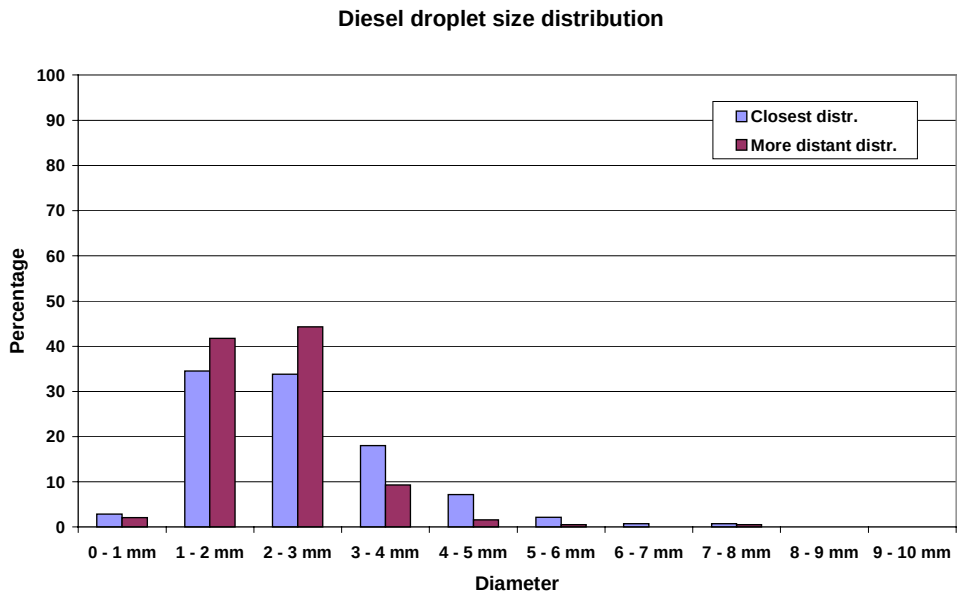

Figure 7.1.17. Distribution of the diesel droplet diameters located between 830 and 789 m depth. Cases 5 (closest distribution) and 6 (more distant distribution). "Close" and "more distant" refer to distance to bottom.

A similar distribution is shown for the volume of the diesel droplets, see Figures 7.1.18 and 7.1.19.

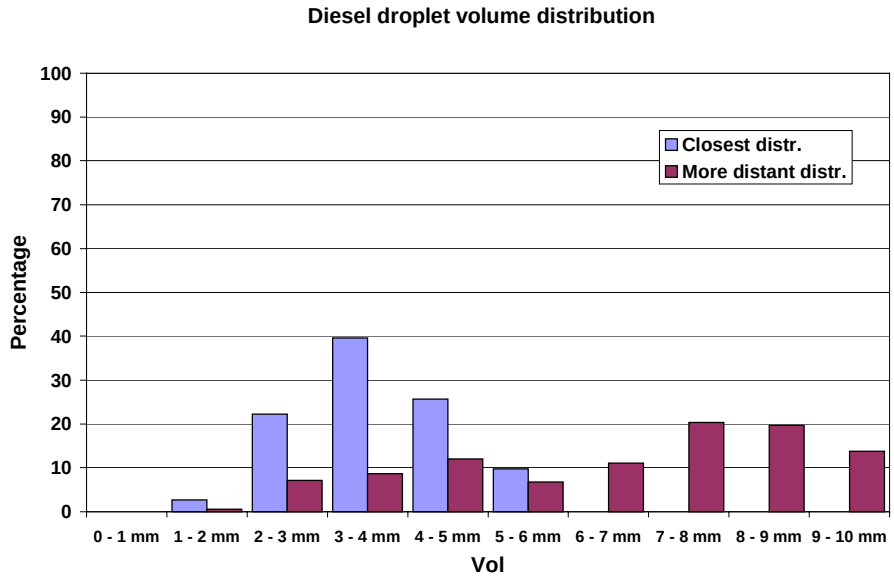

Figure 7.1.18. Distribution of the diesel droplet volumes below 834 m depth. Cases 5 (closest distribution) and 6 (more distant distribution). "Close" and "more distant" refer to distance to bottom.

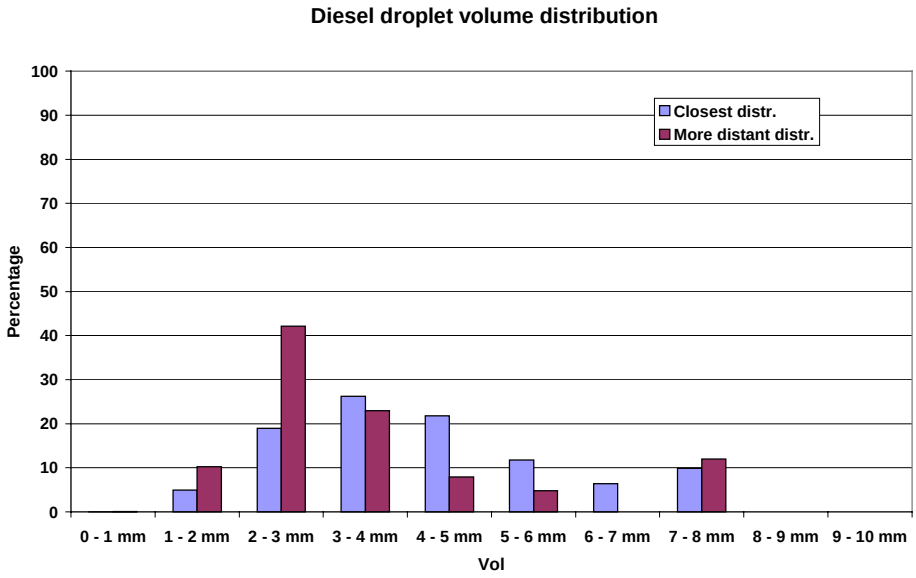

Figure 7.1.19. Distribution of the diesel droplet volumes, between 830 and 789 m depth. Cases 7 (closest distribution) and 8 (more distant distribution). "Close" and "more distant" refer to distance to bottom.

The results from the counts of the diesel droplets may be more difficult to interpret than the gas bubble (methane) release. One of the reasons for this is that the release consists of both gas bubbles (methane) and diesel droplets. In volume, the release consists of about 73 vol% of diesel and 27 vol% of gas at 845 m depth. However, both diesel and methane does not mix with water, and the bubbles/droplets observed may therefore be either methane gas bubbles, diesel droplets, or a mixture of both. It is therefore necessary to distinguish between the gas bubbles and the diesel droplets. This may not be so easy, because they may appear in the plume at the same time.

The first two cases (No. 5 and 6) were both recorded within 11 m from the release opening (at between 834 and 840 m depth). At this stage, the plume consists of a relatively violent mixture of the gas bubbles and the diesel droplets. Also, the vertical ascent of the plume is relatively fast. Simulations of the diesel release with the *DeepBlow* model indicated an average vertical velocity of the underwater plume equal to 0.5 m/s at 834 m depth (this depth corresponds to the end of Case No. 6).

Based on inspection of the ROV recordings, it was possible to distinguish between diesel droplets and gas bubbles. One of the differences in features is that the diesel droplets appear visually to be more "glassy" than the gas bubbles. Another indicator for separating the diesel droplets from gas bubbles is the motion characteristics. The gas bubbles tend to "wiggle" a lot, moving back and forth while ascending. The diesel droplets stay more calmly while they are ascending. The reason for this different motion characteristic is the varying momentum (mass times velocity) between gas bubbles (low momentum) and diesel droplets (large momentum). The Cases 5 and 6 (shown in Figures 7.1.16 and 7.1.17) showed over-all motion characteristics that appeared to be similar to a diesel droplet characteristic. The distributions shown in the Figure 7.1.16 and 7.1.17 are therefore assumed to be basically diesel droplets. However, at larger distances from the release source, the gas bubbles and diesel droplets may separate due to the difference in rise velocities of the individual bubbles/droplets. This is illustrated in the Figure 7.1.20, which illustrates the bent-over of the underwater plume caused by the ambient currents.

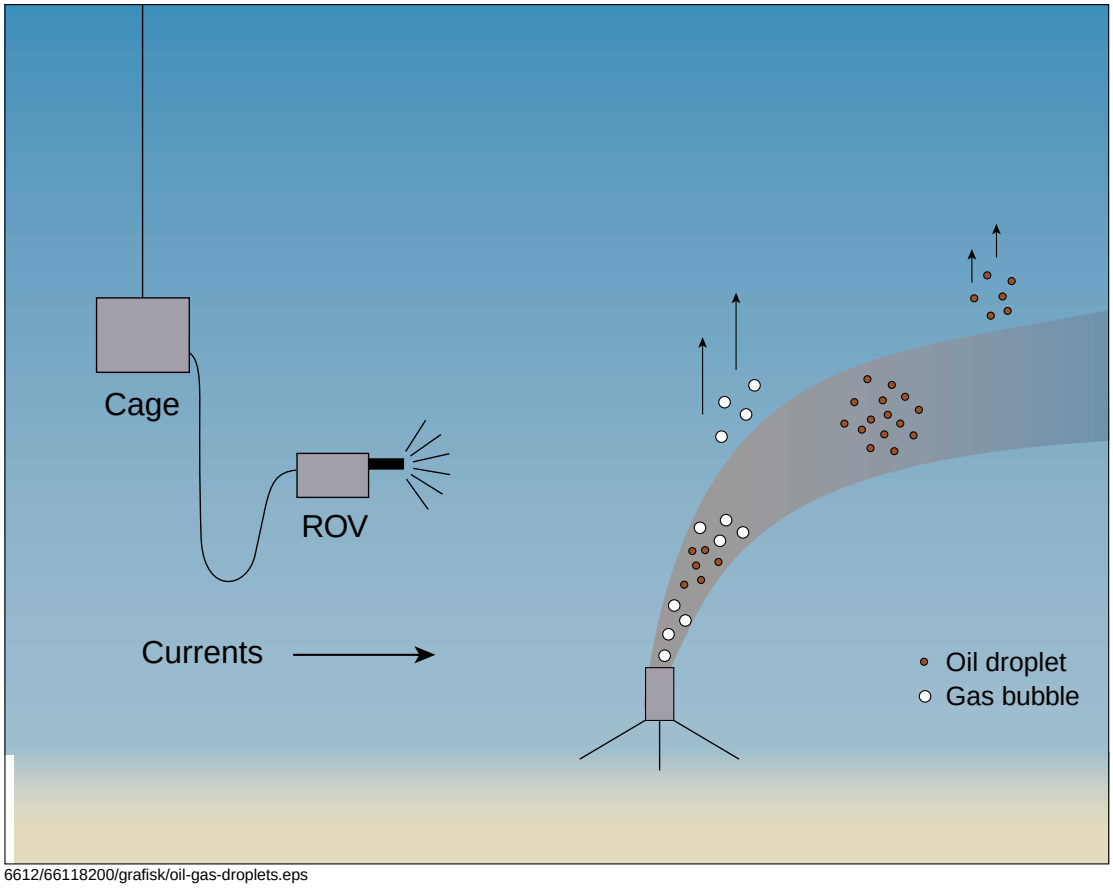

6612/66118200/grafisk/oil-gas-droplets.eps

Figure 7.1.20. Illustration of the leaving of gas bubbles and diesel droplets from a bent plume during the diesel release, release #2. Gas bubbles leave the plume first, due to larger rise velocity of the individual gas bubbles (0.3 m/s), compared to the rise velocity of the individual diesel droplets.

However, the gas bubbles and the diesel droplets have both their own motion relative to the plume due to the buoyancy of the individual droplets/bubbles. This individual motion of the bubbles/droplets will cause the bubbles/droplets to leave the plume, as illustrated in Figure 7.1.20. The gas bubbles will leave the plume first, because their rise velocity (about 0.3 m/s) is larger than the rise velocity of the diesel droplets. This process will thus cause the diesel droplets and gas bubbles to separate into different paths.

From Figures 7.1.16 – 7.1.19, it may seem that the distribution for the cases 7 and 8 are somewhat narrower than the distribution of the diesel droplets shown for the cases 5 and 6. However, this may also not be the case. Firstly, the number of large droplets counted are relatively small all together (for droplets larger than 6 mm, the sum of droplets counted for cases 5 and 6 is 17, while for cases 7 and 8, only 3 diesel droplets were counted). Secondly, the distribution may be biased because different sizes of the diesel droplets may move with different rise velocities if they have left the plume area. This may be the case for the droplets at the largest distance from the source. When the ROV is moving inside the droplet area, some sizes may be easier to be determined if the droplets move with the same velocity as the ROV. The size range of diesel droplets are typically of order 1 – 8 mm, which corresponds to a rise velocity in the range 5 – 12 cm/s. Therefore, the distribution observed may be biased due to a mismatch between the rise velocity of the ROV and the rise velocity of some of the diesel droplet size classes. Therefore it is difficult to conclude on the possible change in droplet size distribution as a function of the distance from the source.

The differences between the two counts may be more clearly seen in Figure 7.1.21, where the data from the two counts are shown together in terms of cumulative distributions. Also here, theoretical curves based on the Rosin-Rammler distribution are shown for comparison.

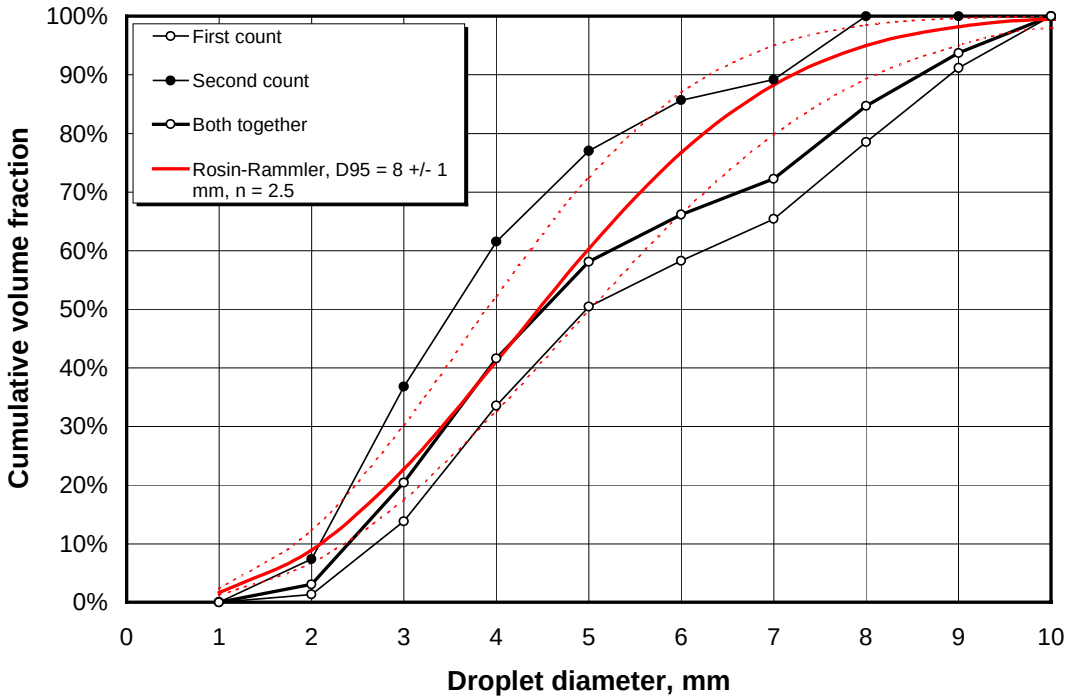

Figure 7.1.21 Droplet size distributions from the two counts shown together with theoretical distributions (Rosin-Rammler).

7.1.6 Conclusions from the ROV recordings.

The ROV cameras recorded on VHS tapes three of the four underwater plumes generated. The recordings were made from visual color camera, visual black/white camera and side-scan sonar.

The conclusions from inspection and analysis of the recordings are:

- The side-scan sonar signal failed to give good interpretation of the underwater plume. The reason for this is interference with noise generated by the cryogenic pump on "*Far Grip*".

- The black/white camera gave good visual impressions of the general features of the plumes generated. The diesel plume showed a clear tendency to meander and/or break up into separate "puffs".

- The color camera was able to track diesel droplet and gas bubble diameters. Both distributions were determined to be located basically between 1 and 8 mm diameter.

7.2 Echo sounder images

During the field trial, echo sounder images turned out to show clear responses on the underwater plumes generated. The images respond on both pure gas releases as well as mixtures of gas and oil/diesel releases. Echo sounder images were collected on both research vessels *Johan Hjort* and *Håkon Mosby*. These images were recorded continuously on tapes while the vessels were navigating to obtain the best possible coverage of the releases. Images for three of the four releases were selected for further processing. These were the releases of marine diesel (release #2), crude oil (release #3) and methane (release #4).

7.2.1 Images as seen onboard

Figure 7.2.1 shows an example of the echo sounder images obtained with the 38 kHz instrument mounted on *Håkon Mosby*. The image is from the crude oil and LNG discharge on June 29. The vertical axis indicates the depth, with the seabed visible at 840 meters. The horizontal axis indicates time (hours and minute), with markers at 6 minutes intervals. Note that the time axis is shifted 4 hours relative to UTC time (add 4 hours to get UTC). The greenish band at 250 to 450 m is biological material (plankton) situated around the perennial thermocline. The plume of oil and gas is visible as reddish “blobs”. The image was obtained while the research vessel was circling around the discharge vessel.

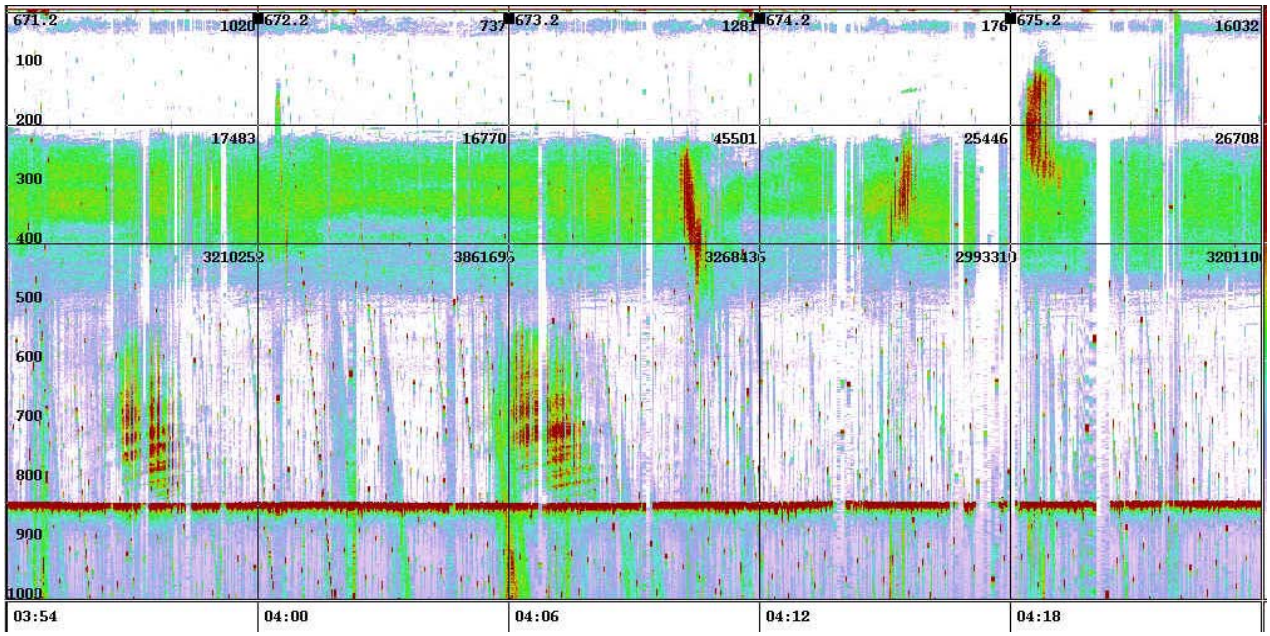

Figure 7.2.1 Echo sounder image as observed on Håkon Mosby during the crude oil and LNG discharge June 29. The horizontal axis indicates time (hours and minute), with markers at 6 minutes intervals. Note that the time axis is shifted 4 hours relative to UTC time (add 4 hours to get UTC). The vertical axis indicates the depth, with the sea bed visible at 840 meters.

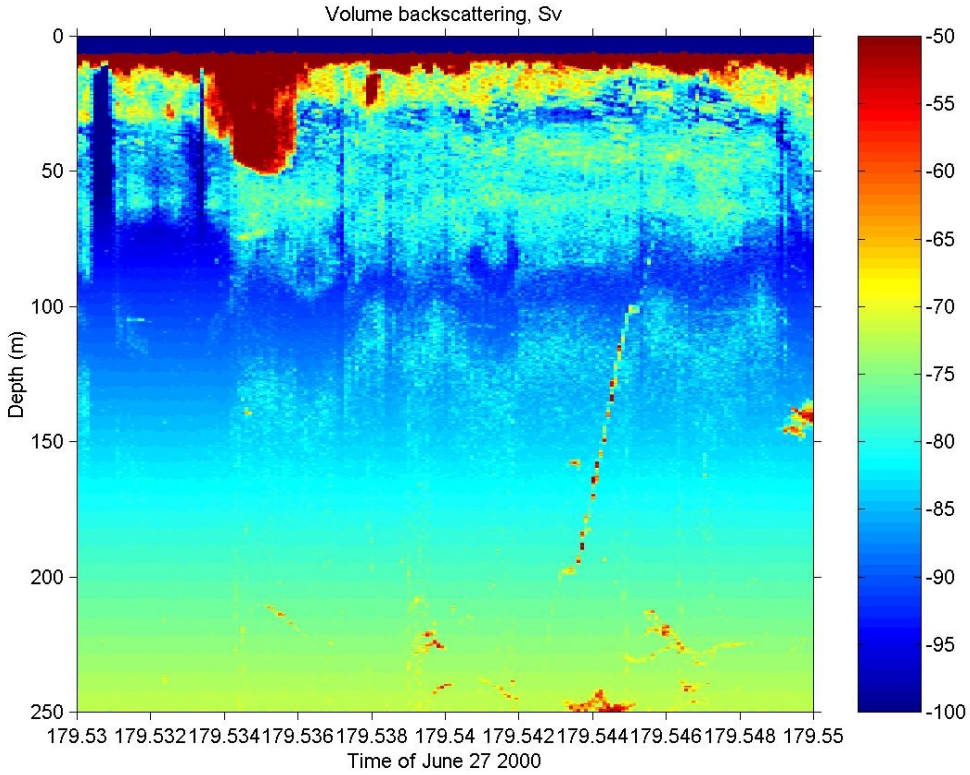

Figure 7.2.2 Image from the 120 kHz echo sounder at Johan Hjort obtained on June 27th during the marine diesel oil and LNG discharge. The picture shows a close up of the depth interval from surface to 250 m. The horizontal axis indicates time in decimal days. The trajectory of the carousel sampler is seen as a dotted inclined line to the right in the picture.

Figure 7.2.2 shows an example of an image obtained with the 120 kHz echo sounder operated from *Johan Hjort*. The figure shows a close up of the depth interval from surface to 250 m depth. The trajectory of the carousel sampler is visible on the image as a dotted inclined line to the right in the picture. The echo sounder on *Johan Hjort* is a multi-frequency system, also operating at 38 kHz and 200 kHz.

7.2.2 Post-processing

The raw data from the echo-sounder measurements are stored in two Excel files in the ECHOdata directory – one file for each research vessel (HakonMosby.xls and JohanHjort.xls). The data are arranged in separate worksheets for June 27 and June 29. Each worksheet contains records with the following parameters:

YEAR, MONTH, DAY:	Date
HOUR, MINUTE:	UTC time
LAT, LONG:	Latitude and longitude in decimal degree
CHAN#:	Channel number; number given to each bin (10 m intervals)
PDMIN, PDMAX:	Top and bottom level of bin, meters
PLANK	Strength of echo-sounder back scattering signal in the bin

During the processing of the data, it turned out that the presentation of the results is not an easy task. The reason for this is that the underwater plumes generated are moving in a 3D space, where the horizontal position is changing with the ambient currents. In addition, the rise of the plume extends far beyond the time instant when the release has been switched off. These effects cause an underwater plume varying in both three dimensions and time, which is difficult to represent in a paper plane. The first type of presentation was made as x-y plots, showing the geographical location of the plume along with the paths of the research vessels. For each of the three releases, 6 plots are shown. Three plots are for various depth intervals (below 600 m, 300 – 600 m and above 300 m depth). These plots were presented for two time intervals, each one lasting for about one hour. The first hour interval corresponds to the time of the release, while the second time interval is representing the hour immediately following the termination of the release.

Since both vessels have the 38 kHz data, these were chosen as the basis for the collocations of the echo-sounder observations shown in Figure 7.2.3. This and the following figures shows a birds eye view of the echo sounder recordings vertically integrated within the three depth ranges, 600 m to bottom, 300 – 600 m, and surface to 300 m depth. Note that the signal from the biological material (plankton) has been subtracted from the data. The plots show the trajectory of the research vessel with the depth integrated strength of the area back scattering signal marked with dots in different colors. The corresponding signal strength is given on the color bar to the right on each plot.

Figures 7.2.9 to 7.2.11 show a second type of presentation in the form of x-z, y-z projections of the data obtained within chosen time intervals. The echo-sounder signals are shown as measured in 10 m depth intervals (bins) with a color code representing the signal strength. One image is shown for each experiment, each covering one hour of data. We will return to these representations of the echo-sounder data in Chapter 9 – dealing with modeling and analysis.

Attempts have also been made to produce 3D presentations of the data. Such plots proved to be quite illustrative, but the actual quantitative aspects of the echo-sounder data were in general difficult to read out of these images.

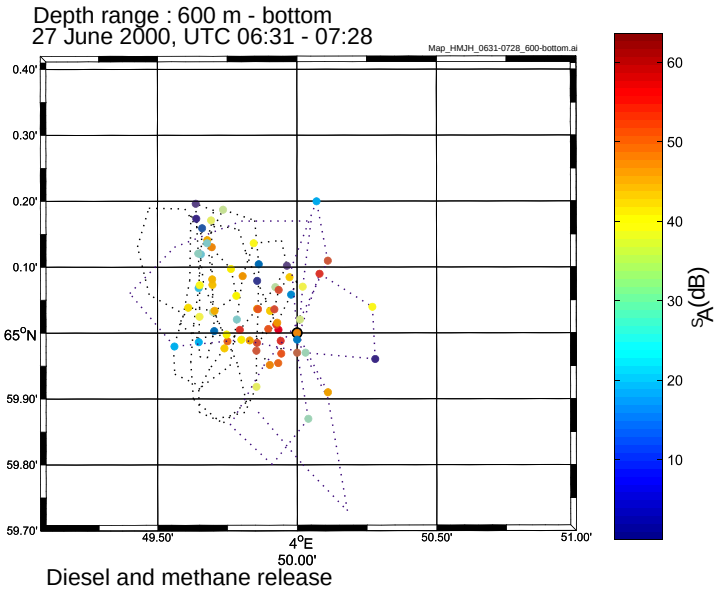

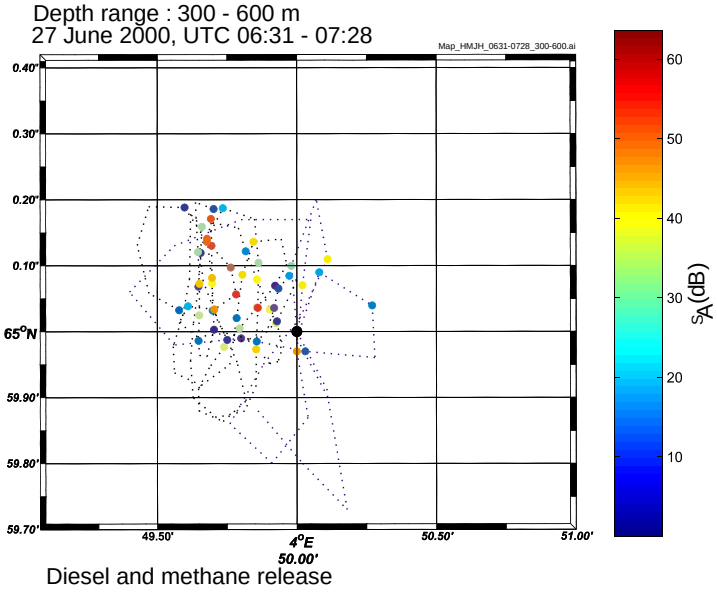

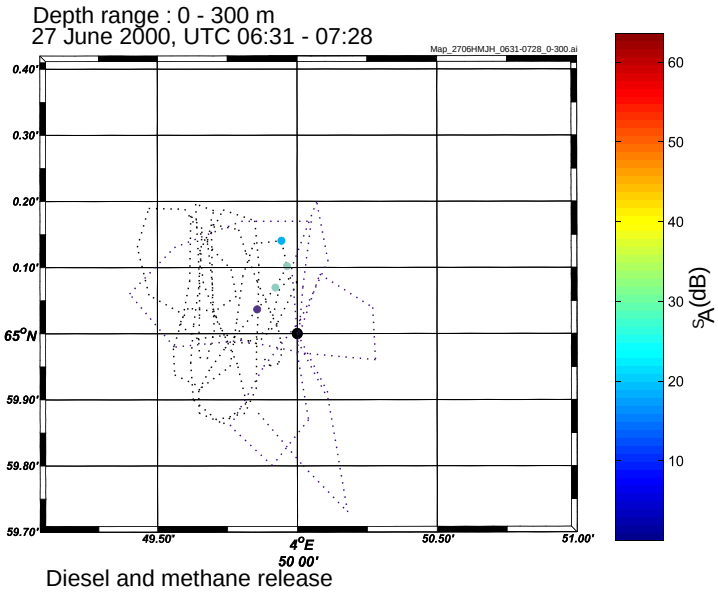

Figure 7.2.3 Birds eye view of the 38 kHz echo sounder data obtained from Håkon Mosby and Johan Hjort. The integral strength of the area back scattering in the given depth range is marked with color coded dots (se color bar to the right). The trajectories of the two vessels are indicated by dotted lines (black for Håkon Mosby, blue for Johan Hjort).

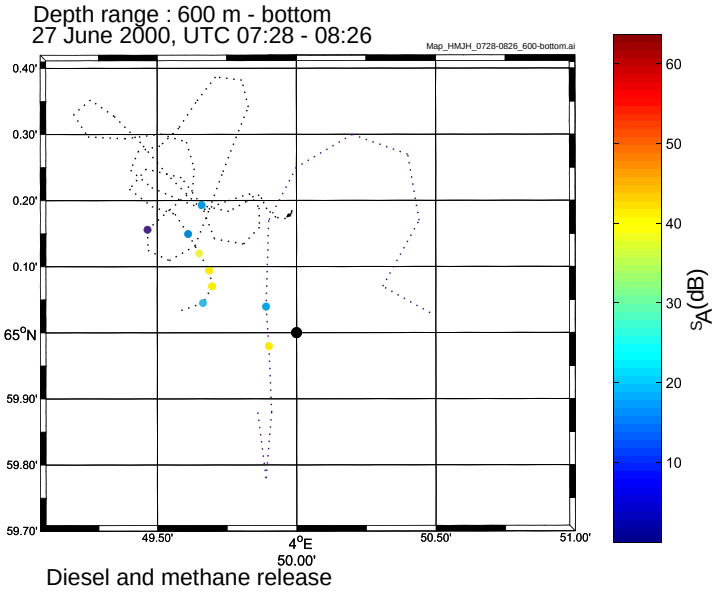

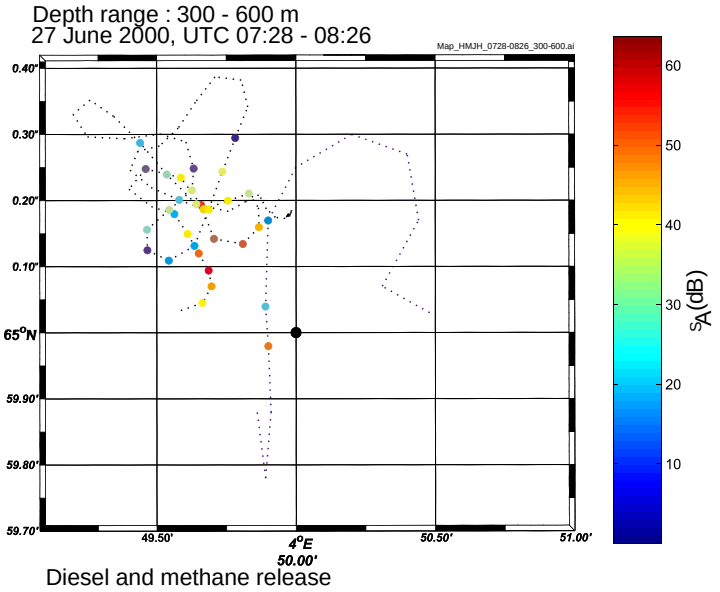

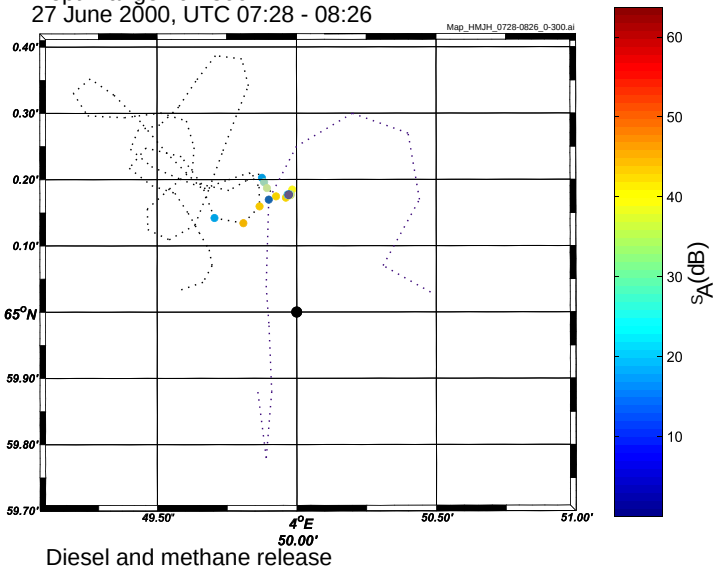

Figure 7.2.4 See Figure 7.2.3 for details

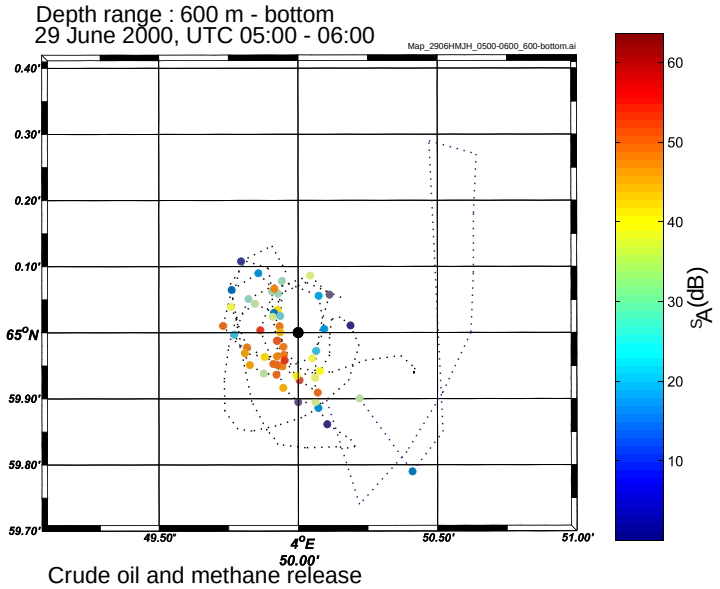

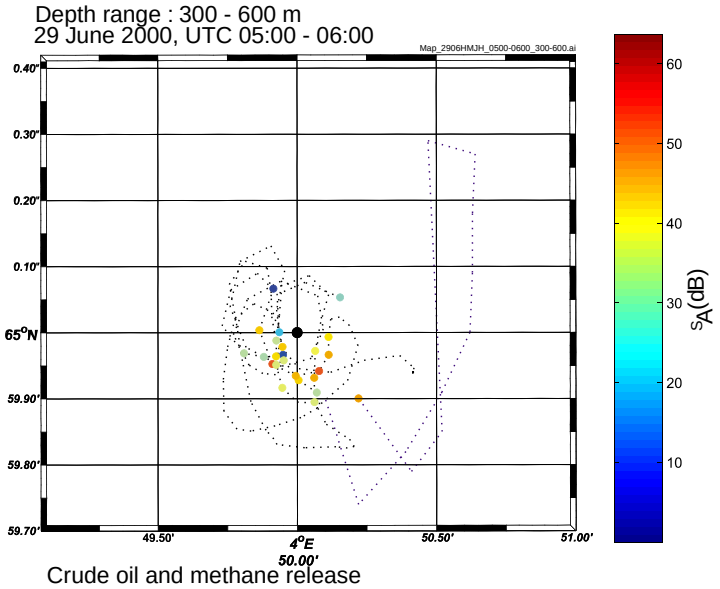

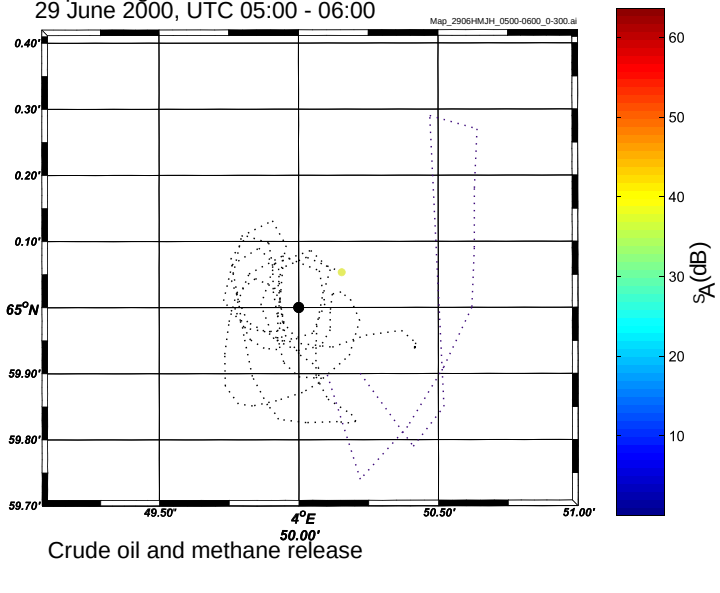

Figure 7.2.5 See Figure 7.2.3 for details

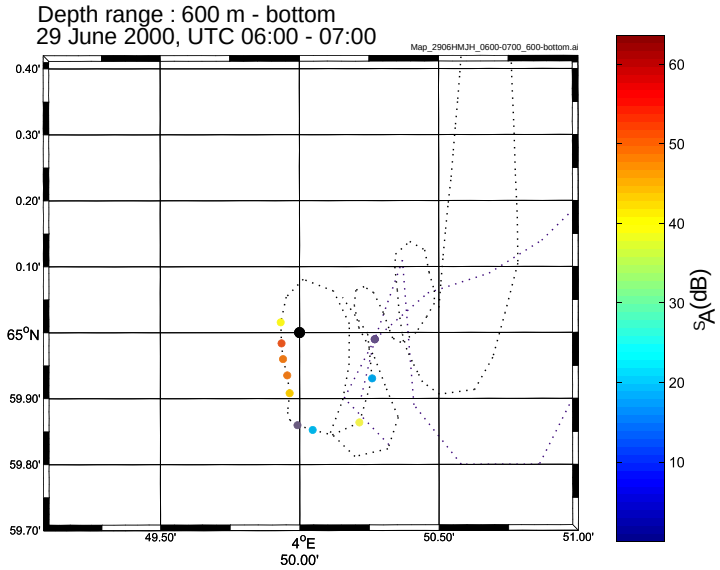

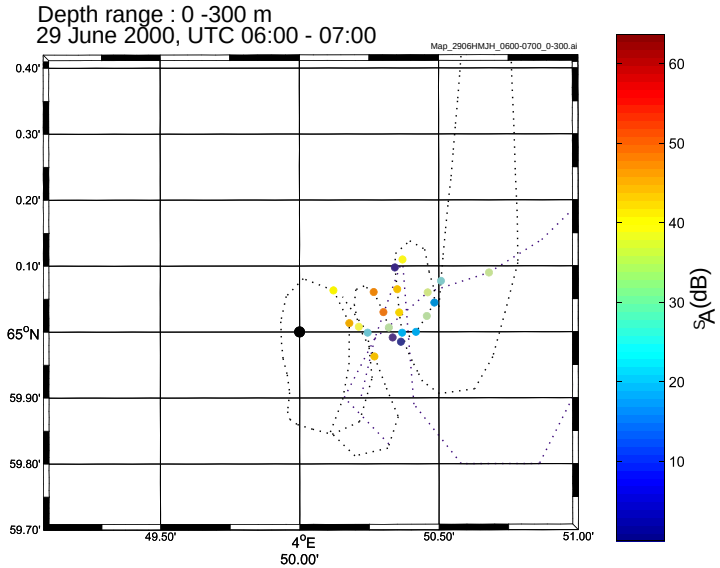

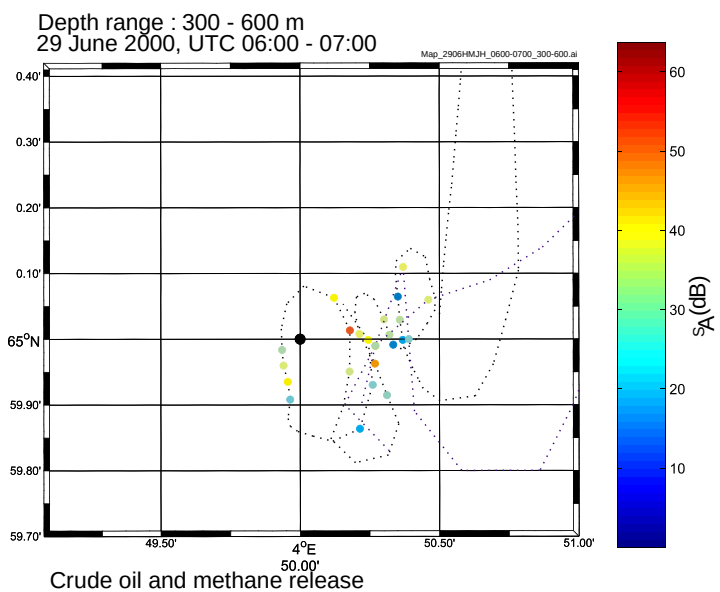

Figure 7.2.6 See Figure 7.2.3 for details

Depth range : 600 m - bottom
29 June 2000, UTC 08:55 - 10:01 Methane release

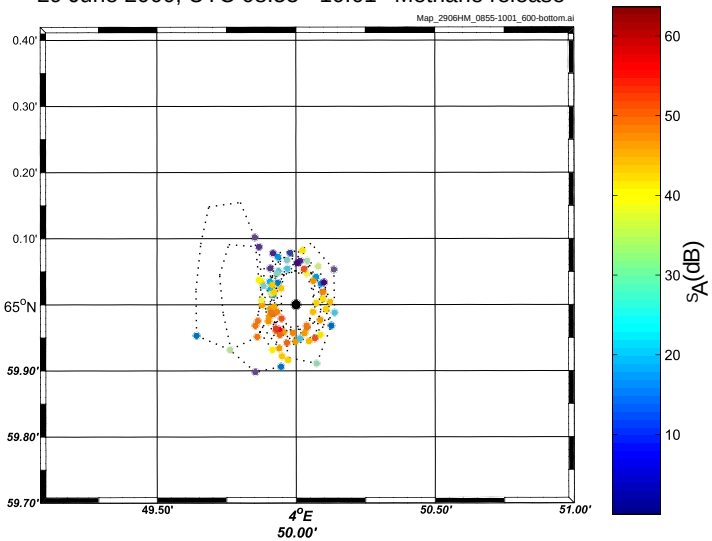

Depth range : 300 - 600 m
29 June 2000, UTC 08:55 - 10:01 Methane release

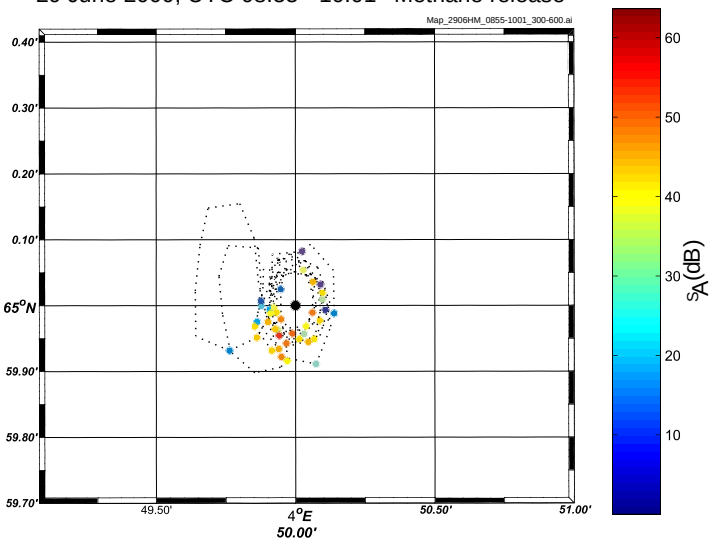

Depth range : 0 - 300 m
29 June 2000, UTC 08:55 - 10:01 Methane release

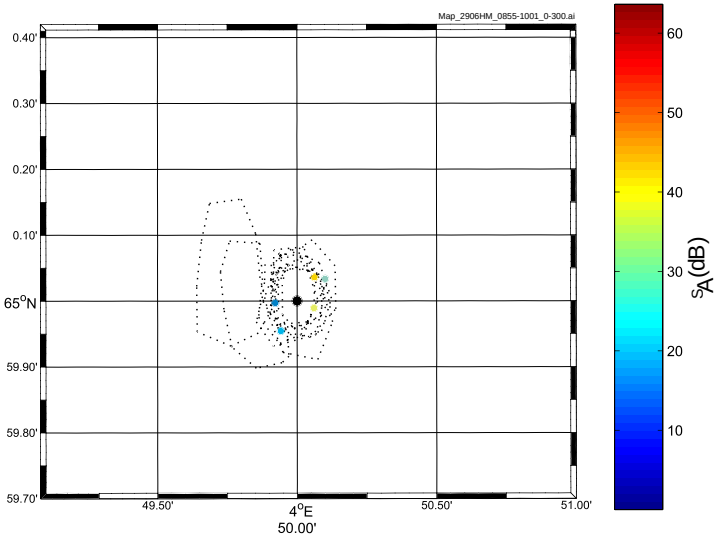

Figure 7.2.7 See Figure 7.2.3 for details

Depth range : 600 m - bottom
29 June 2000, UTC 10:04 - 10:53 Methane release

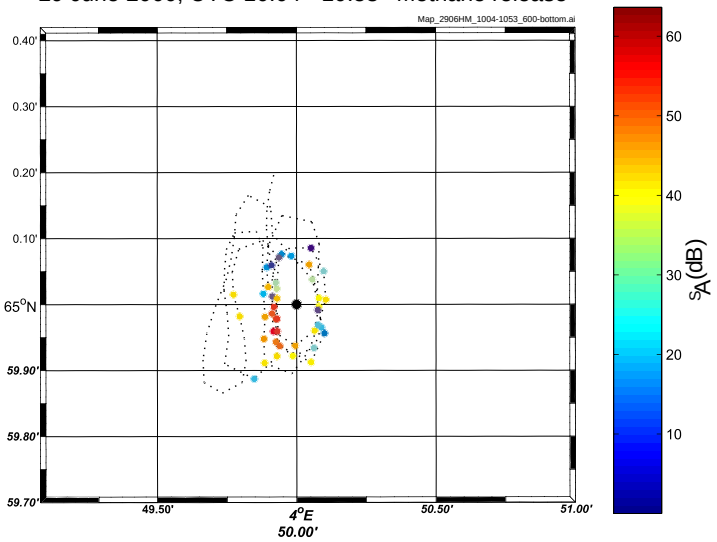

Depth range : 300 - 600 m
29 June 2000, UTC 10:04 - 10:53 Methane release

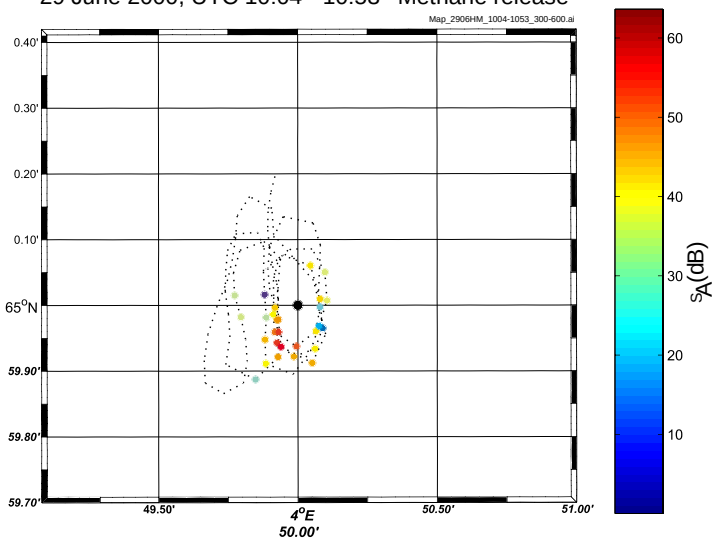

Depth range : 0 - 300 m
29 June 2000, UTC 10:04 - 10:53 Methane release

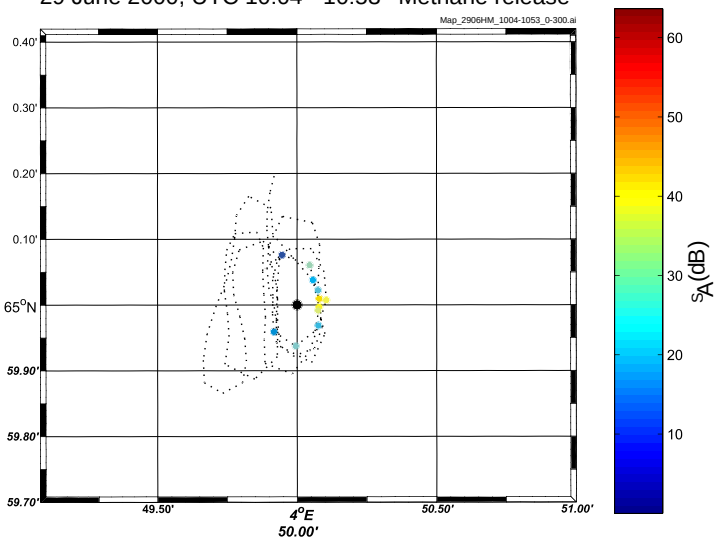

Figure 7.2.8 See Figure 7.2.3 for details

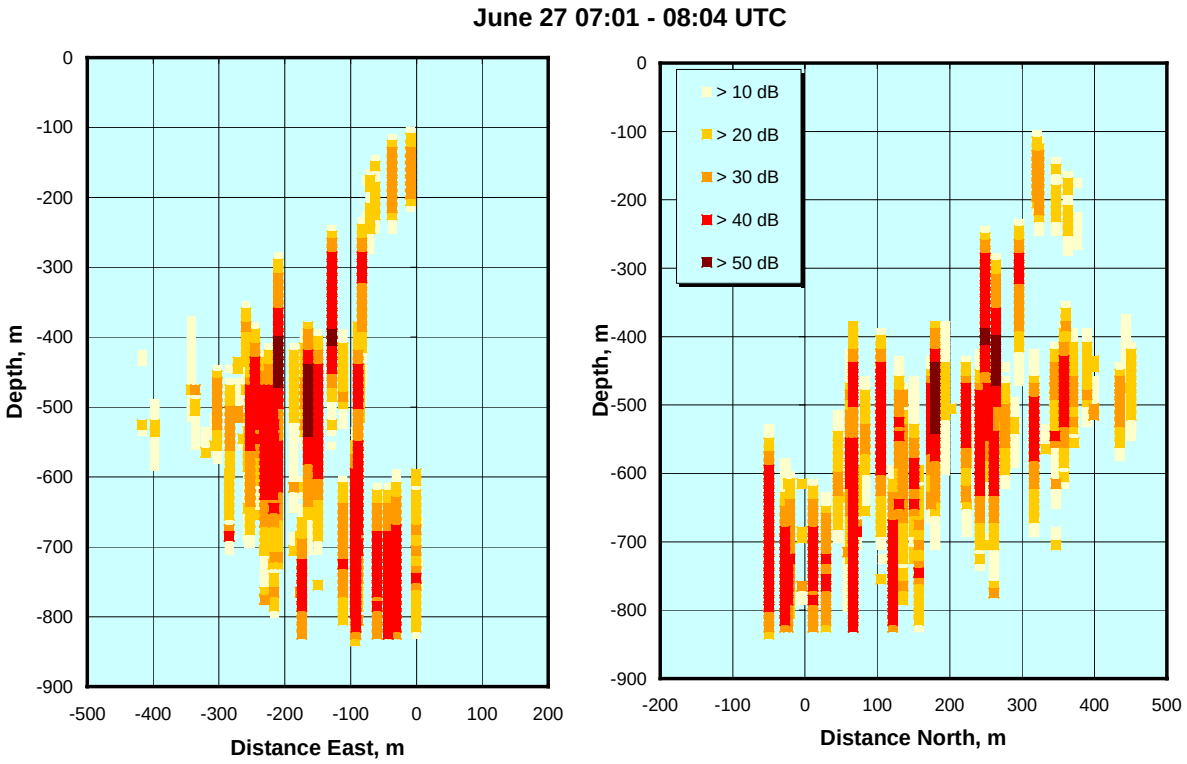

Figure 7.2.9 Example of side view of echo sounder data from the Marine Diesel experiment. The discharge started at 06:30 UTC and lasted for one hour.

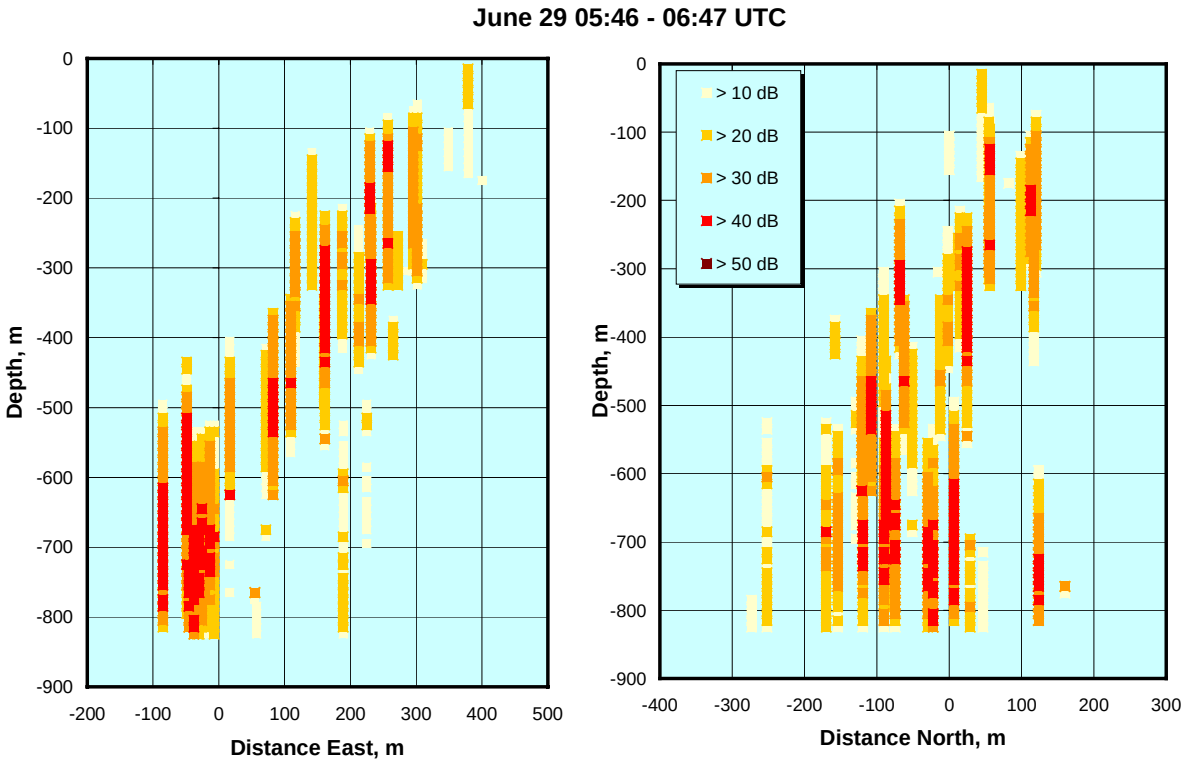

Figure 7.2.10 Example of side view of echo sounder data from the Crude Oil experiment. The discharge started at 05:20 UTC and lasted for one hour.

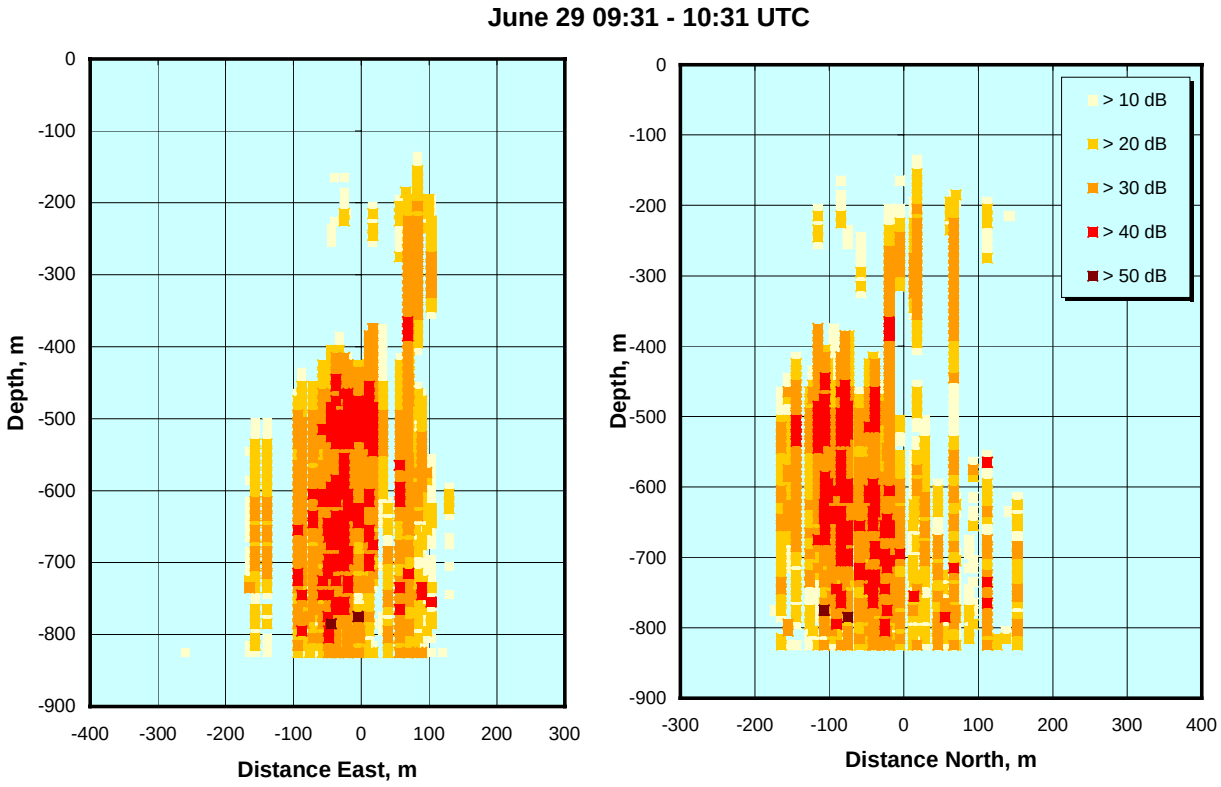

Figure 7.2.11 Example of side view of echo sounder data from the LNG experiment. The discharge started at 09:00 UTC and lasted for two hours.

7.3 Waters samples from the Rosette sampler

7.3.1 General

The release of crude oil and marine diesel at 844 m depth represents a unique opportunity to study the fate of the oil while ascending through the water column to the sea surface. This opportunity was taken care of by carrying out measurements of hydrocarbon concentrations in the water column. Sampling was carried out inside the ascending oil or diesel droplet areas in order to obtain “signatures” of the crude oil or diesel that was (or had been) there.

Oil that ascends through the water column will leave some of its compounds as dissolved matter in the water column. Different compounds will dissolve at different rates. As examples, mono-aromatics, naphthalenes and phenols are all relatively water-soluble compounds. By measuring the concentrations of selected compounds at various depths, information may be obtained on the rates of dissolution of these compounds into the water column. The purpose of the analysis presented here is to exploit the prospects of obtaining dissolution rates of various oil/diesel compounds from the data collected.

The dissolution potential of water-soluble oil components in seawater is an important factor when considering potential ecotoxicological effects from acute releases. This is particularly relevant in connection to underwater releases. Information on dissolution rates of water-soluble components is of special interest due to their bio-availability towards marine organisms. Rising oil droplets in the water column will effectively be extracted in the water, and leave behind a track of dissolved water-soluble oil components.

The kinetics of dissolution of water-soluble components is dependent upon factors as droplet size, droplet composition, viscosity in the oil droplets, diffusion rate, temperature, exposure time (depth) and possible skin formation (which is dependent upon the content of surface active agents in the oil, as waxes, resins and asphaltenes). Laboratory studies of the dissolution rates of water-soluble oil components clearly show great differences in dissolution potential between different groups of components, but it has been difficult to relate these rates to dissolution rates related to a deep blow scenario due to lack of relevant field data.

The *DeepSpill* experiment provides a unique opportunity for study of dissolution of water-soluble components from rising oil or diesel droplets. Sampling was performed using a remote operated rosette sampler lowered in a cable from the research vessel *Johan Hjort*. Positioning of the sampler in the water column was decided on basis of echo sounder images on board *Johan Hjort*. The rosette sampler was also equipped with a UV-fluorometer, and it was initially planned to use signals from this instrument to detect areas with high concentration of oil. The UV-fluorometer, however, did not perform according to specifications, and the rosette sampler was guided by the signal from the echo sounder only. Details of the equipment used are given in Chapter 5.2.3.

Table 7.3.1 gives an overview of water samples taken during the field experiment. Blank water samples was collected the day before the marine diesel release. For both releases, two successful profiles were collected (series MD #2 and MD #3 for the marine diesel and series OB #1 and OB #2 for the oil release).

Table 7.3.1 Water samples taken by rosette sampler during the DeepSpill field experiment. Series 0 represents blind samples and series MD #1 did not hit the volumes of water containing the diesel.

Discharge information	*Series*	*Sample time (local time)*	*Sample depths (m)*
Blind samples, June 26	0	NA	800, 500, and 300
Marine Diesel, June 27	MD #1	0920	No samples. Outside plume area.
Marine Diesel, June 27	MD #2	1100 – 1115	300, 250, 200, 150, 140, 100, 50, 25, and 10
Marine Diesel, June 27	MD #3	1445 – 1500	300, 200, 100, 75, 25, and 10
Crude oil, June 29	OB #1	0800 – 0815	500, 450, 400, 300, 200, and 100
Crude oil, June 29	OB #2	0940 – 0955	250, 200, 100, 50, 25, and 10

The results from the chemical analysis of these samples are stored as Excel-files in the CHEMdata directory. The sampling positions of the rosette measurements are shown in Figure 7.3.1 for the diesel release and Figure 7.3.2 for the crude oil release. The contours of the crude oil and diesel slicks are also shown in order to indicate the position of the sampling locations relative to the positions of the slick areas.

7.3.2 Outline of method

Concentrations of hydrocarbons in the water column has been measured both as total extractable organic compounds (TEOC), which is then the sum of dissolved organic components and the dispersed oil, and as specific PAH compounds.

Analysis of the water samples is based on gas chromatography and coupled gas chromatography / mass spectrometry. The analysis gives concentrations of specific organic compounds, both volatile organic compounds (VOC) and semi-volatile organic compounds (mainly PAH). We are in this report presenting the sum of specific volatile organic compounds (VOC), the sum of specific PAH compounds, and the total concentration of organic compounds, given as TEOC. In addition, we are presenting some examples of detailed analysis of the most water-soluble compounds; BTEX’s and Naphthalenes.

Another group is the “some specific PAH”, including the naphthalenes. These have all carbon numbers larger than 9, and are partly water-soluble. By considering the concentration of the various components (or component groups) as a function of depth, some conclusions can be drawn on the dissolution rates of the various components. This will be explained in the following based on the results from both the diesel and the crude oil release.

It is not possible to distinguish between dissolved hydrocarbons and hydrocarbons present in dispersed oil in the chemical analysis of the water samples. Any change from the original oil/diesel composition in the analysis of the recordings will be an indicator of some dissolution of water-soluble compounds into the water column. The concentration of oil components dissolved in the water column will vary with depth, with the highest concentrations at the point in the water column with the highest integrated exposure of rising oil droplets. The largest concentration of TEOC will be basically inside the “cloud” of rising oil droplets, whereas the peak concentration of

the dissolved compounds may be deeper, due to a larger exposure of oil droplets that have passed by. See illustration in Figure 7.3.3.

In the following, three figures will be shown for each of the four data sets. First figure will show the vertical variation of the TEOC, the VOC and the PAH's. The second figure shows the results when breaking down the sum of specific volatile components (VOC) into different groups of related components (that is, BTEX's, naphtenics and aliphatics).

The third figure may be the most interesting one. In this figure, Naphthalene and its homologous series of alkylated Naphthalenes up to C4 is shown. At the same time, the concentrations have been normalised to the concentration of the Fluoranthene in the oil/diesel (a component which has a negligible solubility in sea water). A normalised value of 100 % of any of the homologues of the Naphthalenes indicates that the component considered has not been depleted from the oil/diesel. Thus, it is possible to study the rate of depletion of specific compounds from the oil, which, in turn, may form a basis for calculation of dissolution rates for different oil components.

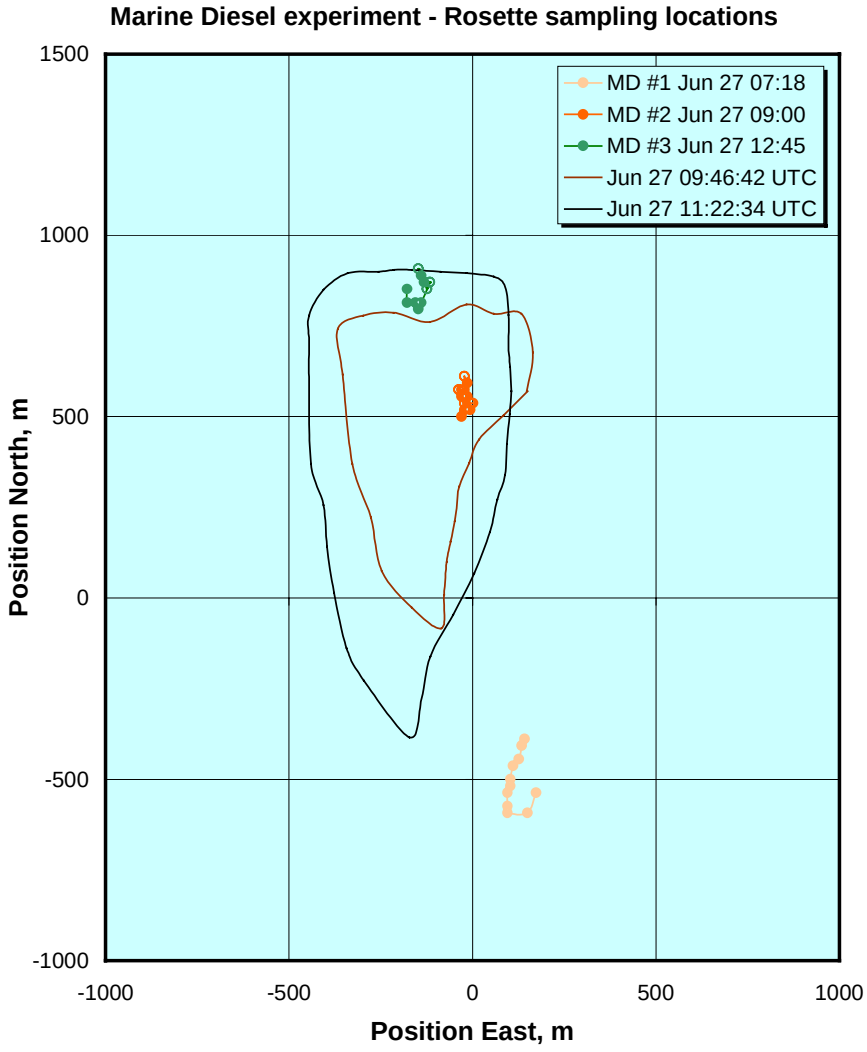

Figure 7.3.1 Position and time of water sampling carried out during the diesel release. Contours of the diesel slick are shown in addition. All hours are given in UTC time. The diesel release took place at about 0630 – 0730 UTC (0830 – 0930 local time).

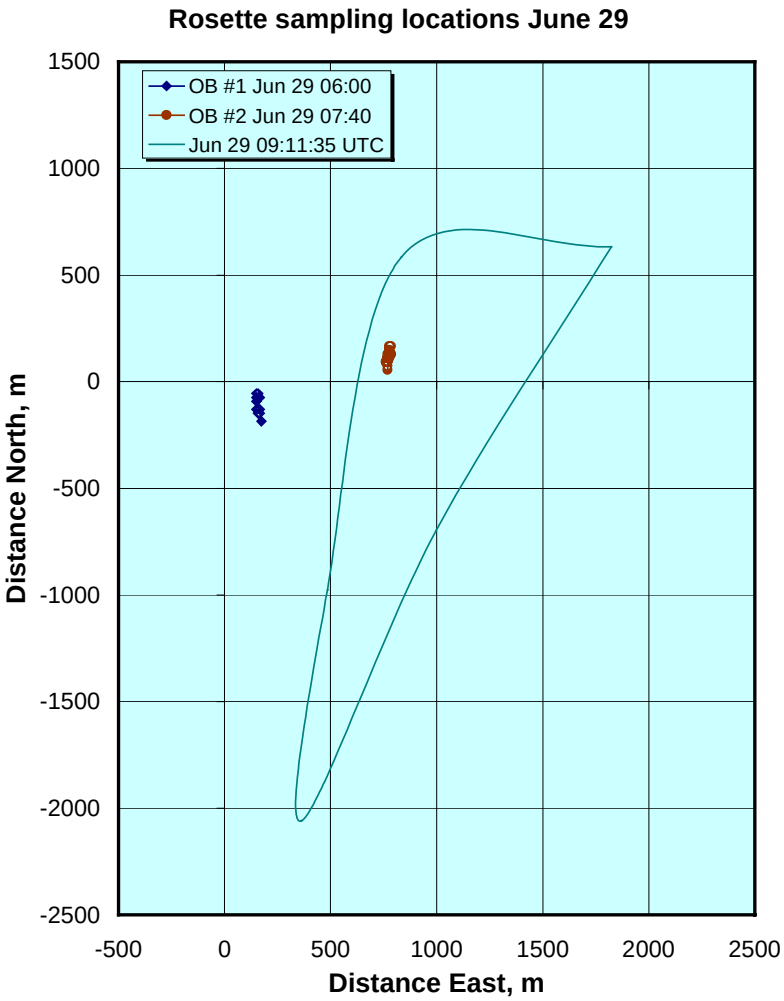

Figure 7.3.2 Position and time of water sampling carried out during the oil release. Contours of the oil slick are shown in addition. Note the distance in time between the sampling with the rosettes and the contour of the slick. All hours are given in UTC time. The oil release took place at about 0520 – 0620 UTC (0720 – 0820 local time).

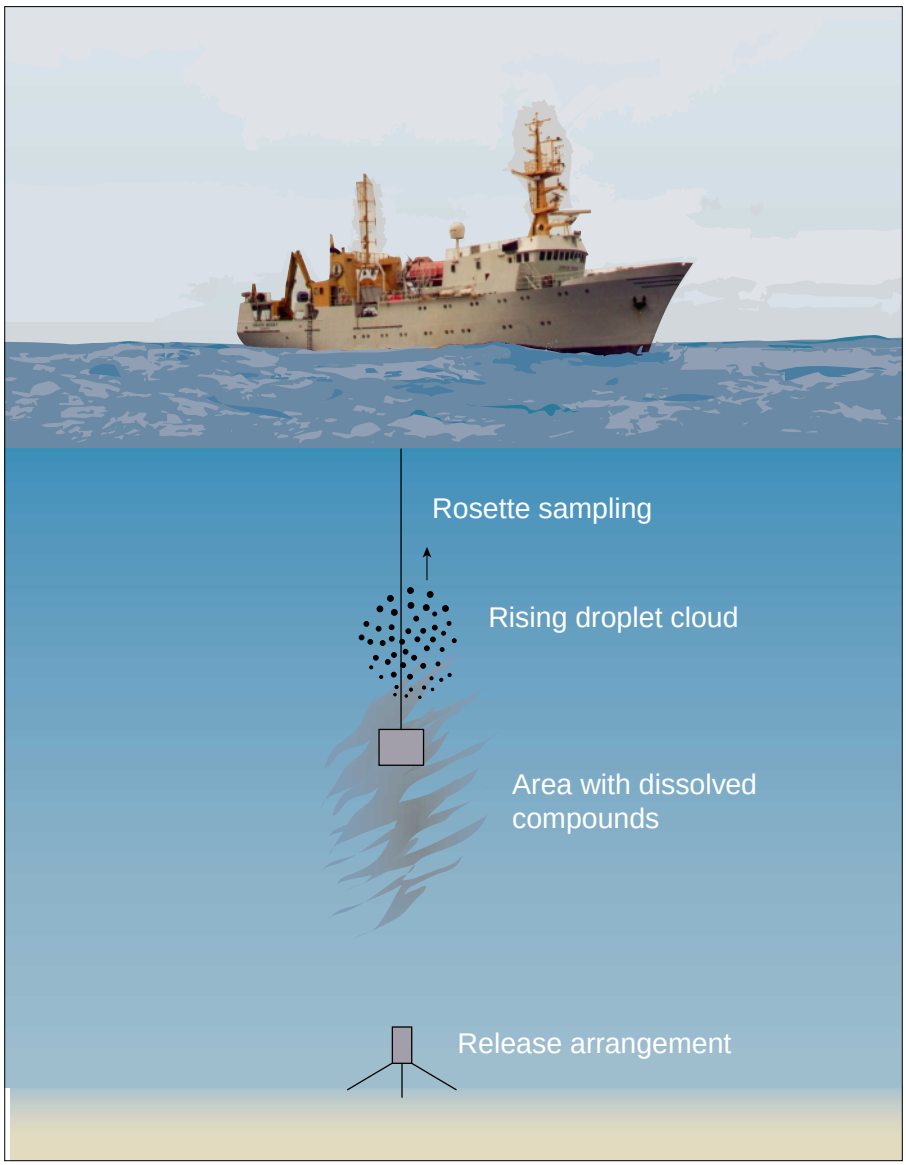

Figure 7.3.3 Illustration of the dissolution of water-soluble compounds from oil droplets into the water column. At the front of the rising oil/diesel droplet cloud: Relatively low contents of water-soluble compounds in the water column, because these compounds have been partially depleted from the droplets at larger depths. Just below the droplet cloud: Relatively high contents of water-soluble compounds in the water column, which have been extracted from the droplets just passed.

7.3.3 Marine diesel release, Series MD #2.

This profile show the concentrations at about 90 minutes after the completion of the diesel release. The bulk of the diesel droplets (or the largest size diesel droplets) may therefore have reached the sea surface at the time of the sampling.

Results for the vertical variation of the TEOC, the VOC and the PAH's are shown in Figure 7.3.4. TEOC and sum specific PAH components show a maximum concentration at 150-200 metres depth. The concentration of the sum of VOC shows a concentration profile that varies and is

apparently not correlated to the concentration profile of TEOC and the sum of specific PAH components.

However, when breaking down the sum of specific volatile components into groups of related components (that is, BTEX's, naphtenics and aliphatics), a different picture appears, as is shown in Figure 7.3.5. The concentration profile of BTEX, with peak concentration at approximately 100 m, is different from the concentration profile of the aliphatics, which has a peak at approximately 250 m.

The total concentration of oil is the sum of dissolved organic compounds and dispersed oil. The sum of specific volatile organic compounds shown in Figure 7.3.4 is therefore the sum of dissolved compounds and compounds in the dispersed oil. The various volatile compounds have different solubility in seawater, where the aliphatic and naphthenic compounds have significantly lower solubility compared to the volatile aromatic compounds (BTEX's). Figure 7.3.5 shows that the peak concentration of aliphatic compounds are found at 250 metres, which correlates reasonably good with the peak concentration of TEOC at approx. 200 metres.

The situation is further clarified in Figure 7.3.6 where the normalised homologous series of Naphthalenes is considered. The normalised profile shows the degree of dissolution of the individual Naphthalenes (a decrease in the ratio between a Naphthalene and Fluoranthene indicates a depletion of the Naphthalene in the sample, compared to the starting point). The normalised concentrations are plotted normalised to the ratios between Naphthalenes and Fluoranthene in fresh marine diesel (set to 100%).

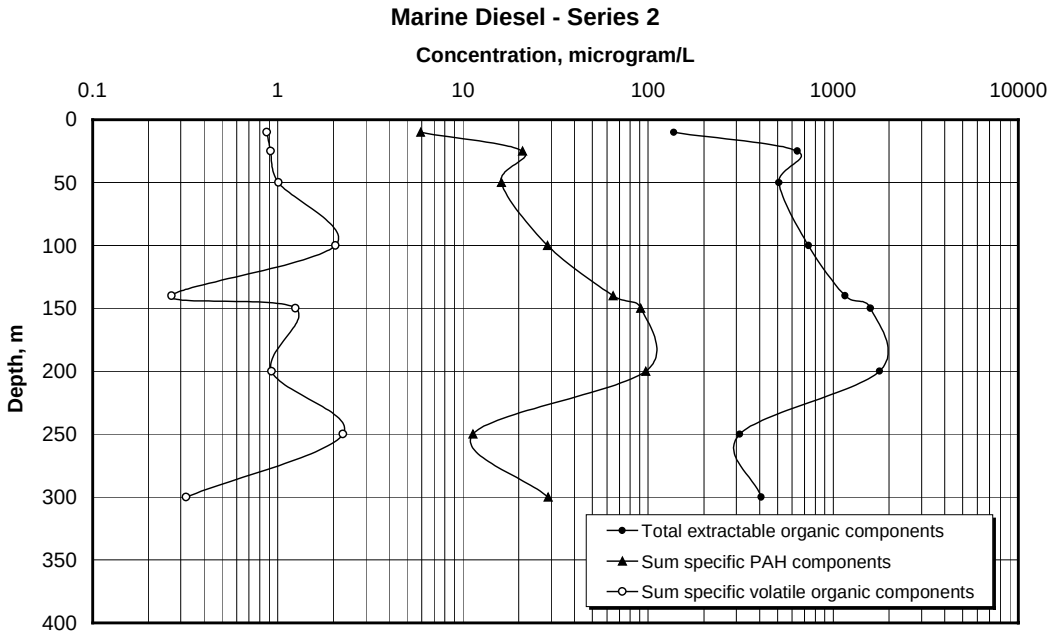

Figure 7.3.4 Concentration profiles of sum specific PAH components, sum specific volatile organic components (VOC), and total extractable organic compounds (TEOC) in the water column during discharge of marine diesel, series MD #2.

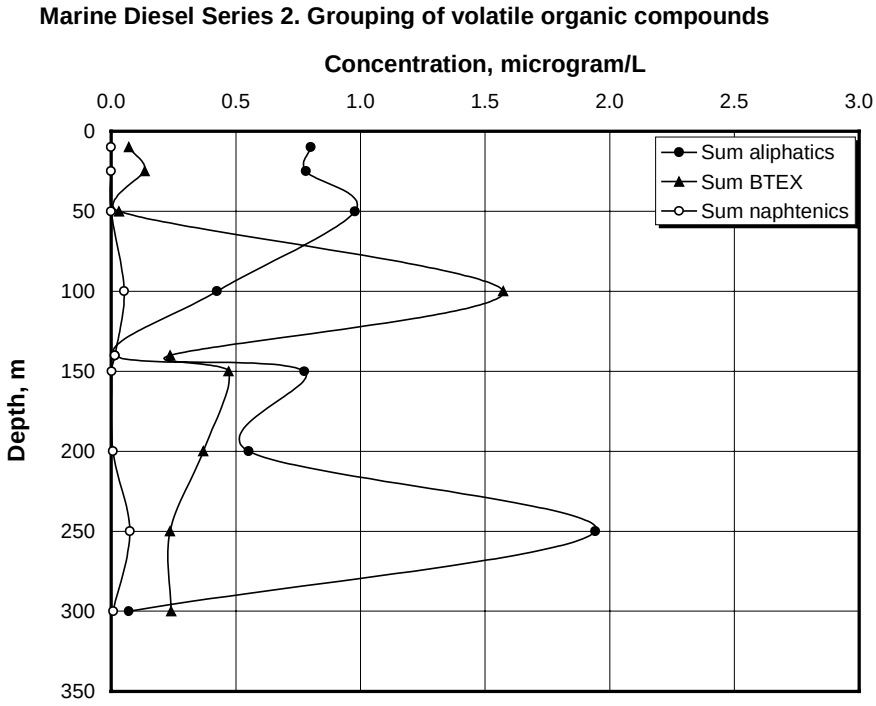

Figure 7.3.5. Concentration profiles of groups of volatile organic compounds in the water column during discharge of marine diesel, series MD #2.

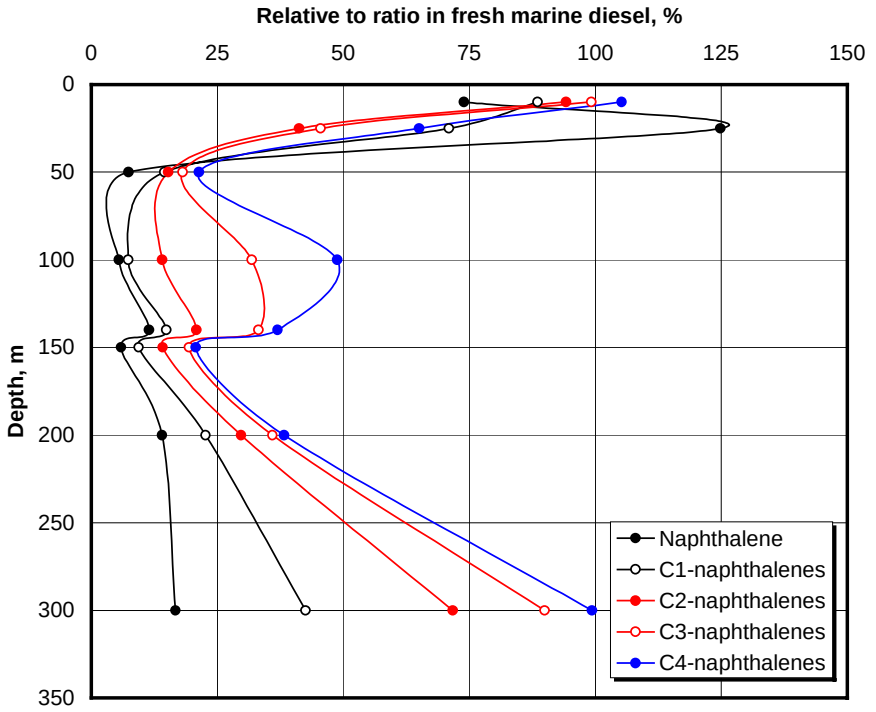

Figure 7.3.6 Profiles of normalised concentrations of selected oil components in the water column during discharge of marine diesel, series MD # 2. The concentrations of the individual components are normalised to the concentration of Fluoranthene, and the ratios are plotted normalised to the corresponding ratios in fresh marine diesel.

The results show one peak ratio between the Naphthalenes and Fluoranthene at maximum depth of sampling (300 m). The different Naphthalenes show a ratio of 20-100% compared to the same ratios in fresh marine diesel. This reflects the initial dissolution of the various compounds from the discharge point and up to 300 meters depth. The Naphthalenes are ranked according to their water solubility (unsubstituted Naphthalene is the most water-soluble component, and C4-Naphthalene is the least water-soluble component). The C4-naphthalene can thus be interpreted as not been dissolved at all (at 300 m depth), while the other compounds have been dissolved to a variable extent (20 – 90 %) on their way up to 300 m depth.

From 300 meters depth and up to approximately 50 meters, the individual ratios decrease to 7-20%, which means a significant dissolution of Naphthalenes from the oil droplets discharged at approx. 800 meters depth. In the samples from 25 and 10 meters depth, it is observed that the ratios rapidly increases back to original ratios in fresh marine diesel near surface. It is believed that this is an effect of the Naphthalenes from accumulated oil on the surface and re-dispersed oil into the upper water masses below the oil slick due to wave action.

7.3.4 Marine diesel release, Series MD #3

This profile shows the situation after more than 5 hours after the completion of the diesel release. At this time, diesel droplets (of smaller sizes) were still arriving at the sea surface. A contour of the surface slick observed about 80 minutes before the time of the sampling is shown in Figure 7.3.1.

Figure 7.3.7 shows the distribution of TEOC and VOC for this case. The PAH's were not analysed in this case. An overall increase of TEOC near surface is observed in this sample series. The explanation for this is that the bulk oil has reached the surface, and the increased concentration of oil in water masses near the surface may be re-dispersed oil from the sea surface.

A corresponding decrease in VOC is also observed at the sea surface. This may be due to evaporation of the VOC compounds at the sea surface.

The results of the VOC analysis show a drop in the concentration in the 75 m sample. This sample is regarded as an outlier in the data analysis.

When breaking down the sum of VOC into groups of related components (see Figure 7.3.8), it can be seen that the concentration profile of the volatile organic compounds, with peak concentration at approximately 100 m, is dominated by the content of aliphatic components in the samples. The very low concentration of aromatics in these samples is explained by the long retention time of the oil in the water column at time of sampling, which results in an almost total depletion of these relatively highly water-soluble components.

Because PAH-s were not analysed, no figure for the normalised PAH concentrations is shown for this case.

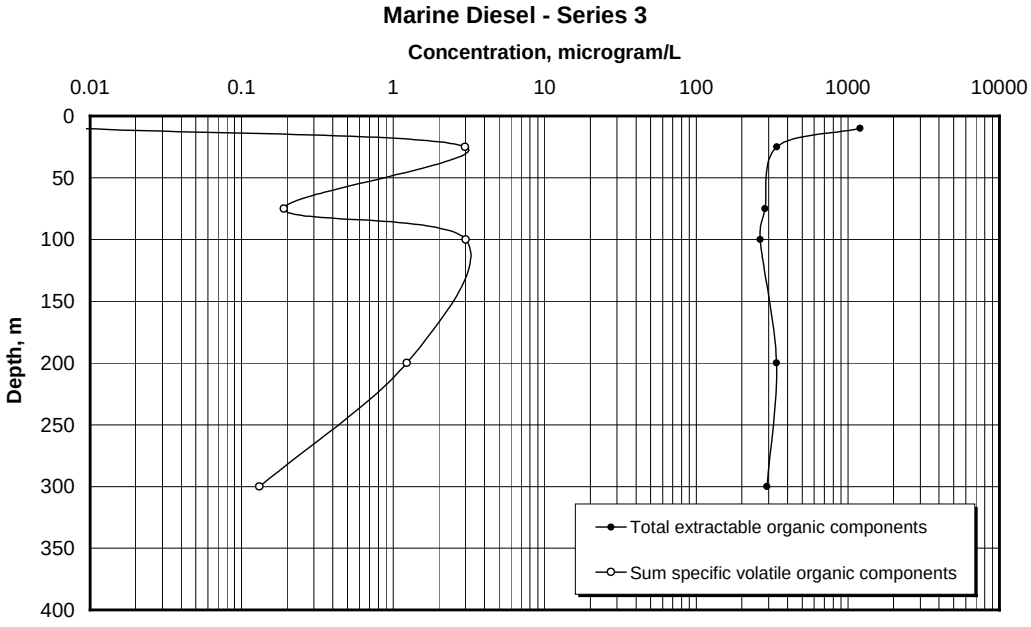

Figure 7.3.7. Concentration profiles of sum VOC and TEOC in the water column during discharge of marine diesel, series MD #3.

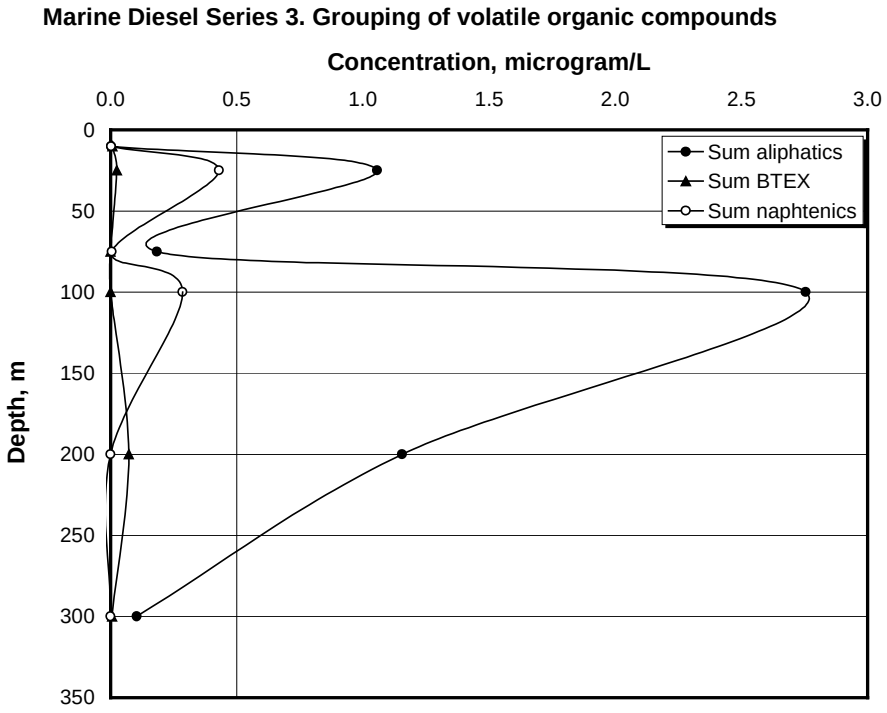

Figure 7.3.8. Concentration profiles of groups of volatile organic compounds in the water column during discharge of marine diesel, series 3.

7.3.5 Crude Oil release, Series OB #1.

This profile was taken at about 15 minutes prior to the completion of the release. The bulk of the oil droplets is therefore distributed in the water column below the sea surface at the time of the sampling.

Figure 7.3.9 shows the total concentration of sum specific PAH components, VOC, and TEOC. The results of the VOC analysis show a drop in the concentration in the 450 m sample, and the sample is regarded as an outlier in the data analysis. All component groups show a maximum concentration at the deepest measurement level (500 m depth), which is natural because the oil is still leaving the release arrangement.

When breaking down the sum of specific volatile components into groups of related components (see Figure 7.3.10) it can be seen that the concentration profile of the volatile organic compounds, with peak concentration at 500 m, is dominated by the content of aromatic components in the samples. This is probably due to a larger contribution from dissolved compounds at this depth. A local maximum at 300 m depth is dominated by the volatile aliphatic compounds, and indicates a relatively higher content of oil droplets compared to dissolved compounds at this depth.

Figure 7.3.11 shows the normalised concentration profiles of the homologous series of Naphthalenes. The results show one peak ratio between the Naphthalenes and Fluoranthene at maximum depth of sampling (500 m). The different Naphthalenes have a ratio of 8-22% compared to the same ratios in fresh crude oil. This reflects the initial dissolution from the discharge point and up to 500 meters depth. The variations in the normalised values above this depth are difficult to explain, but it should be remembered that the absolute concentration of these compounds were quite small at these depths at this early stage of the experiment (see Figure 7.3.10).

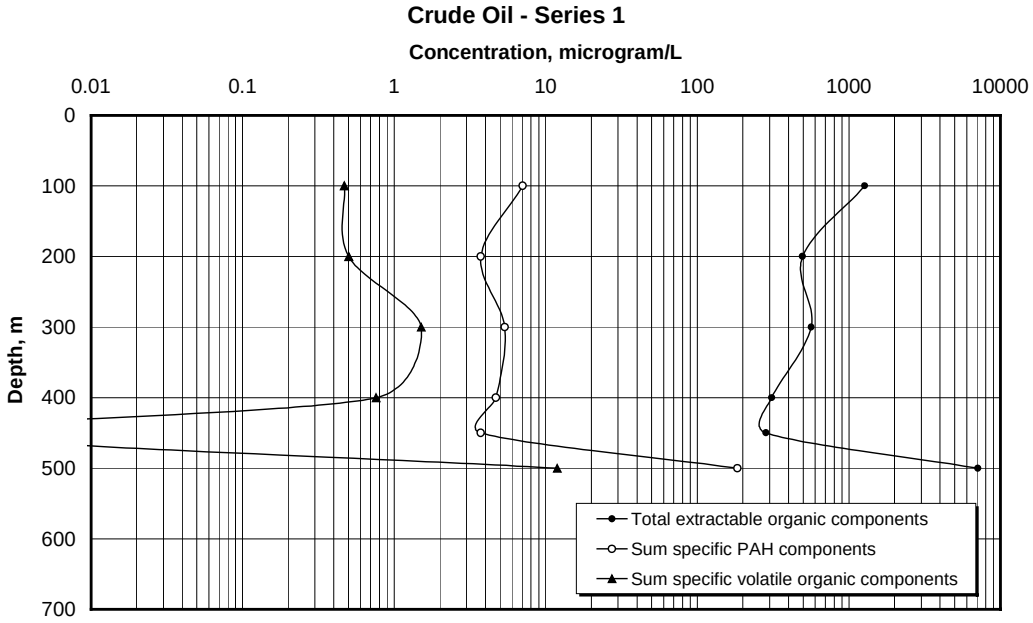

Figure 7.3.9 Concentration profiles of sum specific PAH components, sum VOC, and TEOC in the water column during discharge of crude oil, series OB #1.

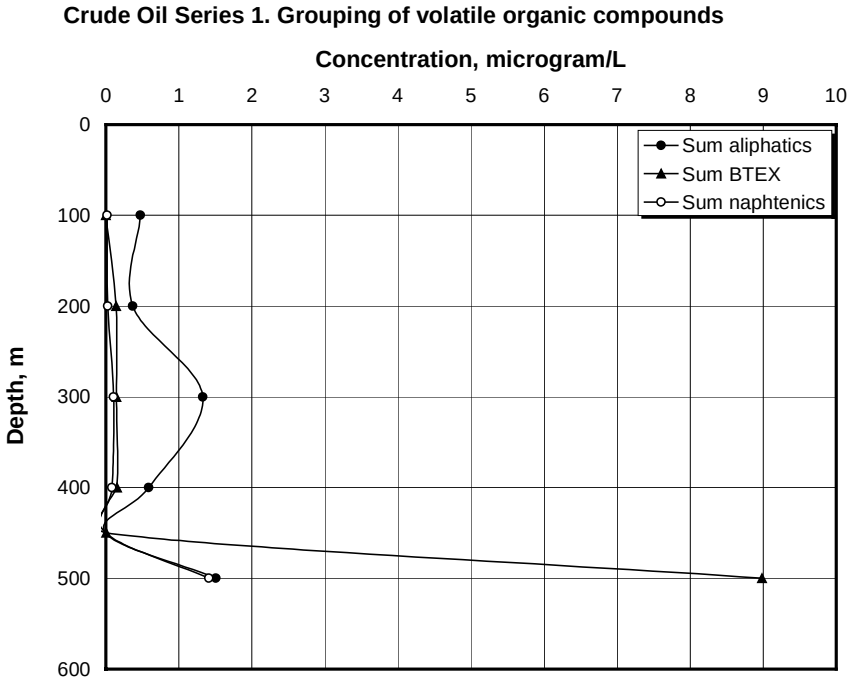

Figure 7.3.10. Concentration profiles of groups of volatile organic compounds in the water column during discharge of crude oil, series OB #1.

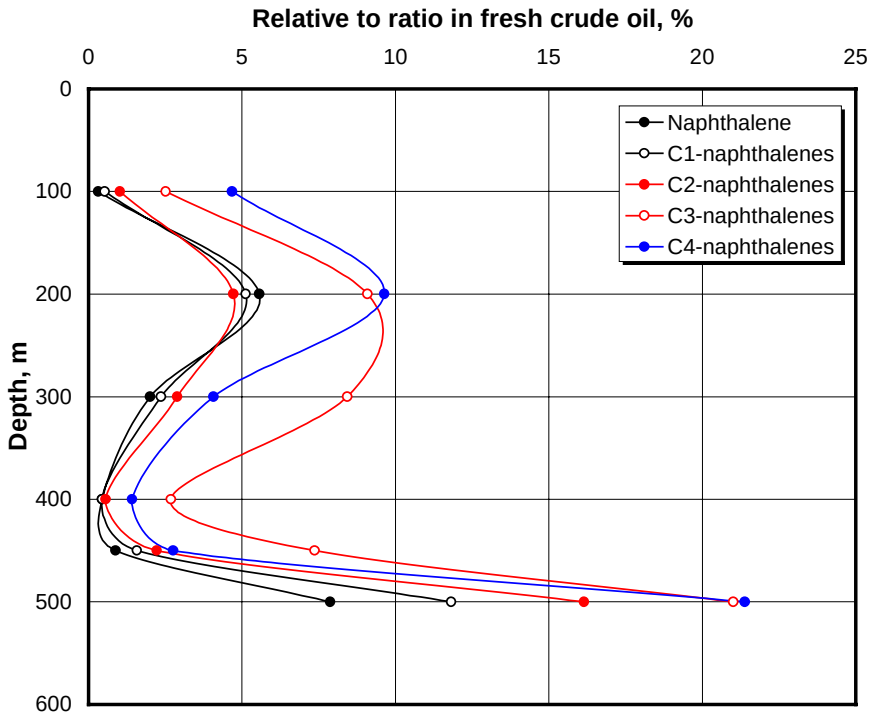

Figure 7.3.11 Profiles of normalised concentrations of naphthalenes in the water column during discharge of crude oil, series OB #1. The concentrations of the individual components are normalised to the concentration of Fluoranthene, and the ratios are plotted normalised to the corresponding ratios in fresh crude oil.

7.3.6 Crude Oil release, Series OB #2.

This profile shows the situation after about 85 minutes after the completion of the release. Some oil is therefore still rising through the water column, but a large part of the oil has reached the sea surface at this time instant.

Figure 7.3.12 shows the total concentration of sum specific PAH components, VOC, and TEOC. Maximum concentrations are now closer to the sea surface, compared to the first rosette sampling for this release (Chapter 7.3.5). The PAH's and TEOC show maxima at 100 – 200 m depth, and the VOC shows a small peak concentration on the samples taken at 25 m depth.

When breaking down the sum of VOC into groups of related components (see Figure 7.3.13), it can be seen that the concentration profile of the volatile organic compounds, with peak concentration at 25 m, is dominated by the content of aliphatic and naphtenic components in the samples. This indicates a relatively higher content of oil droplets compared to dissolved aromatic components at this depth. The peak concentration of sum BTEX is found at 200 m, which correlates to the peak concentration of TEOC and sum specific PAH components.

Figure 7.3.14 shows the normalised concentration profiles of the homologous series of Naphthalenes. The results show the peak ratio between the Naphthalenes and Fluoranthene at maximum depth of sampling (250 m). The different Naphthalenes have a ratio of 15-30% compared to the same ratios in fresh crude oil. This reflects the initial dissolution from the discharge point and up to 250 meters depth. From 250 meters depth and up to approximately 10 meters, the individual ratios decrease to 0.

The interpretation of this result is that the oil is water-extracted on its way up to the sea surface. The rate of this extraction is dependent on the solubility of the compounds in the water, such that the most soluble compounds are dissolved first. Close to the surface, the Napthalenes are almost completely extracted from the oil. These data may thus serve as a basis for estimates of the rates that various water-soluble oil compounds dissolve into the seawater. This is important information, because the water-soluble compounds are generally the most toxic ones when exposed to marine biota. The results from these measurements show that the rising of the oil through the water column represents a kind of a "stripping" process of some of the most toxic compounds in the oil. The end result is therefore that a portion of the most toxic compounds is left in the water column. This is contrasted to a surface generated slick, where a portion the most toxic compounds merely go into evaporation rather than dissolving into the sea.

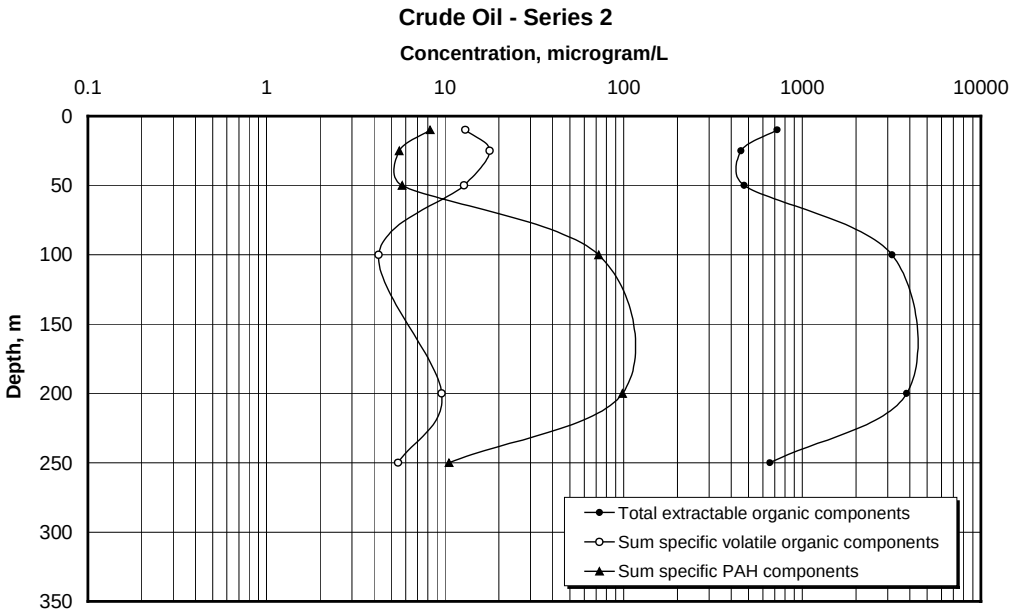

Figure 7.3.12 Concentration profiles of sum specific PAH components, sum VOC and TEOC in the water column during discharge of crude oil, series OB #2.

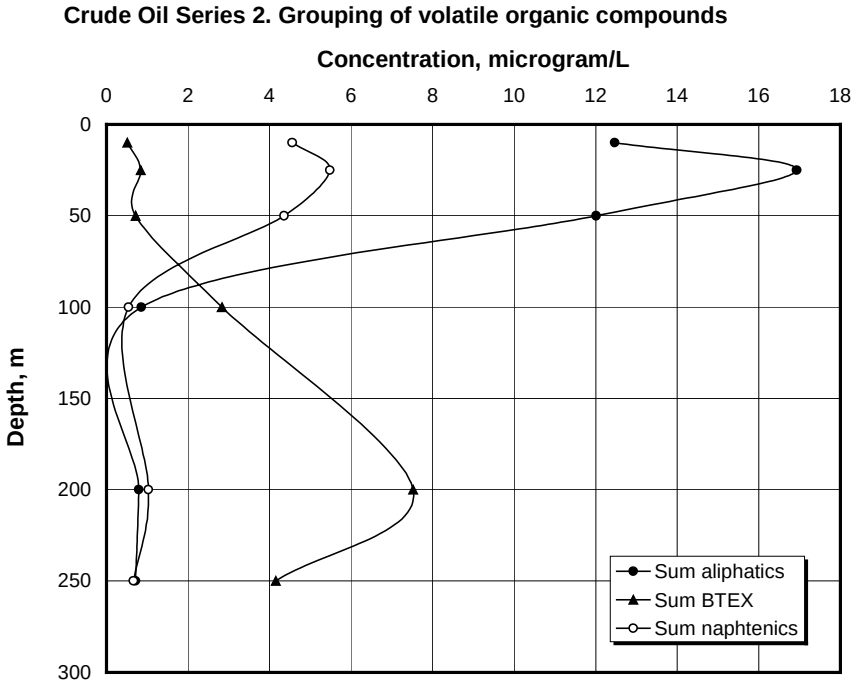

Figure 7.3.13 Concentration profiles of groups of volatile organic compounds in the water column during discharge of crude oil, series OB #2.

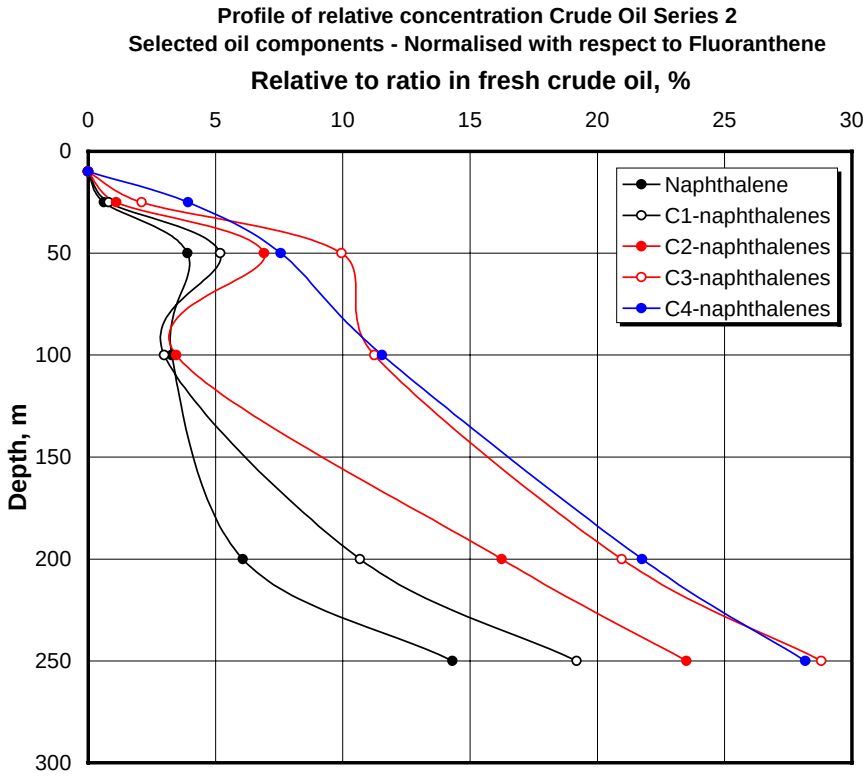

Figure 7.3.14 Profiles of normalised concentrations of selected oil components in the water column during discharge of crude oil, series OB #2. The concentrations of the individual components are normalised to the concentration of Fluoranthene, and the ratios are plotted normalised to the same ratios in fresh crude oil.

7.3.7 Concluding comments

The sampling and analysis of the rosette measurements carried out during the *Deep Spill* field trial have been explained. Results for VOC, TEOC and some specific PAH-s have been presented.

The present review of the water sample data indicates that more extensive analysis of the data set should be considered. It is possible to perform data analysis of these samples for more components than what has been shown here. In addition, the data set has also the potential of revealing dissolution rates for various compounds in the oil/diesel into the water column. In addition, drop size distributions at the depth of discharge are known from the ROV measurements (see Chapter 7.1). This information may, in turn, form a basis for calculating exposures on marine biota caused by underwater releases of oil.

8 OBSERVATIONS OF SURFACE SLICKS

8.1 UV-fluorescence profiles and water samples taken from workboat

This chapter describes the activity of the UV Fluorescence (UVF) workboat, the obtained data and discusses these data and gives recommendation for further work.

8.1.1 Short summary of UVF field operation

The UVF-workboat was operative during both days when oil and gas were released (27.06.2000 and 29.06.2000). Figure 8.1.1 shows a picture of the workboat taken on the day of the crude oil discharge. The table below gives a brief description of the activity of the UVF-workboat for these days.

The UVF measurements were generally made in transects crossing the visible oil slick – starting in clear water outside the slick. The raw data from each of these transects were stored on separate data files, each containing records with date and time, position (latitude and longitude determined with GPS), and the response of the two UVF instruments. All these files have been combined into one excel-workbook – UVF_TRANSECTS.xls, stored in the folder UVFdata. In this workbook, the results of the laboratory and field calibrations have also been taken into account with the aim of presenting the best possible picture of the absolute concentration levels along the transects. Examples of data presentations based on this workbook will be given later in this chapter.

Figure 8.1.1 Picture of UVF workboat taken from far Grip at the day of the crude oil discharge (June 29th).

Table 8.1.1 UVF-workboat activity

Tuesday 27.06.2000

Local time	Event
0900	Start of UVF monitoring - Background survey
0938	The first oil observed on the surface
0951	First response on UVF instrument (1 meter depth)
0930-1204	Monitoring of oil concentrations by performing transects across and along the rising plume.
1204	UVF-workboat on deck on Johan Hjort for exchange of crew
1220	UVF-workboat back on water performing monitoring
1314-1400	”Rescuing” oil samples and personnel from Blue sampling boat.
1400	UVF-workboat was not allowed to continue monitoring due to high sea and malfunction of the other sampling boat.

Thursday 29.06.2000

Local time	Event
0809	Start of UVF monitoring - Background survey
0822	The first oil observed visually on the surface
0819	Oil detected with the UVF instruments
0830	Problems with low power (seawater flooding the battery room!)
0830-0909	Intense sampling activity of surface oil sampling crew
0910	UVF equipment operative (emergency batteries connected)
0910-1149	Monitoring surface oil and sub-surface oil concentration.
1203	UVF-workboat on deck on Johan Hjort for exchange of crew
1245	UVF-workboat back on water performing monitoring
1250-1520	Monitoring surface oil and sub-surface oil concentration.
1610	On-deck Johan Hjort

8.1.2 Field and laboratory calibration of UVF instruments

The UV fluorescence equipment was calibrated in SINTEF’s laboratory against samples of the actual marine diesel and crude oil (Oseberg Blend). In addition, 1-liter water samples were taken during the transects and later analyzed for Total Extractable Organic Hydrocarbons (TEOH). These samples were also used for calibrating the instruments.

After the field trial both instruments were calibrated in the lab with samples of the two oil types used during the Deep Spill field trial. The calibration was performed by successive adding an oil standard (premixed with 2% dispersant) to 20 liter of seawater that were pumped trough both UV fluorescence instruments. The instrument responses versus the concentration of calibration standards are presented in figure 8.1.2 below.

As the figure indicates, the response curves are non-linear, and the data have been fitted to second order polynomials to obtain the shown calibration curves. It should be noted that both instruments also give a certain response for zero oil concentrations. This background signal was subtracted from the measured response to obtain the shown calibration curves. A background signal will also be present in field application, and this signal must be subtracted before the calibration curve was used.

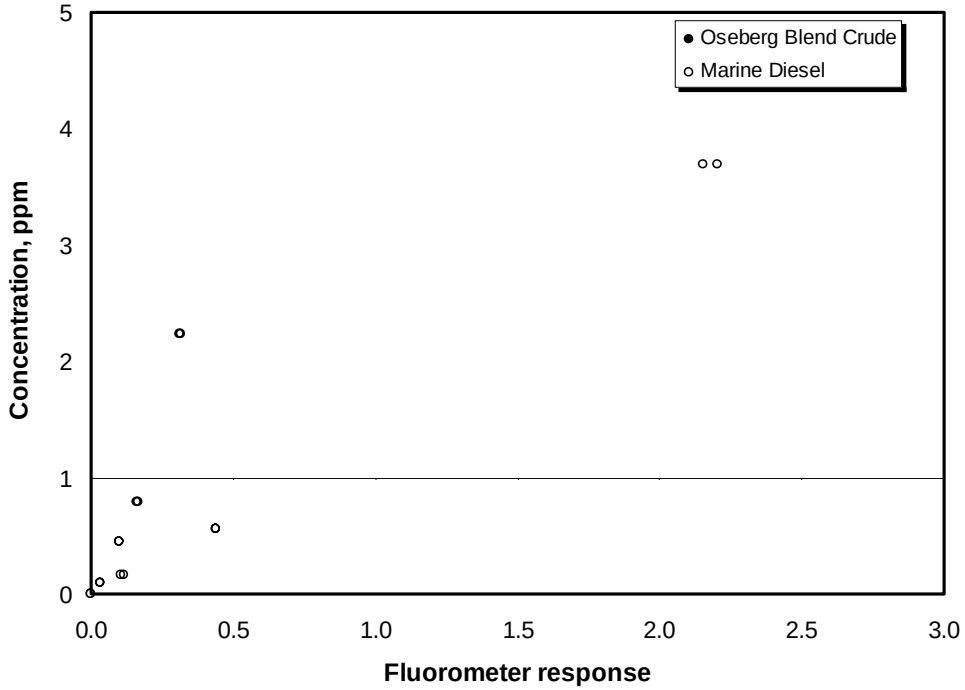

Figure 8.1.2 Laboratory calibration of Oseberg Blend and marine Diesel. Calibration curves giving oil concentration (ppm) corresponding to the response from UVF instruments.

The background signal was in general taken to be the response obtained in clean water outside the visible slick– corresponding to the measurements at the start of each transect. In addition, as shown in the next section – corrections had to be made to the laboratory calibrations based on data from the water samples taken during the transects.

As mentioned earlier, one-liter water samples were taken during UVF transects. The timing of stop and start of sampling were recorded on the internal data logging system onboard the UVF-workboat. The samples with corresponding Total extractable Hydro Carbons (THC) and UVF-response from the Turner instruments are given in table 8.1.2 below.

The UVF response values given in the table above have been calculated from the UVF instrument response by use of the calibration curves obtained in the laboratory (Figure 8.1.1). Note that the background signal – represented by the instrument signal obtained in clean water outside the visible slick – has subtracted from the measured instrument response. A plot of the data is shown in Figure 8.1.3. The x-axis on the graph is the time since start of the discharges, while the y-axis is the ratio between measured concentrations (THC) and the concentrations calculated by use of the laboratory calibration curve. This ratio is called Response Factor – and the actual concentration can be found by multiplying the calculated concentrations with this factor. Note that the power law function fitted to the data is been applied in the Excel workbook mentioned earlier to provide estimates of actual concentration levels along the transects.

It is evident that the calculated concentrations in general underestimate the concentrations in the corresponding water samples, and that the discrepancies are larger for the samples taken short times after the start of the discharge. This time variation indicates that the responses from the UVF instruments could be dependent on the size distribution of the oil droplets in the rising oil plume. The surfacing oil droplets will be large short time after the start of the discharge and will decrease in size with time after the end of the discharge. The instrument response to a certain

concentration could be smaller for these large droplets than for the fine droplets formed in the laboratory calibration samples – probably due to the smaller surface to volume ratio and the fact that the UVF fluorescence to a large extent is a surface phenomenon.

Table 8.1.2 Concentrations in water samples (THC) and corresponding concentrations calculated from the instrument response with the laboratory calibration curve (UVF).

Marine Diesel spill, 1 liter calibration samples :

Sample ID	*Transect ID*	*Local time*	*Depth*	*THC (ppm)*	*UVF (ppm)*
MDV2	1046	10:50:27	8 m	1.30	0.033
MDV3	1115	11:28:56	8 m	0.38	0.431
MDV4	1115	11:29:45	1 m	1.92	0.122
MDV5	1145	11:51:38	1 m	4.03	0.305
MDV6	1145	11:53:12	8 m	8.94	1.059
MDV7	1233	12:39:28	1 m	6.87	3.187
MDV8	1233	12:39:54	8 m	38.5	2.818

Oseberg Blend Spill, 1 liter calibration samples:

Sample ID	*Transect ID*	*Local time*	*Depth*	*THC (ppm)*	*UVF (ppm)*
SB1	1031	10:40:00	9 m	7.21	0.230
SB2	1031	10:43:06	9 m	3.26	0.225
SB3	1330	13:55:58	9 m	0.49	0.124
SB4	1330	13:37:36	9 m	0.90	0.426
SB5	1345	13:52:41	2 m	0.88	0.420

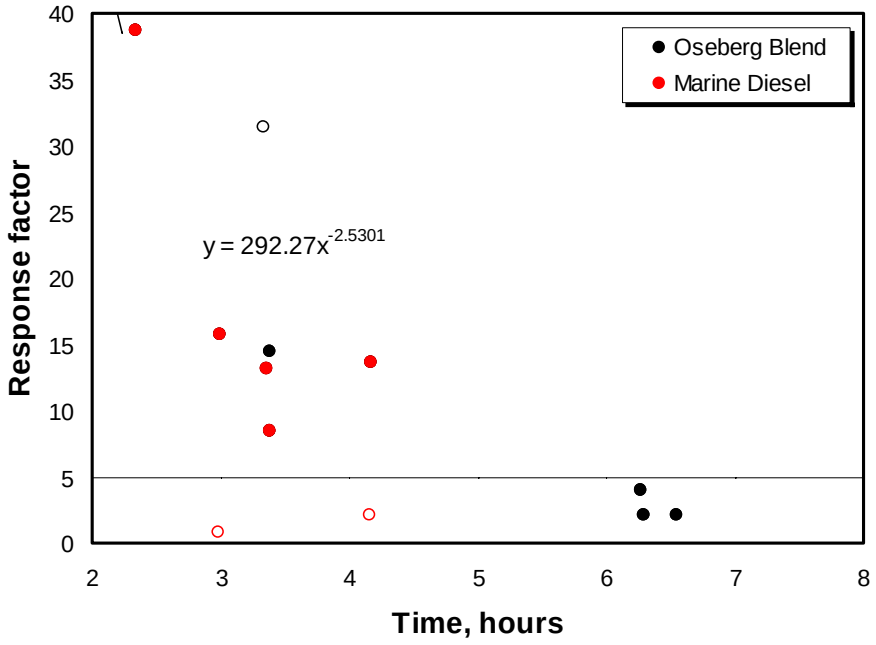

Figure 8.1.3 Response factor as a function of time from start of discharge calculated from the water samples and the measured UVF response. A power law function is fitted to a subset of the data with some obvious outliers omitted.

8.1.3 Oil concentrations along UVF transects

Figures 8.1.4 and 8.1.5 show examples of concentration measurements along the UVF boat transects subsequent to the Marine Diesel and Crude Oil discharges. The presentations are made with the presentation tool included in the Excel workbook mentioned above. Note that the actual measurements were sampled at 2 seconds intervals, but the data were smoothed with a 14 seconds moving average to obtain the data shown at 30 seconds intervals in the following. Each plot covers one hour of measurements – or the period indicated on the respective plots. The concentration values have been calculated from the instrument response by use of the lab-calibration curve for the given oil type (Figure 8.1.2) – corrected with the general time dependent response factor (Figure 8.1.3). A slick contour based on aerial images is shown for reference on each plot.

Figures 8.1.4 and 8.1.5 indicate that the concentration levels measured after the Marine Diesel discharge are significantly higher than the measurement made subsequent to the Crude Oil discharge. The cumulative concentration distributions shown at Figures 8.1.6 confirm this indication, and show another interesting feature: The concentrations measured at the two different depths were almost equal in the Crude Oil experiment, while significant higher concentrations were measured at the shallowest depth in the Marine Diesel experiment. This feature is probably due to the fact that the non-emulsifying marine diesel slick was eroded rapidly by wave action – bringing dispersed oil back into the surface layer.

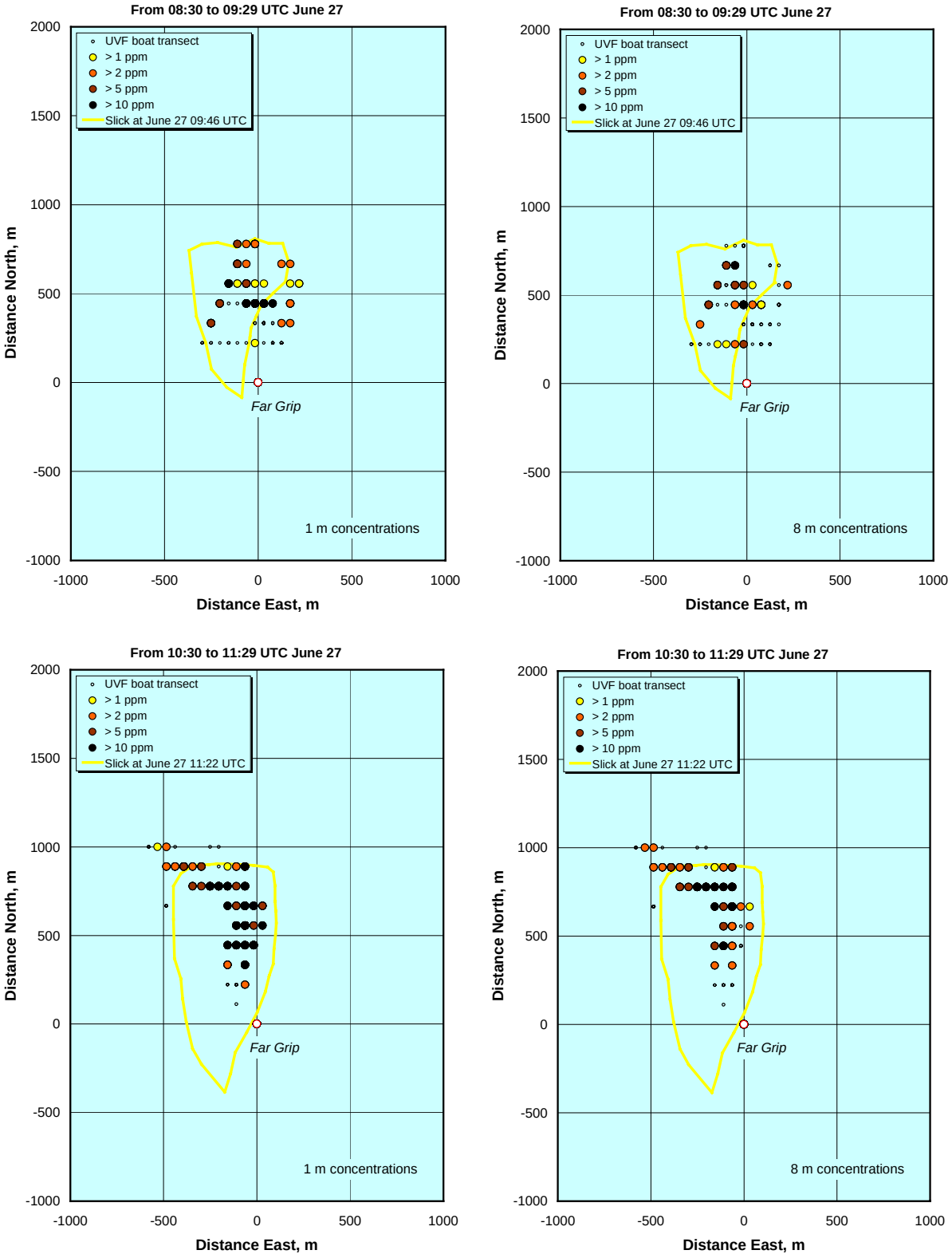

Figure 8.1.4 Examples of concentrations along UVF workboat transects made during the Marine Diesel experiment in the 1 hour periods indicated on the plots. Measurements from 1 m depth are shown to the left, with the measurements from 8 m depth to the right. Concentration levels indicated with color-coded markers (see legend). Slick contour from aerial images shown for reference.

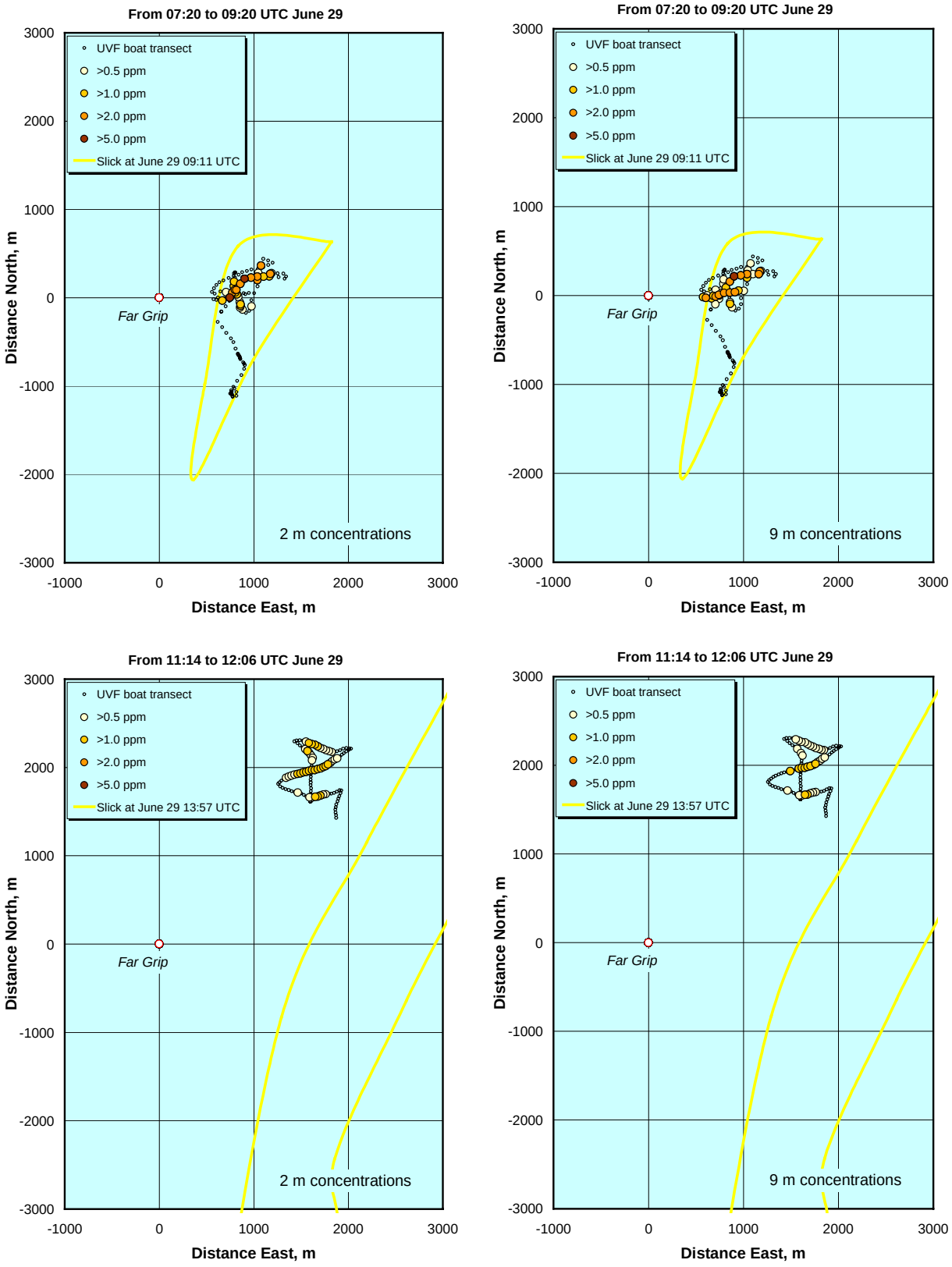

Figure 8.1.5 Examples of concentrations along UVF workboat transects made during the Crude Oil experiment in the 1 hour periods indicated on the plots. Measurements from 2 m depth are shown to the left, with the measurements from 9 m depth to the right. Concentration levels indicated with color-coded markers (see legend). Slick contour from aerial images shown for reference.

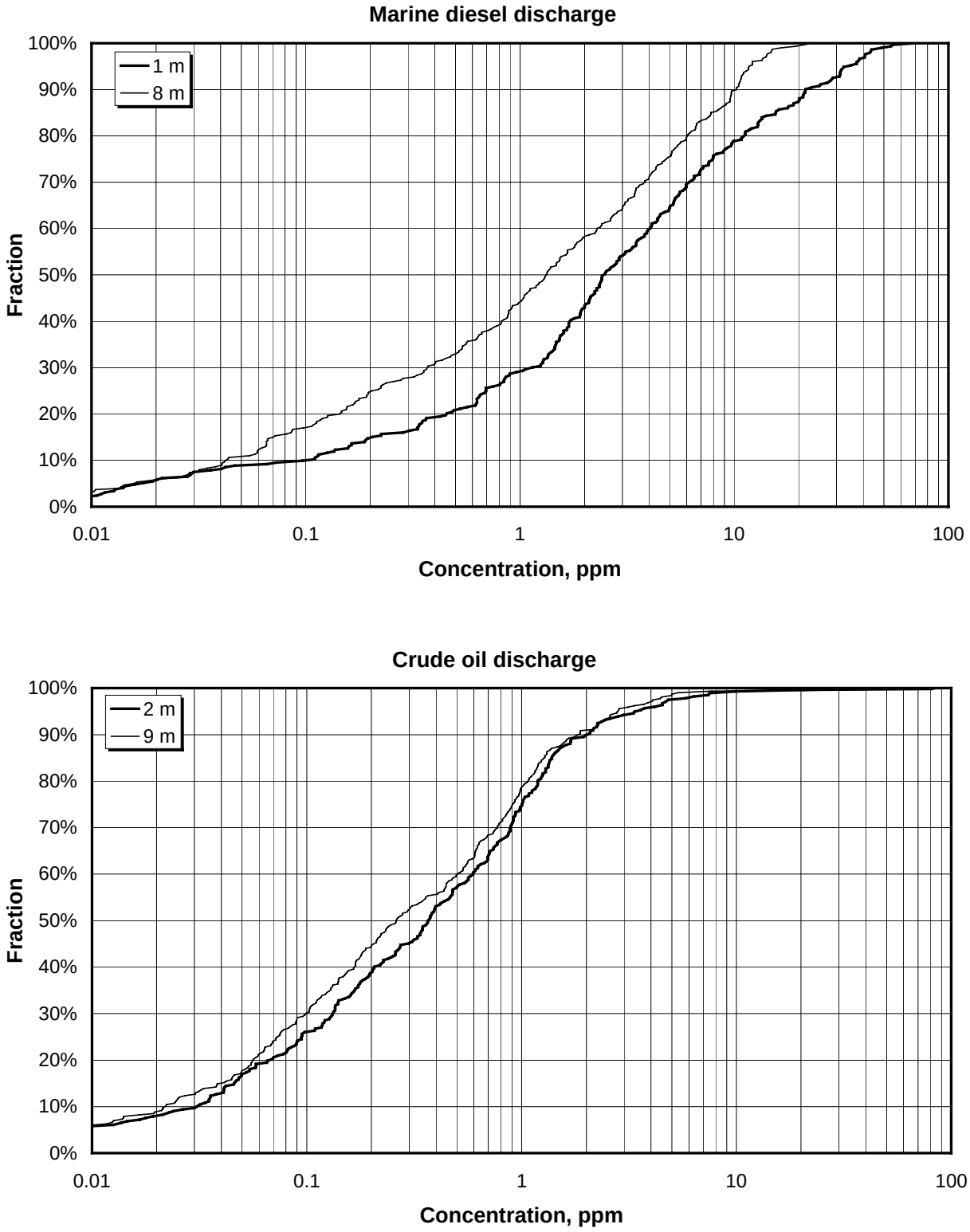

Figure 8.1.6 Cumulative distribution of total oil concentrations derived from the UVF transects after the marine Diesel Discharge (top) and the Crude Oil Discharge (bottom).

8.1.4 Summary and conclusions

The UVF instruments mounted in the workboat were calibrated by a laboratory calibration procedure, but analysis of total hydrocabon in the water samples taken during the monitoring transects indicate that the UVF response are also sensitive to other factors such as the oil droplet size distribution in the samples. The oil droplets in the samples made for calibration purposes were in the micrometer range (the sample oil was premixed with a chemical dispersant). The surfacing droplets in the field were in the millimeter range – but decreasing in size as time elapsed (see Chapter 9 for a calculation of changes in droplet size with time). We have tried to compensate for these effects by using a time dependent response factor (see Figure 8.1.3), but the relatively few water samples taken during the UVF-transects makes this curve uncertain.

However, in total – the results obtained from the different transects seem to provide a fair representation of the extent and location of the area were oil is surfacing, as confirmed by comparison with the available surface oil slicks from aerial images.

SINTEF

8.2 Film thickness measurements and sampling of surface oil

8.2.1 Samples from the Marine Diesel experiment

Table 8.2.1 summarizes the results from the 10 film thickness measurements taken in the Marine Diesel spill.

Table 8.2.1. Emulsion film thickness (μm) - Marine Diesel

Sampling time (local time)	Water content	Film thickness (μm)	Position [1]) Lat	Long	Comments (sampling technique / Visual observations)
0948	-	-	65 00.162	4 50.049	Only GPS positioning
0953	0	0.99	-	-	PP-pad sample. Spot sampling
0955	0	1.49	-	-	Teflon net. Spot sampling
0958	0	0.77	65 00.300	4 50.013	Teflon net. Spot sampling
1005	0	0.14	-	-	Teflon net. Skimming over 10m. Thin oil
1015	0	0.12	-	-	Teflon net. Skimming over 10m. Sheen / Rainbow and some metallic
1020	0	0.28			PP-pad sample. Skimming over 10m
1030	0	0.53			Teflon net. Skimming over 10m
1048	-	-	65 00.012	4 50.075	Only GPS positioning
1035	0	0.40			PP-pad sample. Skimming over 10m
1035	0	0.40			PP-pad sample. Skimming over 10m
1120	0	0.53	65 00.262	4 50.053	Teflon net. Skimming over 10m
1154	0	0.11			PP-pad sample. Skimming over 10m

[1]) Position given in geographical degrees followed by decimal minutes

General comments:

- Due to MOB-Boat failure, the film thickness measurements were limited to the period 0953 to 1154 (local time).
- The visual color code terminology used in this report are based on the following "revised" Bonn Agreement color code:

Code	Description	Film thickness, μm min	max
1	Silvery (sheen)	0.05	0.10
2	Grey (sheen)	0.10	0.30
3	Rainbow	0.30	5.00
4	Metallic	5.00	50.0
5	Discontinuous true colour	50.0	200
6	Continuous true colour	>200	

- The diesel oil came to the surface and spread to a very thin oil film, varied visually between color codes 1, 2, 3 and 4. Due to the rough sea and windy conditions during the experimental period (10-14 m/s wind), the diesel was locally (even within a square meter) very in-homogeneously distributed on the surface, that make the ground-truth film thickness measurements very difficult.

- Both the 3M PP pads and the ETFE Teflon nets fasten on a rod were tried used (see figure 8.2.1 below). Due to the local variations, most samples were taken by skimming PP-pads and

Teflon nets over a distance of 10 m, in order to try to get an average value over 10 m. The distance was measured using a rope with a drogue at the end and a 10 m marker on the rope.

- Most of the results in table 1 give thickness between 0.1 to 1μm. Due to the rough weather, it is to assume that the skimmed area over the 10 m distance was not 100%. This means that the results likely give an underestimation of the average film thickness. The two spot point samples give generally some higher film thickness.

- The surface diesel oil film did not contain any water. One small sample of surface diesel (< 1 ml) was collected and quantified for water content (< 1%).

- From the sampling boat, it was observed foam at sea that became light yellow due to the diesel. Visually, this could easily be mistaken for emulsion.

Figure 8.2.1 Teflon Net for thin oil film thickness measurements, of diesel film under "bad weather conditions

8.2.2 Samples from the Oseberg Blend Crude experiment

Table 8.2.2 summarizes the results of 16 film thickness measurements taken in the Oseberg Blend crude oil slick.

Table 8.2.2 Emulsion film thickness (μm) - Oseberg Blend crude oil

Sampling time (local time)	Water content.[1)]	Emulsion Film thickness (μm)	Position [1)] Lat	Long	Comments (sampling technique / Visual observations)
0902	29	19	65 00.037	4 50.775	PP-Pad, spot sampling / metallic
0904	29	171	65 00.034	4 50.775	PP-Pad, spot sampling / Thick oil (Discontinous / continuos true)
0908	29	38	65 00.009	4 50.772	PP-Pad, spot sampling / thick oil (Discontinous)
0909	29	7	65 00.001	4 50.719	PP-Pad, spot sampling / metallic
1035	29	15	65 00.150	4 51.517	PP-Pad, spot sampling / 4
1036	29	101	65 00.146	4 51.500	samples in thick (discontinous)
1037	29	27	65 00.139	4 51.496	oil and metallic. In an area
1038	29	36	65 00.130	4 51.487	with relatively fresh oil
1100	66	676	64 59.635	4 51.091	PP-pad, spot sampling from emulsified patches
1105	66	1983	64 59.588	4 51.156	PP-pad, spot sampling from thick emulsion
1110	63	1187	64 59.433	4 50.971	Thick emulsion, estimated > 1-3 mm
1116	63	1008	64 59.398	4 50.989	PP-Pad, spot sampling from thick emulsion
1116	63	1902	64 59.398	4 50.989	PP-pad, spot sampling from thick emulsion
1617	69	1264	[2)]		PP-pad in thick emulsion, 3
1617	69	1204			parallel samples
1617	69	777			

[1)] Position given in geographical degrees followed by decimal minutes
[2)] Samples taken in the southern front of the slick (Position not recorded)

Comments:

- Sampling technique: All samples were “spot-sampling" using the polypropylene 3M pads (21x 24 cm sheet connected with a clip and a thread to the to a sampling boat, see figures 1.2 – 1.5). A “spot sample” was taken by placing the sorbing pad gently on the surface. The oil / emulsion present was absorbed immediately by the exposed area of the pad, that was lifted off the surface after 5 to 10 seconds. Emulsion surrounded the sheet, was not observed to “migrate” or to be absorbed to the pad. This is also in accordance with earlier calibration laboratory measurements [1].

- The emulsion thickness were calculated by quantifying the amount of oil (calibrated against a Sture blend 200^{o}C+ residue external standard) and compensate for the water content in the emulsion (obtained in surface samples taken at the same period)

[1] See Ramstad, S.,1999: *The use of colour as guide to oil film thickness; Phase 2 – small scale field experiments*. SINTEF Report STF66 F99083, SINTEF Applied Chemistry, Trondheim, Norway, 39 pp.

- The film thickness of the relatively fresh oil (20 – 200µm, samples taken until about 10.40) is much lower compared to the initial oil film thickness' obtained in the 1994 NOFO-field trial with surface releases of Sture Blend spills. (typically 2- 8 mm during the first 1-2- hours [2]).

- The film thickness obtained in the thicker emulsions (1- 2 mm) after 2- 8 hours on the surface are, however, comparable with the emulsion film thickness' obtained in the 1994 NOFO-field trial with surface releases of Sture Blend spills at the same weathering time at sea [3].This indicates that the surface oil with time, tend to be "packed" into smaller areas of thicker emulsion.

Fig. 8.2.2 Oil film thickness measurements using PP pad (on thicker emulsion). Crude oil experiment June 29.

[2] See Strøm-Kristiansen, T, P.S. Daling and A. Lewis, 1995*: Dispersant trials – NOFO exercise June 1994. Surface oil sampling and analysis*. ESCOST Report No 15, IKU Report No 22.2050.00/95, SINTEF Petroleum Research, Trondheim, Norway, 42 pp.
[3] See Strøm-Kristiansen, T, P.S. Daling and A. Lewis, 1995 (op cit)

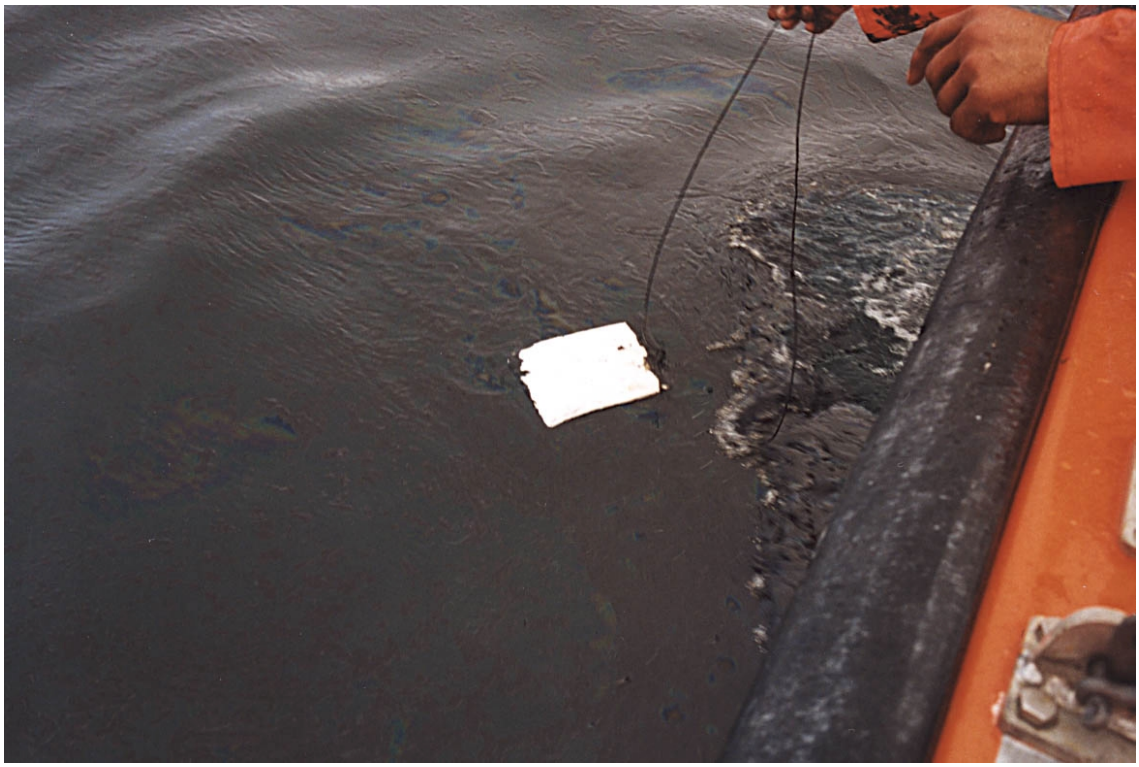

Fig. 8.2.3 Oil film thickness measurements using PP pad (on thicker emulsion). Crude oil experiment June 29.

Fig. 8.2.4 Oil film thickness measurements using PP pad (on thicker emulsion). Crude oil experiment June 29.

Fig. 8.2.5 Oil film thickness measurements using PP pad, on thinner oil film (metallic / discontinous true oil colour)

8.2.3 Physico-chemical properties of surface crude oil / emulsion

The data on the surface oil / emulsion collected from surface slick sampling during the Oseberg Blend release June 29 are listed in table 8.2.2 below.

Figures 8.2.6 – 8.2.8 show some pictures from the sampling and handling of the surface emulsion in the sampling boat.

Figures 8.2.9 – 8.2.12 compares the measured ground truth values with those predicted by the SINTEF Oil Weathering Model[4]. The model predictions are based on:

- Model input data from a laboratory weathering study perform on the same crude oil blend – however named *Sture Blend* at that time.
- Surface sea temperature: 10 ^{o}C . Field measurements of sea-surface temperature. Fixed wind conditions: 5, 10 and 15 m/s. The measured wind during the release varied between 9-12 m/s.
- A constant oil film thickness of 0.5 mm has been use in the predictions.

The weathering time indicated in table 8.2.2 and in the prediction figures are tentatively (based on sampling time and sampling position relative to assumed oil surfacing area).

[4] See Daling, P.S., O.M. Aamo, A. Lewis and T. Strøm-Kristensen: *IKU Oil Weathering Model – predicting oil properties at sea.* 1997 Oil Spill Conference, Fort Lauderdale, Florida, pp 297-307.

8.2.4 Evaporation

Figure 8.2.9 shows that the evaporative loss (measured by GC, using the SINTEF "Evap. Loss program"). The field data are comparable, but slightly higher (2-5 %) than the predictions made by the model at 10 m/s wind conditions.

8.2.5 Properties of water-in-oil emulsions

Figure 8.2.10 shows a kinetic in water uptake that is in fairly good accordance to the model predictions at 10 m/s wind. A maximum in water content of 75 % was obtained after about 5 hours. A slight decrease in water content could be observed in the 6 and 7 h samples. Such decrease has been observed in several earlier field trials [5]. The sample with a weathering time of about 0.5 h at sea surface, showed a low water content (<30% water) that is in accordance to the predicted water uptake that take place on the sea surface at this weather conditions. This indicates that no significant emulsification took place in the oil droplets in the water column during rising to the surface. The volume of the sample (taken 0906) was too low to get viscosity and stability measurements. However, visually, the oil sample was very similar to the properties of fairly fresh Oseberg Blend crude (i.e. black oil, low viscosity, no indication of significant emulsification.

The next surface samples taken show a gradually increasing water uptake up to a maximum of 75 %, at a rate that is in good accordance to the predictions made by the SINTEF OWM. Also the gradually increase in viscosity (figure 8.2.11) and the increase in emulsion density (figure 8.2.12) are in good accordance to the predictions at 10 m/s wind.

Table 8.2.3 shows that all the surface emulsion taken until 1506 (i.e. about 6 h weathering time on the surface) were "semi-stable" emulsions, i.e. that some settling of water will occur during 24 h settling at the ambient temperature (10 ^{o}C). There is a gradually increase in the relative stability (decrease in the dehydration, D-value). The last sample (taken 1620) showed no dehydration to take place over the 24 h settling period. According to SINTEF methodology definitions [6], we consider this emulsion to be a "stable" emulsion.

---

[5] See Daling, P.S. and T. Strøm, 1999: *Weathering of oils at sea: Model/field data comparisons*. Spill Science & Technology Bulletin, Vol. 5, No. 1, pp 63-74.

[6] See Strøm-Kristiansen, T, P.S. Daling, A. Lewis and A.B. Nordvik, 1993*: Weathering properties and chemical dispersability of crude oils transported in US waters.* IKU Report No. 22.2142.00/01/94. MRSC Technical Report Series 93-032. Marine Spill Response Corporation, Washington DC, 219 pp.

Table 8.2.2 W/o emulsion properties

Sampling station	Tentative Weath. time	Density (g/ml)	Viscosity at 10(s^{-1}) (mPas)	Water cont (vol%)	[2)]Emulsion breaker efficiency [1)] D_{4h}	[1)] D_{24h}	Stability [1)] D_{4h}	[1)] D_{24h}	Water free residue properties [3)] Density (g/ml)	Evap loss (wt%) [5)]
906	0.5	0.9259	- [4)]	29.2	- [4)]	- [4)]	- [4)]	- [4)]	0.8852	28.2
920	0.75	0.9550	706	51.5	1.00	1.00	0.50	0.78	0.8806	31.7
1010	1	0.9810	1935	65.8	0.53	0.53	0.16	0.61	0.8962	32.3
1055	1.5	0.9841	3400	67.6	0.82	0.82	0.00	0.27	0.8987	33.5
1116	2	0.9822	3100	66.7	0.83	0.83	0.08	0.41	0.8967	36.2
1427	5	0.9910	7600	75.1	0.61	0.61	0.00	0.00	0.8885	35.6
1506	6	0.9928	5000	72.1	0.69	0.69	0.00	0.24	0.9096	39.3
1620	7	0.9840	6700	68.5	0.73	0.73	0.00	0.00	0.8950	39.3
Fresh crude	-	0.8423	84	-	-	-	-	-	0.8423	-
200°C+	-	0.8903	477	-	-	-	-	-	0.8903	-

1) D is fractional dehydration of emulsion. D_{4h} is effect after 4 hours, D_{24h} is the effect after 24 hours. D=0: no water settled. D = 1: all water settled.
2) Effect of 500 ppm concentration of the emulsion breaker Alcopol O60%, relative to the oil volume
3) Properties of the oil residue after the water has been drained off by 0.5% emulsion breaker Alcopol at 60°C
4) The sample volume was to small to perform the analysis.
5) Evaporative loss quantified by GC – SINTEF Evap-program)

Fig. 8.2.6 Sampling of emulsions and drainage of free water by settling in separation funnels, June 29.

Fig. 8.2.7 Drainage of free water in emulsion sample by settling in separation funnels, June 29.

Fig. 8.2.8 Emulsion sample after free water settling in separation funnels, June 29.

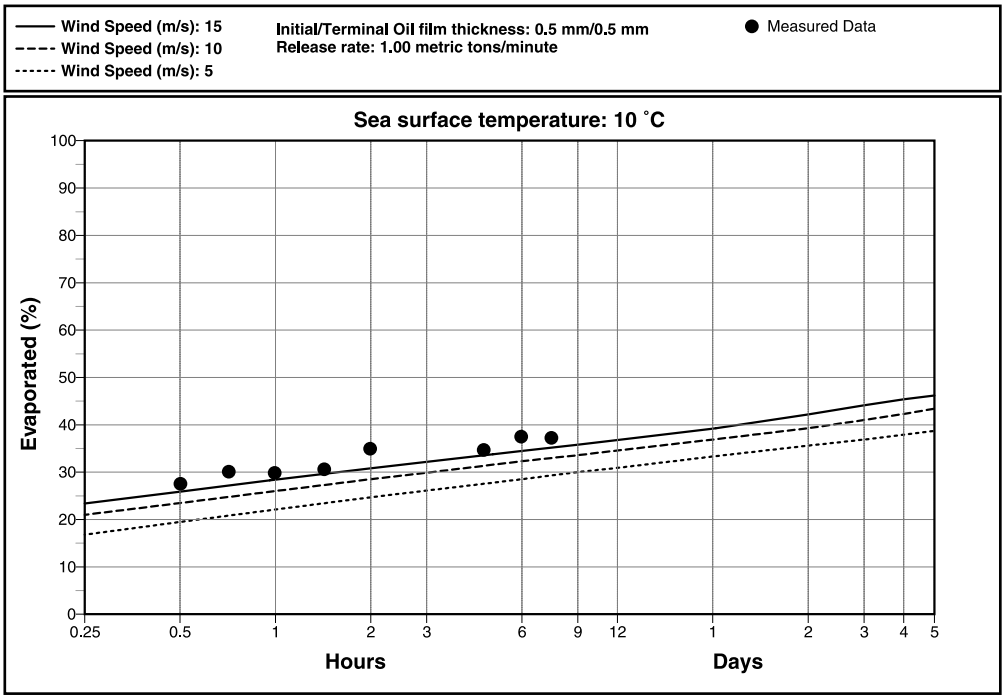

Fig. 8.2.9 Evaporative loss of crude oil after resurfacing. Measured values compared with predictions based on laboratory data obtained from Sture Blend. Note that this is essentially the same blend of crude oils as the Oseberg blend used in the experiment, but previously marketed with another name.

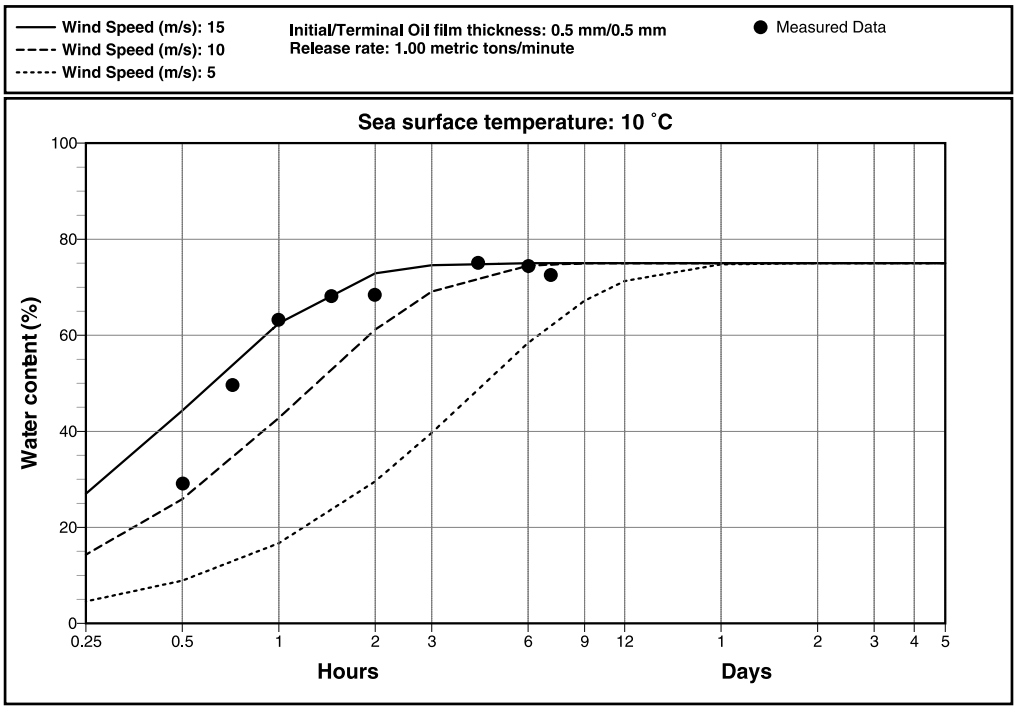

Fig. 8.2.10 Water uptake of Oseberg crude oil after resurfacing. Predicted and measured values.

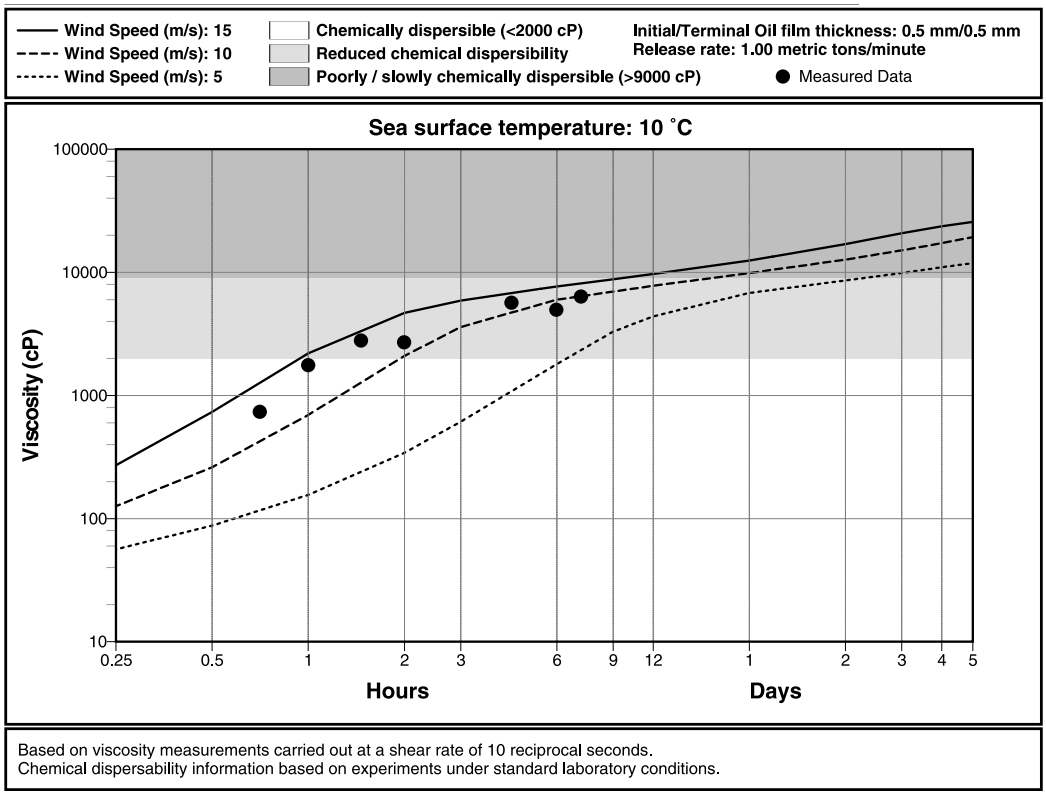

Fig. 8.2.11 Viscosity of emulsion, Oseberg crude oil after resurfacing. Predicted and measured values

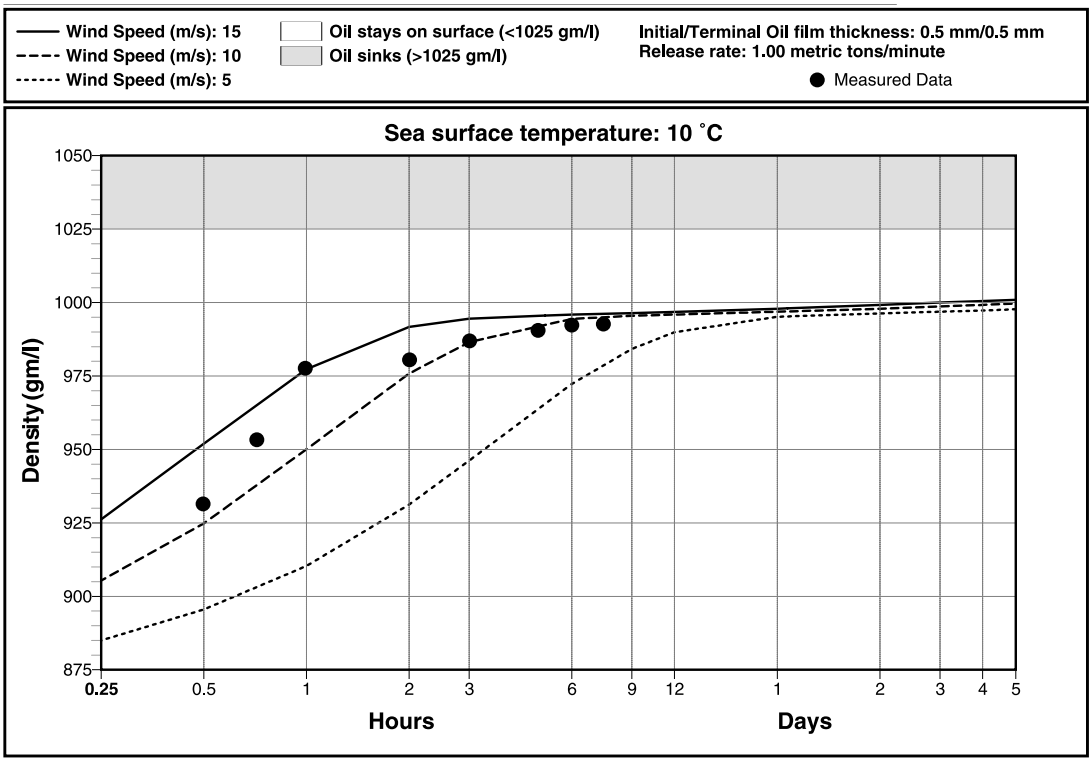

Fig 8.2.12 Density of emulsion formed from Oseberg crude oil after resurfacing. Predicted and measured values.

8.3 Aerial surveillance of surface slicks

From the point of view of the DeepSpill experiment, aerial surveillance was needed for two major purposes:

- Provide guidance for the two workboats in the surface slicks.
- Provide data on the location and spatial extent of the surface oil slicks at different times after the start of each experiment.

Six airplanes provided the aerial surveillance from the same number of European countries – Norway, Denmark, Germany, The Netherlands, France and UK (Figure 8.3.2). The flights were arranged as a part of a Bonn Agreement project with its own agenda – namely to test a special color code designed for determination of oil slick thickness. All planes were operating from Kristiansund Airport, about 250 km south east of the experimental site[7] where also the flight coordinator was stationed. These surveillance airplanes are in general equipped with special imaging facilities, such as infrared (IR) and ultraviolet (UV) scanners and a side scanning radar (SLAR) for mapping oil slicks, and the air crews will normally include specialists in oil spill detection (Figure 8.3.1). Note that all these facilities were not operative on all the participating airplanes, partly due to ongoing repair or replacement of some of the instruments.

Each plane was intended to visit the experimental site for about one hour, when a new plane should take over for the next hour. However – all planes except the Norwegian aircraft belonging to SFT had to depart on June 28 to take care of other obligations. Thus, due to the one-day delay of the last experiment caused by adverse weather, only one plane was available during the crude oil experiment of June 29.

Figure 8.3.1 Inside SFT's surveillance aircraft. View of the SLAR radar image of the crude oil slick.

[7] See map in Figure 4.1 – Part I of the report

Figure 8.3.2 Pictures of three of the surveillance airplanes – from Norway (top), the Netherlands (middle), and Denmark (bottom).

8.3.1 Slick contours

Six flights were made on the day of the Marine Diesel experiment, but only two at the day of the Crude Oil experiment (when only one plane was available), with a flight schedule as listed in Table 8.3.1.

Table 8.3.1 Flight conducted on June 26 and June 29

Aircraft from	*Period at location, UTC time*
June 27	
Norway (SFT)	08:30 – 09:20
Germany	09:25 – 09:55
France	09:50 – 10:35
Denmark	10:23 – 11:00
The Netherlands	11:05 – 11:15
UK	Ca 13:00 – 14:00
June 29	
Norway (Flight 1)	08:00 – 09:15
Flight 2	14:00 – 14:58

Typical examples of images taken during these flights are given in the Figures 8.3.3 to 8.3.6. The first example (Figure 8.3.3) shows a normal photo taken from an oblique angle, showing most of the slick and the different vessels distinguishable in the picture. Figure 8.3.4 shows a combination of three scanner images from the German aircraft – from left to right IR, UV and (PASSIVE) microwave. The next example (Figure 8.3.5) shows a SLAR image from the SFT airplane, taken at June 29 during the crude oil experiment, and the final example (Figure 8.3.6) shows a digital picture of the workboat in the crude oil slick taken by the Norwegian aircraft.

Figure 8.3.3 Picture from SFT aircraft taken June 27 at 0840 UTC. Research vessels Håkon Mosby (left) and Johan Hjort (right) inside the oil slick – together with the two workboats, while the supply vessel far Grip can be seen in the background.

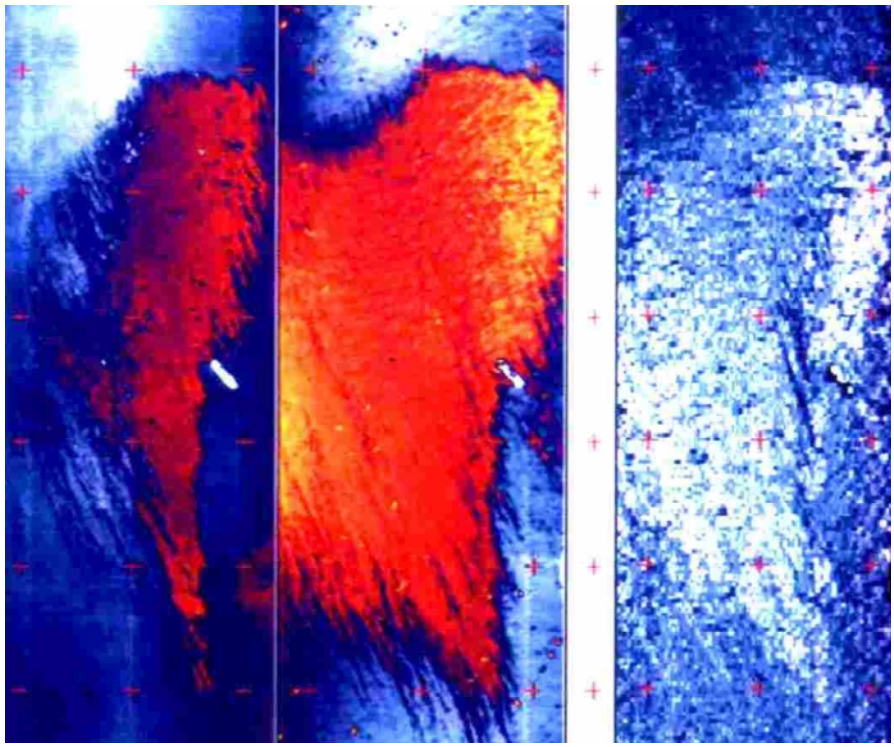

Figure 8.3.4 Combined IR, UV and microwave images from the German aircraft, taken at June 27 0953 UTC. The distance between the markers is 200 m.

Figure 8.3.5 SLAR image from the Norwegian aircraft taken at June 29, 1358 UTC (note that the time stamp on the picture is Norwegian Standard Time – summer saving hour neglected). 10 km distance between markers. The text also contains the heading of the aircraft and a position – with reference to the marker at the top of the bar to the right in the image.

Figure 8.3.6 Digital picture of the UVF workboat taking samples in emulsified patches of the crude oil slick. The picture was taken from the SFT aircraft at 1423 UTC June 29.

We have concentrated on the three first types of images with the aim of mapping the surface slicks. The scanned images are in general most reliable for this purpose, since they are taken vertically and include an explicit scale (markers with fixed distance). The images that are taken with cameras do not possess these features – they contain no explicit scale and are more or less distorted due to the oblique viewing angle. However, there were for several reasons relatively few scanned images (IR, UV and SLAR) available. For this reason, the oblique photos had to be considered as a supplementary source for mapping of the surface slicks. The photos most useful for further analysis had to cover most of the slick – and at the same time include vessels with known identity and position. Fortunately, one of the vessels were in a fixed position in the period of the experiments (the supply vessel *Far Grip*), and both research vessels were keeping a digital log of their positions at short intervals (1 minute). So – from the time tag of the picture and an identification of the visible vessels, a set of fixed positions could be determined in the picture. With these positions known, a rough shape of the slick could then be drawn in scale.

In total – four distinct images of the Marine Diesel slick could be constructed with these methods, while two distinct images could be made from the Crude Oil slick (see Table 8.3.2):

Table 8.3.2 Slick contours derived from aerial surveillance imaging

Date and time (UTC)	*Type of image*	*Slick area, km^2* [a])
June 27 0834	Photo	0.031
June 27 0840	Photo	0.074
June 27 0946	UV (thick slick from IR)	0.271 (0.061)
June 27 1122	UV (thick slick from IR)	0.517 (0.144)
June 29, 0911	SLAR	1.251
June 29, 1358	SLAR	8.016

[a]) Numbers in parenthesis represents the thick part of the slick determined from IR images.

The slick contours that were obtained in this way are stored in digital form in the Excel file Slick_Contours.xls in the SLICKdata directory. This Excel workbook includes a facility for extracting and plotting slick contours for a certain time, with the contours converted into distance in meter from the discharge point. Figure 8.3.7, 8.3.8 and 8.3.9 shows the contours from the four marine diesel slick images and the two crude oil images produced by this facility.

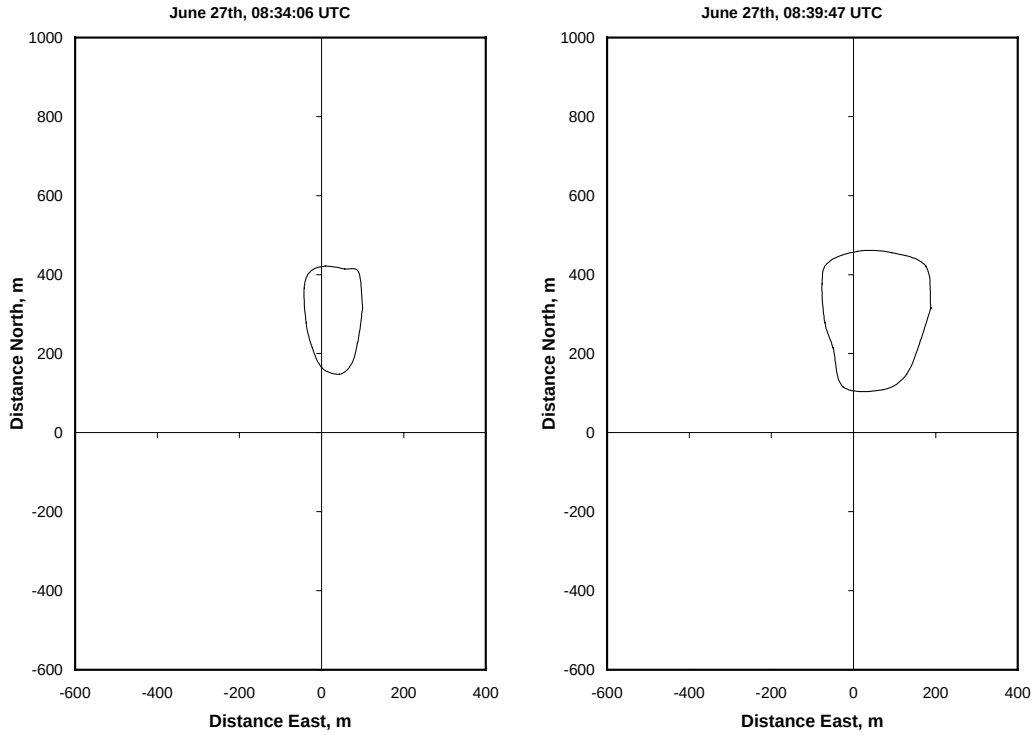

Figure 8.3.7 Slick contours derived from photos taken during the Marine Diesel experiment. Distances are relative to the discharge position (Far Grip). Note that the discharge started at 0630 UTC, with the first oil coming to the surface one hour later.

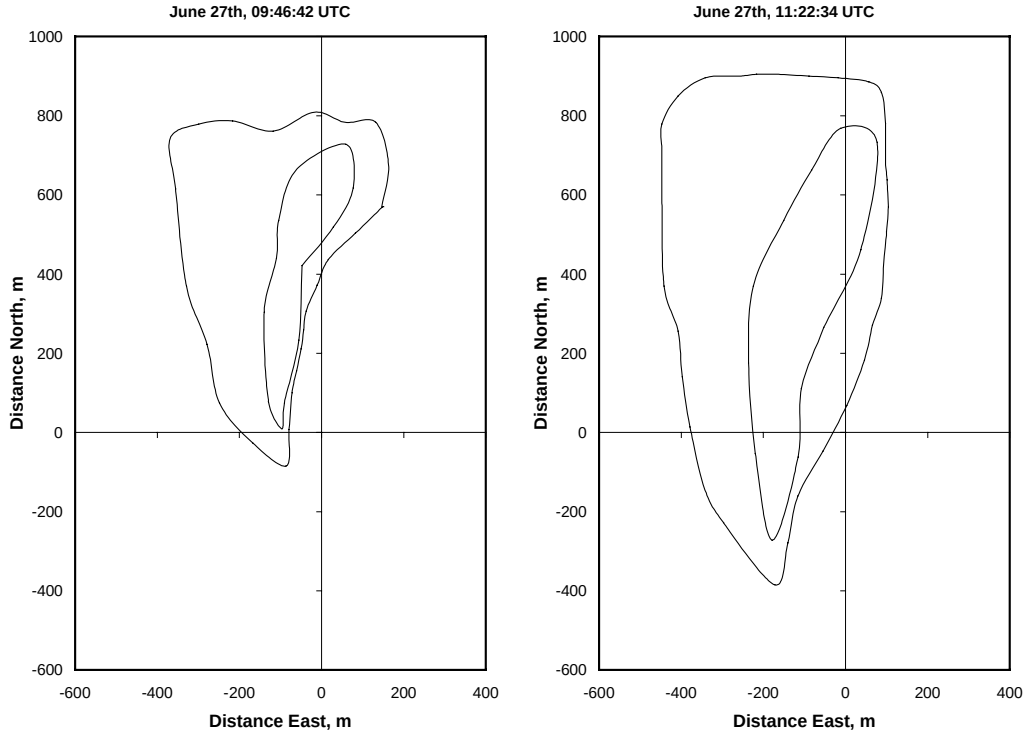

Figure 8.3.8 Slick contours derived from UV and IR-images taken during the Marine Diesel experiment. Distances are given relative to the discharge position. The contours drawn inside the main slick is based on the IR image, representing the thicker portions of the slick, while the outer contours are based on the UV image.

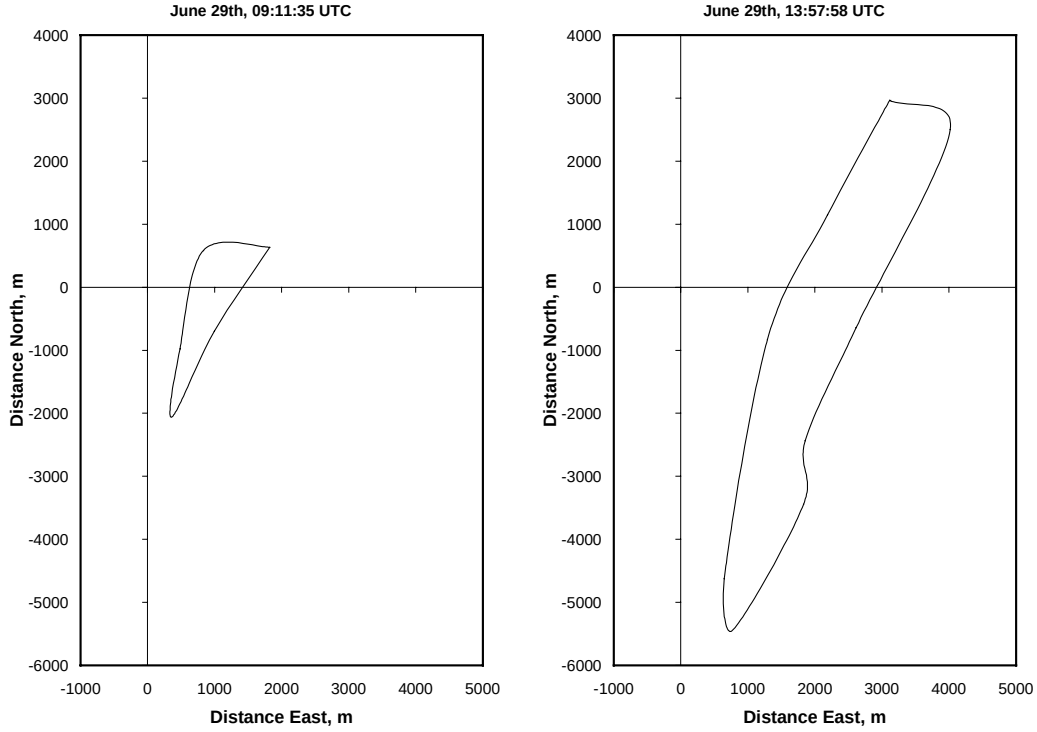

Figure 8.3.9 Slick contours derived from SLAR-images taken during the Crude Oil experiment. Distances are given relative to the discharge position. Note that the discharge started at 0520 UTC, with the first oil coming to the surface one hour later.

8.3.2 Volume estimates

As mentioned before, the aerial surveillance airplanes had an agenda of their own – namely to test a new color code for estimation of surface oil film thickness. The color code includes 6 color categories, each related to a film thickness range:

- Grey: 0.05 – 0.1 μm
- Silvery: 0.1 – 0.3μ m
- Rainbow: 0.3 – 5μ m
- Metallic: 5 – 50μ m
- Discontinuous true color: 50 – 200 μm
- Homogeneous true color: > 200 μm

The actual volume estimates shown in table 8.3.3 were made by estimating the area occupied by each of these color classes in the slick.

Table 8.3.3 Estimates of oil volumes in Marine Diesel Slick made from the surveillance airplanes. Slick volumes in m^3.

Flight	*UTC*	*Min*	*Max*
SFT	8:46	0.2	2.0
Germany	9:30	0.3	3.0
France	10:15	2.0	12.9
Denmark	10:40	1.2	11.4
The Netherlands	11:13	1.7	17.4
UK	14:55	0.003	0.009

The volume estimates in this table are likely to be uncertain, especially due to the fact that this color classification system was new to most of the crews. It should be noted, however, that all numbers are well below the total discharged volume of 60 m^3 probably caused by natural dissipation due to wave action. The rapid dissipation of the surface slick is also confirmed by the last observation at 1455 UTC, when the surface slick had almost totally disappeared.

On June 29 – the day of the Crude Oil discharge, all planes had left except the Norwegian plane operated on behalf of SFT. This plane made two flights, the first in the morning (arrival at about 0800 UTC), the second in the afternoon (arrival about 1400 UTC). A major objective of the last flight was to provide a basis for decisions of what to do with the slick: Should the available oil recovery units be mobilized for clean up, or could the slick be left to vanish on its own? At this time, the slick was about 9 km in length and close to one km in width, mainly consisting of thin sheen with rainbow appearance and small broken patches of emulsion (see picture on Figure 8.3.10). Based on the observations reported from the SFT aircraft, the JIP project manager decided that the slick could be left on its own. Oil recovery was unlikely to be efficient in the thin oil slick, and natural dispersion would eliminate the remaining of the oil slick well before the slick could come to shore. SFT's representative onboard Far Grip had no obligations to this decision, and *Far Grip* and *Håkon Mosby* left the site at 1425 UTC together with the oil recovery vessels from NOFO.

Figure 8.3.10 Oblique view of the crude oil slick from SFT's last flight. Picture taken at 14:20 UTC.

9 MODELLING AND ANALYSIS

In this chapter, model simulations will be compared with observations from the different experiments with the objective to explain some of the major features of the observed behavior of the discharges. In the first section, results from SINTEF's *DeepBlow* model are presented for the three experimental discharges, utilizing the observed stratification and ocean currents at the location as input. Estimates of the mean path of the surfacing cloud of oil droplets are shown in the next section, based on measured current profiles and certain assumptions on the droplet size distribution. Dissolution of gas into ambient seawater from rising methane bubbles is also treated in this section. Predictions of the development of the surface slicks with time are presented in the third section, once more based on the observed variations in ocean currents and wind and certain assumptions about the droplet size distribution. These results are compared with the actual observations when relevant.

9.1 Plume simulations

9.1.1 The *DeepBlow* model

SINTEF has developed a multiphase integral plume model for simulations of the near-field behavior of deepwater blowouts. A comprehensive description of the *DeepBlow* model is given in a recent paper [8], but some of the major features of the model are summarised in the following:

The *DeepBlow* model was developed in response to the increasing interest in petroleum exploration in deep waters, both in Norway and internationally. In this conjunction, deep water implies water depths from 500 to more than 1200 meters. Previously, when releases from more shallow depths were concerned, sub sea blowouts have been modeled as buoyant plumes in stagnant waters, where the buoyancy was mainly related to the gas released at or near the sea bed. However, blowouts from deep waters will behave significantly different in many major aspects:

- For blowouts at shallow to moderate depths the gas may be considered as an ideal gas with a specific volume decreasing linearly with pressure. The volume flux of gas at any depth may then be derived from the gas-to-oil volume ratio at standard conditions (GOR). However, when the blowout takes place at greater depths, the gas can no longer be presumed to behave as an ideal gas, and a pressure and temperature dependent compressibility factor (z-factor) must be introduced in the pressure-volume relationship. This normally implies that the specific volume of the discharged gas will be less than predicted by the ideal gas law.

- At the same time, the fraction of gas dissolved in the oil will increase with pressure. This implies that the vapor mass fraction of the well flow at the outlet will be reduced compared to the mass fraction predicted by the GOR.

- Dissolution of gas from rising bubbles into ambient water may be negligible for blowouts at shallow to moderate depths, since the residence time of the gas bubbles is expected to be short. For blowouts from deep waters — when the rise time of the gas bubbles may be expected to be significantly longer and the solubility of gas in sea water is increased due to

[8] See Johansen, Ø, 2000*: DeepBlow – a Lagrangian plume model for deep water blowouts.* Spill Science & Technology Bulletin, Vol. 6, No. 2, pp. 103 – 111.

larger ambient pressures — a significant reduction in the buoyancy flux may be expected due to dissolution of gas in sea water.

- In addition, natural gas tends to form gas hydrates at elevated pressures and low temperatures. Thus, when a blowout takes place at large depths, the gas may be converted to hydrate in contact with cold bottom water. If that happens, the contribution of the gas to the buoyancy flux will vanish, and the considerably smaller buoyancy caused by gas hydrates and oil will instead drive the rise of the plume.

Together, these factors will cause a significant reduction in buoyancy flux, and as a consequence, the plume may become more sensitive to cross currents and the presence of density stratification in the water masses. In such cases, even small stable density gradients in the ambient water may be expected to cause trapping of the plume. However, the oil may finally arrive at the sea surface due to the buoyancy of individual oil droplets. The resulting surface spreading of the oil will then depend on the size distribution of the oil droplets and the strength and variability of the ambient current.

This situation differs significantly from the situation when blowouts occur at moderate depths. In such cases, the surface spreading of the oil will be governed by the radial outflow of water entrained by the rising gas bubble plume. This implies that without major modifications, existing blowout models will produce unrealistic predictions of plume behavior and surface spreading when applied to blowouts from deep water. As a consequence, in the *DeepBlow* plume model developed by SINTEF, the following major factors have been taken into account in addition to factors included in blowout plume models in general:

- Effects of cross currents and ambient stratification
- Non-ideal gas behavior
- Dissolution of gas and hydrate formation

The first modification (effects of cross currents) implies in the first place the introduction of the mechanism of forced entrainment in the model. However, when this is included, the plume may be found to bend over due to entrainment of momentum from the ambient water. This implies a potential for leakage of gas bubbles from the plume, which has been accounted for in the model.

The second modification (non-ideal gas behavior) implies introduction of a pressure and temperature dependent compressibility factor (*z*-factor) in the pressure-volume-temperature (PVT) relationship of the gas. This *z*-factor depends in addition on the composition of the gas phase, and is a well-known subject in petroleum physics.

The last modification implies that the potential conversion of gas into hydrate in contact with seawater must be introduced in the model. At the same time, the buoyancy of hydrates formed from the gas must substitute the buoyancy of the gas bubbles. Gas that does not form hydrate must be allowed to dissolve in the water masses, causing a corresponding loss in buoyancy from the gas.

Figure 9.1.1 indicates the possible behavior of a deepwater blowout based on these considerations. This figure shows the presence of an underwater plume, containing the oil droplets, the sea water entrained into the plume and the gas, either represented as gas bubbles, hydrate or dissolved gas.

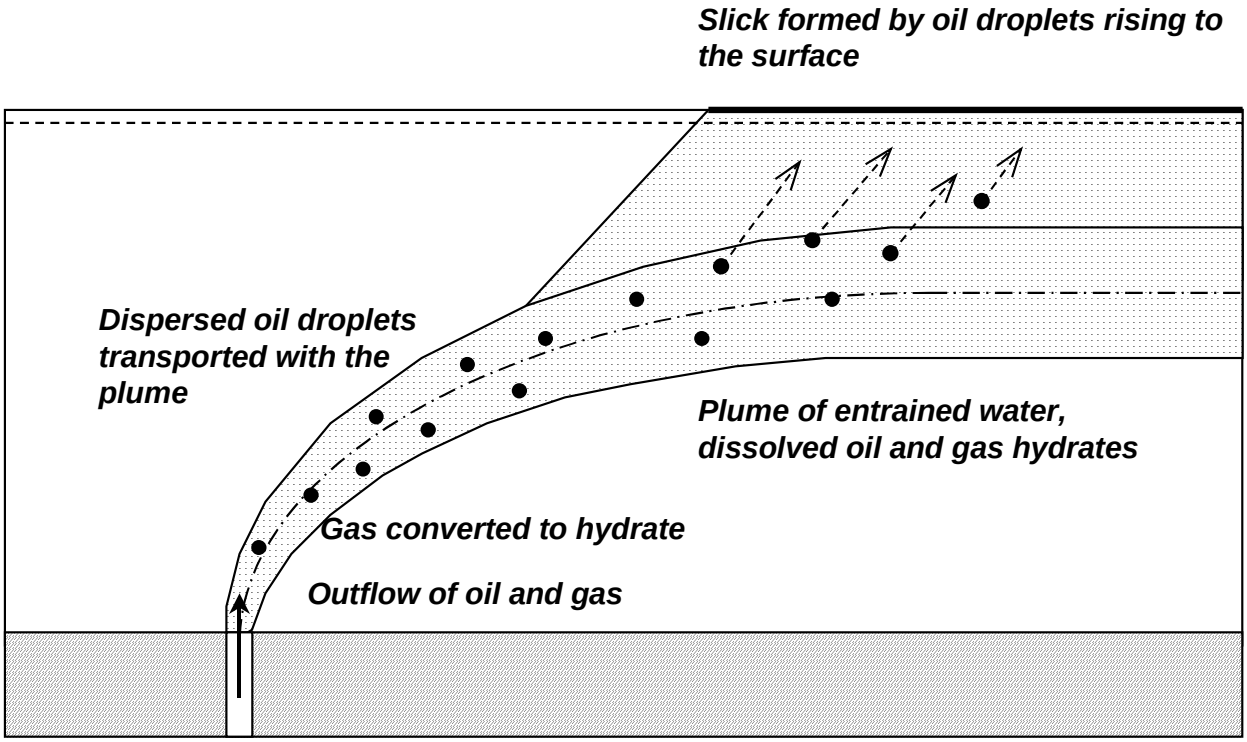

Figure 9.1.1 Sketch of the possible behavior of a plume formed by a deep-sea blowout of oil and gas. Note that it is uncertain whether hydrate formation will take place from rising gas bubbles when the thermodynamic conditions are present. However – dissolution of gas in seawater will to a large extent produce the same overall result (loss of buoyancy related to the gas phase).

While the thermodynamic conditions for hydrate formation are well established, it is still uncertain whether hydrate formation will actually take place, and if that happens - at which rate the gas bubbles will be converted into hydrate. In order to take this uncertainty into account, hydrate formation may be turned on or off in the model to demonstrate the sensitivity of the results to this process.

Once the underwater plume has reached the layer where the plume is entrapped (density of the plume equals the density of the ambient water), the oil droplets will tend to rise out of the underwater plume. The oil droplets will then rise to the sea surface, dependent on their rise velocity (droplet size dependent).

The droplet sizes govern the rise velocity and thus the time for the oil droplet spent on the ascent. The ocean currents will govern the location there the oil droplets will appear at the sea surface. Since these processes are not included in the *DeepBlow* model, a separate model have been developed to represent slick formation.

9.1.2 *DeepBlow* simulations

In the present runs with the *DeepBlow* model, the following input data were used:

Table 9.1 Input data applied in the DeepBlow runs

	Marine Diesel and LNG	*Crude oil and LNG*	*LNG and sea water* [a])
Discharge depth, m	844	844	844
Outlet diameter, m	0.120	0.120	0.120
Oil flow rate, m^3/h	60	60	1
Water to oil ratio, m^3/m^3	0	0.	60
Gas to oil ratio, m^3/m^3	36	42	2520
Density of oil, kg/ m^3	854.8	842.5	842.5
Density of gas, kg/ Sm^3	0.67	0.67	0.67
Salinity of formation water, o/oo	-	-	35.0
Outlet temperature, ^oC	0.0	0.0	0.0

[a]) The oil discharge rate has been arbitrarily set to 1 m^3/h in order to represent the actual discharge rates of gas and water in terms of gas-to-oil ratios and water-to-oil ratios required by the model.

In each case, the measured current profile at the start of the experiment was used, together with the mean vertical hydrographical profile observed in the experimental period (sea temperature and salinity). According to the field observations, the hydrate formation process has been "turned off" in all cases.

The major results from the simulations are summarized in Table 9.1.2 and figures 9.1.2 to 9.1.7. Table 9.1.2 includes the overall results in terms of depth of trapping (DOT) and rise time to this level. As indicated by the marker on Figure 9.1.2, the depth of trapping has been defined as the point of maximum plume rise measured along the plume centerline. As seen from the table, the plume rise is in the order of 200 m, with a variation from 170 to 215 m among the three cases. These variations are mainly due to the variation in the ambient current, and partly due to differences in buoyancy flux (seawater replaced oil in the last experiment).

The values in the last column are calculated by assuming an oil droplet rising with the plume with its own terminal velocity superimposed on the plume rise velocity. However, the extra speed picked up from the plume will cause only minor reductions in the total rise time to the surface. By taking into account the plume rise velocities we find a reduction in the rise time to the surface of respectively 8 and 13 minutes for the two cases with oil discharges.

Table 9.1.2 Overall results from the DeepBlow simulations. All values refer to the depth of trapping – defined as the maximum rise of the plume centerline.

Case	*Current speed, cm/s*	*Plume rise from exit point, m*	*Rise time in plume, sec*	*Rise time of oil droplet, sec* [a])
Marine Diesel	12.2	169	2200	631
Crude oil	6.0	215	1480	636
Methane	3.3	189	1420	-

[a]) This rise time is obtained by superimposing the plume rise velocity on the terminal velocity of oil droplets – here set to 0.15 m/s, which is presumed to be the maximum rise velocity of oil droplets independent of size.

For each case, two figures are shown, one depicting the plume development in terms of a side view and top view of the plume (see for example Figure 9.1.2), while the other illustrates the fate of the gas in the plume (see for instance Figure 9.1.3).

A comparison between corresponding figures shows that the stronger current at the time of the marine diesel discharge causes a significant down-stream deflection of the plume, while the plumes in the two other cases are more upright. The stronger current in the marine diesel case can also explain the more prominent leakage of gas bubbles at an early stage of the plume rise (compare Figures 9.1.3, 9.1.5 and 9.1.7). Note that amount of gas leaked from the plume is the difference between the initial amount of gas (100% at the respective graphs), and the total amount of gas remaining in the plume element. The latter is the sum of gas mass contained in bubbles and present in the dissolved state (and/or trapped in hydrates – when relevant). Note also that in all cases, all the gas is either leaked out or dissolved in the entrained water when the plume reaches the depth of trapping.

In total, these results indicate that most of the gas bubbles and oil droplets will escape from the plume below 100 and 200 m above the exit point. The plume phase as such is thus expected to play a relatively minor role in the ascent of gas bubbles and oil droplets.

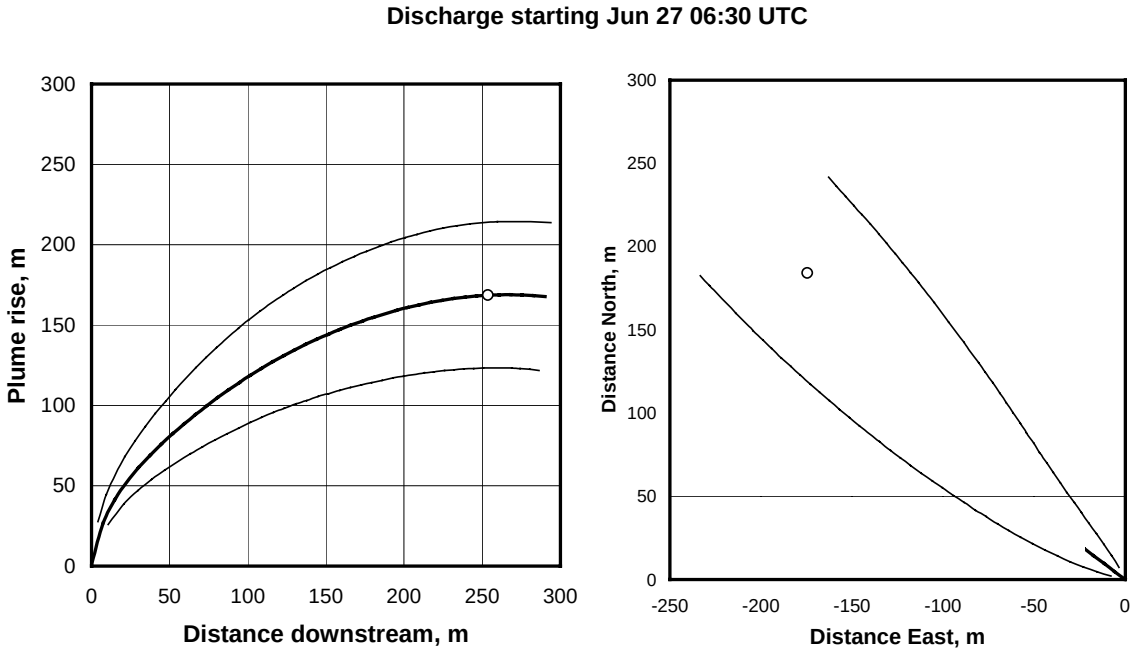

Figure 9.1.2 Results from the DeepBlow simulations: Side view and top view of plume from the Marine Diesel oil experiment. Thick lines represent the plume centerline, while thin lines indicate the radial extension of the plume.

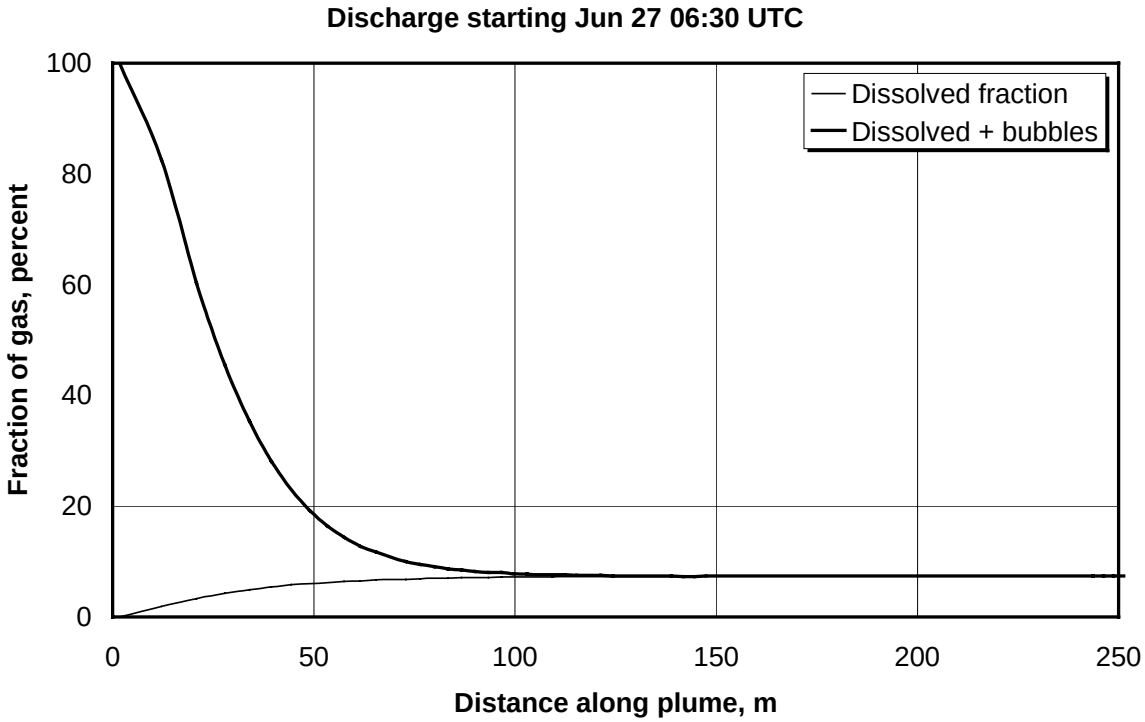

Figure 9.1.3 Results from the DeepBlow simulations: Fraction of gas remaining along plume path for the Marine Diesel experiment.

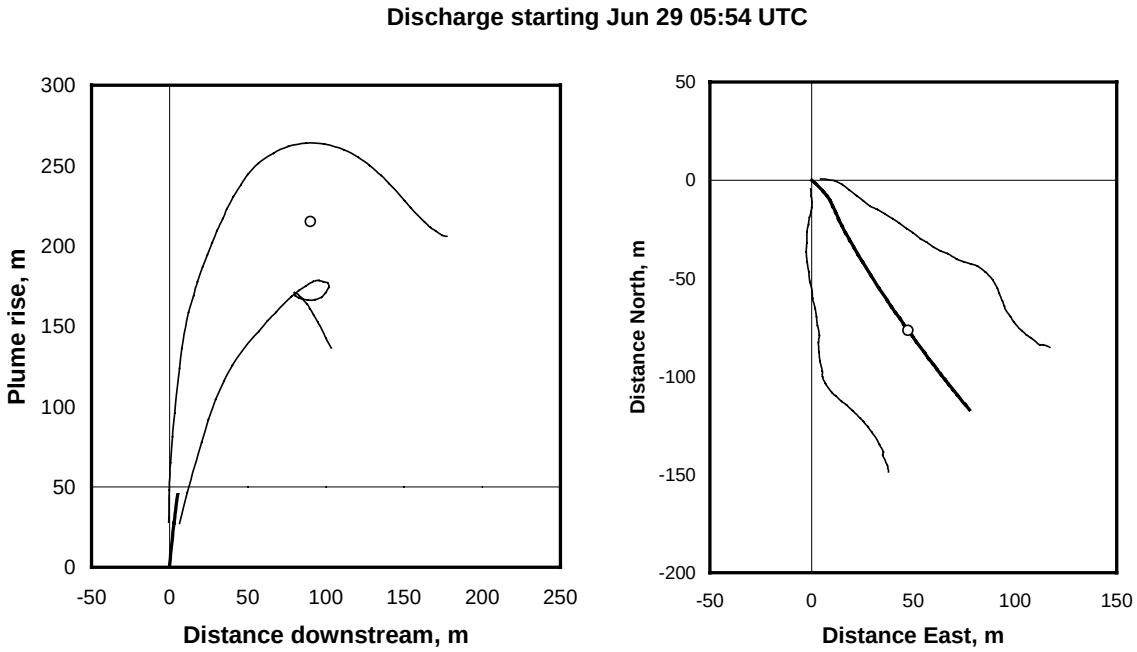

Figure 9.1.4 Results from the DeepBlow simulations: Side view and top view of plume from the Crude Oil experiment.

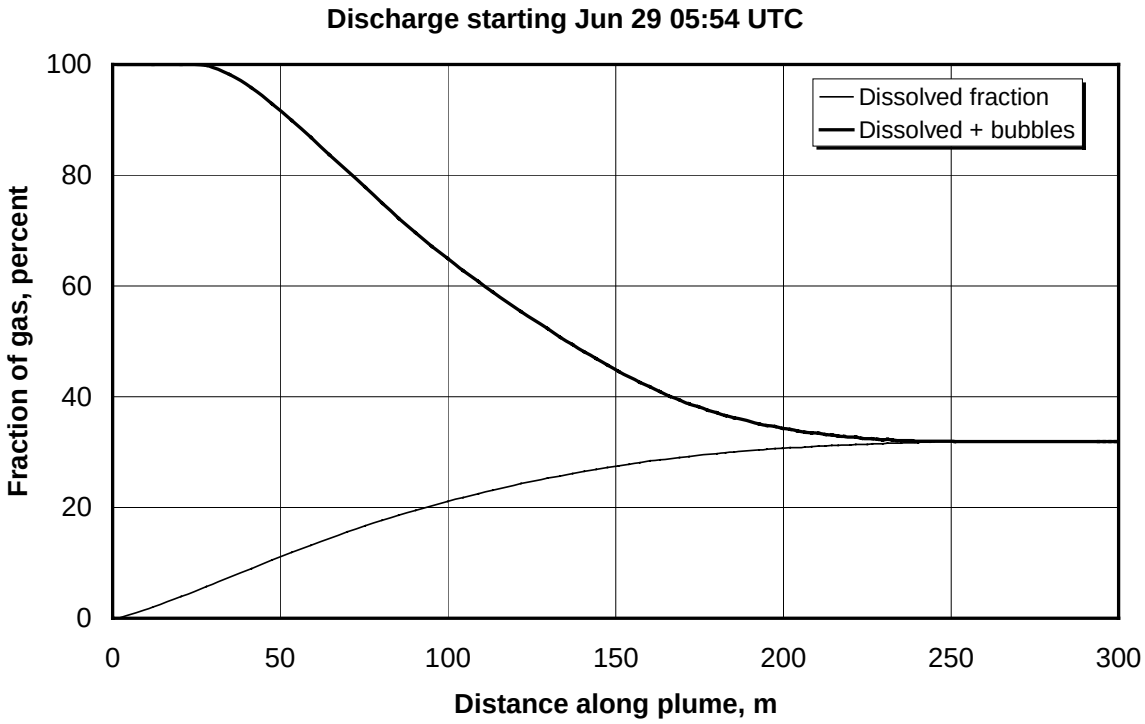

Figure 9.1.5 Results from the DeepBlow simulations: Fraction of gas remaining along plume path for the Crude Oil experiment.

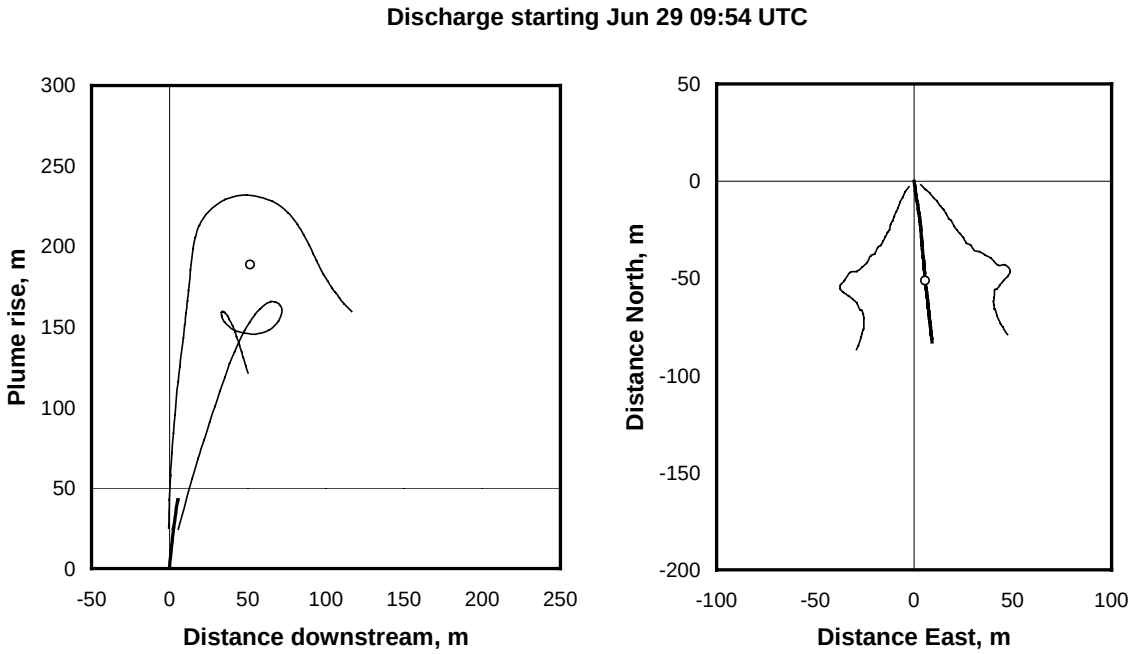

Figure 9.1.6 Results from the DeepBlow simulations: Side view and top view of plume from the Natural Gas experiment.

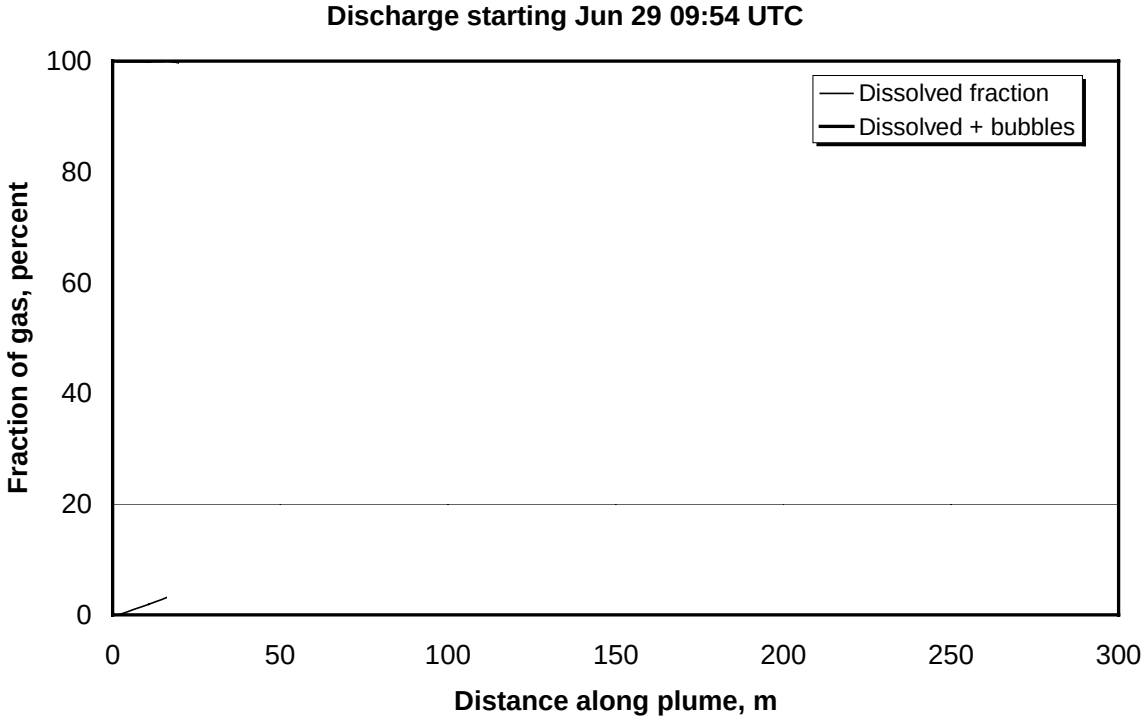

Figure 9.1.7 Results from the DeepBlow simulations: Fraction of gas remaining along plume path for the Natural Gas experiment.

9.2 Surfacing of oil droplets and gas bubbles

As indicated in the last section, oil droplets and gas bubbles will escape from the plume at or before the depth of trapping and then rise to the surface individually. Thus, we can anticipate that the plume phase will be succeeded by rising clouds of dispersed oil droplets and gas bubbles. In this section, we will first present some calculations of the surfacing of oil bubbles, and next consider the fate of gas bubbles in such clouds.

9.2.1 Rise of oil droplets

In this section, we will present calculations of the formation and shape of rising clouds of oil droplets. The centerline of such clouds will to some extent be shaped by the vertical current profile, but the cloud will spread laterally due to variations in the rise velocity of the droplets and bubbles within the cloud. To illustrate this, we have developed an explanatory model based on the following assumptions:

- The measured vertical current profile at the start of each experiment is used to represent the respective cases, and this profile is presumed constant in the period considered.
- The size distribution of the oil droplets is represented by a Rosin-Rammler distribution[9], defined by a maximum droplet size D_{95} = 7 mm and a spreading parameter n = 2.5.
- The rise velocity of the droplets is calculated from the droplet radius and density by a mixed formula[10] – comprising both the Stokes law regime (Reynolds number, Re < 1), the constant drag regime (Re > 1000), as well as the intermediate regime between the asymptotic formulas (see Figure 9.2.1).

The asymptotic equations for droplet rise velocity are expressed as:

$$\text{Stokes law } (\mathrm{Re} \le 1): \qquad w = \frac{D^2 g'}{18\nu}$$

$$\text{Constant drag law } (\mathrm{Re} \ge 1000): w = 1.8\sqrt{g' D}$$

where D is the droplet diameter, $g' = g(\rho_w - \rho)/\rho_w$ is the reduced gravity, and ν is the kinematic viscosity of water.

The mean path of the cloud is estimated in the following way:

A continuous discharge (lasting for e.g. one hour) is represented by a discrete number N of instantaneous releases (here 21) spaced evenly in time. The distance to the surface is divided in a number of discrete levels, spaced at a fixed distance (50 m). At a certain instant t in time – e.g. one hour after the start of the discharge – the rise velocity required for a droplet from each of the discrete releases at times t_j to reach the discrete levels Z_i can be calculated from the equation

$$w_{i,j} = Z_i / \tau_j, \text{ where } \tau_j = t - t_j .$$

[9] See Chapter 3 in Lefebvre, A.H., 1989: *Atomization and Sprays*, Taylor & Francis, USA.
[10] For details, see Johansen, 2000, op cit.

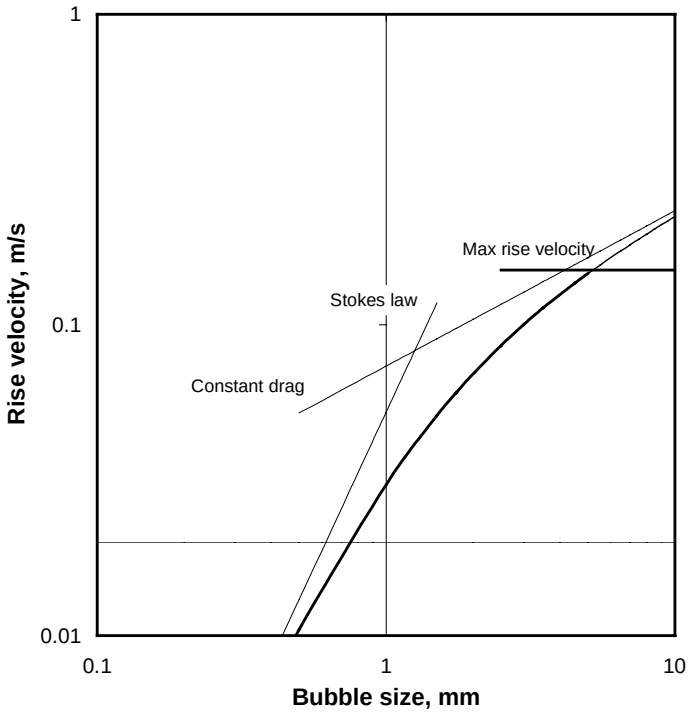

Figure 9.2.1 Rise velocity of oil droplets as a function of size. The oil density is chosen as 850 kg/m^3 as a representative average for the oils involved in the experiment. Thin lines show asymptotic regimes (Stokes law and constant drag law), while the thick line shows the actual rise velocity of oil droplets (mixed formula). A maximum rise velocity of 0.15 m/s is indicated.

The droplet size $D_{i,j}$ corresponding to this rise velocity is derived from the inverse of the rise velocity equation. The cumulative fraction $P_{i,j}$ of oil contained in droplets up to this size is derived from the assumed droplet size distribution, and the fraction $p_{i,j}$ remaining of each discrete release in each discrete layer is obtained as the difference between adjacent layers:

$$p_{i,j} = P_{i,j} - P_{i-1,j}$$

At a certain instant in time, a drifted distance *x*, *y* (corresponding to east and north) can be assigned to each discrete release in each discrete layer:

$$(x, y)_{i,j} = (\bar{u}, \bar{v})_i \, \tau_j \ ,$$

where *u* and *v* with bars are the depth averaged velocities between the exit point and depth level *i*.

The mean path X_i Y_i is then computed as an average of these positions weighted with the corresponding oil mass fraction $p_{i,j}$. A mean droplet size D_i is computed in the same manner from the droplet sizes $D_{i,j}$, paired with the corresponding mass fractions. The model based on these assumptions is referred to as *Cloudrise* in the following. The main results from these calculations for the Marine Diesel experiment are given in Figure 9.2.2, 9.2.3 and 9.2.4.

Figure 9.2.2 shows a top view of the mean path, with depth indicated with markers for each 50 m levels. A slick contour obtained from the aerial surveillance aircraft is shown for comparison. Note, however, that the slick contour was obtained from pictures taken 1 hour after the end of this simulation. The shape of the mean path is clearly reflecting the prevailing currents, turning from a north-westerly current in deep waters towards a north-easterly current in the upper water column.

Figure 9.2.3 shows a side view of the mean path in an east and north projection. The crossbars are drawn to indicate the vertical distribution of the oil mass – expressed as fraction of the total discharge present in each 50 m layer. The crossbars are scaled so that 100 m to each side represents 10 % of the total discharge. As the figure indicates, very small amounts of the oil have reached the surface at this time. The next figure (9.2.4) shows the time development of the vertical distribution of oil mass and mean droplet size. The distribution is seen to change shape as time elapses after the end of the discharge period – with the maximum point rising until it approaches the surface. The mean droplet size changes in a corresponding manner, with the smallest droplets staying behind in the deep layers, while the larger droplets are coming to the surface. Figure 9.2.5 shows a comparison between the computed mean path of the droplet cloud for both oil experiments and the data obtained from the corresponding echo-sounder tracks. The figure indicates that the computed mean path corresponds fairly well with the overall shape of the cloud as observed with the echo-sounder.

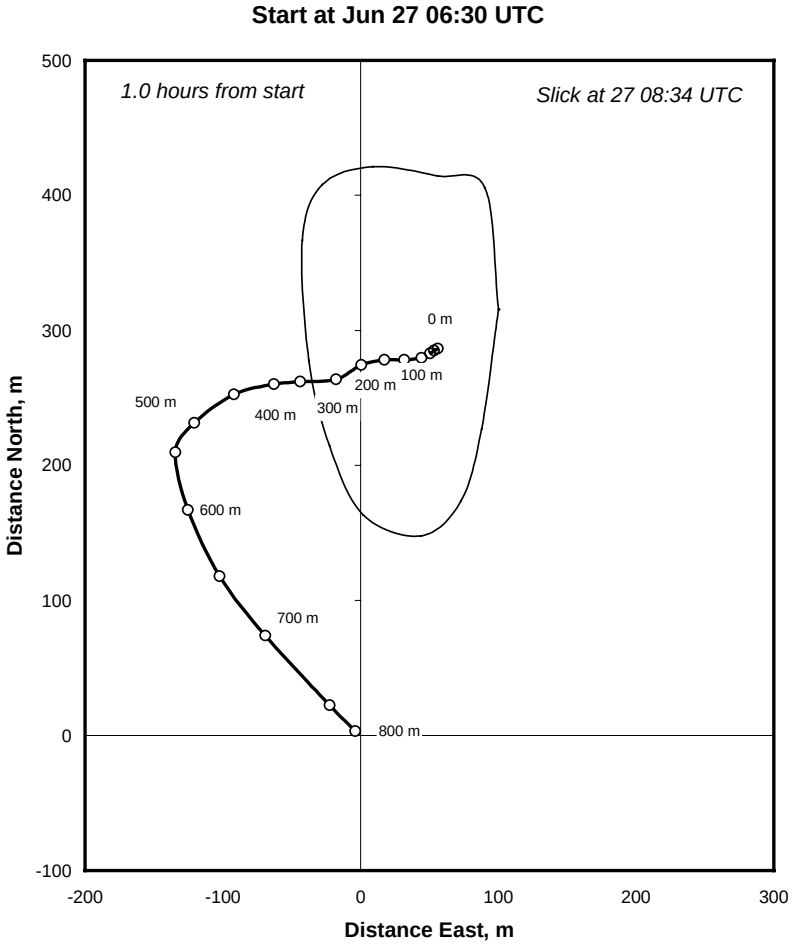

Figure 9.2.2 Cloudrise *calculations applied to the Marine Diesel experiment: Top view of the mean path of a cloud of rising oil droplets with a slick contour obtained from aerial surveillance drawn for comparison.*

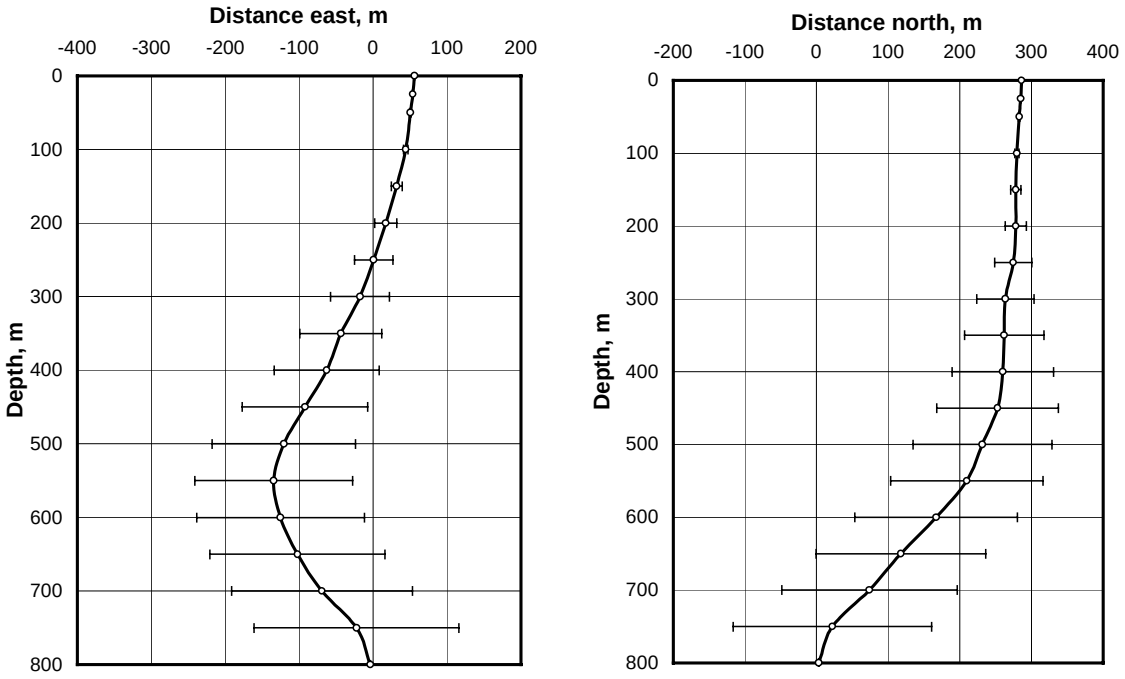

Figure 9.2.3 Cloudrise *calculations applied to the Marine Diesel experiment: Side view of the mean path of the rising droplet cloud one hour after start (east and north projections). The crossbars are drawn to indicate the fraction of the discharged oil remaining in each 50 meters layer. A bar with length 100 m to each side represents 10% of the discharge.*

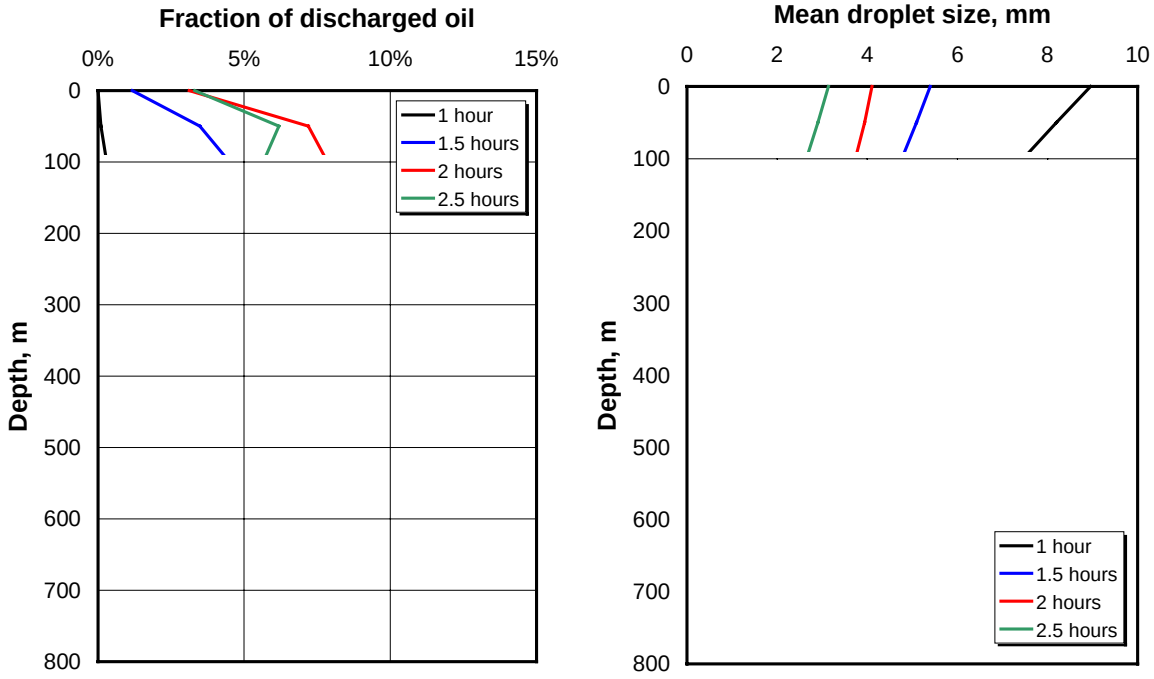

Figure 9.2.4 Cloudrise *calculations applied to the Marine Diesel experiment. Left: Mass fraction of oil in each layer. Right: corresponding mean droplet size. Times relative to start time of discharge.*

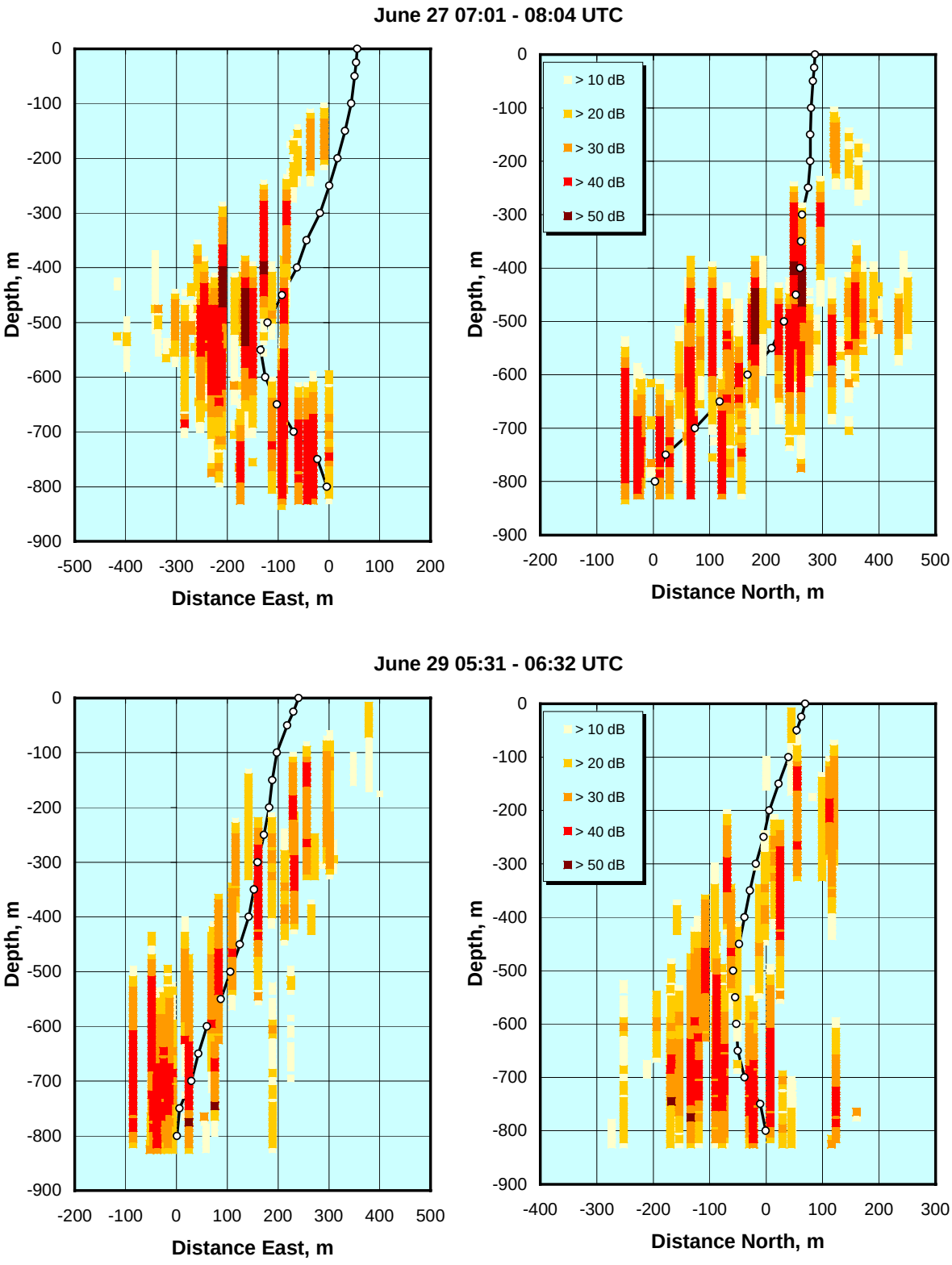

Figure 9.2.5 Cloudrise *calculations applied to the oil discharge experiments: Mean cloud path one hour after start of discharge compared with the echo-sounder data from RV Håkon Mosby. Top: marine diesel experiment. Bottom: Crude oil experiment.*

9.2.2 Rise of gas bubbles

Gas bubbles within the observed size range are expected to show less variation in rise velocity than the oil droplets, primarily due to the existence of an upper limit to the rise velocity in the order of 0.30 m/s. As indicated in Figure 9.2.6, this upper limit is reached for methane bubbles with diameter larger than 3 to 4 mm.

Large bubbles may thus be expected to rise to the surface from a depth of 840 m in about 45 minutes. However, as the echo sounder data shown in Figures 9.2.7 and 9.2.8 indicate, gas was not detected closer to the surface than about 150 m. Figure 9.2.7 shows echo sounder data for the first hour of the experiment, but the situation did not change appreciably in the following hour (the methane gas discharge lasted for two hours), as demonstrated by Figure 9.2.8.

Figure 9.2.8 is based on an inspection of the echo sounder data in intervals of 10 minutes in the early phase of the experiment, and in intervals of half an hour in the later phase (when a quasi-stationary situation was achieved). Within these intervals, the most shallow occurrence of the back scatter signal in each of four classes (10, 20, 30 and 40 dB) have been recorded and plotted as a function of time. On the same plot, lines have been drawn representing the rise of bubbles with constant terminal velocities (0.15, 0.20 and 0.30 m/s).

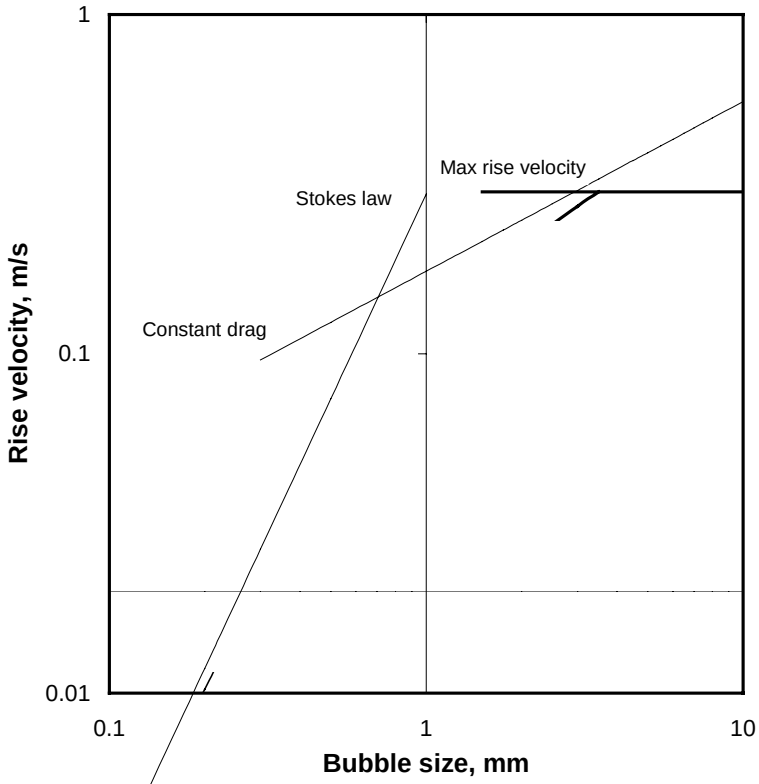

Figure 9.2.6 Rise velocity of methane gas bubbles as a function of bubble diameter. Calculations are made for methane gas at 500 m depth with a temperature of 0 °C, but the results are relatively insensitive to depth. The thick solid line shows the calculated rise velocity limited by a general maximum rise velocity of 0.3 m/s for bubbles. The thin lines are based on the two asymptotic equations – the Stokes law and the Constant Drag Law.

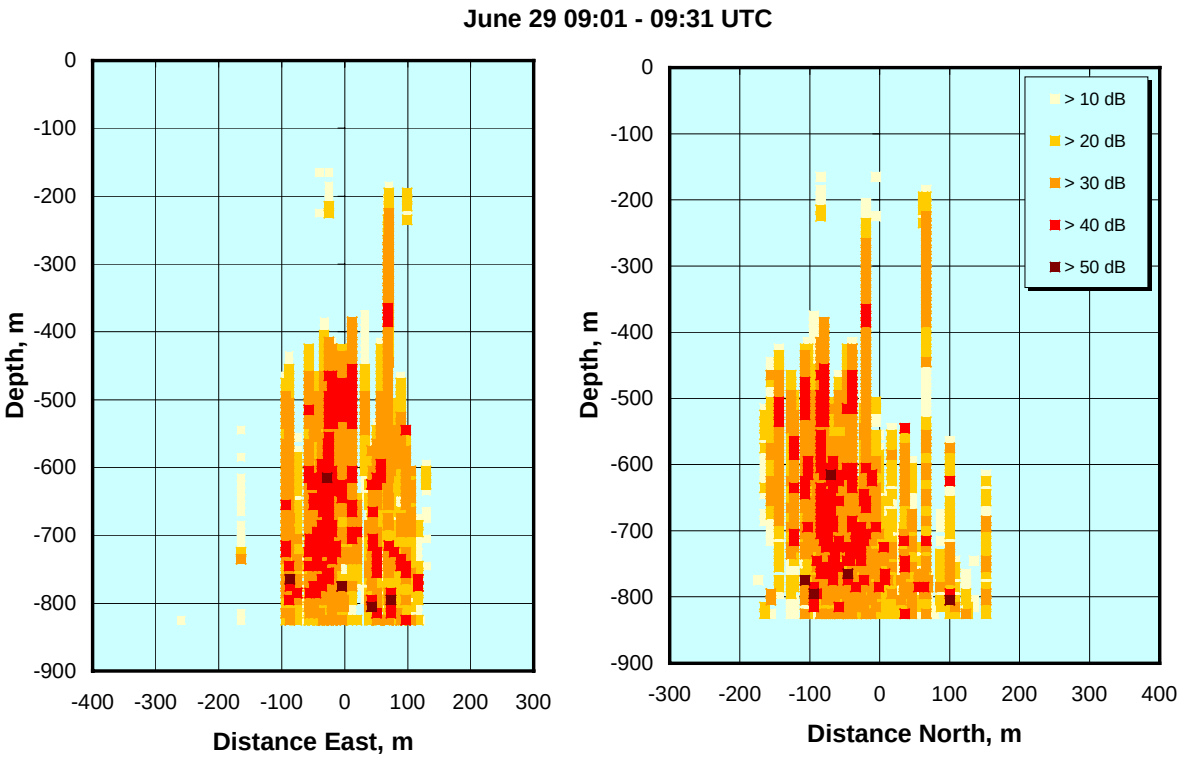

Figure 9.2.7 Echo sounder data from the first hour of the methane gas experiment.

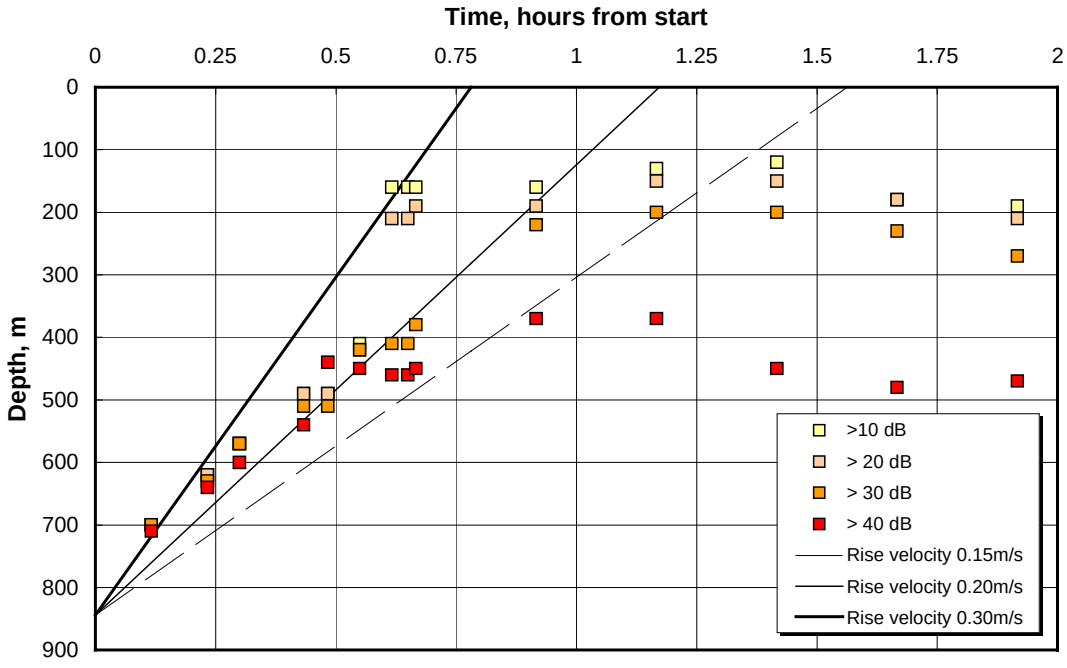

Figure 9.2.8 Time plot of the shallowest registration of echo sounder signals larger than respectively 10, 20, 30 and 40 dB. The straight lines show the trajectory of bubbles with constant rise velocities of 0.15, 0.20 and 0.30 m/s.

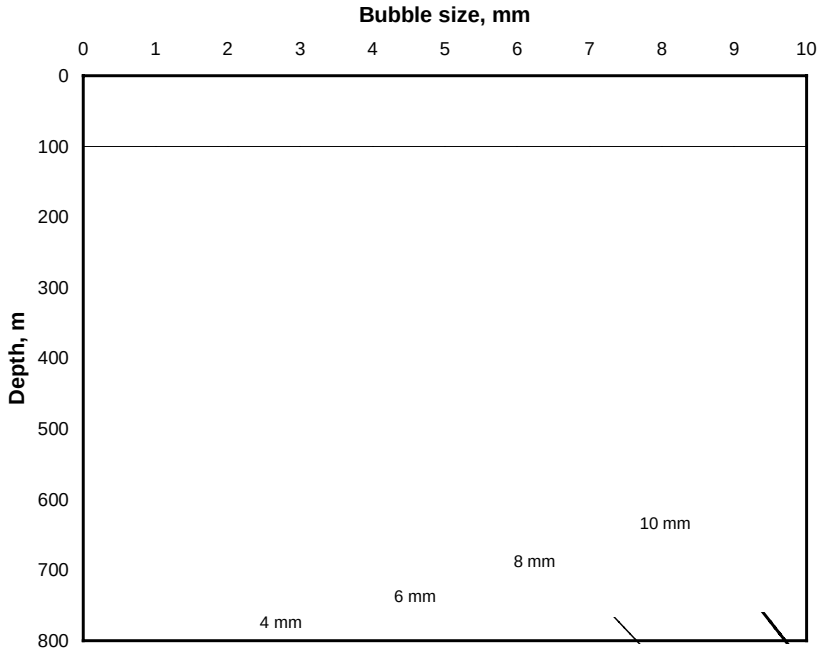

Figure 9.2.9 Reduction in methane bubble diameter due to dissolution of gas into ambient seawater. The bubbles are presumed to start from 850 m depth and rise with their size dependent terminal velocity. The initial bubble size is indicated as parameters on each curve where the subsequent change in bubble size can be read off as a function of depth. Mass transfer coefficient is computed from empirical formulas presented by Hughmark (1967), however reduced with an ad hoc *factor of 0.28 to fit observations of the maximum bubble rise in the methane gas release (see previous figure).*

This figure not only indicates that the bubbles do not reach the surface, but also that the volume of gas (or number of bubbles) tends to be reduced with distance from the exit. Such a loss of gas is very likely to be due to dissolution of gas into ambient seawater. In fact, calculations based on the known solubility of methane gas in seawater[11] and mass transfer coefficients derived from laboratory experiments[12] indicate that even the largest observed gas bubbles (10 mm initial diameter) should have been consumed by the dissolution process after a vertical rise of about 200 m. In order to match the observed maximum vertical rise of gas of about 700 m, an *ad hoc* reduction factor had to be introduced in the mass transfer coefficient (see Figure 9.2.9). An explanation for this significant decrease in dissolution rate has not been found, but other observations in the field of rising bubble clouds or plumes of methane gas seem to indicate the same (unexpected) persistence of the gas bubbles.

9.3 Surface slick formation

While the previous sections have dealt with the fate of gas bubbles and oil droplets in the water column, this section will address the process of surface slick formation. The calculations presented in the following are based on the following main assumptions:

[11] See Chapter 7 in Fogg, P.G.T, 1991: *Solubility of gases in liquids.* Wiley.
[12] See Hughmark, G.A., 1967: *Liquid-liquid spray column drop size, holdup, and continuous phase mass transfer*. I&EC Fundamentals Vol. 6, No. 3, pp. 408-413.

- The oil ascends to the surface as individual droplets from the level of trapping of the plume.
- The rising droplets drift horizontally with the prevailing current (variable with depth and time) until they reach the sea surface.
- Surfaced oil droplets are in addition subject to a wind induced current – to be superimposed on the currents measured in the top layer (25 m depth).
- Surface oil is also subject to weathering, here for simplicity represented as an exponential decay depending on time on sea – parameterised in terms of a chosen half-life.

These assumptions imply that the lateral spreading of the oil will be due to the initial variation in droplet size and the time variations in the current. The resulting film thickness will also be influenced by loss processes such as natural dispersion and evaporation, here represented by an *ad hoc* decay rate or *half-life*.

The following input parameters have used for both oil discharges:

Initial depth (start of "free" ascent):	750 m
Time to reach this level:	600 seconds
Oil density (average for both oils):	850 kg/m^3
Maximum droplets size (D_{95}):	7 mm
Spreading parameter in Rosin-Rammler distribution:	2.5
Ocean current data:	Measured current profiles at 10 min intervals
Wind induced current:	3.5% of measured wind, turned 15 degrees to the right of the wind direction.
Half-life (Marine Diesel experiment):	0.1 hours
Half-life (Crude Oil experiment):	3 hours

The results from the simulations are shown in Figures 9.3.1 (Marine Diesel) and 9.3.2 (Crude Oil). On these plots, the oil film thickness distribution is indicated by colors with reference to oil only, since emulsion formation is not taken into account explicitly. On all plots, observed slick contours are drawn for comparison. These observations have to some extent been used to calibrate the half-life parameter used in these simulations. The short half-life (0.1 hours) that was used in the marine Diesel simulation was chosen to reproduce the limited downstream extension of the observed surface slick in this experiment. A considerably longer half-life (3 hours) had to be used in the Crude Oil case to reproduce the more extended slick formed in that experiment. Note that this first order decay model with a single parameter (half-life) is used here as a provisional representation of much more complex processes (natural dispersion and evaporation). However, the large difference in the half-life parameter required in the two cases is probably a reflection of the fact that emulsion formation were totally absent in the Marine Diesel case, while relatively stable emulsion was formed in the Crude Oil case.

In total, having the above mentioned adjustable parameter in mind – the resulting surface slicks compare quite favorable with the observed slick contours, however with one notable exception: The calculated downwind front of the calculated surface slick on Figure 9.3.2 (8 hours after start) fits well with the observed slick contour, but the calculated slick does not show the same upwind extension as the observed slick contour. This discrepancy may be a result of a secondary spreading process not accounted for in the calculations: Oil droplets entrained from the slick by breaking waves will be mixed down by turbulence and follow the sub-surface current (in this case almost opposite to the wind). As observed in many experimental spills – subsequent resurfacing of these dispersed oil droplets tends to form a thin elongated slick trailing behind the primary surface slick (ref).

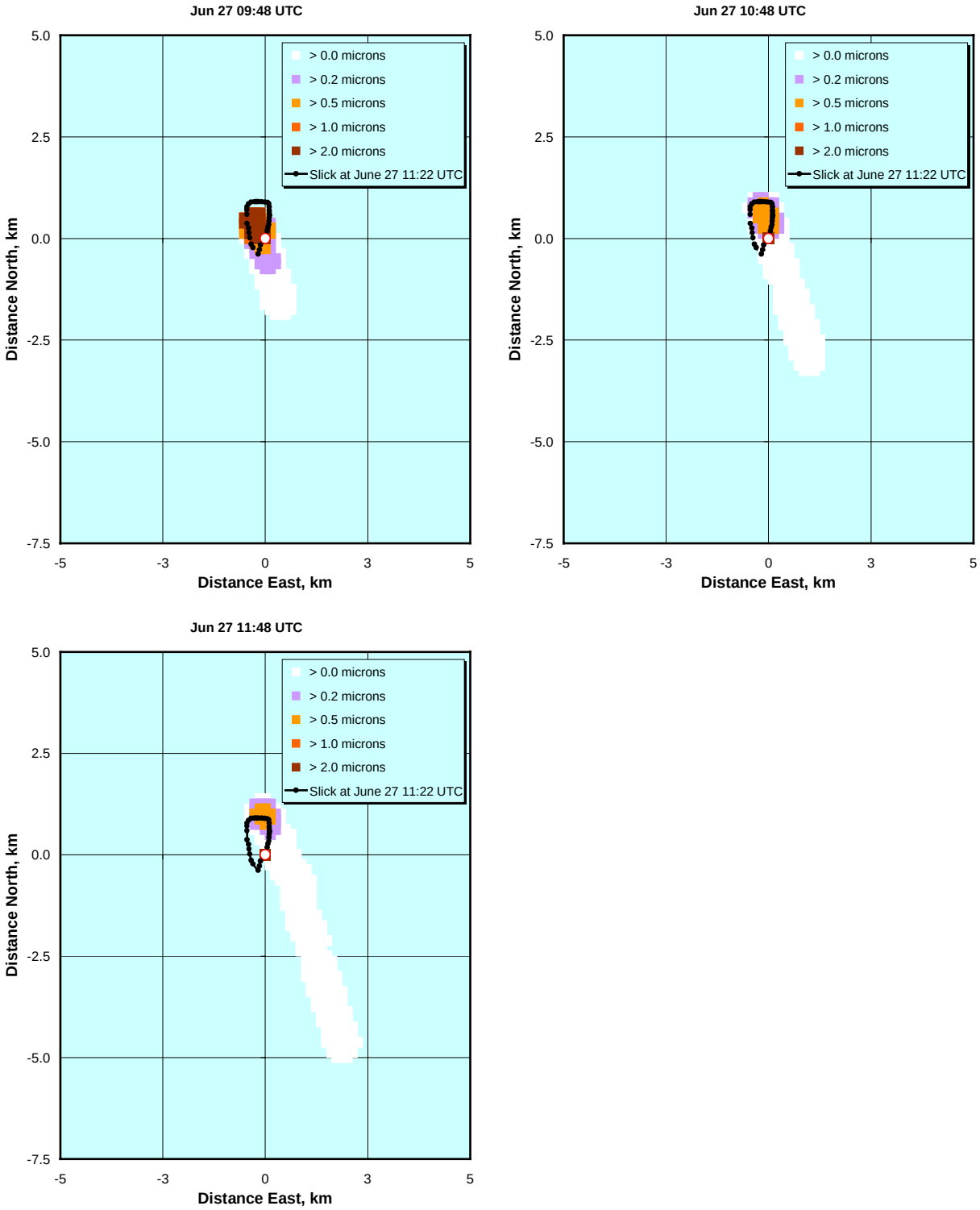

Figure 9.3.1 Simulations of the development of the surface slick from the Marine Diesel experiment. Top: 3 and 4 hours from start of discharge. Bottom: 5 hours from start of discharge. Observed slick contours from adjacent times are drawn on the same plots for comparison.

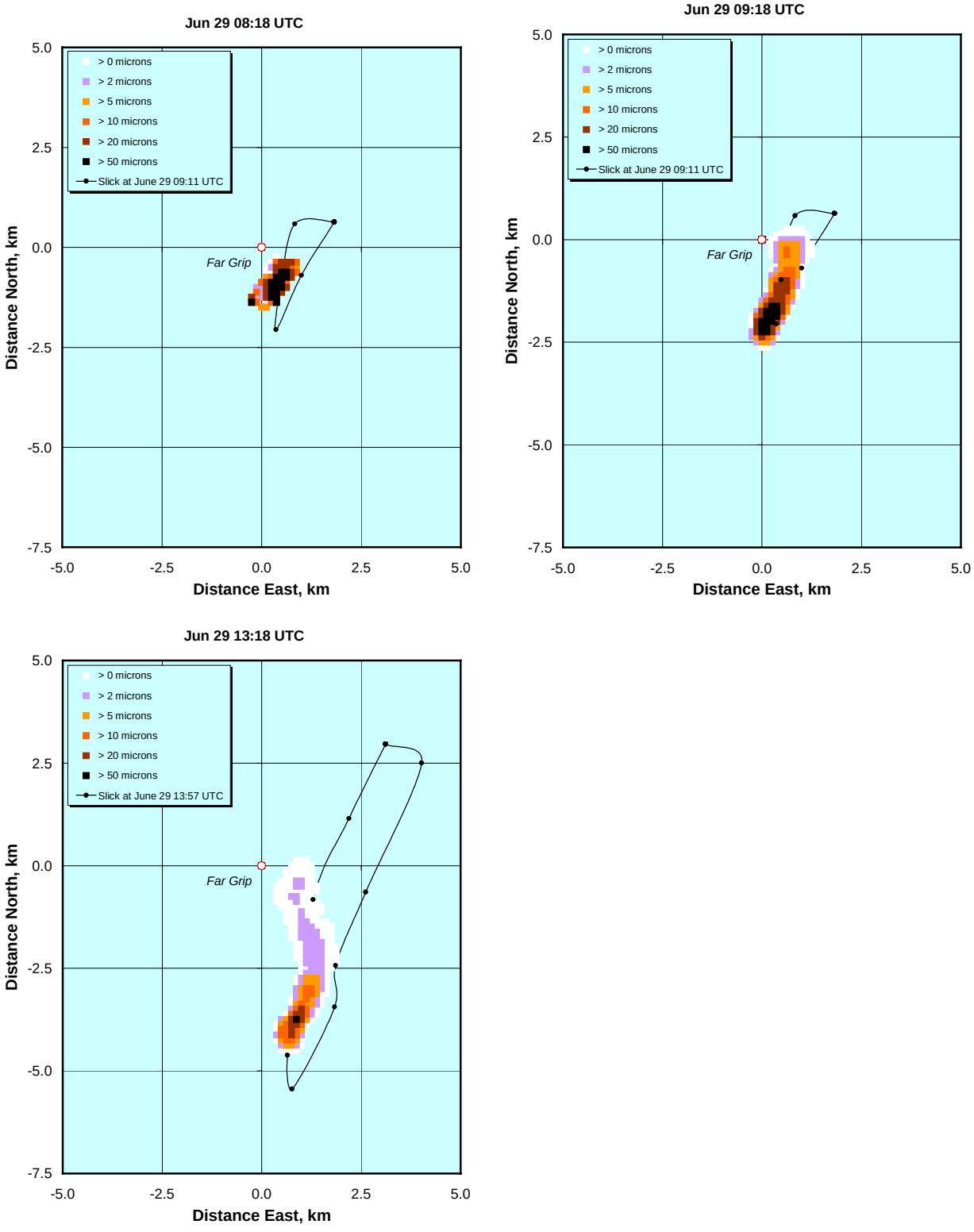

Figure 9.3.2 Simulations of the development of the surface slick from the Crude Oil experiment. Top: 3 and 4 hours from start of discharge. Note that the film thickness distribution shown in the plots are for oil only (exclusive water). Bottom: 8 hours from start of discharge. Observed slick contours from adjacent times are drawn on the same plots for comparison.

Finally, we have included results of two simulations for continuous discharges starting at the time of the Marine Diesel experiment (Figure 9.3.3). The first simulation is made with the same discharge rate and decay rate (60 m^3/ hour and half-life 3 hours) as used in the experimental discharges. The second was made with a discharge rate of 200 m^3/hour and a half-life increased to 6 hours reflecting the increased surface slick thickness (see Figure 9.3.3). The relatively large surface slick thickness resulting from the larger discharge rate will probably provide a basis for emulsion formation in larger areas of the slick, and thus produce a more persistent slick than in the case with the smaller discharge rate.

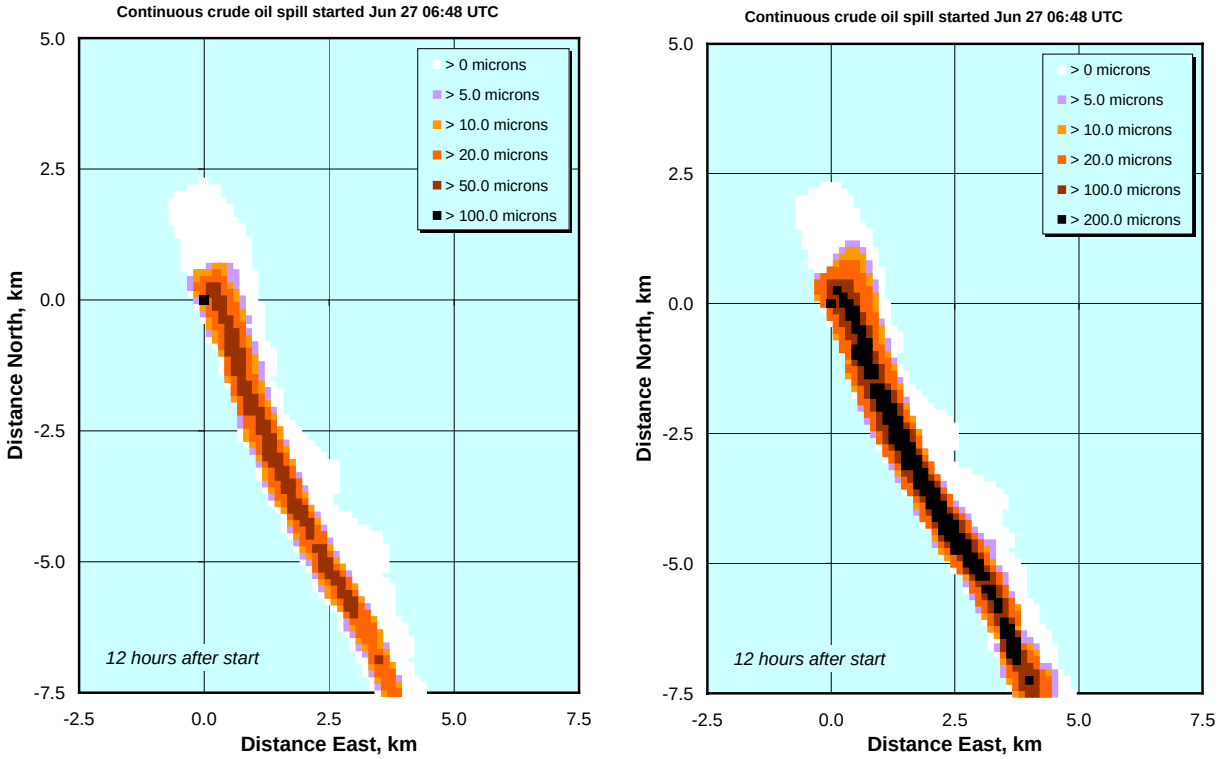

Figure 9.3.3 Simulations of surface slicks from hypothetical continuous discharges, starting at the time of the Marine Diesel experiment. Left: Crude oil discharge of 60 m^3/hour. Right: Crude oil discharge of 200 m^3/hour. Note that the color legend for film thickness is slightly different in the two cases. As before, film thickness is exclusive water (oil only).

9.4 Conclusions from the simulations

The objective of the simulations presented in this chapter has been to provide possible explanations of the observed behavior of the discharges. The major findings will be summarized in this section.

9.4.1 Plume behavior

The first simulations were concerned with the initial plume phase. Unfortunately, the trajectory of the plume as such – consisting of entrained water and dissolved components – could not be observed during the experiment. However, the simulations with the *DeepBlow* model indicated

that the plume rise would terminate between 150 and 200 meters from the exit. In the model simulations the early termination of plume rise was related to loss of gas bubbles from the plume due to deflection of the plume in the prevailing current.

If true, this implies that the plume rise would contribute little to the ascent of gas and oil (i.e. in terms of shortening the rise time). The echo-sounder data from the methane gas experiment indicated that the ascent of the bubble cloud could be related to the typical rise velocity of gas bubbles – without taking into account an initial plume phase. On the other hand, the early appearance of oil on the sea surface (one hour after the start of the discharge) seems to point in the other direction, i.e. that the rise time of the largest oil droplets was shortened due to the initial plume phase. However, these observations are not necessarily contradicting – since the maximum rise velocity of gas bubbles are considerably larger than the maximum rise velocity of oil droplets, any effect of the initial plume phase on the rise time will be more significant for oil droplets.

9.4.2 Rise of oil droplets and gas bubbles

The rise of the clouds of oil droplets was simulated based on a set of assumptions, of which the following were of major importance:

- Current profile as measured at the start of each experiment and constant in time in the time period considered.
- Discharge lasting for one hour.
- Droplet size distribution represented by a theoretical two parameter distribution (Rosin-Rammler).
- The droplets ascend with their terminal velocity derived from droplet size according to a mixed formula (merging Stokes law with the constant drag law).

The fact that the resulting mean path of the droplet clouds were found to compare favorably with echo-sounder observations seems to indicate that the assumptions listed above were reasonable, including the current profiles that were used in the simulations. This is a significant finding, particularly since the ocean current data in the upper half of the water column have been recovered from a (noisy) background of ship motion.

9.4.3 Slick formation

The formation of surface slicks was last item of concern in this chapter. The slick development was modeled with the observed time variable current profiles combined with a wind-induced surface current derived from the wind measurements. To be able to reproduce the development of the marine diesel slick, a tunable half-life parameter was introduced in a first order representation of loss processes (evaporation and natural dissipation). The limited downwind extent of the marine diesel slick (as observed from the surveillance airplanes) could be reproduced reasonably well by using a half-life of 0.1 hours in the simulations. A reproduction of the much larger slick formed in the crude oil experiment required a considerable longer half-life (3 hours was used). With this choice, the location of the downwind front of the slick could be represented reasonably well, but the apparent up-wind lengthening of the slick could not be reproduced. This feature may be interpreted as a result of wave induced entrainment of droplets from the surface slick – a process not accounted for in the present model.

10 SUMMARY, CONCLUSIONS AND RECOMMENDATIONS

10.1 Summary

The *DeepSpill* Joint Industry Project (JIP) was established with the aim of determining the fate of oil and gas released in deepwater by performing full-scale field experimental releases. The main purposes of these experiments were:

- to obtain data for verification and testing of numerical models for simulating accidental releases in deep waters,
- to test equipment for monitoring and surveillance of accidental releases in deep waters,
- to evaluate the safety aspect of accidental releases of gas and oil in deep waters.

Verified numerical models combined with improved surveillance of the releases should then provide a better basis for oil spill contingency planning and environmental impact assessments in conjunction with future deep water exploration, development and production.

10.1.1 Planning and preparations

The project was initiated with a feasibility study in order to develop a strategy for discharging and observing oil and gas in deep water. The feasibility study concentrated on three major issues – i.e. possible arrangements for transport and discharge of oil and gas in deep water, instruments and platforms for monitoring of the deep water plume, and concepts for monitoring the formation of a surface slick. As a result, feasible solutions to these problems were identified:

- The releases should be controlled and operated from surface ships, and not from remotely controlled containers deployed on the sea floor.

- The releases should be pumped down to the sea floor through coiled steel tubes, in separate lines for the oil and the gas.

- Several releases should be arranged in order to allow for redundancy as well as to be able to study different release conditions.

- In addition, the use of Remote Operated Vehicles (ROVs) was found vital due to the large depths encountered.

On this basis, plans for an experimental deepwater discharge of oil and gas were worked out, including work scope, time schedule and budget.

Due to the processing of LNG onboard ship, much attention was directed towards safety issues. Also, the project was recognized to have a large potential for failure on the data recovery side. Therefore, safety workshops (HAZOP) were arranged to reduce the risk when processing LNG onboard ship, and also to increase the possibility of success in collecting the data. Another issue that received considerable attention was the probability of hydrate formation within the coiled steel tubing system.

Another strategy that was emphasized was extensive use of back-up systems and redundancy. A large part of the operations planned had never been attempted before. Due to the high risk of failure for many of the actions planned, a redundancy built into the system would allow for corrective actions on site during the field trials.

10.1.2 Deployment and functioning of release equipment

The supply vessel *Far Grip* was used for deployment and operation of the release arrangement. In addition, two research vessels, *Håkon Mosby* and *Johan Hjort* from the Institute of Marine Research in Bergen, Norway, were engaged for measurements and surveys.

The release arrangement was safely deployed on the sea floor and functioned well during all 4 releases. The release arrangement was also inspected by the ROV once deployed on the sea floor.

10.1.3 Monitoring of the releases

The field trial was carried out in June 2000 at the *Helland Hansen* field in the Norwegian Sea. The sea state during the field trial was in some periods not favorable, with persistent winds above 10 m/s from the north and occasionally occurrence of swell. Due to this, the measurement program was delayed somewhat, but all releases were carried out, mainly within periods of calmer weather.

Four releases were carried out: nitrogen gas, marine diesel, crude oil and methane gas. Both the diesel and the crude oil releases were carried out jointly with methane gas. Table 10.1.1 gives the details of the releases:

Table 10.1.1 Discharges performed during the "Deep Spill" experiment.

Experiment	*Start (local time)*[a]	*Duration*	*Gas rate*	*Water/Oil Rate*
Nitrogen gas and dyed sea water	June 26 1805	40 minutes	0.6 Sm^3/s	60 m^3/hour
Marine diesel and LNG	June 27 0820	60 minutes (oil)	0.6 Sm^3/s	60 m^3/hour
Crude oil and LNG	June 29 0715	60 minutes (oil)	0.7 Sm^3/s	60 m^3/hour
LNG and sea water	June 29 1105	120 minutes	0.7 Sm^3/s	60 m^3/hour

[a] Local time in Norway in summer is 2 hours ahead of UTC (UTC + 2 hours)

Most of the measurements were carried out according to plan, but some of the equipment did not always work as intended. In particular, the ROV operated from *Håkon Mosby* and equipped for monitoring of the underwater plume, failed at an early stage. However, this loss was compensated by activating the back-up ROV installed on *Far Grip*. Also, it turned out that echo sounders on both research vessels monitored the underwater releases better than expected. The sampling of the water column carried out with the rosette sampler on *Johan Hjort* provided additional supportive data on plume behavior. These three contributions compensated to a large extent for the ROV failure.

The gas releases were thus monitored by the work ROV and echo sounders on both research vessels. For the marine diesel and crude oil releases, monitoring in the water column, at the sea surface and aerial surveillance were carried out in addition. The measurements or observations carried out during the field trial are summarized in Table 10.1.2.

Table 10.1.2 Overview of measurements and observation made at the DeepSpill field trial

Objective	*Methods*	*Period*	*Comments*
Documentation of experimental conditions	Weather station on research vessel. CTD operated from research vessel. ADCP mounted on research vessel and bottom mounted ADCP with acoustic link to research vessel.	Wind and current data sampled at 10 minutes intervals. Sea temp and salinity profiles measured minimum once a day.	Wind measured 10 m above sea level. Ocean currents sampled at 25 m intervals from 50 m above seabed to 25 m below sea surface. Sea temp and salinity measured at 1 m spacing from surface to seabed.
Observation of oil droplets, gas bubbles and transition to hydrate	Visual video recorded by work ROV	During discharge periods	Clouds of gas bubbles pictured from outside of plume. Close up of oil droplets and gas bubbles inside plume.
Mapping of plume trajectory	Visual video, sonar, UV-fluorescence meter, methane detector mounted on observation ROV. Remote operated sampling flasks (rosette sampler) deployed from research vessel. Echo sounders operated from research vessels.	During and after each discharge period	No measurements obtained from the ROV mounted due to operational problems with the observation ROV. Echo sounder images were used to guide the rosette sampler was guided into the rising plume of gas bubbles and oil droplets.
Surfacing of oil droplets, thickness and properties of surface oil	UV-fluorescence meter, sampling pads and flasks operated from two workboats.	Subsequent to oil discharges	Workboats guided into surface slick by aircraft.
Extent of surface slick	SLAR, UV and IR imaging from aircraft	Subsequent to oil discharges	Surveillance shared by six airplanes during marine diesel experiment (June 27). Only one aircraft available during crude oil experiment (June 29).
Supplementary information	Sea bird surveillance. Sampling and surveillance of marine organisms.	Prior to and during field trials.	Carried out from *RV Johan Hjort* by specialists from NINA and IMR

The variety of observations and collected data has provided a relatively complete and consistent picture of the features that were to be studied in the field trial. One of the major objectives of the field trial was to make data available for verification of deep-water plume models. In order to facilitate this verification process – and to promote further analysis of the data – data files

covering most aspects of the measurements performed during the experiments have been collected on a special CD-ROM. A list of content of this CD is given in Appendix C of this report.

10.1.4 Results obtained

Observations of the underwater plume by video camera operated from ROV provided close up pictures for determination of droplet and bubble size of the diesel and methane gas releases. No hydrate formation was observed from these video sequences, although the releases were made under conditions where gas hydrates would be thermodynamically stable.

Echo sounders mounted on the research vessels provided useful images of the clouds of oil droplets and gas bubbles rising to the sea surface. Analysis of water samples taken with a rosette sampler – guided by the images from the echo sounder – revealed how the composition of the crude oil and marine diesel changed on its way to the sea surface due to dissolution of the water soluble components into the ambient water.

The echo sounder images indicated that the methane gas did not reach the sea surface, with the signal from the rising cloud of gas bubbles vanishing from the images at about 150 m depth, probably due to the dissolution of the gas into the ambient water. However, both the crude oil and the diesel releases reached the sea surface, but the average rising time was somewhat shorter than expected.

Concentrations in the upper water column were monitored with UV-fluorimeters lowered from workboats. Workboats were also used to sample the crude oil and marine diesel slick at the sea surface. The weather conditions were similar during the crude oil and the marine diesel releases, but the marine diesel dispersed rapidly compared to the crude oil.

The surface oil film thickness produced in the two releases was also significantly different. Typical thickness of the marine diesel slick was of order of 1 μm, while within the thicker parts of the crude oil slick the thickness reached order of 1 mm. The marine diesel did not show any sign of emulsion formation, but the crude oil release did form water-in-oil emulsion. Analysis of oil samples from the surface slicks provided weathering characteristics in terms of reductions with the time of volatile components in the oil (evaporation), increase in water content (crude oil), and changes in physical properties (viscosity).

Aerial surveillance of the two slicks gave supplementary information on the slick sizes and also provided a basis for estimates of the amounts of oil in the slicks. In particular for the marine diesel release, amounts of diesel in the slick were small, compared to the amounts released (60 m^3). The reason for this was attributed to the rapid dispersion of the diesel slick into the surface layers due to wind/wave action.

10.2 Conclusions

This chapter gives some preliminary conclusions related to the objectives formulated for the sea trial, namely to form a data basis for verification of numerical simulation models, to test equipment for monitoring and surveillance and assess possible implications of safety issues.

10.2.1 Verification or validation of the model

The data collected form a good basis for comparison with numerical simulation models of deep-water releases. In this report, the *DeepBlow* model developed by SINTEF has been compared with the field data. This model is designed to include effects of hydrate formation, dissolution of gases in the plume, effects of cross currents and ambient stratification on the underwater plume, trapping of the underwater plume in the recipient, as well as leakage of gas bubbles in a bent-over plume. Different models were used to represent the ascent of oil droplets from the trapped plume to the sea surface, the formation and thickness of the slick on the sea surface, and finally the dissipation of the surface slick due to wind/wave action.

The *DeepBlow* model was adjusted to the observations by turning off hydrate formation in the model, and adjusting the gas dissolution rate to the observed behavior of the methane gas release (disappearing at about 150 m depth). The model was then run with the actual release conditions and the observed ambient currents and stratification. The models for rising droplets and slick formation were run with the observed droplet size distribution and the observed current and wind conditions. An *ad hoc* decay parameter – representing losses due to evaporation and natural dispersion – was adjusted to match the observed persistence of the surface slicks.

The model results show generally good agreement with the observations. The simulated underwater plume behavior was similar to that observed (e.g. gas bubbles leaking out of the plume at an early stage). The calculated paths of the rising clouds of oil droplets and gas bubbles were in good agreement with the images obtained from the echo sounders. The simulated development of the surface slicks was similar to that observed, although some differences in the shape and extension of the slicks were noted. These discrepancies could be due to model limitations as well as inaccuracies in the input data (measured ocean currents and wind).

10.2.2 Implications for the monitoring of the releases

The monitoring conducted during the experiments included use of an ROV at the release site, echo sounders and water sampling for monitoring of the releases in the water column, work-boats for sampling of oil in the surface slick and in the surface waters, and the use of surveillance aircraft.

During actual deep-water spills – all information that can support the tracking of the underwater plume and the subsequent motion of the oil (and the gas) should be made available on site. Such information could be made by different means, such as:

- ROV observations of the underwater plume
- Echo sounder recordings of the oil droplets and gas bubbles
- On-line transfer of concentrations recorded in the underwater plume area
- Real-time model simulation of the underwater spill on site
- Real time measurements of the ambient conditions (winds, currents and stratification) on the site

All these monitoring methods were tested during the field trial. The experiences gained are as follows:

The ROV operated from *Far Grip* performed successfully. The use of a "cage" from which the ROV operated turned out to be successful. No tangling problems were experienced with this ROV, although the "cage" was lowered close to the discharge arrangement. The other ROV – that was operated from *Håkon Mosby* and guided by an umbilical from the surface – did have problems with tangling. Large drag forces on the umbilical also hampered the operability of this vehicle. Therefore, we recommend that an ROV system of the cage type – as the one operated from *Far Grip* – should be preferred in future subsea monitoring operations.

The echo sounders on the research proved to be effective for imaging of the ascending clouds of gas bubbles and oil droplets from the discharges. This method requires that the vessel operating the echo sounder can move freely and be in position above the discharge area more or less continuously.

The UV-fluorimeter that was mounted on the rosette sampler was intended to provide in-situ readings of concentration within the oil droplet cloud ascending from the trapped plume. This instrument failed for unknown reasons during the field trial, and the sampling of the droplet cloud was therefore guided by the images from the echo sounder. This worked well, but the results from the sampling had to await laboratory analysis of the data. No results from the measurements within the oil droplet area were therefore available during the field operations. In an accidental spill situation, such information should be available in-situ. In order to assure this, testing and calibration of a UV-fluorimeter in combination with a rosette sampler should be made under realistic conditions.

Vertical profiles of sea temperatures, salinity and ocean currents were made available in real time during the field trial. This was important for the planning of the monitoring. In addition, the *Deep Blow* model was run (based on the real time current and density profiles) on site for the prediction of the expected paths of the releases. This information facilitated the guidance of the monitoring instruments, as well as the positioning of the research vessels.

During the present sea trial, three ships were in action, one in a fixed position (*Far Grip*), while the other two were free to move for the tracking of the discharge under water. The ROV system used at *Far Grip*, including the operation of the ROV from a "cage" may impose restrictions on the motion of the ship. Therefore, two ships may be an absolute minimum for surveying an underwater release. This will allow for the necessary flexibility in the positioning of the ships. Preferably, the ship with the ROV should be located closest to the discharge point. The other ship(s) will then be free to move in order to track the release in the water column with echo sounders or with other equipment.

10.2.3 Implications for the safety

One of the purposes of the sea trial was also to look for new information related to safety issues when gas is discharged in deep water (explosion danger). When the gas plume (or cloud of bubbles) reaches the sea surface, a danger for explosion arises. Today's practice involves a removal of the platform or the surface-operating unit from the blowout site in order to reduce the explosion danger.

The results from the *DeepSpill* experiments indicate that this practice may not be always necessary for deepwater blowouts. During the crude oil and marine diesel releases, the observers in the MOB boats could see clearly oil droplets "bursting" at the sea surface, but no gas bubbles

were observed. During the crude oil release, the echo sounder images showed sign of the release up to the surface, while during the methane gas release, all signs of the release vanished at about 150 m depth. The observed disappearance of the gas is expected to be due to dissolution of gas into ambient waters. With this in mind, the risk for gas explosions may be considerably lower for deepwater blowouts. This would, in turn, increase the possibility of keeping the operating unit on site to control (or improve on) the blowout situation.

10.3 Recommendations

10.3.1 Model development

One of the purposes of the *Deep Spill* sea trial was to generate data for verification of numerical simulation models. SINTEF's *DeepBlow* model showed reasonably good correspondence with the observations generated in the experiment, but some modifications had to be made in the model. In accordance with existing theory – hydrate formation was presumed to take place under the prevailing release conditions, but no indications of this process was seen during the releases. The process of dissolution of gas to seawater was implemented according to well-established chemical engineering practice – but the observed dissolution rates were smaller than predicted by theory. Verification runs with other similar models would reveal if this is a model specific problem – or if the problem are of a more general nature.

The data generated in this project will also be suitable for testing of other models presently available or under development. To facilitate this – a special CD-Rom has been prepared with data-files comprising all quantitative information gathered during the experiments. See appendix C for a list of contents of this CD.

A substantial part of this data set has been presented and analyzed in the present report, but there are still unexplored potentials for testing and verification of models. As an example, data were collected on concentrations of specific oil components (such as BTEX, naphthalenes, alcanes, and naphthenes) present in the oil or dissolved in the water. Concentrations of these compounds were obtained for both the water column and the surface oil slicks. These results would be very useful for testing and verification of oil spill simulation models incorporating the dissolution process.

10.3.2 Oil spill contingency planning

Oil spill contingency planning for surface spills could include chemical dispersion of the oil, as well as mechanical recovery. So far, the options for oil spill combat in deep water will be the same as for surface spills. The surface slick formed after the crude oil release contained patches of water-in-oil emulsion with film thickness more than adequate for containment with oil booms, and also with sufficient thickness for efficient treatment with chemical dispersant. The potential life-time of the crude oil slick on the sea surface was however was however judged to be short – and for this reason the slick could be left to disperse naturally without attempting any mechanical combat.

This might indicate that for deepwater blowouts far offshore and far from sensitive biological resources, a third oil spill response option could be viable, i.e. to monitor the surface and subsea spreading of the release, without any combat measures. Even if combat measures have to be planned for, monitoring will be required for decision making and public information.

To monitor the subsea spreading of deepwater blowouts, methods are needed that can provide real-time data of concentrations of oil (oil droplets and dissolved oil) and dissolved gas (methane), in the water masses. This information should be supported with real time current data and hydrographic profiles (sea temperature and salinity) to facilitate the monitoring task. All this, of course, comes in addition to the use of echo sounders and ROV inspection of the release.

10.3.3 Further research

Most of the results from the various experiments turned out as expected, but some unexpected results were found as well. One of these was that no hydrate formation was observed during the sea trial, even while methane gas are known to form thermodynamically stable hydrates under the release conditions. The absence of hydrate formation was apparent from close up video images of gas bubbles made in the vicinity of the exit and out to a distance of about 150 meters above the exit. The fact that the echo-sounder signal of the gas cloud was visible up to a depth of 150 m (700 m above the release point) during the methane gas release also supports this notion: The bubbles could not have ascended to such heights if hydrate formation had been effective.

Presently – no convincing hypothesis has been found for the absence of hydrate formation, but most probably, the problem is related to the kinetics of hydrate formation. In laboratory experiments – hydrate formation from gas bubbles have been observed under corresponding conditions, but there are indications that the onset of hydrate formation required that the ambient water had been saturated with gas [13]. Since the seawater surrounding a rising gas bubble would be constantly replenished – the absence of gas saturation might be the factor retarding the onset of hydrate formation at the surface of a rising bubble in natural conditions. Laboratory studies similar to the ones referred to above, but with constantly replenished water could confirm this hypothesis, or lead to better explanation of the observations.

Presently, we also have no convincing explanation for the apparently smaller dissolution rate of gas compared to theory. Some kind of surface coating on the gas bubbles ("dirty bubbles") could be one possible explanation [14] – but this notion could not be confirmed by visual inspection: The close up video images shoved clearly transparent bubbles. However, we might speculate if high pressure could play some unknown role in the mass transfer process, besides the well-known effect of increased water solubility of gas with increasing pressure. Laboratory studies with natural gas bubbles in high-pressure chambers could throw more light upon this puzzle.

Prior to the sea trial, there were some doubts about whether the oil would reach the sea surface. It apparently did so during these experiments, but if the size of the oil droplets formed at the exit had been sufficiently small, the oil might not have surfaced. During the present sea trial, the exit

[13] Maini, B.B. and P.R. Bishnoi, 1981: *Experimental investigation of hydrate formation behaviour of a natural gas bubble in simulated deep sea environment.* Chemical Engineering Science Vol 36, pp 183-189.
[14] Leifer, I. and R.K. Patro, 2000: *The bubble mechanism for transport of methane from the shallow sea to the surface: A review and a sensitivity study*. Paper manuscript submitted for publication in Continental Shelf Research. Preprint.

nozzle was designed to produce an exit velocity of about 2 m/s. This is within the possible range for potential blowouts in deep waters, but larger exit velocities might also occur that might produce considerably smaller droplets.

The experiment also indicated that the rise time of the largest oil droplets were somewhat shorter than expected. To account for the observed rise time of 1 hour from a depth of 844 m, the rise velocity must have been considerably larger than the presumed maximum rise velocity of oil droplets of about 0.13 m/s [15]. Some shortening of the rise time might have been gained by the more rapid rise of the droplets in the plume stage, but this effect does not seem to be large enough to account for the observed difference.

We therefore recommend that the drop size formation processes as well as the rise velocity of oil droplets are considered further. It may be that laboratory tests will be the most efficient way to arrive at results for these two items. For the rising velocity of oil droplets, it should also be considered what influence the presence of gas in the release might have.

Finally – there might be worthwhile to consider methods for subsea surveillance and monitoring that have not been tested in the present experiment, such as Autonomous Underwater Vehicles (AUV) that can be pre-programmed to follow a certain track. AUVs designed for the US Navy have been equipped with various sensors, including CTD, side scan sonar, fluorometer, optical backscatter sensors, 1200 kHz and 300 kHz ADCP, 150 kHz phased array ADCP, various camera systems including low-light video, and acoustic Doppler velocimeter [16]. Such sensors could be prove useful for subsea monitoring in case of accidental deepwater releases or blowouts.

[15] Shengen Hu and R.C. Kintner, 1955: *The fall of single liquid drops through water*. A.I.Ch.E. Journal, pp. 42-48.
[16] See *Office of Naval Research's* website onr.navy.mil/sci_tech/ocean

APPENDIX A – SUMMARY OF APPLICATION FOR PERMIT

Application to SFT (Norwegian Pollution Control Authority) for permission to carry out an experimental oil release in deep waters in the Norwegian Sea.

Norsk Chevron A/S, on behalf of a group of oil companies and organizations, is planning an experimental release of oil and gas in the Norwegian Sea (west of the Haltenbank) in June 2000. The releases are planned on 800 – 1000 m depth, and is motivated by the need for increased knowledge about the behavior of eventual accidental spills in deep waters (depth more than 400 – 500 m).

Applicant:
Norsk Chevron A/S, on behalf of a group that consists of

- Norsk Chevron AS
- BP Amoco Norge AS
- Norsk Conoco AS
- Elf Petroleum Norge AS
- Norsk Hydro AS
- Minerals Management Service (U. S. Dept. of Interior)
- Texaco Exploration and Production Inc.

wish to carry out experimental releases of oil and gas in the Norwegian Sea at 800 – 1000 m depth.

Time and place for the releases:
The releases are planned to be carried out during week 25 (19-23 June) this year (2000). The release site is located close to the "Helland Hansen" area west of the Haltenbanken area. The release site is located within the area:

$64^o\ 45'$ - $65^o\ 15'$ N, $4^o\ 00'$ - $5^o\ 00'$ E

What and how much is to be released:
Four experimental releases are planned, comprising of different combinations of oil, natural gas and nitrogen. Also, Rhodamine added as a tracer is also planned. Two releases are planned to see how the different types of oil affect the results. The release amounts to be applied for are:

- 60 m^3 of light oil or condensate
- 60 m^3 of a typical North Sea crude
- 10 kg of the tracer Rhodamine

Basis for the releases:
New discoveries of oil resources are expected at increasing sea depths. The operators therefore need to increase their basic knowledge if the exploration activity should cause accidental releases of oil and gas. The operators need to be as well prepared as possible when searching for oil in deep waters. The purposes of these release trials are:

- to obtain data for verification and testing of numerical models for simulating accidental releases in deep waters.
- to test equipment for registration and surveillance of accidental releases.
- to evaluate the safety aspect of accidental releases of gas and oil in deep waters.
- to make more reliable estimates of environmental impacts by the use of verified numerical models.

The use of models combined with improved surveillance of the releases will then serve as a basis for the planning of optimum contingency.

Environmental effects of the releases:

Calculations have been made on possible effects of the planned releases, both for oil in the water column and for oil on the sea surface. The release is located in deep waters outside the shelf area (the Haltenbank). Some of the oil is expected to enter the water column / water masses. Calculations show that this is expected to happen at large depths (lower than 400 – 500 m depth), so that the water masses on the continental shelf (shallower than 400 m depth) will not be affected. Oil drift and fate computations show that the oil on the sea surface is expected to break down quickly (mix into the water masses). Due to the long distance to shore, no oil is expected to reach the shore.

Co-ordination with the NOFO oil spill trial:

The experiment is coordinated with NOFO who is carrying out their oil spill trial at the same time and place. The engagement of NOFO is coordinated so that they will be on site with necessary oil recovery equipment when the oil releases have been performed.

Result accessibility for operators on the Norwegian Continental Shelf:

The aim with this release trial is to provide data on the behavior of accidental released in deep waters, in order to verify numerical models for such releases. Models verified on the basis of data from the experiment will be accessible for all operators on the Norwegian Continental Shelf, but operators not participating in the project will have to pay a fee for the use of such models for their own purposes. In particular, the experimental data will be used to verify a deepwater spill model that will be implemented in an improved oil drift forecast system under development for NOFO and SFT. This forecast model will be operated by the Norwegian Meteorological Institute and on behalf of NOFO and SFT in oil spill exercises or actual spill situations on the Norwegian Continental Shelf.

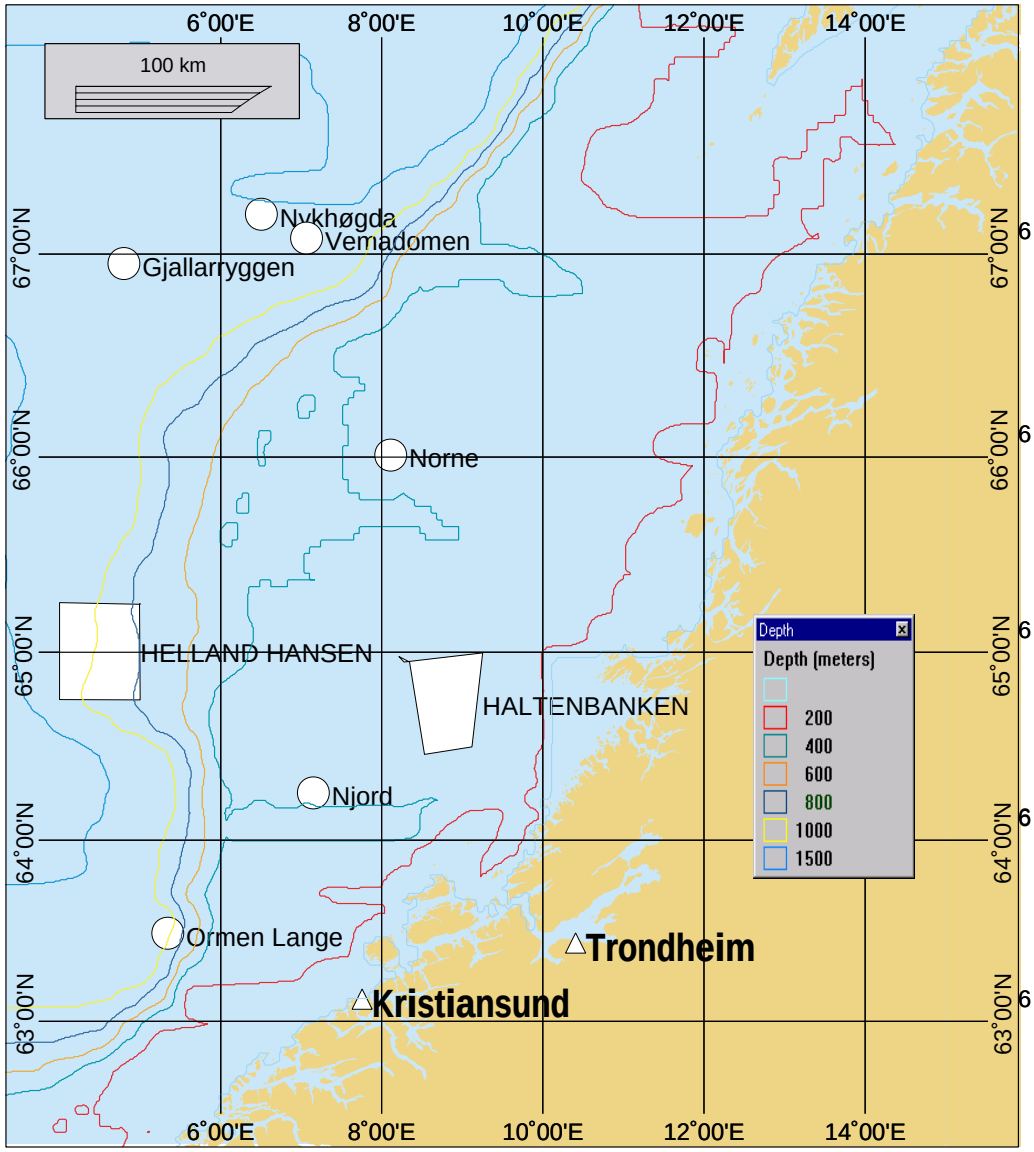

Map over the Helland Hansen experimental area. Existing oil fields are basically located between Njord and Norne. Areas where oil exploration in deep water has been taken place are at Ormen Lange, Helland Hansen, Gjallarryggen, Vemadomen and Nykhøgda.

SINTEF

APPENDIX B – PARTICIPANTS IN THE DEEPSPILL PROJECT

B.1 Participants in the DeepSpill JIP (listed in alphabetic order)

Company	City	Country	Contact person
AGIP UK	Aberdeen	Scotland	Paolo Linzi - Safety & Envir Mgr
BHP Petroleum Inc	Houston TX	USA	Ron Campbell
BP Amoco Norge AS	Stavanger	Norway	Hans Grüner - Sr Envir Advisor
Chevron Petroleum Technology Co.	San Ramon CA	USA	Cortis Cooper – Sr. Staff Scientist
Devon Energy	Houston TX	USA	Lynn Travis
Dominion Exploration & Production	New Orleans LA	USA	David J. McBride
EEX Corporation	Houston TX	USA	Joseph Kilchrist
El Paso Production Company	Houston TX	USA	Reese Mitchell
Elf Petroleum Norge AS	Stavanger	Norway	Bertrand Gaudebert
Exxon Upstream Research	Houston, TX	USA	Jean Bruney
Kerr-McGee Oil & Gas Corporation	Houston TX	USA	Cary V Bradford - Mgr Regulatory Affairs
Marathon Oil Co	Lafayette LA	USA	Michael W Miller - HES Mgr
Mariner Energy	Houston TX	USA	Blain Dinger
Minerals Management Service (MMS) - U.S. Dept. of the Interior	Herndon VA	USA	Jane M Carlson - Contracting Officer
Murphy Exploration & Production Co	New Orleans LA	USA	Don Evans, S. J. Carboni, Jr.
Newfield Exploration Co	Houston TX	USA	Gary Harrington
Norske Conoco AS	Stavanger	Norway	May Roesand
Norsk Hydro	Oslo	Norway	Odd-Arne Follum
Phillips Petroleum Co	Houston TX	USA	Mike Metz
Shell Exploration & Production Co	New Orleans LA	USA	Kent Satterlee
Statoil	Stavanger	Norway	Arne Myhrvold
Texaco Exploration & Production Inc	New Orleans LA	USA	Paul Broussard
Unocal Corporation	Sugar Land TX	USA	Terry James
Vastar	Houston TX	USA	Richard Tink

SINTEF

B.2 Subcontractors and major providers to the DeepSpill project

Institution/Company	*Location*	*Provider of*
Alun Lewis Oil Spill Consultant	Staines, Middlesex, UK	▪ Co-ordination of aerial surveillance flights
AGA	Oslo, Norway	▪ Liquefied Nitrogen (LIN)
Argus Remote Systems as	Bergen, Norway	▪ Observation ROV (Aglantha)
Det Norske Veritas (DnV)	Høvik, Norway	▪ Safety seminars (HAZOPs)
Institute of Marine Research (IMR)	Bergen, Norway	▪ Research vessels "Johan Hjort" and "Håkon Mosby" ▪ Met-ocean data ▪ Echo-sounder data ▪ Marine biological survey
JM Consult as	Stavanger, Norway	▪ Design and fabrication of – Discharge unit – Deck arrangement – Platform for Work ROV
Krytem GmbH	Willich, Germany	▪ Cryogenic pump and evaporator for gas supply system
MARINTEK	Trondheim, Norway	▪ Design and operation of gas supply system
Norsk Hydro Produksjon AS	Oslo, Norway	▪ Crude oil (Oseberg Blend) for experimental discharge
Norwegian Clean Sea Associates (NOFO)	Stavanger, Norway	▪ Oil spill contingency (on site)
Norwegian Institute of Nature Research (NINA)	Trondheim, Norway	▪ Sea bird survey
Norwegian Meteorological Institute (DNMI)	Bergen, Norway	▪ Weather forecasts (on site)
Norwegian Pollution Control Authority	Horten, Norway	▪ Aerial surveillance airplanes from Norway, Denmark, France, Germany, The Netherlands and UK
Oceaneering A/S	Stavanger, Norway	▪ Work ROV
Schlumberger Norge A/S	Stavanger, Norway	▪ Coiled Tubing and accessories ▪ Pump unit for oil
Seabrokers Chartering AS	Stavanger, Norway	▪ Supply vessel "Far Grip"
Statoil Norge AS	Oslo, Norway	▪ Liquefied natural gas (LNG) ▪ Marine Diesel for experimental discharge
Taylor Minster Leasing	Marlow, UK	▪ Cryogenic tank containers

B.3 Participating vessels and cruise members

Function	*Far Grip*	*Håkon Mosby*	*Johan Hjort*
TAC Representative		1 Cort Cooper, Chevron US	
Project supervisor	1 Bob Watson, Norsk Chevron		
Safety officer	1 Roger Tailby		
Response Officer	1 Odd Arne Follum, Norsk Hydro		
DeepSpill Camera man	1 Steve Kane		
SINTEF cruise coordinators	1 Hans Jensen, SINTEF	1 Øistein Johansen, SINTEF	
Discharge system supervisor	1 Kenneth Maribu, Schlumberger		
CST operators	4 Schlumberger		
LNG/LIN operators	2 Stein Inge Lien, Marintek Harald Haltstrand		
ROV operators	3 OCEANEERING	4 ARGUS	
Subsea monitoring	1 Henrik Rye, SINTEF	1 Alf Melby, SINTEF	
Workboat # 1(SINTEF)			2 Per Dahling Ivar Singsaas
Workboat #2 (SINTEF)			2 Per Johan Brandvik Frode Leirvik
SINTEF Lab container			1 Kirsti Almås
Cruise leader IMR		1 Bjørn Serigstad	1 Tor Knutsen
Oceanographic data aqui.		1 IMR	
Plankton trawling			2 IMR
Chemical analysis			1 IMR
Acoustics			1 IMR
Ornitholog			1 Nils Røv, NINA
DeepSpill JIP observers		1 Mary Boatman, MMS	1 Arne Myhrvold, Statoil
		1 Paul Broussard, Texaco	1 Bela James, Equilon
External observers			
Norwegian Pollution Control			
Authority, SFT	1 Jørn Harald Andersen		
NOFO			1 Kari Stokke
CO_2 experiment		1 Arvid Sundfjord, NIVA	

APPENDIX C – OVEVIEW OF DATA SETS STORED ON CD-ROM

```
 Directory of D:\DATA_FILES

WINDdata
ADCPdata
CTDdata
UVFdata
ECHOdata
CHEMdata
SLICKdata

 Directory of D:\DATA_FILES\WINDdata

HAKON_MOSBY_WIND.DAT                21 250 bytes
Total                               21 250 bytes

 Directory of D:\ DATA_FILES\ADCPdata

ADCP_DATA.xls                      997 888 bytes
Total                              997 888 bytes

 Directory of D:\ DATA_FILES\CTDdata

CTD_St500.prn                       13 141 bytes
CTD_St2001.prn                      21 019 bytes
CTD_St2002.prn                       2 247 bytes
CTD_St488.prn                       20 941 bytes
CTD_St489.prn                       22 163 bytes
CTD_St490.prn                       20 109 bytes
CTD_St494.prn                       20 395 bytes
CTD_St495.prn                       21 435 bytes
CTD_St496.prn                       21 435 bytes
CTD_St499.prn                       20 317 bytes
CTD_stations.prn                       415 bytes
CTD_MeanProfiles.prn                 1 469 bytes
Total                              185 086 bytes

 Directory of D:\ DATA_FILES\UVFdata

UVF_TRANSECTS.xls                4 760 064 bytes
Total                            4 760 064 bytes

 Directory of D:\ DATA_FILES\ECHOdata

HakonMosby.xls                   7 347 200 bytes
JohanHjort.xls                   2 980 864 bytes
Total                           10 328 064 bytes

 Directory of D:\ DATA_FILES\CHEMdata

Rawdata Volatile Organic Compounds Rosette Samples.xls          41 984 bytes
Rawdata Semi Volatile Organic Compounds Teflon Pads.xls         27 648 bytes
Rawdata TEOC Blank Samples .xls                                 16 384 bytes
Rawdata TEOC Rosette Samples.xls                                19 456 bytes
Rawdata Volatile Organic Compounds Oils.xls                     19 456 bytes
Rawdata Volatile Organic Compounds Rosette Blank Samples.xls    20 480 bytes
Rawdata Semi Volatile Organic Compounds Rosette Samples.xls     60 416 bytes
Rawdata Semi Volatile Organic Compounds UVF ..
                                  ..Calibration Samples .xls    37 888 bytes
Rawdata TEOC Teflon Pads.xls                                    14 336 bytes
Rawdata TEOC UVF Calibration Samples .xls                       15 360 bytes

Rawdata Semi Volatile Organic Compounds Rosette ..
                                       ..Blank Samples.xls      23 552 bytes
Chemical analysis of organic compounds.doc                      67 072 bytes
Total                                                          364 032 bytes
```

```
 Directory of D:\ DATA_FILES\SLICKdata

Slick_Contours.xls                                  83 968 bytes
Total                                               83 968 bytes

Total Files Listed                              16 740 352 bytes
```